Exploring the role of ERβ2 at different subcellular locations in breast cancer

Emily Louise Smart BSc (Hons)

Submitted in accordance with the requirements for the degree of Doctor of Philosophy

The University of Leeds
School of Medicine

September 2015

The candidate confirms that the work submitted is her own and that appropriate credit has been given where reference has been made to the work of others.

Acknowledgements

I would like to thank my primary supervisor, Professor Valerie Speirs for her guidance, dedication and patience throughout this project. Val's continued support has made this project possible and has helped me develop as a scientist and I greatly appreciate the time she has put into me.

Thanks also go to my co-supervisors; Dr Thomas Hughes, for his vastly extensive knowledge on just about everything and his ability to encourage me when things get tough; cake is often the answer apparently, Professor Andrew Hanby for his encouragement and help with all things pathology and Laura Smith for her reassurance and support.

I would also like to thank Euan Baxter (PhD), a Post- doctorate and former member of the Breast Research Group for the additional support and guidance and for the excellent grounding he has given me in many aspects of molecular biology. Euan is credited with performing some aspects of the molecular cloning in this project. Thanks to Professor Eric Lam for providing the original ERβ2 construct so we were able to proceed with the cloning work. A particularly special thank you goes to Claire Nash (PhD) for taking me under her wing the moment I arrived in Leeds and supporting me throughout my project both as a colleague and a friend.

Additional thanks goes to The Pathological Society of Great Britain and Ireland for funding my project and allowing me to present and communicate my work at their annual conferences.

Finally I would like to thank my family and significant other Matt Ward for their continual financial and emotional support and helping my keep my mental state intact over the last four years, and to Georgia Mappa, Rob Danks and Rich Powell for giving me a place to stay during my write up.

Abstract

Two estrogen receptors exist, ERα and ERβ. ERα is often over-expressed in breast cancers, frequently coupled with ERβ downregulation.

The complex function of ERβ is not fully understood. There are 5 ERβ isoforms, ERβ1-5, and three are present in breast tissue (ERβ1, -2 and -5). Knowledge surrounding the role of the ERβ2 in breast cancer is limited; however its cellular location has been demonstrated to have predictive prognostic ability; nuclear expression was associated with better prognosis and cytoplasmic with poorer prognosis. Aside from acting as a repressor of ERα in breast cancer cells, little is known about the function of ERβ2.

The aim of this thesis was to improve our understanding of ERβ2 and its potential role in breast cancer. ERβ2 expression was characterised in a range of breast cancer cell lines representative of five major molecular subgroups where it was expressed in both the nucleus and cytoplasm. Nuclear ERβ2 was largely expressed in a speckled pattern while cytoplasmic ERβ2 colocalised with mitochondria in all cell lines.

ERβ nuclear speckles were explored further by immunofluorescence. ERβ2 speckles did not colocalise with other known nuclear speckled proteins, including nuclear speckles, PML and cajal bodies. Speckle numbers changed in response to 4-OHT, DPN and genistein treatment but not E2, and disappeared following transcriptional or translational inhibition with actinomycin D and cyclohexamide respectively. Numbers of ERβ2 speckles decreased during G2/M phase of the cell cycle.

The physiological function of ERβ2 was explored by overexpressing ERβ2 in luminal and triple negative cell lines. ERβ2 overexpression resulted in suppression of proliferation in luminal cells whereas in triple negative cells, proliferative response was cell line-dependent. Cell migration was decreased in all cell lines. ERβ2 overexpression additionally influenced gene transcription of some nuclear

genes i.e. *BCL-2, CDK6, S100A7* and *RIP140* and also some mitochondrially transcribed genes i.e. *ND1, ND2, CYB* and *ATP6*.

In summary, ERβ2 was expressed in the nucleus as speckles; dynamic structures which changed in number in response to external stimuli. Cytoplasmically expressed ERβ2 colocalised with the mitochondria may influence transcription of some mitochondrial genes.

Table of Contents

List of Figures

List of Tables

Abbreviations

Abbreviation	Definition
4-OHT	4-Hydroxytamoxifen
ActD	Actinomycin-D
ADT	Adenosine diphosphate
AF-1	Activation function 1
AF-2	Activation function 2
AKT	Protein kinase B
AP-1	Activator protein 1
AR	Androgen receptor
ARE	Androgen receptor element
ATCC	American Type Culture Collection
ATP	Adenosine triphosphate
ATP	Adenosine triphosphate
BLAST	Basic Local Alignment Search Tool
BLM	Bloom syndrome protein
bp	Base pairs
BPE	Bovine Pituitary extract
BrUTP	Bromouridine-triphosphate
ChIP	Chromatin immunoprecipitation
ChIP-Seq	Chromatin immunoprecipitation sequencing
CHX	Cycloheximide
CS-FCS	Charcoal stripped foetal calf serum
CTC	Circulating tumour cells
DAPI	4’6-diamidino-2-phenylindole
DBD	DNA binding domain
DCIS	Ductal carcinoma in situ
DFC	Dense fibrillar component
DFS	Disease free survival
DMSO	Dimethyl sulphoxide
dNTP	Deoxyribonucleotide triphosphate
DPBS	Dulbecco’s Phosphate Buffered Saline
DPN	Diarylpropionitrile
E2	17β-estrodiol
EDTA	Ethylenediaminetetraacetic acid
EGF	Epidermal growth factor
EGFR	Epidermal growth factor receptor
EMT	Epithelial to mesenchymal transition
ER	Estrogen receptor
ER+	Estrogen receptor positive
ERE	Estrogen Response Element
ERK	Extracellular-signal-regulated kinase
ERβ	Estrogen receptor alpha
FC	Fibrillar centre
FCS	Fetal Calf Serum

FITC	Fluorescein isothiocyanate
GC	Granular component
GF	Growth factor
GFR	Growth factor receptor
GM	Genetically modified
HER2	Human Epidermal Growth Factor Receptor 2
HI FCS	Heat Inactivated Fetal Calf Serum
HRP	Horseradish peroxidise
IF	Immunofluorescence
IHC	Immunohistochemistry
IM	Immunomodulatory
kb	Kilobases
kDa	Kilodaltons
LAR	Luminal androgen receptor
LB	Luria-Bertani
LBD	Ligand binding domain
LCIS	Lobular carcinoma in situ
MAPK	Mitogen-activated protein kinase
MCS	Multiple cloning site
MSL	Mesenchymal stem like
mtDNA	Mitochondrial DNA
NST	No special type
OS	Overall survival
PBS	Phospho buffered saline
PCC	Pearson's correlation coefficient
PCR	Polymerase Chain Reaction
PFA	Paraformaldehyde
PI	Propidium Iodide
PI3K	Phosphoinositide 3-kinase
PML	Promyelocytic Leukemia
PR	Progesterone receptor
RIPA	Radioimmunoprecipitation assay buffer
RNA Pol I, II, III	RNA polymerase I, II, III
ROI	Region of interest
ROS	Reactive oxygen species
rRNA	Ribosomal RNA
RT	Reverse transcription
RWD	Relative wound density
SDS	Sodium dodecyl sulfate
SM	Second messenger
SP-1	Activation protein 2
Src	Proto-oncogene tyrosine-**protein** kinase
STR	Short Tandem Repeat
TATA-BP	TATA-binding protein
TBS	Tris buffered saline
TBS-T	Tris buffered saline Tween
TDLU	Terminal ductal lobular unit
TN	Triple negative

TNBC	Triple negative breast cancer
tRNA	Transfer RNA
UV	Ultraviolet
WB	Western blot
WT	Wild type

1.0 Chapter 1: Introduction

1.1 Normal Breast Anatomy

The normal breast contains a series of structures that contribute to its main function; production and expression of milk during lactation. It is made up of a series of lobules and ducts, which are surrounded by connective tissue also known as stroma, shown in Figure 1.1. Lobules are made up of small rounded structures known as acini, which contain epithelial and myoepithelial cells contained within a basement membrane. The epithelial cells are located on the inside edge of the ducts and lobules and are responsible for secreting milk upon stimulation with hormones after giving birth. Estrogen is responsible for the growth and differentiation of the ducts and lobules and similarily progesterone influences the size of the acini (1). Both inhibit lactation until birth, when levels of estrogen and progesterone drop and prolactin causes epithelial cells to secrete milk (2). The myoepithelial cells surround the outer edge of the epithelial cells and function to contract in order to eject secreted milk into the ducts (3). Both cell types are surrounded by a protein rich basement membrane. The ducts are in continuity with the lobules and serve as a drainage system to the nipple. Together the smaller ducts and the lobule are known as terminal ductal lobular units (TDLU), considered the major functional structural component of the breast (4). Other components of the breast include the stroma or connective tissue which also plays a functional role. It contains cells such as fibroblasts (which secrete collagen), endothelial cells, adipocytes, stem and immune cells, and serves to provide a matrix in which the TDLUs can grow and help create the structure of the breast (5).

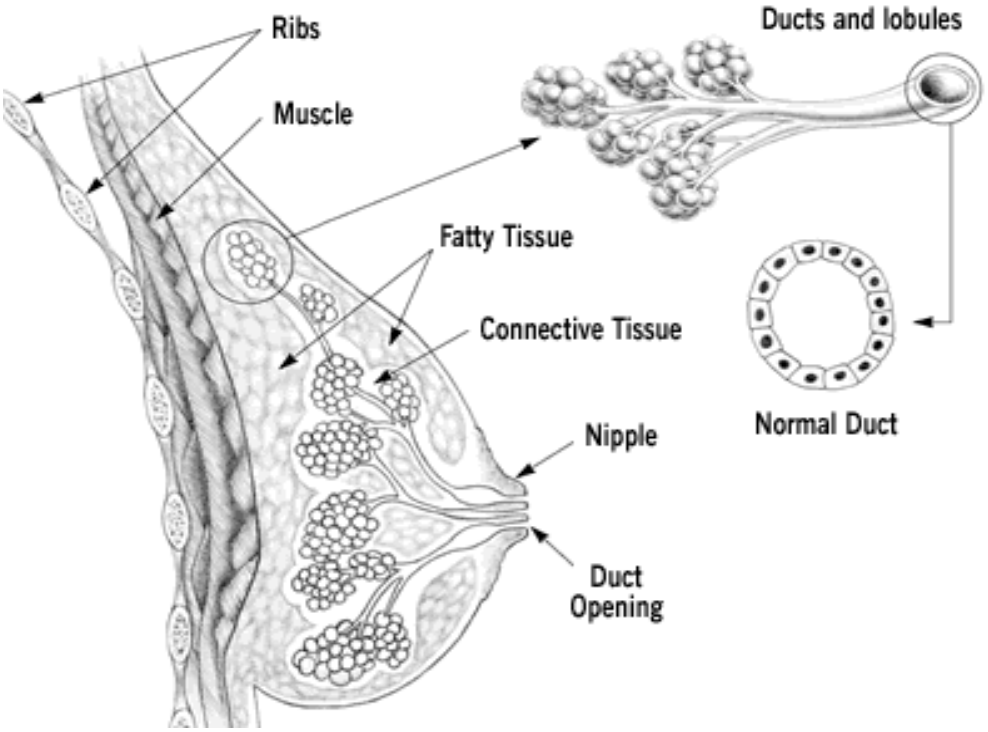

Figure 1.1. Diagrammatic representation of breast anatomy. Taken from [3] with author's permission.

1.2 Breast cancer

1.2.1 Epidemiology

Breast cancer is responsible for 23% of new cancer cases per year worldwide and is the most frequently diagnosed cancer in women. It is attributed to 14% of total cancer deaths (6) and is estimated to affect 1 in 8 females in their lifetime (7). It is also one of the most treatable cancers with 78% of women in England and Wales surviving 10 or more years after diagnosis (8). With breast cancer being so prevalent among the population, it is not surprising there is considerable research into this disease.

1.2.2 Pathology

In western society, breast cancer is the most common type of malignancy in females. Breast cancers generally arise in the epithelial cells of the ducts or lobules. The myoepithelial cells are thought to be tumour suppressive as it has been suggested they regulate the in-situ to invasive process by contributing to the control of epithelial cell cycle progression, invasion, migration and cell polarity (9).
At its earliest stages carcinomas are confined to ducts or lobules, and have not breached the basement membrane and invaded surrounding tissue. These non-invasive cancers are more commonly known as ductal carcinoma in situ (DCIS) or lobular carcinoma in situ (LCIS). Invasive carcinomas are characterised by the breach of the basement membrane in ducts or lobules, by the tumourous epithelial cells, whereby they “invade” the surrounding tissues. It is hypothesised that myoepithelial cells lose their tumour suppressive properties at this point allowing epithelial invasion and proliferation (9). The most common group of invasive breast cancers are infiltrating ductal carcinoma of no special type (NST), with around 75% of invasive breast cancers belonging to this group. Infiltrating lobular carcinomas account for a much lower percentage (10%) of invasive breast cancers. Other types

include mucinous, tubular, papillary and medullary, which are all rarer forms of the disease (4). Figure 1.2 illustrates the morphological differences in normal breast tissue, DCIS and invasive breast cancer.

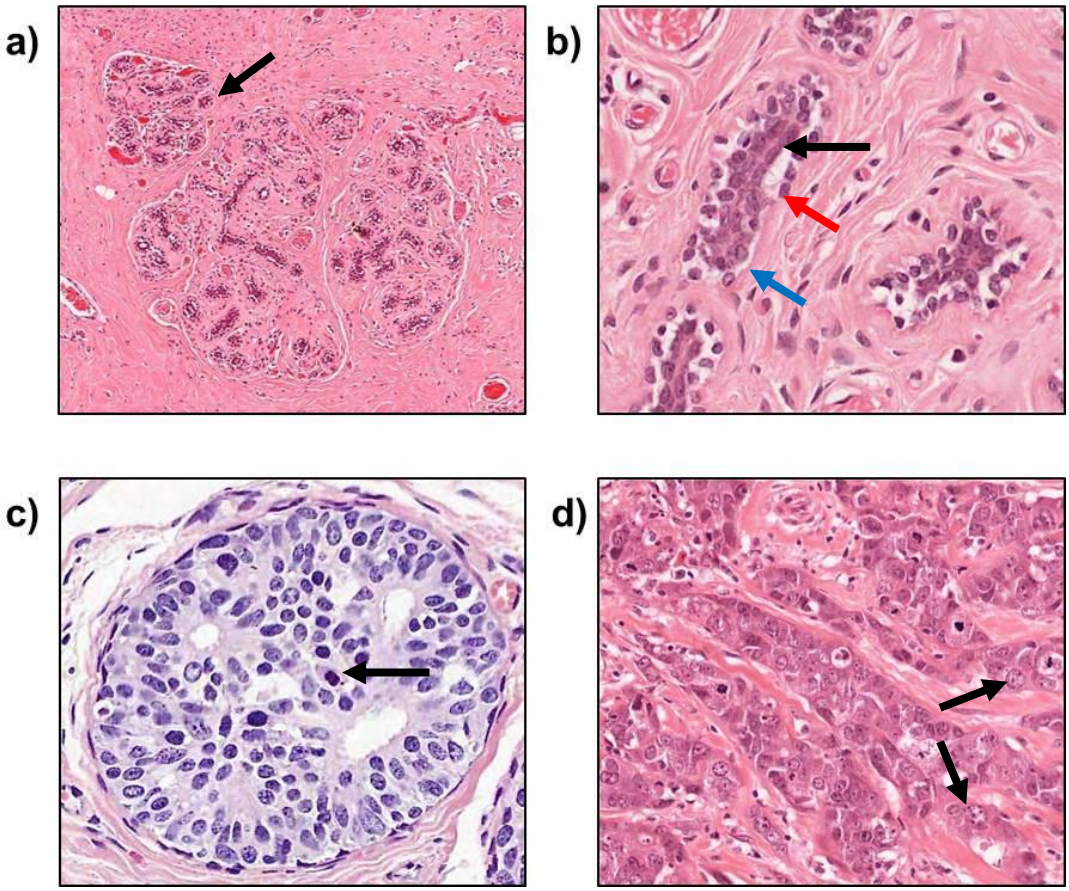

Figure 1.2. H&E stained sections of breast tissue.
(a) Normal benign breast tissue, low magnification. Image shows distinct organised structure of the lobule. Highlighted (arrow) is an individual acinus
(b) Normal benign breast tissue, high magnification. Individual acini can be seen in detail, showing two cell layers. The black arrow denotes the luminal epithelial cells and the red arrow indicates the myoepithelial cells. These cells are encased in a basement membrane (blue arrow)
(c) DCIS, high magnification. Epithelial cells have proliferated into the ductal space (arrow) but are still contained within the basement membrane; the tumour remains non-invasive.
(d) Invasive breast carcinoma, high magnification. Illustrates disorganised arrangement without two organised cell layers as seen in normal breast tissue. Large pleomorphic nuclei are shown by the arrows.
Images were provided by Professor A Hanby, Professor of Breast Cancer Pathology at the University of Leeds

1.2.3 Risk factors

Risk factors associated with the development of this disease include increased age, obesity, familial history, environmental factors such as higher alcohol consumption or lack of exercise, increased duration between menarche and menopause, use of oral contraceptives and levels of endogenous sex hormones (10). Familial history predominantly refers to genetic risk factors such as the presence of mutant *BRCA1* or *BRCA2* gene, which can increase the lifetime risk of developing the disease by 45-90% (11). Other genetic variants that predispose to breast cancer have also been identified and include *TP53* (12) and *PTEN* (13), which have been shown to significantly increase breast cancer risk. In addition *CASP8* and *FGFR2*, to name a few, are demonstrated to be commonly defective in breast cancer and having a variant for of these genes increases the risk of breast cancer. Other rarer genetic variants that influence breast cancer prevalence include *CHEK2, ATM, BRIP1* and *PALB2* (12, 14-16). Still, mutations in these genes only account for around 25% of hereditary breast cancers. With lifestyle factors thought to cause around 27% of breast cancers, everyday changes to habits could reduce incidence (17). A diet low in saturated fat and alcohol, maintenance of a healthy weight and regular exercise could all contribute to lower the risks of developing breast cancer. When familial history pre-disposes a person to breast cancer, options such as a mastectomy or prophylactic tamoxifen/raloxifene, two selective estrogen receptor modulators, treatment could benefit the person (18).

1.2.4 Prognosis

Prognosis of a patient with breast cancer depends on how advanced the disease is. At a rudimentary level breast cancers can be categorised into early breast cancer, locally advanced breast cancer and secondary or metastatic breast cancer. Early breast cancers are still confined to the breast whereas locally advanced breast

cancer is characterised by a larger size and presence in lymph nodes of the armpit or in the skin or muscle surrounding the breast. Secondary or metastatic breast cancers are those that have spread to other parts of the body. A more detailed method used by breast pathologists during diagnosis measures the size, grade and stage of the tumour, often referred to as TNM (tumour, node, metastases) breast cancer staging. These three parameters can be utilised to determine prognosis using the Nottingham Histologic Score system (or Nottingham prognostic index) (the Elston-Ellis modification of Scarff-Bloom-Richardson grading system (19). Grade is derived from a composite score, summating attributes of tubule formation, nuclear pleomorphism and mitotic activity. Grade inversely mirrors the degree of differentiation seen and a number is allocated based on this. Grade 1 tumours are well differentiated tumours and carry a better prognosis. Grade 2 tumours are moderately differentiated and cells look less normal, are faster growing and are often varied in size and shape. Grade 3 tumours are poorly differentiated and fast growing and tend to have much worse prognosis. Alone, this system over-simplifies complex underlying taxonomy. Tumours are also defined by their stage. This refers to the extent of spread, invasion and metastasis of the cancer. They are defined as stage 1-4, each with a series of subcategories. Low stage tumours are small and are contained within the breast, mid stage tumours are characterised by a larger size and spread to local lymph nodes whereas high stage tumours are typified by their large size and metastatic spread to nodes and distant sites (4). In order to metastasise, it is thought the tumour cells undergo a process called epithelial-mesenchymal transition (EMT). This happens when cells at the outer edge of the invasive tumour undergo a phenotypic change, usually characterised by loss of the adhesion molecule E-cadherin, which allows them to break free from the primary tumour and enter the lymphatic system or blood vessels (20, 21). Here, the circulating tumour cells (CTC) can travel to distant sites, for example breast tumours commonly metastasise to the bone, liver, lungs and brain, where they

undergo the reverse process, mesenchymal-epithelial transition, to regain epithelial properties and form distant tumours (22). High stage tumours tend to have the worst prognosis.

Prognosis not only depends on morphological features of breast cancer, but also its biology. Tumours can be characterised by their expression of a number of targetable proteins which can be exploited for therapeutic purpose. Expression of ERα, which occurs in around 70% of breast cancers, greatly improves prognosis as these tumours tend to be less aggressive and can be targeted with endocrine therapies (23, 24). In these ER positive breast tumours survival statistics and prognosis are good. A large study on over 111,000 patients with ERα positive tumours graded 1-3 found that 90-95% of patients survived beyond 5 years (25). Expression of the HER2 protein, which occurs in around 15-20% of breast cancer cases may mean the tumour can be targeted with monoclonal antibody (e.g. trastuzumab) therapy targeted to the HER2 protein. This type of breast cancer is the second most aggressive form with poorer prognosis and survival statistics than ERα+ breast cancers and is correlated with more invasive tumours (26). However prognosis does improve if the tumour responds to trastuzumab. Triple negative breast cancers (TNBC) have the worst prognosis as they tend to be highly aggressive invasive metastatic tumours (27-29). Around 10-17% of breast tumours have a triple negative phenotype (30-33). TNBCs have a much higher mortality rate and tumours are often of a higher grade. A study that examined 1600 women with breast cancer, found that triple negative patients have an increased risk of recurrence and death within 5 years of diagnosis (34). By definition they lack ERα, PR and HER2 expression and cannot therefore be treated with targeted therapies, which contributes to their poor prognosis, Instead these tumours are routinely treated with chemotherapy. Prognosis between races can also vary dramatically and affect survival rates. Black women have a 3 fold higher chance of developing

TNBC than white populations (33). Hispanic populations also have an increased incidence of TNBC compared to the white population (35). The knock on effect of this is that the rate of mortality in these populations is also increased.

A lack of molecular targets for TNBCs and incidences of resistance to HER2 and endocrine therapy means there is still huge scope for new and improved treatment options that are drastically needed for the 22% of breast cancer sufferers (11,643 people in 2012 in the UK) (8) who still die from breast cancer.

1.3 Molecular classification of breast cancer

Breast cancer is a multi-faceted heterogeneous disease, and to try to treat the disease with a 'one size fits all' approach would be out of place. Instead molecular

advances have allowed clinicians to tailor treatments based on expression of specific proteins. Breast cancers can be classified into groups depending on their gene expression profile. Originally 5 subgroups were identified and characterised; Luminal A, luminal B HER2, basal and normal (36). Although defined by expression of a number of genes, for clinical use these groups are defined by the expression of ER, PR and HER2. The luminal groups are defined by their expression of estrogen receptor alpha (ERα) and progesterone receptor (PR). HER2 breast cancers overexpress the membrane bound protein epidermal growth factor receptor 2 (HER2), however luminal B tumours express HER2 as well as ER/PR. Basal types are usually negative for ER, PR and HER2. The normal group contained tumours that had variable gene expression and prognosis so could not be classified in any of the other groups. A claudin-low subgroup was later identified (37). This group was characterised by a lack of expression of HER2 and luminal markers such as ER and PR, along with inconsistent expression of basal keratins, and unlike basal tumours, low expression of the proliferation marker ki67. A more recent publication indicates that realistically there are probably at least 10 subcategories of breast cancer (38). Gene expression patterns of just under 1000 tumours were analysed and authors discovered that tumours clustered into 10 groups with distinct outcome. These clusters were based on copy number variations but researchers also included information about single nucleotide polymorphisms (SNPs) and gene expression patterns, and added independent predictive value away from size, grade, and nodal status. Interestingly, one of the subgroups identified was a mix of ERα positive and negative tumours that were grouped due to a strong immune and inflammatory gene signature with lymphocytic infiltration.

In addition, to further add a layer of complexity to the heterogeneity of breast cancer, 6 subgroups of triple negative breast cancer have also been identified by cluster analysis of 587 TNBC tumours. These include 2 basal-like groups (BL1 and

BL2), immunomodulatory (IM), mesenchymal (M), mesenchymal stem-like (MSL) and luminal androgen receptor (LAR) subtype (39).

For the purpose of this study, the cell lines used were grouped based on 5 subtypes; luminal A, luminal B, HER2, basal and claudin-low and Table 1.1 summarises receptor expression and characteristics of these 5 subgroups.

Subgroup	Receptor Expression	Characteristics	Therapy	Survival
Luminal A	ER+, PR+/-, HER2-	Slow growing (low Ki67), less aggressive	Respond to endocrine therapy	Longest overall survival
Luminal B	ER+, PR+/-, HER2+	Fast growing (Ki67 high), less aggressive	Usually respond to endocrine therapy	Increased survival
HER2	ER-, PR-, HER2+	Fast growing (high Ki67), aggressive, but less so than TNBC.	Trastuzumab and chemotherapy responsive	Decreased survival
Basal	ER-, PR-, HER2-	Fast growing (high Ki67), cytokeratin 5/6+, some EGFR+	Often chemotherapy responsive	Shortest overall survival
Claudin-low	ER-, PR-, HER2-	Slow growing (low ki67), aggressive, invasive (loss of E-cadherin), Claudin-3, claudin-4 & 7 low	Intermediate response to chemotherapy	Decreased survival

Table 1.1. Classification of 5 subgroups of breast cancer (36, 37) used in this study Adapted from Holliday et al 2009 (40)

1.4 Mechanisms of estrogen action in the breast

ERα+ breast cancers proliferate in response to the hormone estrogen. There are 3 major naturally occurring estrogens produced in the body; estrone (E1), estradiol (E2) and estriol (E3), and E2 is the most potent form requiring lower doses to produce an effect (41). Estrogen is predominantly synthesised and secreted by the ovaries upon stimulation with follicle-stimulating hormone, which is produced in the pituitary gland. Estrogens can also be secreted by adipose tissue (body fat) (42). Estrogens have numerous functions in the body and a key role is in the development of female sexual characteristics. They also have function in the skin, heart and various biochemical processes such as protein synthesis, control of cholesterol levels and various hormones. Estrogen has important function in the morphological development of the prostate, lung, brain, ovaries, uterus and breast (43).

In the breast estrogen is essential for normal regulation of the growth and differentiation of breast tissue (44). Estrogen signalling is mediated by estrogen receptors. There are two subtypes of estrogen receptor identified; ERα, first identified in rat uterus in 1966 (45) and ERβ, first described in rat prostate and ovary in 1996 (46). On a molecular level, estrogen receptors function as transcription factors when activated either in a ligand dependant, or ligand independent manner. Both regulate a distinct subset of genes often involved in proliferation and apoptosis (47). Figure 1.3 describes the different activation pathways of ERs, which results in target gene transcription. Simplified, ligand dependant activation involves the binding of a ligand to the estrogen receptor, which then translocates to the nucleus and dimerises with other ERs. This receptor dimer then recruits co-regulators that bind to the promoter region of the target gene where transcriptional machinery is recruited and the gene transcribed. There are a number of promoter regions that ERs bind to, which regulate different genes.

Originally it was thought that binding only to estrogen response elements (EREs) in the promoter region of estrogen responsive genes would initiate transcription. It is to these response elements that ERs bind directly. However transcription can also be initiated by the interaction of ER dimers with other transcription complexes which then target other response elements on different subsets of genes. ER interaction with the Fos/Jun complex regulates transcription at AP-1 promoter sites and interaction with SP-1 results in binding to SP-1 motifs in target gene promoters (43, 48, 49). However, estrogen signalling in this way is more complex and target gene regulation depends on the type of ligand or the dimerisation combination that occurs. Agonists and antagonists will initiate different transcriptional responses. For example, agonists may result in a confirmation change in ERs that allows co-activators to be recruited and gene transcription to be initiated. When the antagonist tamoxifen binds, the resultant conformational change initiates recruitment of co-repressors, which prevents transcription (50, 51). This recruitment of co-activators/repressors is mediated through binding to the AF-2 domain on the ER, contained within its ligand binding domain.

The combination of ER dimers that form upon activation also influences response. ERα homodimers result in co-activator recruitment and active transcription (52). ERβ has much lower trans-activation ability on ERE regulated genes. When ERα/ERβ forms a heterodimer, suppression of ERα activated genes is observed due to the recruitment of co-repressors (53). Heterodimerisation is preferential when both receptors are present thus ERβ has a dominant effect over ERα (54). ERα action can also be negated by formation of ERβ homodimers, which regulates genes that oppose the action of ERα regulated genes. ERα or β homodimers regulate the majority of the same genes, involved in processes such as proliferation, cell cycle, apoptosis and cell motility but in a manner thought to give opposing action.

Estrogen signalling is complex, and not yet fully understood. The nature of the ligand, co-expression of ERs, cross talk with other signalling pathways and the added complexity of ERβ isoforms and their role in signalling indicates further scrutiny is vital.

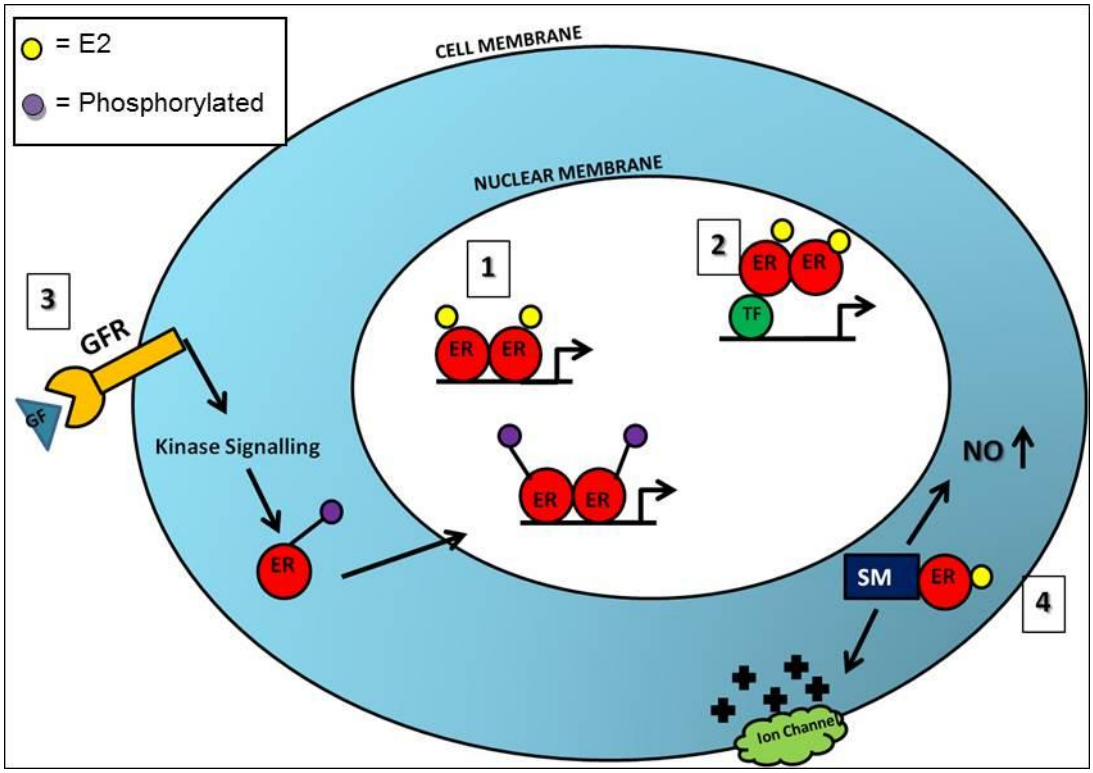

Figure 1.3. Simplified diagrammatic representation of ER activation pathways.
1) Direct activation. The ligand binds the ER, causing the receptor to dimerise and bind directly to the estrogen response element (ERE) on the target gene (55).
2) Indirect activation. The ligand bound ER dimers bind to genes which do not contain EREs, by protein-protein interaction with other transcription factors (41).
3) Ligand-independent regulation occurs through other signalling pathways such as the growth factor signalling. Activated kinases phosphorylate the ER resulting in dimerisation with other ERs followed by binding to EREs in target genes regulating their transcription (41).
4) Non-genomic regulation. Rapid physiological response is caused by the interaction of ligand bound ER with second messengers. Second messengers may affect ion channels or increase nitric oxide levels in the cytoplasm through PI3K/AKT dependent pathway activation
GFR= Growth Factor receptor, GF= Growth Factor, SM= Second Messengers

1.5 Estrogen receptors

As previously mentioned there are 2 types of estrogen receptor ERα and ERβ. Their genes are located on different chromosomes with ESR1 (coding for ERα) found on chromosome 6 at position q25.1 (56) and ESR2 (coding for ERβ) on chromosome 14 at position 14q22-24 (57). They are thus products of independent genes. They share variable homology on regions of their protein. Both ER proteins contain an N-terminal domain, a DNA-binding domain, a hinge region, a ligand-binding domain and a C-terminal domain. The DNA binding domain shares 95% homology with ERα, which explains why the two estrogen receptors interact with the same response elements in target genes. However the ligand binding domain has only 55% homology, and as a consequence ERβ has lower affinity for its ligand (58).

1.5.1 Normal breast

In normal breast ERβ is the principally expressed isoform, while ERα is infrequently expressed in normal breast cells (59). Only around 10% of normal breast epithelia express ERα (60). This is restricted to the epithelial cells of breast and no ERα expression was reported in other breast cell types. ERβ is also present in these epithelial cells and is observed in addition within myoepithelial and some stromal cells (59, 61). ER levels change during the menstrual cycle as estrogen stimulates growth of breast ducts and lobules. Proliferation of breast epithelia is influenced by a fine balance between ERα and ERβ (53). During the first half of the menstrual cycle (day 1-14), ERα expression is observed in 31% of epithelia, whereas no expression of ERα is present during the second half (day 15-27) (62). Knockout mouse models have demonstrated that ERβ does not appear to influence mammary development. Mammary gland structure develops normally and after pregnancy, lactation and mammary gland differentiation also appears normal (63-

65). ERα however is essential for breast development and function. ERα knockout mice have a rudimentary ductal system with no epithelial branching and lobular development, and demonstrate a loss of lactation functionality (66). In normal breast it is important to note that ERs also appear in the stromal component. Both stromal and epithelial ERα is required for full mammary development; it was found that if given E2, stromal ERα was sufficient for complete development. Without any ERα present only a rudimental ductal system develops (67).

1.5.2 Breast cancer

70% of breast cancers are diagnosed as ER positive (ER+), and this refers to the expression of the ERα receptor in the tumour. An ER+ breast cancer occurs when the balance of estrogen receptors in the breast epithelia is disrupted and ERα becomes overexpressed (68). ERα overexpression leads to constitutive activation of estrogenic responsive genes many of which result in cell growth, proliferation and suppression of apoptosis (69, 70). ERα overexpression is often coupled with down-regulation of ERβ (71). Reasons for this respective up and down-regulation and the subsequent oncogenicity are unknown, however given that ERβ is the dominantly expressed ER in normal breast and ERα is rarely expressed (59), loss of ERβ may be as important in tumourigenesis as ERα overexpression.

1.6 ERβ

Five isoforms of ERβ have been identified. Isoforms 1, 2 and 5 are present in the breast tissue. The isoforms are formed by alternative splicing at exon 8. (54). Figure 1.4 depicts the ERβ gene and the resulting 5 protein isoforms. The ERβ isoforms only differ in their C-terminus affecting their ligand binding domains. ERβ1 is the ligand binding isoform. The position of helix 12 in the LBD is important for ligand binding. In ERβ1 it is positioned so when a ligand is bound, co factors can be recruited and transcription activated. In the shorter ERβ2, helix 12 is folded differently and the binding pocket is much smaller so binding is blocked. In ERβ5, the C-terminal is much shorter and no binding pocket is formed due to an absent helix 12 (54). The action of ERβ1 homodimers and heterodimers is described in section 1.4. The ERβ2 and ERβ5 isoforms cannot form homodimers and have little function on their own. They exert their action by heterodimerising with ERα or other ERβ isoforms to repress or enhance their activity (72).

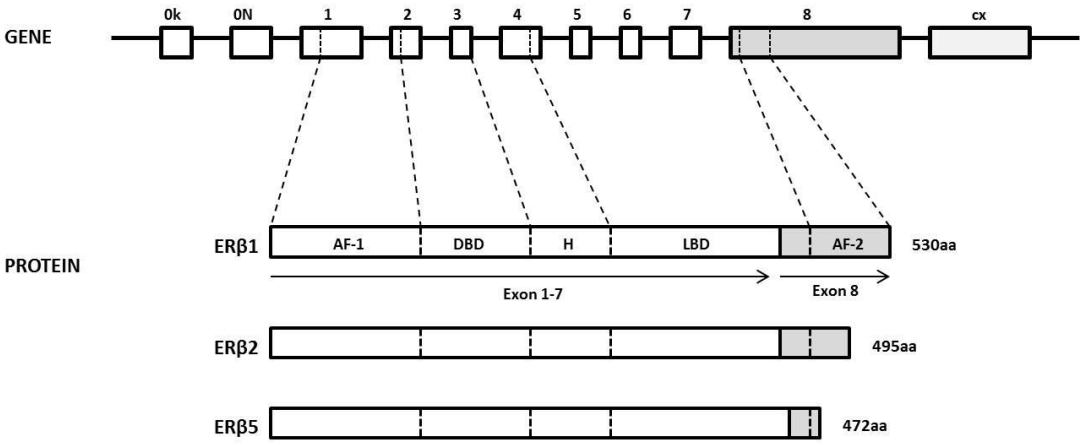

Figure 1.4. Diagram representing the ERβ gene and the different protein isoforms found in breast; a consequence of alternative splicing at the last exon (depicted in grey).
0k and 0N represent 2 untranslated exons at the 5' end of the gene, exons 1-8 are represented by boxes and introns by lines. cx represents a 3' exon present in the long form of ERβ2 protein (ERbcx). Dotted lines link areas of the ERβ gene that code for each protein domain. AF-1: activation function-1 (ligand independent), DBD: DNA binding domain, H: hinge region, LBD: ligand binding domain, AF-2: activation function 2 (ligand dependent). Number of amino acids (aa) that make up each isoform is displayed at the ends of the proteins. Taken from Smart et al (2013) with author's permission (73)

1.6.1 ERβ1 and breast cancer

The most well studied ERβ isoform in breast cancer is ERβ1. ERβ1, the ligand binding isoform of the ERβ receptors, is widely believed to be tumour suppressive and its function protects against breast cancer. Numerous clinical studies have identified ERβ1 expression in all molecular subgroups of breast cancer. A large cohort of 2170 patients revealed that 72% of luminal A, 68% of luminal B, 55% of HER2 and 60% of basal tumours expressed ERβ1 (74). ERβ1 expression is demonstrated to be associated with small tumour size, negative lymph node status and low histological grade (75). Most studies also correlate ERβ1 expression with a better prognosis (76-78) and a loss of ERβ1 in the primary tumour has been associated with poor survival and higher grade more aggressive tumours (79). Investigation of ERβ1 on a functional level has been widely studied, commonly through overexpression of the protein. Common observations in the literature have determined that overexpression of the ERβ1 protein *in-vitro* triggered effects such as reduced proliferation and invasiveness and inhibition of tumour formation (80-83). Suppression of the cell cycle may contribute to reduced proliferation as ERβ1 overexpression has been demonstrated to cause G1 arrest as a result of cyclin D1 down-regulation (84). High levels of ERβ in tumours have been shown to correlate with a better response to tamoxifen and longer overall survival time, giving evidence to support the theory that ERβ may act as a tumour suppressor (85, 86).

There are incidences where ERβ1 has been linked to poor outcome (87, 88). One study correlated ERβ mRNA with poor prognosis, identifying mRNA levels as an independent prognostic marker in breast tumours (89). However, this study not only measured total ERβ (all isoforms) but also mRNA levels, which have been demonstrated to not always correlate with protein levels (90) add ref 88, 90, 173). ERβ1 has also been correlated with Ki67, a proliferation marker, in clinical tumour

samples (91). On a functional level, there are incidences where ERβ overexpression has been associated with increased proliferation. Two studies have associated ERβ1 expression with increased proliferation. Both have investigated ERβ1 overexpression in triple negative breast cancer cell lines. Tonetti et al (2003) (92) demonstrated increased proliferation with ERβ1 overexpression. However this study used a truncated shorter form on ERβ1, which may have influenced the outcome, as this protein lacked a complete AF-1 domain, which may have influenced ligand independent activation. The other study by Hou et al (2004) (93) used MDA-MB-435 cells which have since been identified as a melanoma cell line. The major ERβ1 functional studies in breast cancer cell lines are summarised in Table 1.2.

1.6.2 ERβ2 and breast cancer

Much less is known about ERβ2 in breast cancer than ERβ1. ERβ2 has been demonstrated to be expressed in all histological grade breast tumours (79). Positive expression appears to vary between studies. In a cohort of 713 patients, 83% of tumours expressed nuclear ERβ2 (94). However in another study only 32% of tumours expressed nuclear ERβ2 (60). This may be due to variation in staining techniques, sample preparation and antibodies used, illustrating a need for standardisation. Much of the literature agrees that ERβ2 expression is positively correlated with ERα (75, 94), but it is also regularly observed in ER/PR negative tumours (95). The clinical data pertaining to its prognostic ability is just as conflicting. It has been implicated in both good and poor outcome. ERβ2 expression has been associated with low histological grade and high expression of both mRNA and protein correlated with better disease free and overall survival (75). Its presence has also been associated with better response to endocrine therapy (96). Low ERβ2 expression has been demonstrated to correlate with high Ki67 expression, a marker of proliferation (97) suggesting loss of ERβ2 may result in increased proliferation. However some studies also reported correlation

with poor overall and disease free survival and ERβ2 presence in the primary tumour was associated with metastasis (98). ERβ2 expression has also been demonstrated to increase in invasive tumours compared to adjacent 'normal' tissue possibly implicating ERβ2 in tumourigenesis (99). The varied prognostic ability of ERβ2 may be due by an association with ERα. Generally ERα positive tumours have a better outcome, and as around 70% of tumours express ERα, this may heavily influence ERβ2's prognostic ability, given that ERβ2 has been demonstrated to be correlated with ERα. Another possible source of variation could be due to the location of ERβ2 within the cell. Nuclear ERβ2 is associated with better prognosis and overall survival and cytoplasmic ERβ2 with poor prognosis (94, 100), thus it may be important to distinguish the location of the staining before reporting on prognosis. ERβ2 has also been shown to have a strong prognostic ability in other tissues. In prostate cancer ERβ2 was the predominantly expressed ERβ isoform and was largely expressed in the cytoplasm with only around 10% of cells displaying nuclear ERβ2. In this context nuclear ERβ2 was associated with shorter time to postoperative metastasis and poorer survival (101). In advanced serous ovarian cancer, cytoplasmic ERβ2 expression was associated with significantly worse outcome and chemo-resistance (102). The clinical data regarding opposing prognosis between cytoplasmic and nuclear expression may indicate ERβ2 has a separate function in these compartments.

In terms of its function, little is known about ERβ2 in breast cancer. It is believed to function by forming heterodimers with ERα or ERβ1. Similarly to ERβ1, it has been shown to be a tumour suppressant in ERα+ cells, when dimerised with ERα (95). It preferentially forms a heterodimer with ERα (103). This negative effect has not been observed when heterodimerising with ERβ1. It has been proposed that it enhances the transcriptional ability of ERβ1 (54), therefore potentially co-regulating some of the same sets of genes. In ERα positive MCF-7 cells, ERβ2 overexpression resulted in a reduced S-phase cell population suggesting growth

ability was impaired (104). This may be due to its interaction with ERα. Zhao et al (2007) demonstrated ERβ2 induced proteasome-dependant degradation of ERα, and that its expression reduced the recruitment of ERα to estrogen response elements (95). It appears that in the presence of ERα, ERβ2 may be tumour suppressive. However without ERα co-expression, the function of ERβ2 in breast cancer remains unclear. When overexpressed in the triple negative cell line HS578T, ERβ2 had no effect on growth (105). Studies examining ERβ2 overexpression in breast cancer cell lines are summarised in Table 1.2.

In other tumour types ERβ2 overexpression did affect proliferation. In the prostate cell line PC3, ERβ2 overexpression resulted in increased proliferation and upregulation of the proliferation marker gene *c-Myc* (106). They also observed an upregulation of *RUNX2* mRNA by ERβ2 overexpression, a transcription factor shown to increase the metastatic potential of prostate cancer cells. Other studies in prostate have also demonstrated an ERβ2 mediated increase in invasive potential (101). These studies appear to show a distinct role for ERβ2 dependent on cellular context

1.6.3 ERβ5 and breast cancer

Very few studies have examined ERβ5 function in normal breast and breast cancer. Like ERβ2, it does not bind a ligand or form homodimers, but it thought to exert its effect by heterodimerising with other ERs to alter their function (54). One study, summarised in Table 1.2, found ERβ5 had no effect on growth of breast cancer cell lines but did sensitise cells to apoptosis (107).

There is also a lack of studies examining ERβ5 expression patterns in clinical breast cancer samples. One major study by Shaaban et al (2008) examined ERβ5 expression in a cohort of 757 patent tumour samples.754 of these patient tumours expressed nuclear ERβ5. Nuclear expression was significantly associated with better overall survival only when 65% positive nuclei was used as a cutoff, suggesting only high expression is associated with better outcome. Unlike ERβ2, cytoplasmic ERβ5 expression was rare (94). ERβ5 expression has also been investigated in other tumour types. In advanced serous ovarian cancer ERβ5 expression was nuclear and rarely cytoplasmic (102). However in prostate tumour specimens, ERβ5 was primarily located in the cytoplasm and this correlated with short postoperative metastasis. Ectopic expression of ERβ5 in prostate cancer cells enhanced invasion and migration of cells (101).

ER isoform	Cell line	Receptor classification	Observation	Effect on Tumour	Reference
ERβ1	MCF-7	ERα+	Growth suppression-G2 cell cycle arrest Prevents xenograph tumour formation	Tumour suppressive	Paruthiyil et al 2004 (80)
	MCF-7	ERα+	Cell cycle arrest-CDK1 inhibition by induction of gadd45a and btg2	Tumour suppressive	Paruthiyil et al 2011 (81)
	MCF-7	ERα+	Growth suppression	Tumour suppressive	Murphy et al 2005 (83)
	MCF-7	ERα+	Growth suppression	Tumour suppressive	Hodges-Gallagher 2008 (108)
	MCF-7	ERα+	Reduced S-phase population resulting in growth suppression	Tumour suppressive	Omoto et al 2003 (104)
	MCF-7	ERα+	Growth suppression	Tumour suppressive	Treeck et al 2007 (109)
	T47D	ERα+	Decreased tumour size in xenographs	Tumour suppressive	Horimoto et al 2011 (110)
	T47D	ERα+	Growth suppression	Tumour suppressive	Strom et al 2004 (82)
	SKBR3	HER2	Growth suppression	Tumour suppressive	Treeck et al 2007 (109)
	HS578T	TN	E2 stimulated growth suppression, decreased S-phase population	Tumour suppressive	Secreto 2007 (105)
	HS578T	TN	E2 stimulated growth suppression	Tumour suppressive	Shanle et al 2011 (111)

Table 1.2. ERβ overexpression cell line models in breast cancer and resultant phenotypic change. TN: triple negative

ER isoform	Cell line	Receptor classification	Observation	Effect on Tumour	Reference
ERβ1	MDA-MB-231	TN	Ligand independent growth inhibition	Tumour suppressive	Lazennec et al 2001 (112)
	MDA-MB-231	TN	Increased proliferation	Tumourigenic	Tonetti et al 2003 (92)
	MDA-MB-453	TN	Increased proliferation	Tumourigenic	Hou et al 2004 (93)
ERβ2	MCF-7	ERα+	Induced ERα degradation and inhibited recruitment to ERE-Reduced growth	Tumour suppressive	Zhao et al 2007 (95)
	MCF-7	ERα+	Decreased S-phase population	Tumour suppressive	Omoto et al 2003 (104)
	HS578T	TN	No effect on growth	None	Secreto et al 2007 (105)
ERβ5	MCF-7 MDA-MB-231	ERα+ & TN	No effect on growth, sensitised cells to apoptosis	Unknown	Lee et al 2013 (107)

Table 1.2 continued. ERβ overexpression cell line models in breast cancer and resultant phenotypic change. TN: triple negative

1.7 Sub-cellular localisation of ERβ

As a member of the nuclear receptor super-family, most studies have generally focused on nuclear expression of ERβ. However reports of extra-nuclear expression have been published, suggesting sub-cellular location of ERs may be important for function. These studies show ERβ expression in the nucleus, cytoplasm and mitochondria (113, 114). The location of ERβ within the cell has been shown to affect prognosis. Nuclear expression of ERβ1 and ERβ2 is associated with good prognosis and cytoplasmic with a poor prognosis. This may infer that ERβ has an alternate function in different compartments of the cell.

1.7.1 Nuclear ERβ

Nuclear ERβ it widely recognised to act as a transcription factor when located in the nucleus of a cell and its mechanism of action is described in section 1.4.
Nuclear expression of ERβ has been associated with better overall prognosis in patients with breast cancer (81-83, 94, 96). It is thought ERβ1 regulates genes in 2 ways; either as homodimers or as a heterodimers by altering the gene regulation of ERα. The other ERβ isoforms can enhance ERβ1 gene regulation by forming heterodimers with ERβ1. It has been shown, that ERβ regulates genes in an opposing manner to ERα i.e. ERβ1 down-regulates genes that are upregulated by ERα, and vice versa. For example genes that are frequently downregulated include those that promote the cell cycle and are anti-apoptotic. For this reason ERβ has been established as tumour suppressive in ERα+ tumours. Some examples of these genes are listed in table 1.3.
There have been a small number of major genome wide studies investigating ERβ gene regulation using ChIP-Seq (47) and RNA-Seq technology (115). Ch-IP Seq identified ERβ binding sites in MCF-7 cells producing a comprehensive list of genes that are regulated directly by ERβ. This includes genes regulated by the ERβ1

homodimer or the ERβ1/ERα heterodimers. It does not however give any information as to whether ERβ1 heterodimerised with other ERβ isoforms. The study identified that ERβ regulated gene expression through binding promoters including AP-1, ERE, SP-1 and E2F sites. They identified 9702 binding sites for ERβ1 and 6024 binding sites for ERα. 4506 of these overlapped and were binding sites for both ERα and ERβ1. The genes that were identified as being regulated by ERβ1 included transcription factors and key proteins involved in cell cycle regulation, cell survival and differentiation pathways. Examples of these genes include *CDK6*, *IGFBP-4, MYC, TGFβ-2*, and *TGFβI*. The functional effect of ERβ1 in MCF-7 cells was also observed, and it was found that proliferation was inhibited by the presence of this receptor, suggesting regulation of these genes by ERβ1 leads to tumour suppression rather than a mitogenic effect as observed with ERα activation (47).

One limitation of this study is that it was performed in MCF-7 cells, which are positive for ERα expression, and with E2 stimulation only. It is suggested that under different ligand stimulation, gene targets and how they are regulated may be changed. There is a wealth of knowledge available pertaining to ERβ1 expression in ERα+ tumours but much less investigating its function in ERα- tumours.

Another recent genome wide study aimed to investigate ERβ1 gene regulation in ERα negative tumours (115). A similar technique, RNA-Seq (which measures the transcripts rather than location of transcription factor binding), was used. ERβ1 was overexpressed in the MDA-MB-468 TNBC cell line and gene transcript levels measured. Ligand-dependent and independent target genes were identified. Altogether 930 genes were differentially regulated between wt-MDA-MB-468 cells and ERβ1 overexpressing MDA-MB-468 cells. As in ERα+ cells, these genes were involved in the regulation of growth and proliferation, survival, cell death and motility. Gene targets identified in this study also correlated with ERβ1 in a cohort of clinical samples, further supporting the role that ERβ1 has in TNBC. The functional

effect of ERβ1 expression in these cell lines was also investigated. Inhibition of tumour growth due to G1 cell cycle arrest, inhibition of tumour growth and formation in xenographs and tumour regression after stimulation with E2 were all reported. There are very few studies that have investigated gene regulation by other ERβ isoforms. A microarray study investigating a subset of genes identified that ERβ2 regulated similar genes to those of ERβ1 in MCF-7 cells. These included *IGFBP4* (involved in cell growth control) and cathepsin D (linked to poor prognosis in breast cancer), which were both downregulated (104).

The consensus regarding the effect of ERβ1 on gene expression in breast cancer seems to agree with its tumour suppressive status, with genes that suppress the cell cycle and promote apoptosis commonly identified. Gene regulation by ERβ2 and ERβ5 still needs investigation to determine their function in breast cancer.

Target Genes	Function	Regulation by ERβ	Molecular Effect	Cellular Effect	Reference
GADD45A, BTG2	Inhibit CDK1 cell cycle regulator	upregulation	G2 cell cycle arrest	Proliferation inhibition	Paruthiyil et al 2011 (81)
c-myc, Cyclin D1, Cyclin A	Stimulate cell cycle progression	downregulation	Cell cycle arrest	Proliferation inhibition	Paruthiyil et al 2004 (80)
P21, p27	Inhibit cell cycle progression	upregulation	Cell cycle arrest	Proliferation inhibition	Paruthiyil et al 2004 (80) Lazennec et al 2001 (112)
Integrin α1 & β1	cell surface receptor involved in adhesion and migration	upregulation	Enhanced adhesion to extracellular matrix proteins	Decreased migration	Lindberg et al 2011 (116)
Cyclin D1	Regulates cell cycle progression at G1 checkpoint	downregulation	Cell cycle arrest	Proliferation inhibition	Strom et al 2004 (82)
TGF-β genes	Growth repressor when stimulated with E2	downregulation	Cell cycle arrest	Proliferation inhibition	Chang et al 2006 (117)
FOXM1	regulates cell cycle progression	downregulation	Cell cycle arrest	Proliferation inhibition	Chang et al 2006 (117)
E2F1	regulates cell cycle progression	downregulation	Cell cycle arrest	Proliferation inhibition	Chang et al 2006 (117)
BCL-2	Anti-apoptotic	downregulation	Activation of apoptosis	Increased cell death	Ruddy et al 2014 (118)

Table 1.3. Summary of nuclear action of ERβ isoforms on gene regulation function
(ChIP-Seq and RNA-Seq gene expression data (47, 115) not included, but described in section 1.7.1)

1.7.2 Cytoplasmic and mitochondrial ERβ expression

It has been shown that prognosis varies between patients who exhibit cytoplasmic vs. nuclear ERα expression in breast cancer. One group were able to demonstrate ERβ1 nuclear expression correlated with a favourable response to endocrine therapy and cytoplasmic ERβ2 expression correlated with poor response to therapy (100). This was also demonstrated by Shaaban et al, who correlated ERβ2 expression in the cytoplasm, either alone or in combination with nuclear expression, with a significantly poorer overall survival rate. Those with no nuclear ERβ2 at all had a much worse survival rate (119). The prognostic differences with ERβ location was also demonstrated in other cancers. Cytoplasmic expression of ERβ predicts poor clinical outcome in advanced serous ovarian cancer (102).

The differential prognostic significance of cytoplasmic or nuclear ERβ suggests it may have an alternative function in each compartment. It has been well reported that ERβ also functions in the mitochondria. Estrogen is believed to have a role in mitochondria possibly functioning in E2 mediated regulation of the mitochondrial respiratory chain (120). Numerous studies have produced evidence for the localization of ERβ in mitochondria (121) (122). Upon examination using immunogold electron microscopy it was found to be in the mitochondrial matrix. With E2 stimulation the levels of ERβ in the mitochondria increased. A later study discovered ERβ shifts from the nucleus to the mitochondria during tumourigenesis. Grober et al (47) discovered an ERβ binding site in the mtDNA, but no ERα sites when they analyses ERβ genome binding in MCF-7 cells by ChIP-Seq. ERβ was demonstrated to bind to the D-loop region on the mtDNA genome when incubated with E2 or DPN, which is the region that controls transcription of mitochondrially encoded genes. When the mitochondrial fraction of these activated cells was separated by fractionation, western blotting confirmed the presence of the ERβ

protein (47). Due to the presence of mitochondrial ERβ in normal tissues, all with high energy demands, it could be speculated that ERβ may be involved in regulation of energy production by interacting with the mitochondrial respiratory chain process. In agreement with this theory, the normal breast epithelial cell line MCF-10F demonstrated a significant increase in expression of CO1, CO2 and ND1, three mitochondrial DNA (mtDNA) encoded genes, upon DPN (ERβ selective agonist) incubation (122). This upregulation of mtDNA encoded genes was also seen in other tissues. In the cardiac tissue of rats following trauma, mitochondrial ERβ increased along with an increase in mtDNA encoded mitochondrial respiratory complex IV genes upon DPN administration (123).

There is some evidence that ERβ may be an inhibitor of oxidative phosphorylation, which is contradictory to the examples above. However these papers describe inhibition due to regulation of nuclear encoded mitochondrial proteins. This fits with the observation that nuclear ERβ is a good prognostically as nuclear ERβ is correlated with a decrease in cellular energy. For example in malignant mesothelioma cells ERβ was correlated with low levels of succinate dehydrogenase B (SDHB). This is a protein involved in oxidative phosphorylation as part of the respiratory chain complex II. Activation of ERβ resulted in downregulation of complex II and IV and reduced ATP production and cellular energy (124).
In cases where ERβ is within the mitochondria, the consensus is that mitochondrial ERβ increases cellular energy production possibly by upregulation of components of the mitochondrial respiratory chain. However it is not yet clear whether this regulation is by ERβ alone, or mediated by nuclear regulated genes that are also involved in mtDNA regulation. The increase in energy production seen in some of these studies may be to fuel increased growth and proliferation of the cell, or to fuel invasion and migration processes, characteristics of a more aggressive cancer.

This may clarify why cytoplasmic ERβ has been commonly associated with a poorer prognosis.

Mitochondrial ERβ has also been implicated in tamoxifen resistance. In tamoxifen resistant MCF-7 cells, tamoxifen acts as an agonist rather than an antagonist and thus fails to increase reactive oxygen species to cause apoptosis. The agonistic activity of tamoxifen on mitochondrial ERβ promotes cell survival (125). It is unclear why tamoxifen acts as an agonist in this setting.

1.7.3 Membrane bound ERβ

It is thought that ERβ located in the cell membrane of some breast cancer cells may contribute to ERβ signaling, activating non-genomic pathways to exert its regulatory effects (55). Membrane ERβ activation is a rapid (within seconds) process that results in activation/repression of downstream kinase signaling such as mitogen-activated protein kinase (MAPK) pathways. Membranous ERs interact with Gα and Gβγ proteins resulting in calcium and cAMP generation, and the activation of kinases such as Src, PI3K, ERK and AKT (126). These pathways are associated with breast cancer cell function. At present the role of membrane ERα is well established. ERα has been shown to interact with IGF, resulting in MAPK activation (127), and with EGFR, which activated G proteins and increased ERK and PI3K/AKT signaling (128). These pathways all result in cellular proliferation. ERβ on the other hand is much less well studied at the cell membrane but it has been reported that E2 bound to ERβ reduced ERK activity in porcine smooth muscle cells (129). The ERβ-E2 complex has also been demonstrated to activate the p38 MAPK pathway which is known to induce apoptosis and therefore mediating its anti-proliferative properties (130). Membrane ERα activation results in proliferative pathway activation (131).

1.8 Breast cancer treatment

Breast cancer is one of the most treatable cancers thanks to identification of molecular therapeutic targets. Overall around 78% of patients diagnosed with breast cancer are expected to survive 10 years (8). Treatment is defined by tumour gene expression profiles, and expression of targetable receptors can drastically improve patient prognosis.

1.8.1 Current treatments

The inherent heterogeneity of breast cancer means treatment can be complex and often patients do not respond to therapy as expected. Currently expression of ERα or HER2 in breast cancers will determine treatment options. Breast cancers that express ERα are often termed ER positive (ER+). These are targetable with hormone therapies such as tamoxifen or aromatase inhibitors. Tamoxifen acts as antagonist to ERα, inhibiting estrogen binding to this receptor and preventing proliferative activity. As estrogen 'feeds' these ERα+ tumours to grow this is an effective treatment. Aromatase inhibitors prevent the production of estrogen by blocking the enzyme aromatase from converting androgen to estrogen. Luteinising hormone therapy can also be given to pre-menopausal women to block signalling from the pituitary gland to the ovaries thus preventing estrogen and progesterone production. Expression of HER2 in a breast tumour, also allows for targeted treatment in the form of a HER2 specific monoclonal antibody therapy. Commonly this is with the drug trastuzumab (Herceptin). This drug works in a number of ways. Trastuzumab blocks the HER2 receptor from dimerising, which is a requirement for activation of the downstream signalling of PI3K/AKT pathway. It also up-regulates PTEN suppressing PI3K/AKT signalling, and restores p27 levels, resulting in cell cycle arrest. All three of these actions result in inhibition of cell cycling and proliferation. Trastuzumab has also been demonstrated to trigger HER2

internalisation and subsequent degradation by ubiquitination. As trastuzumab is an antibody, when it binds to HER2 it attracts natural killer immune cells thus marking the tumour cells for degradation (132). It is suggested that this is the reason why tumours with high HER2 expression respond better to trastuzumab than low expressers.

Triple negative breast cancers are often more aggressive partly due to their lack of expression of targetable receptors. Chemotherapy is often given in combination for the best outcome and includes drugs such as cyclophosphamide, fluorouracil and epirubucin. The drugs are cytotoxic and kill the cancer cells as well as any other dividing cells within the body. It is not a targeted treatment such as tamoxifen or trastuzumab. The effectiveness of chemotherapy depends on how advanced the tumour is with lower grade and stage tumours having the best prognosis.

Radiotherapy is also used as a treatment for breast cancer, and is a common treatment option post-surgery. It reduces the risk of local recurrence and increases survival rates.

1.9 ERβ; is there potential as a therapeutic target?

ERβ has been widely shown to be anti-proliferative and pro-apoptotic in breast cancer, and is believed to have a protective role in normal breast tissue. It has also been suggested it may be a strong prognostic and therapeutic response predictor, especially ERβ2. This coupled with the fact it is often expressed in all molecular subgroups means ERβ may serve as an attractive target for therapy.

Tamoxifen therapy has been suggested for ERα negative tumours that express ERβ. One study demonstrated that in TNBC patients treated with adjuvant tamoxifen therapy, ERβ1 positivity was associated with increased DFS and OS (86). This finding was supported when another group found that high ERβ1 expression correlated with tamoxifen response in ERα negative patients. These high expressers had better OS and relapse-free survival rates (133). Tamoxifen has also been proposed as a prophylaxis for BRCA1/2 mutation carriers, with a 50% reduction in contra-lateral breast cancer development seen if given tamoxifen treatment upon initial diagnosis (134). This data indicates tamoxifen treatment in ERα negative patients may be beneficial. This is being investigated in the ANZ 1001 SORBET clinical trial.

As ERβ biology is not yet fully understood there are a number of factors which may need consideration. Firstly it is unclear as to whether ERβ should be agonised or antagonised. Tamoxifen is traditionally an ER antagonist, however as ERβ is believed to be tumour suppressive, tamoxifen may be acting agonistically. ERβ activation not only suppresses ERα protein action but has also been shown to down-regulate ERα mRNA (135) so ERβ agonism may be effective in enhancing endocrine treatments. It has been documented that E2 stimulation of TNBC cell lines resulted in an upregulation of cell cycle suppressive genes. This was coupled with a decrease in cellular proliferation (112). Even without the presence of ERα in the tumour, E2 may also be an effective therapeutic strategy. Other ERβ agonists have also been developed that may prove effective. 2,3-bis(4-hydroxy-phenyl)-

propionitrile (DPN), genistein, MF101, ERB-041 and WAY-202196 are just some ERβ agonists that have been developed. Drugs such as genistein have multiple functions. It is a potent ERβ agonist but can also agonise ERα. Its effectiveness may depend on the co-expression of ERα and ERβ. When both receptors are present low doses actually induce proliferation and at higher doses anti-proliferation and increased apoptosis is observed (136-139) . In other cancer types without the presence of ERα e.g. colon (140), pancreatic (141) and bladder cancer (142), tumour growth and metastasis is inhibited by genistein. This drug may prove more effective in ERα negative environments. Genistein is also a tyrosine kinase inhibitor and suppresses kinase signalling. Resistance to therapies is often seen due to the cross talk between signalling pathways (143, 144). When one pathway is suppressed in the cell, others may become activated. Genistein may both suppress ER and kinase proliferative signalling, overcoming this problem of resistance. Given its probable tumour suppressive nature, up-regulating or reintroducing ERβ in breast cancers may be an effective therapeutic strategy to regaining the sensitive balance between ERα and ERβ as seen in normal breast. A study investigating the androgen receptor (AR) in breast cancer found an androgen response element (ARE) in the promoter of the ERβ gene. When AR was activated with a synthetic ligand, ERβ mRNA and protein was increased (145). Using a combination of AR and ERβ agonists may be a viable way of restoring ERβ and normal ER signalling within the cell.

There is growing knowledge surrounding ERβ, and the majority refers to ERβ1. The importance of considering each ERβ isoform separately is becoming apparent as it is emerging that they have very distinct functions. ERβ2 expression is dominant in normal breast tissue over other ERβ isoforms suggesting this isoform is important in the maintenance of a normal breast environment. Identified as a strong prognostic marker in breast cancer, ERβ2 certainly warrants further study

especially given the contradictions in the literature regarding whether this protein tumour suppressive or oncogenic. This study will begin to address these discrepancies by exploring ERβ2 expression and function in breast cancer.

Hypothesis and Aims

ERβ2 has distinct function in breast cancer cells depending upon co-expression with ERα or its location within the cell.

Specific aims of this project were to:

- explore the expression patterns of ERβ2 in subcellular compartments in breast cancer cell lines
- determine the presence of ERβ2 in the mitochondria and establish a role in mtDNA gene regulation
- investigate and characterise the dynamic nature of ERβ2 nuclear speckles in breast cancer cells
- explore the physiological effect of ERβ2 overexpression on breast cancer cell lines including determination of its effects on proliferation, migration and target gene regulation

2.0 Chapter 2: Methods

This chapter outlines the common methods used throughout the project. More specific methods relating to a particular chapter can be found in their respective chapter.

2.1 Short Tandem Repeat (STR) testing

All cell lines were STR profiled annually to assess their authenticity. This was performed in-house by Dr Claire Taylor at the CRUK genomics facility, University of Leeds. This was performed using Powerplex-16 reagents (Promega) where PCR amplification of sixteen loci is performed; Penta E, D18S51, D21S11, TH01, D3S1358, FGA, TPOX, D8S1179, vWA, Amelogenin, Penta D, CSF1PO, D16S539, D7S820, D13S317 and D5S818. Data was analysed using GeneMapperR *ID* software. Profiles of each cell line were compared to the reference STR profiles provided on the ATCC (American Type Culture Collection) website. Cells that were not authentic were discarded along with all stocks and replacements were ordered from the ATCC.

2.2 Cell Culture

Eleven breast cancer cell lines were used in this study, which represent the major molecular subtypes of breast cancer (36). Details of these cell lines, their molecular profile, growth media and passage specifics are summarised in Table 2.1. Cells were maintained in humidified incubators at 37°C with 5% CO_2, in T75 flasks (Corning) with vented caps. Prior to use, the foetal calf serum used to supplement the culture media was heat inactivated at 56^{o}C for 30 minutes. Cells were tested every 6 months for mycoplasma infection in-house by Sarah Perry (Laboratory Manager, University of Leeds) using the MycoAlert^{TM} Mycoplasma Detection Kit (Lonza). Cell lines were consistently negative for mycoplasma infection.

2.2.1 Cell Passage

Cells were washed with 1x Dulbecco's phosphate-buffered saline (DPBS, Gibco). BT-20 and LGI1T cells required incubation with 0.1% EDTA in 1x DPBS for 3-5 minutes at 37°C after the initial wash. Cells were incubated for approximately 1-3 minutes in 2ml of 1x Trypsin-EDTA (diluted from 10x stock of 0.5% trypsin EDTA, in DPBS, Gibco). Cells were resuspended in their appropriate media and diluted for passage (see weekly passage, Table 2.1). LGI1T cells were resuspended in RPMI 1640 media containing 5% FCS to deactivate the trypsin and then centrifuged for 3 minutes at 290 x g, after which the cell pellet was resuspended in keratinocyte growth media and diluted in the appropriate amount of media for passage.

2.2.2 Cell freezing

At least 10 vials of each cell line were frozen at the beginning of the project to allow return to a standard passage number if and when required. All cells were frozen in 90% HI FCS (Biosera), and 10% sterile filtered DMSO (Sigma). Cells at 60-70% confluency were washed in 1x DPBS and trypsinised as previously described in 2.2.1. Cells were resuspended in 10ml of media containing FCS, and centrifuged at 290 x g for 3 minutes to pellet. The cell pellet was resuspended in 4ml of freeze media and 1ml of suspension was aliquoted into each cryovial (Nuncbrand). These vials were transferred to an isopropanol filled container (Mr. Frosty™ freezer container; Nalgene*)* to ensure optimal cooling rate, and stored at -80 overnight. The following day frozen stocks were transferred to liquid nitrogen for long term storage until required.

2.2.3 Thawing cells

Cells in culture were discarded at a maximum of 20 passages after their first use and replaced with a new stock vial. When cell stocks were thawed from liquid nitrogen they were cultured for at least 1 passage before use in experiments. Frozen vials were thawed quickly by placing in a water bath at 37 C for 30 seconds. Cells were mixed with 9ml of their respective media and centrifuged at 290 x g for 3 minutes to pellet. The media supernatant was removed and the cell pellet resuspended in 10ml of its respective media. The cell suspension was placed in a T75 flask and placed in an incubator. The following day cells were washed and media replaced to remove cell debris.

Cell Line	Classification	Immuno-profile	Growth Medium	Weekly passage
MCF-7	Luminal A	ER+, PR+, HER2-	RPMI 1640 + 5% FCS	1:20
T47D	Luminal A	ER+, PR+, HER2-	RPMI 1640 + 5% FCS	1:8
BT-474	Luminal B	ER+, PR+, HER-2+	DMEM (glutamax)+ 10% FCS	1:8
MDA-MB-231	Claudin-Low	ER-, PR-, HER2-	RPMI 1640 + 5% FCS	1:12
MDA-MB-436	Claudin-Low	ER-, PR-, HER2-	RPMI 1640 + 10% FCS	1:8
MDA-MB-468	Basal	ER-, PR-, HER2-	RPMI 1640 + 5% FCS	1:12
LGI1T	Basal	ER-, PR-, HER2-	Keratinocyte + BPE + EGF	1:12
BT-20	Basal	ER-, PR-, HER2-	RPMI 1640 + 10% FCS	1:8
SK-BR-3	HER2	ER-, PR-, HER-2+	DMEM (glutamax)+ 10% FCS	1:6

Table 2.1. Details of the 9 cell lines used in this study.
Classification adapted from (146-150). Culture medium used in line with Breast Group SOPs. Culture media supplied by Gibco and FCS by Biosera. BPE (bovine pituitary extract) and EGF (epidermal growth factor) supplied by Gibco.

2.3 Measurement of cell proliferation

Proliferation of cells was analysed by performing growth curves. Growth curves were performed on MCF-7 wild-type cells and transduced vector control MCF-7, T47D, MDA-MB-231 and MDA-MB-468 cells as well as their ERβ2 overexpressing counterparts. The number of cells seeded per well were as follows: MCF-7; 40,000 cells/ml, T47D; 80,000 cells/ml, MDA-MB-231; 40,000 cells/ml, MDA-MB-468; 50,000 cells/ml. Cells were washed and trypsinised then resuspended in media up to 10ml. 1ml aliquots were placed onto the Vi-Cell (Beckman Coulter), an automated cell counter, which adds trypan blue to the aliquot and counts based on an exclusion method, where stained dead cells are not counted and unstained live cells are. The Vi-Cell performed counts on 100 images per sample, as cells were pumped through the flow cell and imaged at 6.75 x magnifications. Cells were diluted to their respective seeing densities and plated into 6 well plates using the following calculation; c1v1=c2v2, which translates to:

$$v1 = \frac{c2v2}{c1}$$

Where:

v1= volume of undiluted cell suspension required (ml)

c1= undiluted cell concentration (cells/ml)

c2= final concentration of cells required (cells/ml)

v2= final volume of diluted solution, after addition of diluted cells

The total volume of media (v2) minus the amount of cell suspension required (v1) was added to the appropriate volume of media to make up to the total volume required (v2). Counts were performed in duplicate at 48, 72, 96 and 120 hours for each cell line, so a total of 8 wells of each cell line were plated in 6 well plates. 1ml of fresh media was added to each well and plates were placed in a humidified

incubator (37^{o}C @ 5% CO_2). Cells counts using the Vi-Cell (described above) were performed at each time point and total number of cells was plotted on growth curves.

2.4 Migration assay

Collagen 1 (Corning) was diluted to 50µg/ml in 0.02M acetic acid on ice, pipette mixed and 100µl was added to each well of a 96-well ImageLock tissue culture plate (Essen BioScience). This was left to set for 1 hour in a humidified cell culture incubator (37^{o}C with 5% CO_2). The following day the cells were rinsed with DPBS 3 times to remove excess acid. MCF-7, T47D, MDA-MB-231 and MDA-MB-468 ERβ2 overexpressing cells and their empty vector counterparts were counted as described in section 2.3 and 20,000 cells were transferred to each well. Three wells were used per cell line to represent technical replicates. Cells were left to adhere overnight. The following day using the WoundMaker™ (Essen BioScience) according to the manufacturer's procedure, wounds were created in each well. Media was then aspirated and wells gently washed twice to remove cell debris. 100µl of the appropriate media was then added to the wells and the plate was placed into the IncuCyte™ (Essen BioScience) and allowed it to equilibrate for 5 minutes. Repeat scanning was scheduled for every 30 minutes for 72 hours, whereby one image per well was taken, using the IncuCyte™ software, and the scan type set to scratch wound. Data was analysed by the software and relative wound density was calculated for each scanned image, a metric used to measure the density of the wound region relative to the density of the cell region (%).

2.5 Immunofluorescence

All incubation steps were performed at room temperature. Details of antibodies used, their working concentrations and diluents used are detailed in Table 2.2. Cells were visualised on a Nikon A1R confocal microscope at 60x magnification and images acquired using the accompanying NIS elements software (v4.2). Images were acquired within 2 weeks of staining. Slides were stored in the dark at 4^{o}C until image acquisition. A negative slide where the primary antibody was omitted was included for every immunofluorescent experiment. These demonstrated staining for DAPI but did not display any signal for the protein in question. Negative controls were viewed prior to the samples. Images captured and presented from immunofluorescent experiments were representative of the whole slide. Biological replicates were performed for every experiment and results shown are a typical subset.

2.5.1 Cell seeding and fixing

Round coverslips (Scientific Laboratory Supplies) were sterilised with 70% ethanol made up in dH_2O, and placed into the wells of a sterile 12 well plate (corning). Cells were plated onto the coverslips at around 40% confluency. Cells were allowed to fully adhere for 48 hours. Cells were washed twice in 1x DPBS then incubated for 15 minutes with 4% paraformaldehyde solution (Sigma) made up in 1x PBS (Sigma). Cells were then gently washed twice with 1x TBS, and then incubated with 0.2% Triton X-100 (Sigma) solution made up in 1x TBS for 10 minutes to permeabilise the cells. Cells were washed gently in 1x TBS twice, and stored until use.

2.5.2 Avidin/Biotin immunofluorescence

This more sensitive immunofluorescence method was used when staining with ERα, ERβ1 or ERβ2 antibodies, as ERβ1 and ERβ2 protein were present at low levels in breast cancer cell lines. ERα was also stained in this way for consistency. All washes were performed using 1x TBS (Sigma). Fixed and permeabilised cells were washed once before incubation in an egg white block (1 egg white to 100ml dH_20) for 20 minutes. Cells were washed again then a 0.01% biotin block solution (Sigma) made up in 1x TBS was applied to the cells and incubated for 15 minutes. The biotin block was removed; coverslips were washed twice and inverted into 100µl of diluted primary antibody dotted onto parafilm and incubated for 1 hour. Coverslips were placed back into wells and gently but stringently washed (3X 5 minute washes). 100µl of biotinylated secondary antibody was dotted onto fresh parafilm and coverslips inverted onto the antibody for 1 hour. Coverslips were washed (3X 5 minute washes) and the avidin conjugated alexa fluor 488 was diluted as per Table 2.2. 100µl was dotted onto fresh parafilm, and coverslips inverted onto the antibody and incubated for 1 hour in the dark. Coverslips were washed (3X 5 minute washes) and mounted onto labelled slides cell side down using Vectashield Mounting Media, hard set containing DAPI. Slides were then stored at 4°C in the dark until image capture.

2.5.3 Dual colocalisation immunofluorescence

Dual staining immunofluorescence was performed using known nuclear speckled protein antibodies; SC-35 (nuclear speckle antibody), PML (pro) and coilin (marker of cajal bodies), and the ERβ2 antibody. Cells were plated as described in 2.5.1 and ERβ2 antibody staining was performed as per section 2.5.2 but coverslips were not mounted onto slides. Cells were then stained with either SC-35, PML or coilin antibodies as follows. Coverslips were blocked with 1x casein (made up in TBS) for

1 hour then incubated with one of the following primary antibodies; SC-35, PML or coilin. Antibodies were diluted as per Table 2.2 and coverslips were incubated with 100 µl for 1 hour in the dark. Coverslips were washed (3X 5 minute washes) then incubated for 1 hour in the dark with the appropriate texas red secondary depending on antibody species. Cells were washed (3X 5 minute washes) then mounted onto glass slides using Vectashield mounting media containing DAPI and left to dry in the dark at 4^{o}C overnight. Two control slides were obtained, omitting both primary antibodies individually (ERβ2 and either SC-35, PML or coilin). In the case of SC-35, due to both primary antibodies being mouse, an additional control omitting just SC-35 was obtained to check there was no unbound ERβ2, which had the potential to bind the texas red secondary.

2.5.4 Mitochondrial staining for ERβ2 colocalisation investigation

Cells were seeded at ~40% confluency in 12 well plates onto sterilised glass coverslips and left for 48 hours. Mitotracker dye (Invitrogen) was diluted to 500nM in media and incubated with the cells for 1 hour in humidified incubators at 37°C with 5% CO_2 to allow mitochondrial labelling. Cells were fixed with 4% PFA for 15 minutes at room temperature, and then permeabilised with 0.2% Triton x-100 for 10 minutes both in the dark and processed for ERβ2 immunofluorescence as described in 2.5.2.

Negative controls were also carried out to enable calculation of colocalisation that occurs by chance using cyclophilin A antibody instead of ERβ2. Cyclophilin A staining was performed on MCF-7 and MDA-MB-231 cells.

Antibody details	Species	Assay	Working concentration	Diluent
ERβ2 (57/3) (AbD serotec, #MCA2279)	Mouse	IF	1:50	1x casein
ERβ1 (PPG10/5) (AbD serotec, #MCA1974GA)	Mouse	IF	1:50	1x casein
ERβ-total (14C8) (Abcam, #ab288)	Mouse	WB	1:50	5% milk
ERα (1D5) (Dako, #M3643)	Mouse	IF	1:200	1x casein
SC-35 (Sigma, #S4045)	Rabbit	IF	1:1000	1x casein
PML (Abcam, #ab53773)	Rabbit	IF	1:50	1x casein
Coilin (SantaCruz, #sc-32860)	Mouse	IF	1:50	1x casein
Biotinylated IgG (Dako, #E0354)	Goat	IF	1:600	1x casein
Alexa fluor 488-avidin conjugated (ThermoFisher, #A-21370)	n/a	IF	1/1000	1x casein
Texas red (ThermoFisher, #T-6390)	Goat anti-	IF	1/1000	1x casein
Texas red (ThermoFisher #T-2767)	Goat anti-	IF	1/1000	1x casein
Flag M2 (Sigma, #F1804)	Mouse	WB	1:500-1:1000*	5% milk
Tata bp (Proteintech, #22006-1-AP)	Rabbit	WB	1:400	5% milk
Cytochrome C (Proteintech, #10993-1-AP)	Rabbit	WB	1:200	5% milk
β-actin (Sigma, #A5441)	Mouse	WB	1:10000	5% milk
Cyclophilin A (Abcam, #ab41684)	Rabbit	WB	1:10000	5% milk
		IF	1:1000	1x casein
HRP-conjugated (SantaCruz, #sc-2005)	Goat anti mouse	WB	1:10,000	5% milk
HRP-conjugated (SantaCruz, #sc-2030)	Goat anti rabbit	WB	1:10,000	5% milk

Table 2.2. Antibodies and their dilution details, used throughout this project
1x casein was made up in 1x TBS and 5% milk made up in 1x TBS-T
*MCF-7 cells incubated with 1:500, MDA-MB-231 cells with 1:**1000 o/n**
WB= western blot, IF= Immunofluorescence

2.6 Estrogenic ligand treatment for ERβ2 speckle analysis

Glass coverslips were sterilised with 70% ethanol in dH_2O, and placed into 12 well plates. MCF-7 and MDA-MB-231 cells were plated onto these coverslips at 40% confluency and allowed to adhere overnight. In parallel to this cells were placed in T25 flasks at 40% confluency and allowed to adhere overnight. All cells were then placed in 5% charcoal stripped foetal calf serum (CS-FCS) RPMI 1640 media for 24hrs. This was followed by incubation for 24 hours with one of the following estrogenic ligands diluted in 5% CS-FCS RPMI 1640; E2-1nM, 4-OHT-50nM, DPN-10 nM, Genistein-30 µM. Cells on coverslips were fixed and permeabilised as described in 2.5.1 and immunofluorescence with ERβ2 antibody performed as per 2.5.2 and images acquired on the Nikon A1R-A1 confocal microscope at 60x magnification and images acquired using the accompanying NIS elements software (v4.2). Speckle number analysis methodology is detailed in chapter 5.3.1. The cells in T25 flasks were washed in DPBS, detached from the flask using 1ml of 1x trypsin EDTA for 1-3 minutes and centrifuged at 290 x g for 3 minutes to pellet. Cell pellets were used for RNA extraction, cDNA synthesis and qRT-PCR to measure ERβ2 mRNA levels. Detailed protocols for RNA extraction, DNase treatment and cDNA synthesis and qRT-PCR can be found in section 2.12, 2.13 and 2.14 respectively.

2.7 Cell synchronisation for ERβ2 speckle analysis

Cell synchronisation was performed on MCF-7 cells using a double thymidine block, then analysed for ERβ2 protein expression (immunofluorescence) and cell cycle distribution (flow cytometry). Incubations were performed in a humidified cell culture incubator at 37^{o}C with 5% CO_2. Cells were seeded to achieve around 60% confluency when adhered into 6 well plates and 12 well plates that contained sterilised (with 70% ethanol) coverslips, and allowed to adhere overnight. Thymidine was diluted in fresh RPMI 1640 media supplemented with 5% FCS to a concentration of 2mM, was added to the cells and plates were incubated for 16 hours. Cells were then washed thoroughly three times with DPBS to remove the block and incubated for 10 hours in fresh media, after which media was replaced with fresh media containing 2mM thymidine and incubated for a further 16 hours. Media was removed, cells were washed three times in DPBS and fresh media was added. At 0, 8, 10, 12 hours post thymidine release cells in 12 well plates grown on coverslips were fixed, permeabilised and processed for immunofluorescence with ERβ2 antibody as described in section 2.5.1 and 2.5.2. Cells in the 6 well plates were trypsinised at each of the time points as previously described in 2.2.1, resuspended in media, and centrifuged at 290 x g for 3 minutes to pellet. Pellets were resuspended in 300 µl of ice cold 70% ethanol, then 3ml of ice cold DPBS was added. The fixed cell suspension was stored at -20°C until processed for flow cytometric analysis.

2.7.1 Cell cycle distribution measurement by flow cytometry

Samples were removed from -20°C storage and centrifuged at 290 x g for 3 minutes to pellet the cells. Cell pellets were resuspended in 400µl PBS and passed through a cell strainer into to a 5ml round bottom falcon tube (both BD Biosciences) for flow cytometry. Propidium iodide (PI) staining solution was made up by addition

of 250 µl PI stain stock solution at 50 µg/ml (Sigma), 700µl 0.5% Triton X-100 (Sigma) and 50µl RNAse at 100 µg/ml (Sigma) to a 1.5ml microcentrifuge tube (kept in the dark). 150µl of this staining solution was added to the resuspended cells, pipette mixed and incubated in the dark for 30 minutes at room temperature. Samples were then run on the LSRII flow cytometer using the blue laser at an excitation of 488 nm. 10,000 events were counted from each sample. Data was analysed using Modfit software and parameter set using a 'normally distributed' unsynchronised sample from the same cell line. Peaks representing G1 and G2 were identified on the histogram generated. S-phase was identified as the area between these two peaks. The percentage of cells in each phase was generated from the area under the peaks. An example histogram is displayed in figure 2.1.

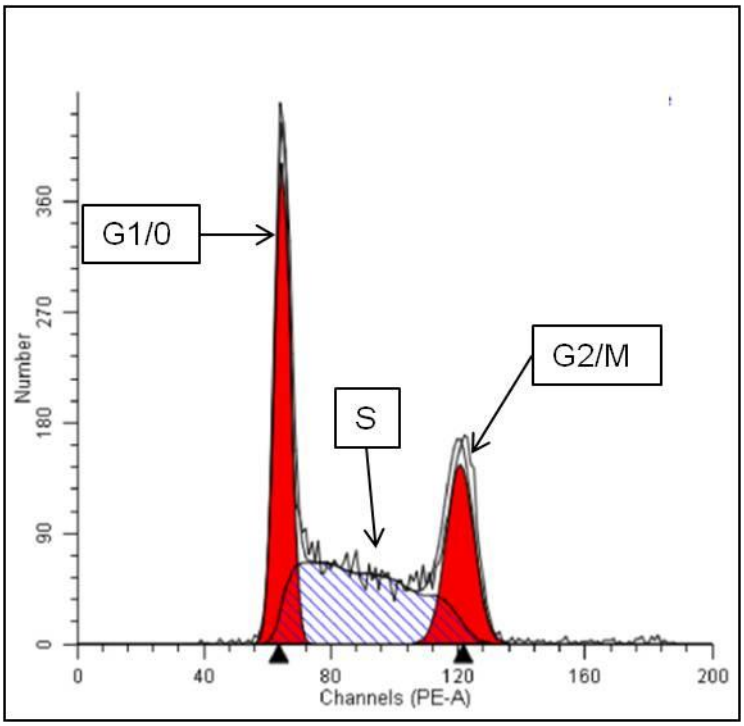

Figure 2.1. Cell cycle distribution analysis using ModFit software
Thymidine treated MCF-7 cells was analysed by flow cytometry and output data was examined using ModFit software. The proportion of cells in G1/0, S and G2/M were calculated as the area under each section of graph, and are labelled on the Figure.

2.8 Actinomycin D (ActD) and Cyclohexamide (CHX) treatment

MCF-7 vector control and ERβ2 overexpressing cells were plated at 40% confluency out onto sterile glass coverslips (pre-soaked in 70% ethanol) in 12 well plates and allowed to adhere for 48 hours. Cells were also placed into T25 flasks and T75 flasks for RNA and protein extraction respectively and allowed to adhere. At 60% confluency all cells were incubated with ActD (5µg/ml) or CHX (20µg/ml). At 30 minutes, 1,2,4,8,16 and 24 hours after initial incubation, cells on coverslips were fixed and permeabilised as described and processed for ERβ2 immunofluorescence analysis (2 wells per time point) described in 2.5.1 and 2.5.2. Cells in T25 flasks were pelleted, as previously described, at these time points for RNA extraction, cDNA synthesis and qRT-PCR for ERβ2 mRNA quantification, protocols for which are detailed in 2.12, 2.13 and 2.14. Cells in T75 flasks were used for protein extraction and subsequent western blot, protocol details of which are described in 2.9 and 2.10. Western blots were done using the FLAG M2 antibody (Sigma) to detect ERβ2 and both protein extraction and western blot was performed on ERβ2 overexpressing MCF-7 cells only. All other assays in this experiment were performed on both vector control and ERβ2 overexpressing MCF-7 cells.

2.9 Protein extraction and quantification

Cells for protein extraction were grown in either T75 or T150 vented cap cell culture flasks (Corning) depending on the concentration of protein required. Protein was extracted from cells when they were ~60% confluent using a lysis buffer containing a 1:1 ratio of 1x RIPA buffer (300nM NaCl, 4nM EDTA, 2% NP40, 0.5% Na deoxycholate (all Sigma) and 1x protease inhibitor mini protease cocktail EDTA free tablets (Roche). Briefly, cells were washed once with ice cold DPBS, then ice cold lysis buffer was added (T75 flask; 500µl lysis buffer, T150 flask; 1000µl lysis buffer). This was placed on ice for 2 minutes ensuring the buffer covered the cells. Using a

cell scraper, cells were removed from the flask and transferred to a sterile pre-chilled 1.5ml microcentrifuge tube (Starstedt). This was placed on a rocker at 4^{o}C for 10 minutes. The protein extract was then centrifuged at 16100 x g for 10 minutes at 4^{o}C until a cell debris pellet formed. The supernatant (protein) was removed and placed into a new pre-chilled sterile 1.5ml microcentrifuge tube and either used fresh or aliquoted and stored at -80 C until required.

Protein concentration was determined using the DC protein assay (Biorad) as per the manufacturer's instructions. Briefly, 5µl of the protein standard samples of known concentration (0.1875mg/ml, 0.5mg/ml, 1mg/ml, 2mg/ml) and the samples to be quantified were added to separate wells of a flat bottom 96 well microtitre plate (Corning). 25µl of reagent A + S (alkaline copper tartrate solution) was added to these wells followed by 200µl of reagent B (Folin reagent). The plate was incubated at room temperature in the dark to allow colour change then analysed at a wavelength of 750nm on a Berthold Mithras LB94 plate reader. A standard concentration curve was generated using the readings from the standards to determine sample protein concentrations. Protein samples were diluted to the same concentration in deionised water before western blot.

2.10 Western blot

22.5µl of diluted protein extract was added to 7.5µl of 4x SDS buffer (sodium dodecyl sulphate, Novex) containing 0.5% β-mercaptoethanol (Sigma), into a fresh pre-chilled 1.5ml microcentrifuge tube and pipette mixed. Protein samples were boiled to 105^{o}C for 5 minutes, vortexed and briefly centrifuged then cooled on ice. 25µl of each sample along with 7µl of dual colour protein plus standard (Biorad) was loaded on a precast NuPAGE® Novex® 4-12% Bis-Tris Protein Gels (1.0 mm, 10 well) used with Xcell Surelock Mini-Cell apparatus submerged in 1x NuPAGE MOPS SDS Running Buffer (all Invitrgen). Electrophoriesis was performed at 120v for 1-1.5 hours. Protein was transferred to a Hybond-P PVDF protein transfer

membrane (Amersham). Before use the membrane was pre-activated by soaking for 20 seconds in methanol then soaked in 1x NuPAGE Transfer buffer diluted in dH_2O with 10% methanol. Protein samples were then transferred using the Xcell II Blot Module SureLock™ in transfer buffer at 30 volts for 2 hours. The membrane was then blocked with 5% milk made in TBS-T (10mM Tris-HCl, pH 8.5, 150mM NaCl, 0.1% Tween-20) for 1 hour at room temperature. The primary antibody (dilution details in Table 2.2) was incubated with the membrane overnight at 4°C, followed by washing (3 x 10 minutes) with TBS-T, then incubation with a HRP-conjugated secondary antibody for 1 hour at room temperature (dilution details in Table 2.2). The membrane was washed 3 x 10 minutes with TBS-T then developed using SuperSignal West Pico Chemiluminescent Substrate (ThermoScientific) and visualised using a BioRad Universal Hood II ChemiDoc® MP imaging system. The membrane was then washed with TBS-T (3 x 10 minutes) and re-blocked in 5%milk in TBS-T for 1 hour. The membrane was incubated with the relevant loading control antibody (details in Table 2.2) overnight at 4°C, followed by washes in TBS-T (3 x 10 minutes) and incubated with the relevant secondary HRP conjugated antibody for 1 hour at room temperature. The membrane was washed (3X for 10 minutes) in TBS-T and developed using SuperSignal West Pico Chemiluminescent Substrate (ThermoScientific) and visualised using a BioRad Universal Hood II ChemiDoc® MP imaging system

2.11 Subcellular fractionation

MCF-7 and MDA-MB-231 ERβ2 overexpressing cells were trypsinised and counted using the ViCell automated system as described in section 2.3. $6.6x10^6$ cells were pelleted by centrifugation at 290 x g for 3 minutes. A Cell Fractionation Kit – Standard kit (Abcam) was used for protein extraction from the cells. 2X buffer A was diluted to 1X by addition of dH_2O. The cell pellet was resuspended in 150 µl of 1X Buffer A. Buffer B was prepared by diluting detergent I 150-fold in 1X buffer A. 150 µl of buffer B was added to the resuspended cell pellet incubated on a rotator for 7 minutes at room temperature to lyse and break down the cell membrane. Samples were then centrifuged at 10,000 x g for 1 minute at 4^oC and supernatant removed. This was centrifuged at 10,000 x g for 1 minute at 4^oC and transfer to a new tube. This was the cytoplasmic fraction. The pellet was resuspended in 150µl of 1X Buffer A. Buffer C was prepared by dilution of detergent II 25 fold in 1x buffer A.150µl of Buffer C was added to the resuspended cell pellet to lyse the mitochondrial membranes and incubated on a rotator for 10 minutes at room temperature, followed by centrifugation at 5000 x g for 1 minute at 4^oC. The supernatant was removed and put into a new clean 1.5ml microcentrifuge tube, while the pellet was put on ice. The supernatant was re-centrifuged at 10000 x g for 1 minute at 4^oC, and the supernatant was transferred to a new microcentrifuge tube. This was the mitochondrial fraction. The cell pellet was resuspended in 300µl of 1x buffer A and centrifuged at 5000 x g to wash the pellet. The supernatant was discarded and the pellet was resuspended in 300µl of 1x buffer A. This was the unlysed nuclear fraction. The cytoplasmic, mitochondrial and nuclear protein fractions were then processed by western blotting for protein detection as described in 2.10.

2.12 RNA extraction

RNA extraction was performed using a RNeasy Mini Kit (Qiagen) according to the manufacturer's protocol. Briefly, cells were trypsinised as previously detailed and centrifuged at 290 x g for 3 minutes to pellet. Buffer RTL (lysis buffer) was added to the pellet and pipette mixed. The cell suspension was homogenised by centrifugation of the sample through a Qiashredder column for 2 minutes for 16000 x g at room temperature. 70% EtOH was added to the sample, pipette mixed and placed in an RNeasy spin column and centrifuged for 15 seconds at 8000 x g. The column was then washed firstly by addition of RW1 buffer followed by centrifugation for 15 seconds at 8000 x g, then twice with RPE buffer for 15 seconds at 8000 x g. RNA was eluted by addition of 50µl RNase-free water to the column membrane, placed in a new clean 1.5ml microcentrifuge tube, and centrifuged for 1 minute at 8000 x g. RNA samples were then DNAse treated as described in 2.13.

2.13 DNase treatment and cDNA synthesis

To remove any residual DNA that may be present, RNA samples were treated with DNase using a TURBO DNase kit (Ambion). Briefly, 5µl of 10x Turbo DNase Buffer was added to 50µl of RNA sample followed by addition of 1 µl of Turbo DNase 1, and incubated at 37^{o}C for 30mins. 5µl of DNase Inactivating Agent was then added to the sample and incubated for 2 minutes at room temperature, flicking after a minute to ensure mixing. Samples were centrifuged for 1.5 minutes at 8000 x g. The supernatant was transferred to a clean 1.5ml microcentrifuge tube ready for further processing.

DNase treated RNA samples were quantified on a Nanodrop ND-1000 spectophotometer. RNA samples were diluted to the same known concentration in Ambion® Nuclease-Free Water (Life technologies). The following was prepared on ice in a microcentrifuge tube; 10µl RNA sample, 1µl of random hexamers at 50µM (Invitrogen) and 1µl of 10nM dNTP (Promega), and incubated at 65^{o}C for 5 minutes

then placed on ice to cool for 2 minutes. The following were then added to the sample; 4µl 5x First Strand Buffer, 2µl 0.1M DTT, 1µl RNase OUT (all Invitrogen), and incubated at 42^{o}C for 2mins. 1µl of Superscript II enzyme (Invitrogen) was then added to the samples and incubated at 42^{o}C for 50 minutes, followed by 70^{o}C for 15 minutes. Samples were then stored at -20^{o}C until use.

2.14 qRT-PCR with TaqMan® gene expression assays

cDNA samples were diluted to 10ng/µl as recommended by the manufacturer in Ambion® Nuclease-Free Water (Life Technologies). Samples were run in triplicate for each TaqMan® probe used. RPLP0 was used as a reference gene and was also run in triplicate with each sample. Reactions were set up in a UV sterilised hood. Each reaction was 20 µl total volume made up of 9µl cDNA sample (diluted to 10 ng/µl), 1 µl TaqMan® probe, 10 µl gene expression master mix and was transferred to a MicroAmp® optical 96 well plate then sealed with optical sealing tape (all Applied Biosystems). All samples were run in triplicate and a no RT control (one prepared per cDNA synthesis experiment) and no cDNA control were processed with each gene expression assay. Amplification was performed on an ABI 7500 real-time PCR system with the following cycling parameters; 2 minutes @ 50^{o}C, 10 minutes @ 95^{o}C, then 40 cycles of 15 seconds @95^{o}C and 1 min @ 60^{o}C. After amplification, ct values were obtained using a threshold line placed through the exponential area of the curve and data exported to an excel sheet. Relative expression; 2(-$\Delta\Delta Ct$) (151) or fold change compared to the relevant control sample were calculated.

2.15 ERβ2 Molecular Cloning

To enable the creation of ERβ2 over expressing cell lines, cloning of ERβ2 into a retroviral vector using PCR and recombination techniques cloning along with retroviral transduction were used to generate stable transfected cell lines that overexpress ERβ2.

2.15.1 Amplification of ERβ2 fragment

PCR reactions to amplify the ERβ2 coding sequence were performed using a pCDNA3 plasmid containing the coding sequence for the ERβ2 protein, a gift from Professor Eric Lam, Imperial College London. The primers were designed to create ends complementary to the pFB-NeoFLAG3 when cut with EcoR1 and BamH1 restriction enzymes (New England Biosciences) and the primer sequences are detailed in Table 2.3. The PCR reaction was carried out in 0.2ml PCR tubes (Axygen), and the reagents added are detailed in Table 2.4.

Primer Name	Primer sequence
ERβ2 Exon1 F	5'-TAAAGCTAGCGAATTCATGGATATAAAAAACTCACC-3'
ERβ2 Exon 8 R	5'-GCCGCTCGAGGATCCTCACTGCTCCATCGTTGCTTC-3'

Table 2.3. Primer sequences for amplification of the ERβ2 fragment
Primers were designed in-house and supplied by Sigma Aldrich. Upon receipt, primers were resuspended according to the manufacturers accompanying data sheet.

PCR Master Mix Component	Volume per reaction (µL)	Thermal Cycling Conditions		
		Stage	Temperature (°C)	Time (mm:ss)
dH_20	10.5	Hold	98	0:30
Buffer GC	4			
dNTP (10mM)	1	Cycle- (30 Cycles)	98	0:15
ERβ2 Exon1 F primer	1			
ERβ2 Exon 8 R primer	1		63	0:30
Phusion Taq	0.5			
pcDNA ERβ2 plasmid template	2	Elongation	72	2:00

Table 2.4. Reaction details for amplification of the ERβ2 fragment from pCDNA3 ERβ2 plasmid.
Total reaction volume was 20µl.

2.15.2 Recombination

The amplified ERβ2 fragment was cloned into a pFB-NeoFLAG3 vector. This vector was a gift from Professor Maggie Knowles of The Molecular Biology of Urothelial Cancers group in Leeds. The original pFB-Neo vector was supplied by Agilent Technologies. A map of the vector is shown in Figure 2.2. Briefly, the pFB-NeoFLAG3 vector was digested using the restriction enzymes EcoR1 and BamH1 by addition of the following in order to a microcentrifuge tube; 10 µl pFB-NeoFLAG3 vector, 15.7 µl dH_20, 3 µl Buffer 3, 1 µl EcoR1, 1 µl BAMH1 (all New England Biosciences). The amplified ERβ2 fragment and digested vector were then recombined using the In-Fusion HD Cloning Kit (Clontech). The following reagents were placed into a microcentrifuge tube followed by incubation at 50°C for 15 minutes; 2µl dH_20, 1 µl of vector, 1µl ERβ2 DNA and 1µl In-phusion enzyme. A negative vector only control was also prepared, with dH_20 substituting for ERβ2 DNA.

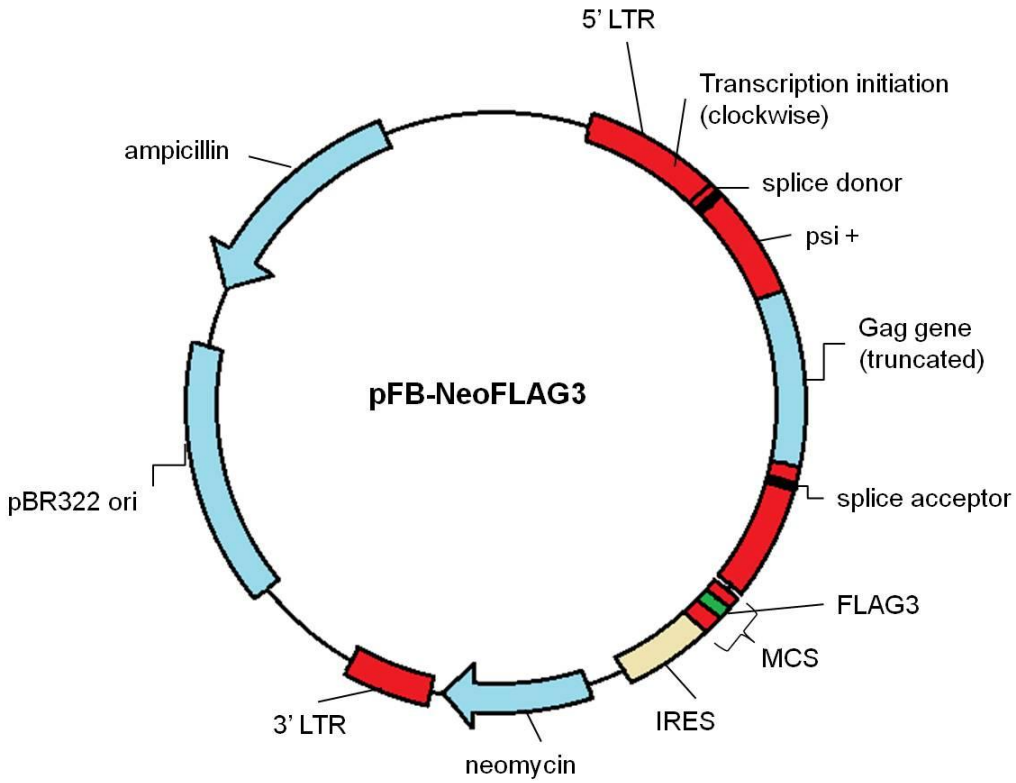

Figure 2.2. Map of the pFB-NeoFLAG3 vector used for recombination of ERβ2 into the multiple cloning site (MCS).
Features of the vector are labelled and include a neomycin resistance gene for selection purposes. Adapted from Agilent Technologies pFB-neo retroviral vector instruction manual

2.15.3 Transformation

Competent DH5α E. coli were used for transformation of the recombined ERβ2 pFB-NeoFLAG3 plasmids. 1µl of ERβ2 vector or negative control was added to 50µl DH5α E. coli and incubated on ice for 30 minutes. Following heat shock (90 seconds at 42°C), they were returned to ice for a further 2 minutes then smeared on sterile LB (lysogeny broth) agar plates containing 100 µg/ml ampicillin. Plates were incubated overnight at 37°C, where positive recombination clones would produce colonies on the agar plate.

2.15.4 Positive clones

Colonies from the positive plates were picked, and bacteria grown in 5ml of sterile LB (made up in dH_2O, Sigma) containing 0.1% ampicillin overnight in a shaking incubator at 37°C. The following day 750µl of bacterial suspension was added to 250 µl of 80% glycerol, and stored at -80. These would be used if clones were demonstrated to be positive for ERβ2 incorporation. 1.5ml of bacterial suspension was aliquoted into a microcentrifuge tube and centrifuged for 5 minutes at 2300 x g, then the supernatant discarded and the pellet DNA purified using a QIAprep Spin MiniPrep Kit (Qiagen), following the manufactures instructions. Briefly, bacterial cell pellets were resuspended in Buffer P1. Pellets were lysed by addition of 250 µl of buffer P2 and 350µl buffer N3 followed by centrifugation at 16100 x g. The supernatant was removed and added to a QIAprep spin column and centrifuged at 16100 x g for 1 minute to bind the DNA. The column was washed by addition of 750µl buffer PE and centrifuged at 16100 x g for 1 minute. The column was then placed in a new sterile microcentrifuge tube and DNA eluted by addition of 50µl buffer EB and centrifugation at 16100 x g for a further minute. The purified DNA from the minipreps was digested with EcoR1 by addition of the following in order to a microcentrifuge tube; 10µl miniprep DNA, 11.5µl dH2O, 2.5µl NEB Buffer 4, 1µl

EcoR1 enzyme. The samples were digested at 37°C for 3 hours, and then loaded onto a 1% agarose gel containing ethidium bromide for visualisation and electrophoresis was performed. Positive clones were identifiable by bands of sizes of 6.8kb and 1.1kb. Clones with 2 bands of the above sizes were digested further with EcoRV by addition of the following in order to a microcentrifuge tube; 10µl miniprep DNA, 11.5µl dH2O, 2.5µl NEW Buffer 4, 1µl EcoRV enzyme and incubated at 37^{o}C for 3 hours. Samples were loaded onto a 1% agarose gel containing ethidium bromide for visualisation and electrophoresis was performed. Positive clones presented bands of 80bp, 2150bp, 2800bp and 3050bp. Using the glycerol stocks previously made, samples deemed positive from both digests were grown up in 50ml Lysogeny broth (made up in dH_2O,Sigma), containing 0.1% ampicillin, overnight in a shaking incubator at 37°C.

The DNA was purified using the NucleoBond Xtra Midi kit (Macherey Nagel) according to the manufactures instructions. Briefly; bacterial cells from the LB broth were pelleted by centrifugation at 5000 x g for 10 minutes at 4^{o}C. The pellet was resuspended in 8ml of Buffer RES then lysed by addition of 8ml of Buffer LYS. 12ml of buffer EQU was added to the NucleoBond® Xtra Column together with the inserted column filter and allowed to empty by gravity. 8ml of Buffer NEU was added to the sample then this was applied to the NucleoBond® Xtra Column filter, which was allowed to empty by gravity. The column was then washed by addition of 5ml of Buffer EQU followed by 8ml of Buffer WASH and allowed to drain after addition of each. Plasmid DNA was eluted into a 15ml ultracentrifuge tube (Corning) by addition of 5ml of Buffer ELU to the column. The eluate was precipitated by addition of 3.5ml of isopropanol and centrifuged at 4500 x g for 15 minutes. The supernatant was discarded and 2ml of 70% ethanol was then added followed by centrifugation at 15000 x g for 5 minutes. The supernatant was removed and the pellet allowed to air dry, after which the pellet was dissolved in dH2O.

To ensure that our ERβ2 gene coding sequence was recombined into the pFB-NeoFLAG3 vector and to verify it was in frame with the start codon, the two positive clones identified and purified were sequenced in house by Dr Euan Baxter on an ABI 3130xl Genetic Analyzer using a BigDye® Terminator v3.1 Cycle Sequencing Kit with 200ng starting material. Sequencing primers were designed to cover the whole ERβ2 coding sequence, the FLAG3 sequence and multiple cloning site, and their primer sequences are displayed in Table 2.5. Sequencing data was analysed using ABI Seq Scanner 2 software and readouts were aligned to the reference genome by performing a BLAST search (appendix 7.1).

Primer Name	Primer sequence 5'-3'
pFB-Neo FWD	GGCTGCCGACCCCGGGGGTGG
pFB-Neo RVS	GCCAGGTTTCCGGGCCCTCAC
F1	TCCAGCTACAAATCAGTGTAC
F2	CTGGAAATCTTTGACATGCTCC
F3	GATGGAGGTGTTAATGATGGG
R1	GTACACTGATTTGTAGCTGG
R2	GGAGCATGTCAAAGATTTCCAG

Table 2.5. Details of the sequencing primers used to confirm the in frame presence of ERβ2 gene sequence in pFB-NeoFLAG3 vector.

2.15.5 Transfection of pFB-NeoFLAG3 ERβ2 Vector into viral packaging cells for virus particle production

All transfection and transduction work was carried out in a GM Class 2 facility with approved risk assessments specific to this project in place. A T75 flask containing Phoenix Ampho (phoenix A) retrovirus producer cell lines grown to around 60% confluency in DMEM Glutamax media supplemented with 10% FCS was transfected with the pFB-NeoFLAG3-ERβ2 construct. Another T75 flask of Phoenix A cells was prepared and transfected with the empty vector (pFB-NeoFLAG3), to be utilised as the control cell counterpart for downstream experiments. Briefly, 24µl of Lipofectamine 2000 reagent® (Invitrogen) was added to 1600µl of serum free DMEM glutamax media (Gibco) in a sterile universal tube. 50µl (containing 8µg total DNA) of plasmid DNA was added, gently mixed by flicking the tube and incubated at room temperature for 20 minutes. The solution was then added to 10ml of DMEM Glutamax in a universal tube, and used to replace the media on the Phoenix A cells. Cells were incubated overnight at 37^{o}C in a humidified incubator with 5% CO_2. The day after, media was removed and 10ml of fresh media applied to the cells for 24 hours after which an additional 10ml media change was performed the following day. The day after the media was removed (viral supernatant) and syringe filtered through a Millex® 0.45µm syringe filter (Millipore) and stored at -80^{o}C.

2.15.6 Transduction of viral particles into breast cancer cell lines

MCF-7, T47D, MDA-MB-231 and MDA-MB-468 cells were seeded into T25 flasks and allowed adhere and reach 40% confluency. Two flasks were seeded per cell line, one to be transduced with the empty vector (pFB-NeoFLAG3) and the other with the pFB-NeoFLAG3-ERβ2 construct. Polybrene stock (@ 80mg/ml) was diluted to 8µg/ml by addition of 1µl to 10ml of DMEM glutamax media supplemented with 10% FCS. Polybrene solution was added to the cells at 1µg/ml;

so for each flask of cells, 250µl of polybrene solution was added to 1750µl of viral supernatant. This viral solution (2ml) was then added to the flasks of cells after media aspiration, and incubated overnight at 37^{o}C in a humidified incubator with 5% CO_2. The following day fresh media was applied and the cells were left for 48 hours before selection with geneticin, detailed in 2.15.7.

2.15.7 Selection of positively transduced cell lines

To select the effective dose to cause cell death wild type cell lines used for transduction, a geneticin (G418) kill assay was performed prior to selection. Each wilt type cell line, MCF-7, T47D, MDA-MB-231 and MDA-MB-468, was seeded into five T25 flasks at around 30-40% confluency and allowed to adhere overnight. Geneticin was diluted in the appropriate media to the following concentrations; 100, 200, 400, 800 and 1000µg/ml and each dose was applied to a flask of every cell line. Cells were observed under the microscope and photos taken during a period of 10 days. At the end of the selection period the lowest dose of geneticin, specific to each cell line, which resulted in complete cell death, was used to select for successfully transduced cell lines.

Geneticin was diluted in the appropriate media for each cell line to a concentration demonstrated to result in cell death after 10 days in wild type cells (detailed in chapter 4.3.2) as follows; 500µg/ml for MCF-7, T47D and MDA-MB-231 cells, 200µg/ml for MDA-MB-468 cells. Retrovirally transduced cell lines were incubated with their cell specific dose of genistein for a period of 10 days (@37^{o}C with 5% CO_2) to select for positively transduced cells. After 4 days the media was replaced with fresh media containing the appropriate doses of geneticin. After the 10 day section period cells were washed in DPBS and media was replaced. Cells were grown up and stocks made for long term storage (10 vials each) at low passage. Cells were then used for downstream experiments detailed in chapter 4.

3.0 Chapter 3: Examination of ER expression in a range of breast cancer cell lines representing 5 major molecular subgroups

3.1 Introduction

3.1.1 ER expression in breast cancer cells

ERα expression is only present in luminal A and B tumours whereas ERβ is expressed across all molecular subtypes. The expression patterns of ERβ1 was established in a large cohort of 2170 breast cancer patient samples, where immunohistochemistry analysis revealed that 72% of luminal A, 68% of luminal B, 55% of HER2 overexpressing and 60% of basal breast cancers expressed ERβ1 (74). ERβ1 expression has been widely associated with a better prognosis and DFS regardless of molecular subtype (75, 77, 86). Only a handful of studies have contradicted this and described a correlation with poor outcome (87, 88). Studies have identified ERβ2 expression in breast tumours and have reported that around half express this protein (76, 91, 98, 152). ERβ2 has repeatedly been positively correlated with ERα expression (75, 90) however expression has also been observed in 57% of ERα negative tumours (91). The implication of ERβ2 expression on prognosis and survival is far more complex and contradictory than for ERβ1. Some associate ERβ2 protein expression with a better prognosis (75, 90, 96), while others with a poorer prognosis (98, 152). Other than potential differences in IHC (immunohistochemistry) staining protocol, sample handling, tissue fixation methodology and antibodies used, there is another factor that may explain these differences. The location of the ERβ2 protein within the cell appears to affect prognosis. In a study of 757 invasive breast cancer samples, nuclear ERβ2 expression resulted in a good prognosis whereas cytoplasmic ERβ2 was a poor

prognostic marker (94). This observation has been corroborated by Yan et al, 2011 (100) in a cohort of 123 breast cancer samples.

Expression of ERβ1 and ERβ2 has been observed in breast tumours of all molecular subtypes; however the implication on prognosis does appear to vary and the location of the protein within the cell may not have been considered in the vast majority of studies. The purpose of this chapter was to explore expression patterns of estrogen receptors in breast cancer cell lines of differing molecular subgroups. This was done using immunofluorescence, allowing precise analysis of expression patterns in cellular compartments including nucleus, cytoplasmic and mitochondria. There are various technical considerations which need to be addressed during such analysis, and these are described in detail below.

3.1.2 ER antibody specificity

Much of this project relied upon the use of antibodies, specifically the ERβ2 57/3 clone (Serotec); therefore it was important that this antibody was demonstrated as reliable in the literature. There are relatively few studies that have used this antibody; however it has been validated in the literature as specific for the ERβ2 isoform in a number of cases. Peptide pre-absorption has been performed prior to the antibody use and no signal was detected upon ERβ2 immunohistochemistry (94, 153) or western blot (154). However one study did demonstrate that the ERβ2 antibody was not specific, as the use of siRNAs to ERβ2 failed to negate signal when ERβ2 antibody was applied (155). However details of the siRNA knockdown efficiencies were not given. There is much variability in the efficiency of knockdown using siRNAs (156). As siRNAs target the mRNA, the incubation time used in this study (24 hours) will only silence newly synthesised ERβ2 and could provide a possible reason for lack of signal negation. This method of antibody specificity validation may not be suitable for already synthesised longer lasting proteins, as siRNAs cannot silence proteins whereas peptide pre-absorption can.

3.1.3 Immunofluorescence and confocal microscopy

In this study we required a technique that could allow us to observe subcellular compartments and expression pattern in detail. Confocal immunofluorescence microscopy allows detailed observation of cellular proteins at high resolution and provides the means to view cells in 3D by creating z-stacked images, or allowing analysis of an individual slice from the stack. It was deemed the most appropriate and flexible practice for our study. This technique also allows for protein colocalisation experiments and subsequent quantification using sophisticated software.

3.1.4 Colocalisation

Colocalisation immunofluorescence describes the spatial overlap of signals at a pixel location from two or more different fluorophores. These fluorophores are attached to antibodies which bind to specific proteins of interest, and provides information as to whether two targets are located in the same cellular space (157). Colocalisation doesn't directly prove that two proteins are interacting, but it does provide valuable information about their characteristics. This technique is most often used to determine whether proteins are associated with cellular structures e.g. those located to endosomes, mitochondria etc., or those located to specific nuclear structures such as the nucleolus or in nuclear speckles, or to suggest interaction between two proteins. Colocalisation describes co-occurrence of signal in the same pixel location and their correlation. It is common in the literature, for colocalisation studies to investigate the overlap of two entities labelled with red and green fluorophores and identify yellow colocalised areas without any further analysis. Although appropriate for some incidences for example when the colocalisation is obvious to the eye, when colocalisation is more subtle or when one entity is stained more intensely and masks the other, the use of an automated method with the

ability to quantify colocalisation may be appropriate. This has the added advantage of not being subjective or misleading, and results in consistency in analysis between images. Provided images are uniform in their acquisition or the colocalisation calculation used eliminates any potential human variation, accurate quantification of colocalisation can be obtained. Special attention must be paid to ensure:

- Z-stacks are acquired and analysis is performed on a slice of the image
- pixels are not saturated (by lowering the gain)
- background is greatly reduced
- chromatic aberration (when the lens distorts and fails to focus the colours on the same point) is avoided or corrected.

3.1.5 Colocalisation coefficients

There are two metrics typically used in quantifying protein colocalisation; the Pearson's correlation coefficient and the Mander's overlap coefficient. These are used to quantify the degree of colocalisation between fluorophores by correlation, and the two calculations possess subtle differences in how they are measured. The Pearson's correlation coefficient (158) is robust and well characterised method widely used to measure correlations, but its use in fluorescence is a relatively recent occurrence (159). It measures the linear correlation between two variables and generates a value of between +1 and -1, where +1 signifies total correlation, 0; no correlation and -1; total negative correlation. In the context of immunofluorescent colocalisation, it measures the level of colocalisation between two colour channels based on the intensity distribution between them. It is determined using the following calculation (157), which assumes the two channels are red and green:

$$= \frac{\sum_i (R_i - \overline{R}) \times (G_i - \overline{G})}{\sqrt{\sum_i (R_i - \overline{R})^2 \times \sum_i (G_i - \overline{G})^2}}$$

R_i refers to the intensity of the red channel in each pixel and likewise G_i represents intensity of the green channel in each pixel. R and G (with a horizontal line above) refer to the mean intensities of the red and green channels respectively across the whole defined region of interest (ROI). As this coefficient subtracts the mean intensity from pixel intensity, it is not influenced by signal levels and background (offset) (160). This makes it a preferable method for colocalisation when comparisons between images are being made, as it is not affected by differences in image acquisition or processing (changes in gain and offset) and free from user bias. Its disadvantage however is that the data must follow a linear relationship in order to gain meaningful information from this coefficient. For example if red pixel intensity is increased, so is green pixel intensity. Generation of a simple scatterplot of red vs. green pixel intensity in the region of interest (ROI) on an image will determine linearity and the appropriateness of this calculation (157). The Mander's coefficient is similar to the Pearson's correlation coefficient and is calculated using the equation below (161):

$$= \frac{\sum_i (R_i \times G_i)}{\sqrt{\sum_i R_i^2 \times \sum_i G_i^2}}$$

Again R_i and G_i represent red and green pixel intensity respectively. It was developed specifically for use in immunofluorescence to address the deficiencies of using the Pearson's correlation, and eliminates the process of subtracting the average intensity values for the ROI from each pixel intensity value (160). This removed potential for negative values to arise, which are often confusing to interpret. Rather than basing the calculation on departure from the mean intensity, it

is a measure of absolute intensity. It is a more complex interpretation of colocalisation but is useful for data that does not follow a linear distribution. It is insensitive to variations such as efficiency of antibody binding, sample photo-bleaching or microscope differences. It also excludes areas where both probes are absent, so defining regions of interest would not be necessary, provided background is eliminated. However alteration of the offset (background) does heavily influence the values. An accurate Mander's coefficient would depend upon the user reliably and consistently eliminating all background. Manually interpreting what is or isn't background could prove erratic especially when dealing with multiple images.

3.2 Aims

To investigate ER protein expression in a range of breast cancer cell lines representing five major molecular groups by:

- establishing the expression patterns and cellular location of ERα, ERβ1 and ERβ2 protein using confocal immunofluorescence
- ascertaining whether cytoplasmic ERβ2 colocalises with mitochondria and quantifying levels of colocalisation in this organelle

3.3 Methods

The following describes the analysis performed to determine ERβ2 and mitochondrial colocalisation. All other methods are described in chapter 2.

3.3.1 Colocalisation analysis

Colocalisation levels in each cell line were analysed as follows. An image slice from around the centre of the z-stack was selected. The cytoplasm of each cell was specified by manually drawing around the cytoplasmic region of each cell as depicted in Figure 3.1a. A scatter plot was created for each image to ensure the intensity distribution was linear, an example of this is illustrated in Figure 3.1b .A Pearson's correlation coefficient (PCC) was generated for each cell in the image and values were exported to an excel spreadsheet. Values from individual cells were plotted on a frequency distribution histogram, one for each cell line, using GraphPad Prism 6 software. This experiment was repeated at least three times and until a minimum of 30 cells from each cell line were analysed. This number proved sufficient as cumulative data analysis of colocalisation values for MDA-MB-231 was performed, whereby 30 cells was sufficient to result in stabilisation of histogram shape (appendix 7.4).

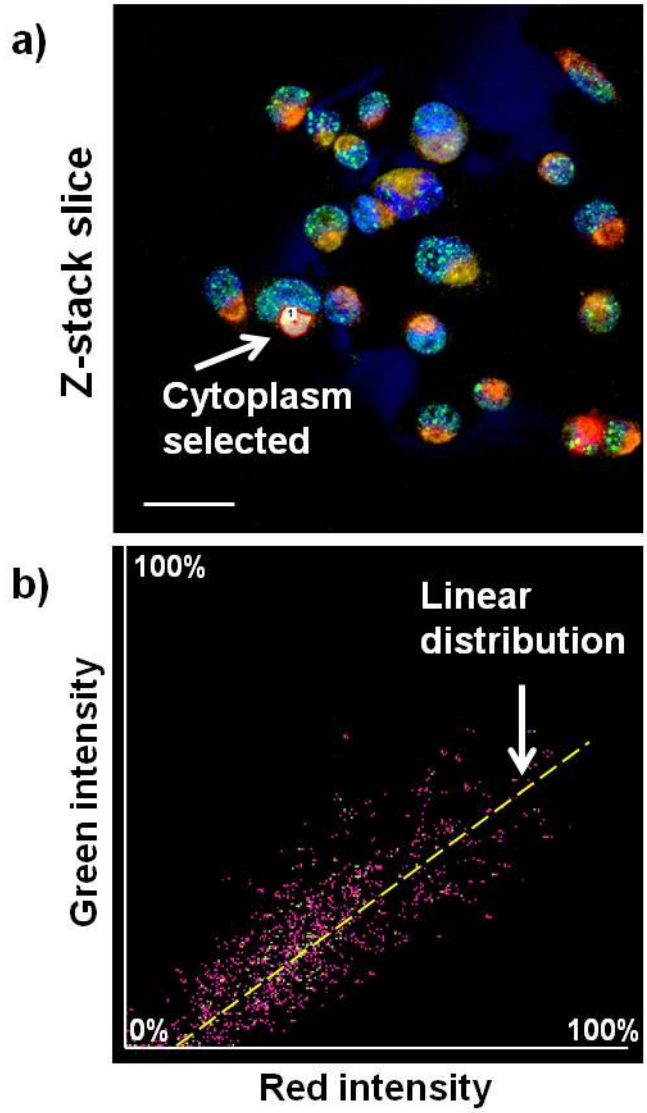

Figure 3.1. Quantification analysis of ERβ2 and mitochondria colocalisation
a) The cytoplasmic region was selected in each cell (MDA-MB-231 cells shown) by manually drawing around the cytoplasm, illustrated by the white arrow, using the region of interest (ROI) drawing tool in the Nikon A1R confocal elements software v3.2. Scale bar = 50µm
b) A red/green pixel intensity scatterplot was generated for each cell and a Pearson's colocalisation coefficient value calculated by the software. Each dot on the plot represents a pixel with red and green staining. The yellow dotted line shows the linear relationship of pixel intensities.

3.4 Results

3.4.1 Immunofluorescent analysis of ERα ERβ1 and ERβ2 expression in breast cancer cell lines

Expression of ERα, ERβ1 and ERβ2 was investigated in a range breast cancer cell lines representing 5 major molecular subgroups to explore its localisation in cellular compartments. This was done by immunofluorescence analysis and evaluation of expression patterns using confocal microscopy.

3.4.1.1 Luminal A cell lines

Figure 3.2 illustrates expression patterns of ERα, ERβ1 and ERβ2 in MCF-7 cells. ERα expression in MCF-7 cells (b) was localised to the nucleus indicated by the white arrow. Staining intensity varied between cells, suggesting levels of ERα protein differed from cell to cell. Intensity of ERβ1 expression (e) also varied between cells, with some cells displaying stronger nuclear expression than others. Again expression was localised to the nucleus signified by the white arrow in image (f). ERβ2 expression was both nuclear and cytoplasmic. Staining intensity was even between cellular compartments. Nuclear staining is indicated by the white arrow in Figure 3.2h, and cytoplasmic by the red arrow in figure 3.2i. Distinct nuclear ERβ2 expression patterns were also observed as speckles in the cell nucleus of around half the cells examined indicated on Figure 3.2i by the yellow arrow.

In T47D cells displayed in Figure 3.3, expression or ERα was nuclear (white arrow, c). This nuclear expression varied in intensity between cells with some cell displaying much stronger staining (white arrow, image b). ERβ1 expression in T47D cell was uniformly nuclear indicated by the white arrow in image (f). Intensity was consistent between cells. Unlike MCF-7 cells there was weak cytoplasmic expression of ERβ2, in T47D cells ERβ2expression was predominantly nuclear. T47D cells also had a nuclear speckled pattern of ERβ2 expression signified by the yellow arrow in image (i). These were in every cell and are much greater in number than in MCF-7 cells. Speckles varied in number and size, with some cells having up to 10 well defined speckles (red arrow).

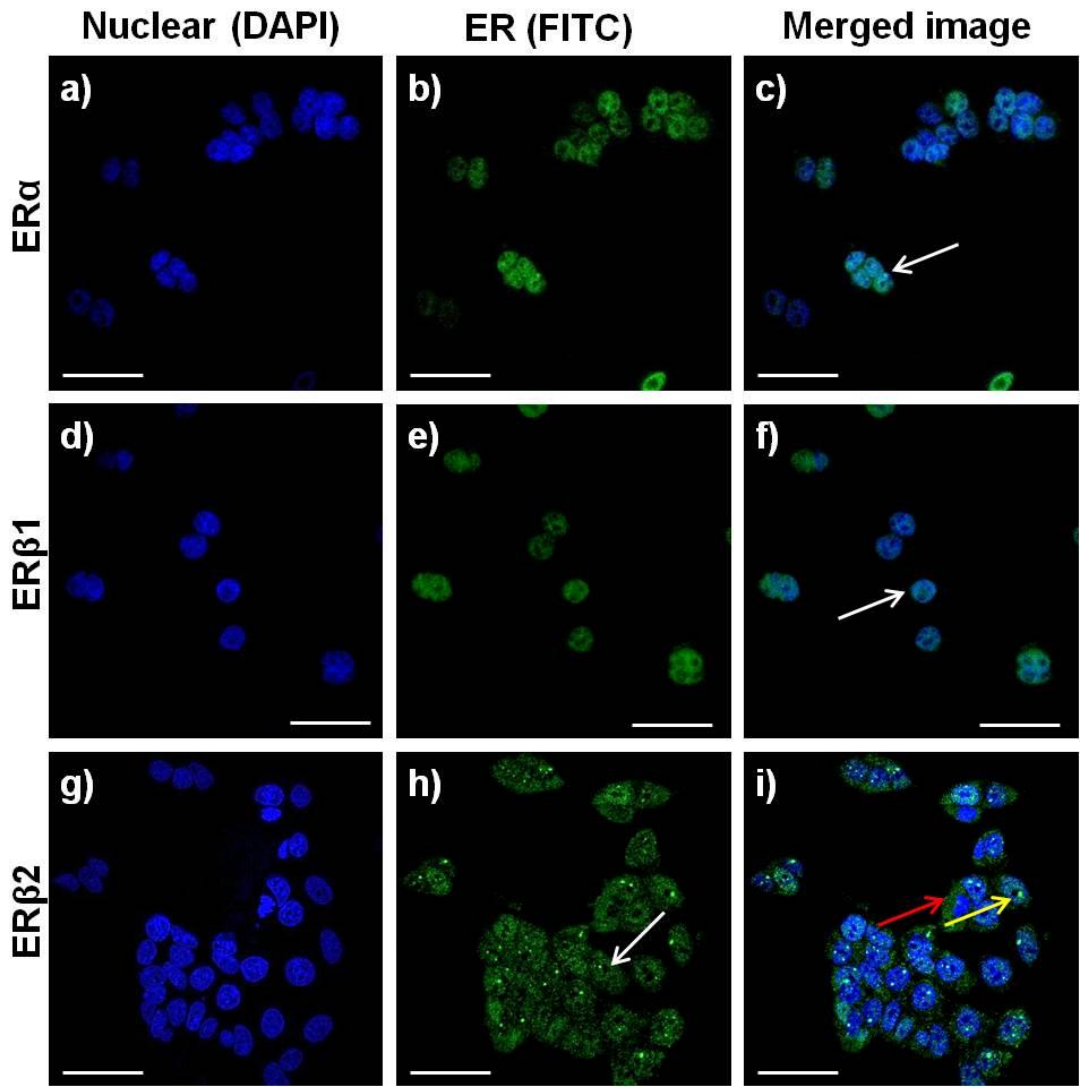

Figure 3.2. Immunofluorescence images of ERα, ERβ1 and ERβ2 expression patterns in the luminal A cell line MCF-7
(a, d, g) Cell nuclei were labelled with DAPI (blue), (b, e, h) ER proteins are visualised in green (FITC), (c, f, i) Merge image; DAPI and FITC overlaid
ERα expression was present in the nucleus of MCF-7 cells (white arrow, c)
ERβ1 expression was present in MCF-7 cells and was nuclear (white arrow, f)
ERβ2 expression in MCF-7 cells was present in both the cytoplasm (red arrow, i) and in the nucleus. Nuclear ERβ2 expression was also present as speckles (yellow arrow, i).
60 x magnification. Scale bars =50µm.

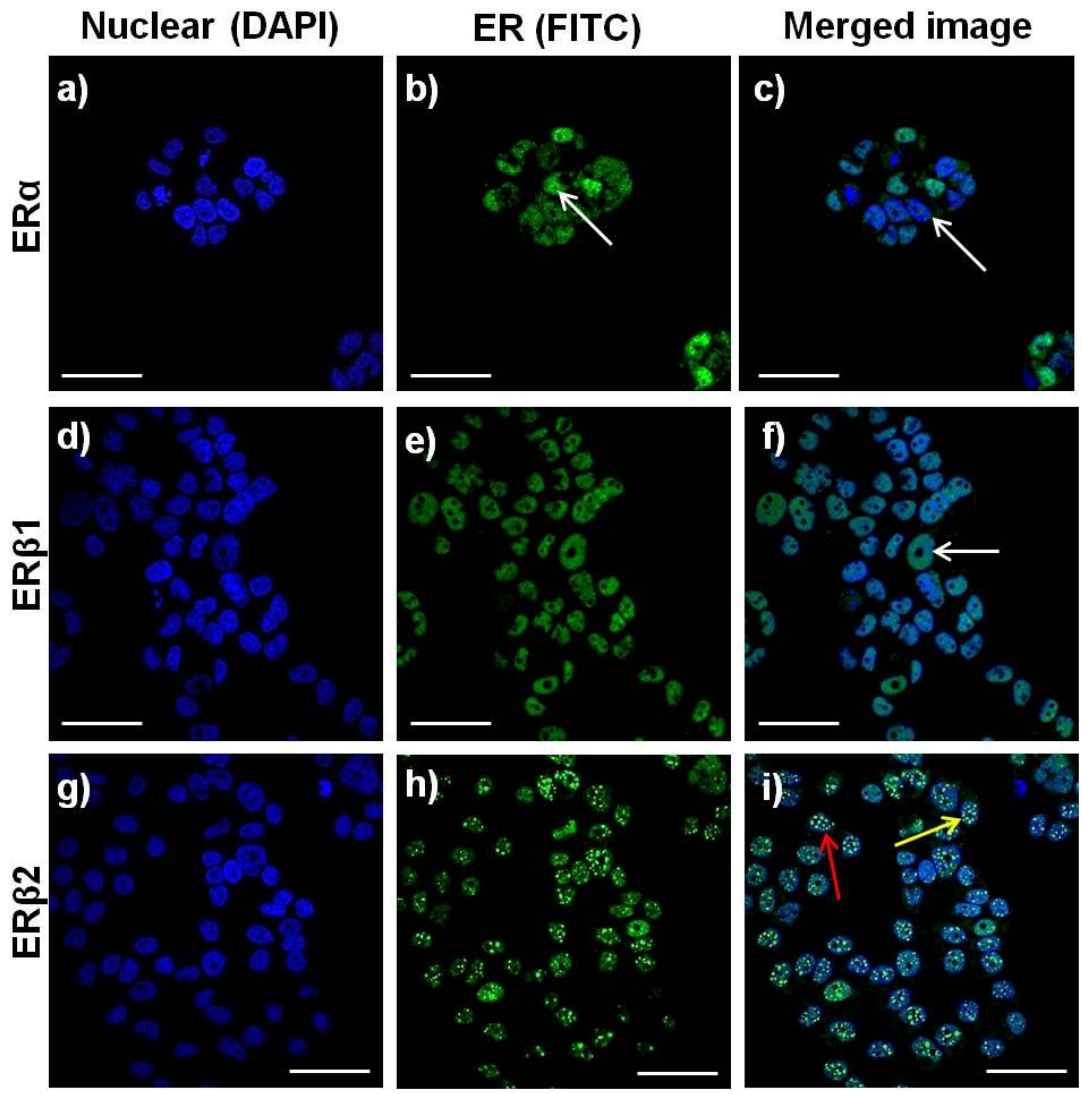

Figure 3.3. Immunofluorescence images of ERα, ERβ1 and ERβ2 expression patterns in the luminal A cell line T47D

(a, d, g) Cell nuclei were labelled with DAPI (blue), (b, e, h) ER proteins are visualised in green (FITC), (c, f, i) Merge image; DAPI and FITC overlaid
ERα expression was present in the nucleus of T47D cells (white arrow, b, c)
ERβ1 expression was present in T47D cells and was nuclear (white arrow, f)
ERβ2 expression in T47D cells was present in both the cytoplasm (red arrow, i) and in the nucleus. Nuclear ERβ2 expression was also present as speckles (yellow arrow, i).
60 x magnification. Scale bars =50µm.

3.4.1.2 Luminal B Cell Line

The only cell line representative of luminal B phenotype used in this study was BT474. Figure 3.4 demonstrates the expression patterns of ERα, ERβ1 and ERβ2. ERα expression (b) was variable with more intense staining observed in some cells than others, signified by the while arrow in image (b). ERβ1 expression in BT474 cells (e) was present in the nucleus and cytoplasm. The intensity of staining was relatively even between cytoplasm and nucleus. The cytoplasmic stain was only observed within the cluster of cells (white arrow, f), with no expression observed around the periphery of the cluster. ERβ2 expression (h) was predominantly nuclear in these cells signified by white arrow in image (h). ERβ2 speckles were also detected in the nucleus of the majority of these cells (yellow arrow, i). Cytoplasmic staining was observed in between cells (red arrow, i) but this was much fainter than nuclear staining.

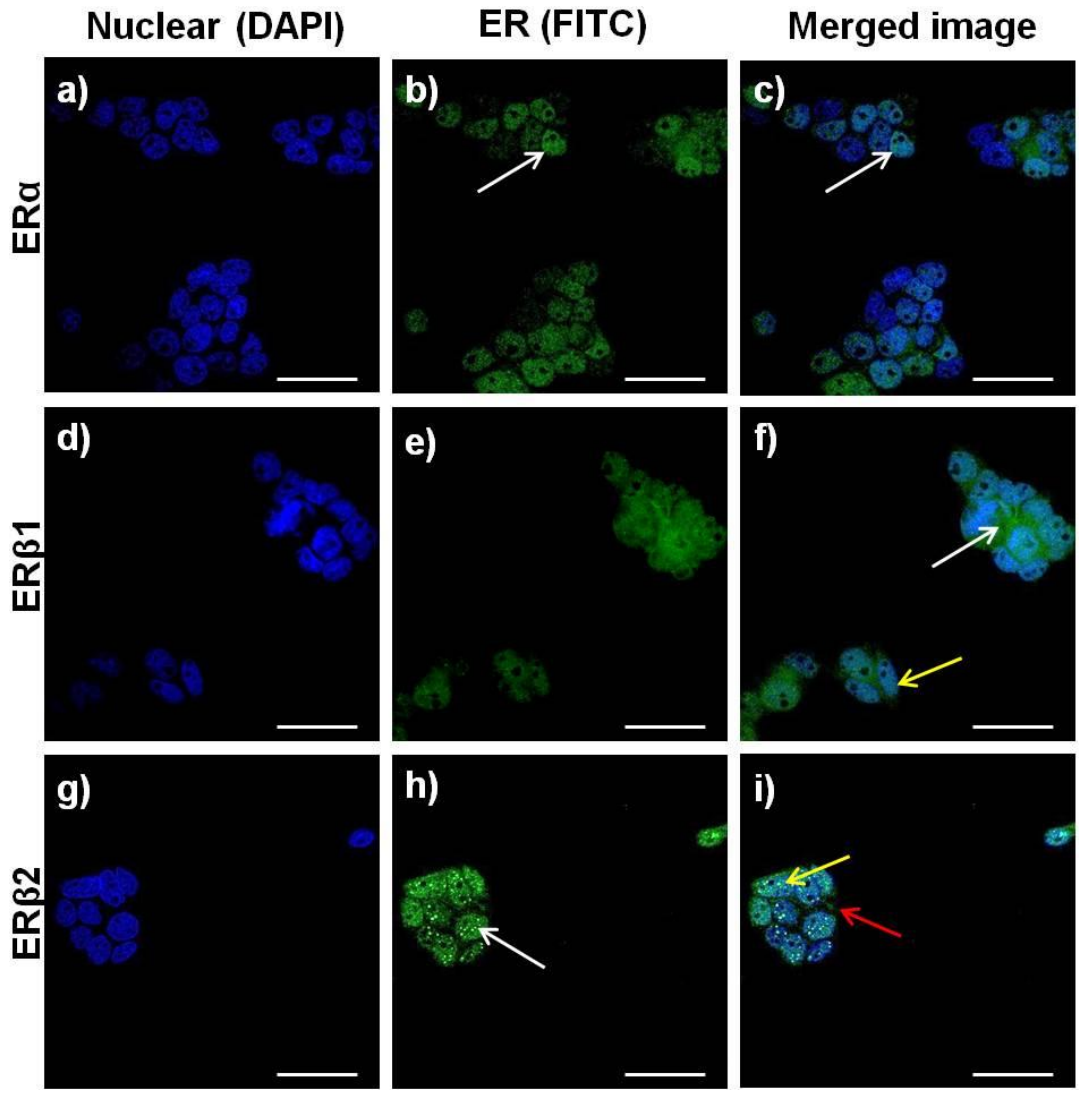

Figure 3.4. Immunofluorescence images of ERα, ERβ1 and ERβ2 expression patterns in the luminal B cell line BT474
(a, d, g) Cell nuclei were labelled with DAPI (blue), (b, e, h) ER proteins are visualised in green (FITC), (c, f, i) Merge image; DAPI and FITC overlaid

ERα expression was present in the nucleus of BT474 cells (white arrow, c)
ERβ1 expression was present in BT474 cells and was nuclear (white arrow, f) and cytoplasmic (yellow arrow, f)
ERβ2 expression in BT474 cells was present in both the cytoplasm (red arrow, i) and in the nucleus (white arrow, h). Nuclear ERβ2 expression was also present as speckles (yellow arrow, i).
60 x magnification. Scale bars =50µm.

3.4.1.3 HER2 Over-expressing Cell Lines

The SKBR3 cell line is representative of HER2 overexpressing breast cancers. Figure 3.5 demonstrates ERβ1 and ERβ2 expression patterns in these cells. All cell lines were negative for ERα staining (data not shown).

ERβ1 staining (b) was nuclear, with intense staining in most cells. Cytoplasmic staining was only visible in the cell undergoing mitosis signified by the white arrow in image (c). In this case cytoplasmic ERβ1 would be expected due to the breakdown of the nuclear membrane. ERβ2 expression (e) was both nuclear and cytoplasmic. Nuclear staining varied in intensity and was stronger in some cells signified by the white arrow in image (e). ERβ2 speckles were also seen in the nucleus of these cells and similar to the other cell types, varied in size, number and intensity (yellow arrow). Cytoplasmic staining was present in all cells analysed shown by the red arrow on image (f).

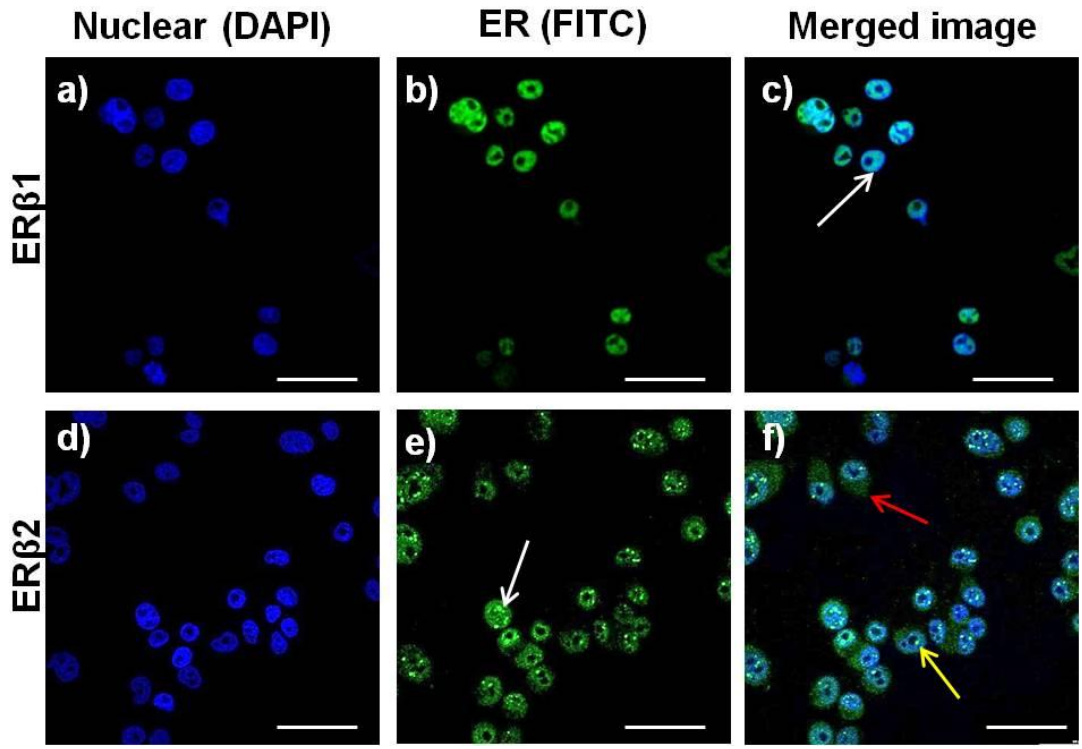

Figure 3.5. Immunofluorescence images of ERβ1 and ERβ2 expression patterns in the HER2 cell line SKBR3
(a & d) Cell nuclei were labelled with DAPI (blue), (b & e) ER proteins are visualised in green (FITC), (c & f) Merge image; DAPI and FITC overlaid
ERβ1 expression in SKBR3 cells was entirely nuclear located (white arrow, c).
ERβ2 expression in SKBR3 cells was present in both the cytoplasm (red arrow, f) and in the nucleus, which was also expressed as ERβ2 nuclear speckles (yellow arrow, f).
60 x magnification. Scale bars =50µm.

3.4.1.4 Basal Cell Lines

Staining for ERβ1 and ERβ2 expression in the basal phenotype cell lines LGI1T, BT-20 and MDA-MB-468 are shown in Figures 3.6, 3.7 and 3.8. All cell lines were negative for ERα staining (data not shown).

Figure 3.6 displays ERβ1 and ERβ2 expression in LGI1T cells. ERβ1 expression in LGI1T cells (b) was nuclear and intense staining can be seen in all cells (yellow arrow, c). There was no evidence of cytoplasmic staining apart from in the cell marked with a white arrow in image (c). This cell is characteristically undergoing mitosis with a rounded overall appearance, unique nuclear shape as a result of the condensed chromatin and has cytoplasmic ERβ1 expression due to a breakdown of the nuclear membrane. This cell line exhibits both nuclear (white arrow, e) and cytoplasmic ERβ2 expression (red arrow, f), and nuclear expression appeared greater indicated by the stronger staining present in the nucleus. Although one or two very small nuclear ERβ2 speckles can be observed in the merge image (f) indicated by the yellow arrow, they were absent from most cells.

ER staining of BT-20 cells is visualised in Figure 3.7. Images b and c illustrate ERβ1 expression in BT-20 cells. Expression was predominantly nuclear indicated by the white arrow in image (c). ERβ2 expression in BT20 cells was both nuclear and cytoplasmic, and the staining intensity was uniform between both compartments, suggesting similar protein levels. The merged image (f) shows very strong cytoplasmic staining which was present in the majority of the cells (red arrow). Nuclear expression was seen in all cells at an even intensity. Nuclear ERβ2 speckles were present in the majority of cells at variable number indicated by the yellow arrow in image (f).

Expression of ERs in MDA-MB-468 cells is illustrated in Figure 3.8. ERβ1 expression demonstrated a nuclear staining pattern indicated by the white arrow in image (c). The intensity of staining was similar between individual cells. MDA-MB-468 cells exhibited cytoplasmic expression of ERβ2, in only a few cells. Cells with

and without cytoplasmic expression are indicated by the red arrows in image (f). ERβ2 nuclear speckles were sparse in MDA-MB-468 cells; however some were still present as indicated by the yellow arrow in image (f).

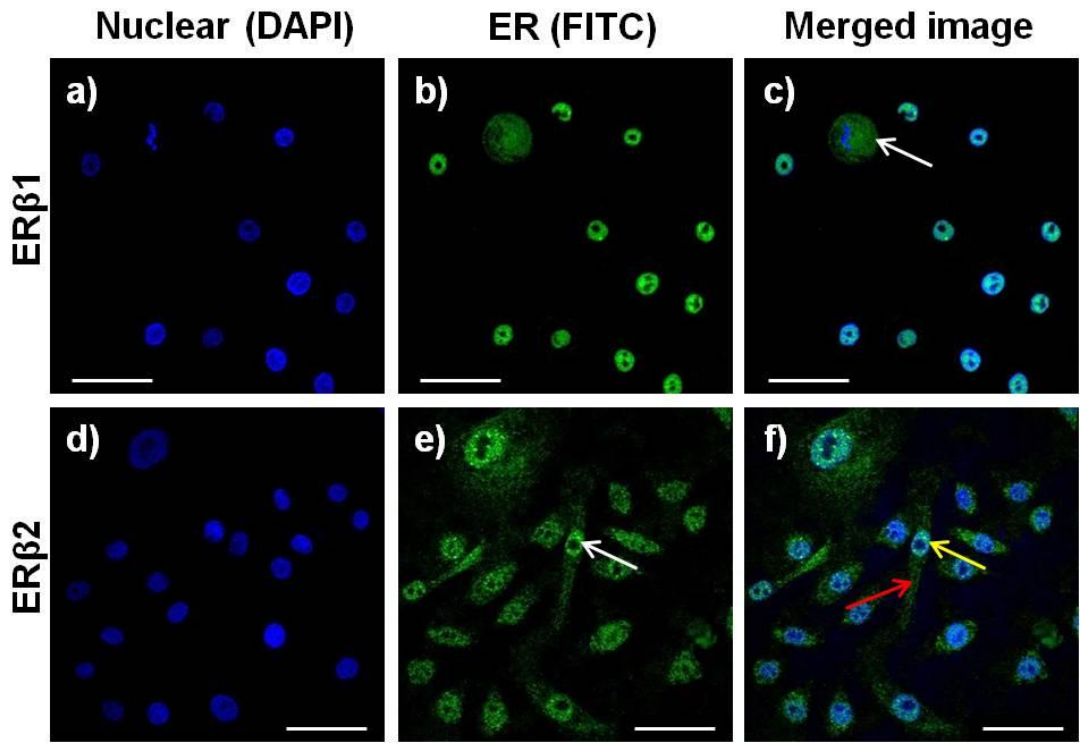

Figure 3.6. Immunofluorescence images of ERβ1 and ERβ2 expression patterns in the basal cell line LGI1T
(a & d) Cell nuclei were labelled with DAPI (blue), (b & e) ER proteins are visualised in green (FITC), (c & f) Merge image; DAPI and FITC overlaid
ERβ1 expression in LGI1T cells was located to the nucleus (yellow arrow, c), except in the cell undergoing mitosis (white arrow, c).
ERβ2 expression in LGI1T cells was present in both the cytoplasm (red arrow, f) and in the nucleus, which was also expressed as ERβ2 nuclear speckles (yellow arrow, f).
60 x magnification. Scale bars =50µm.

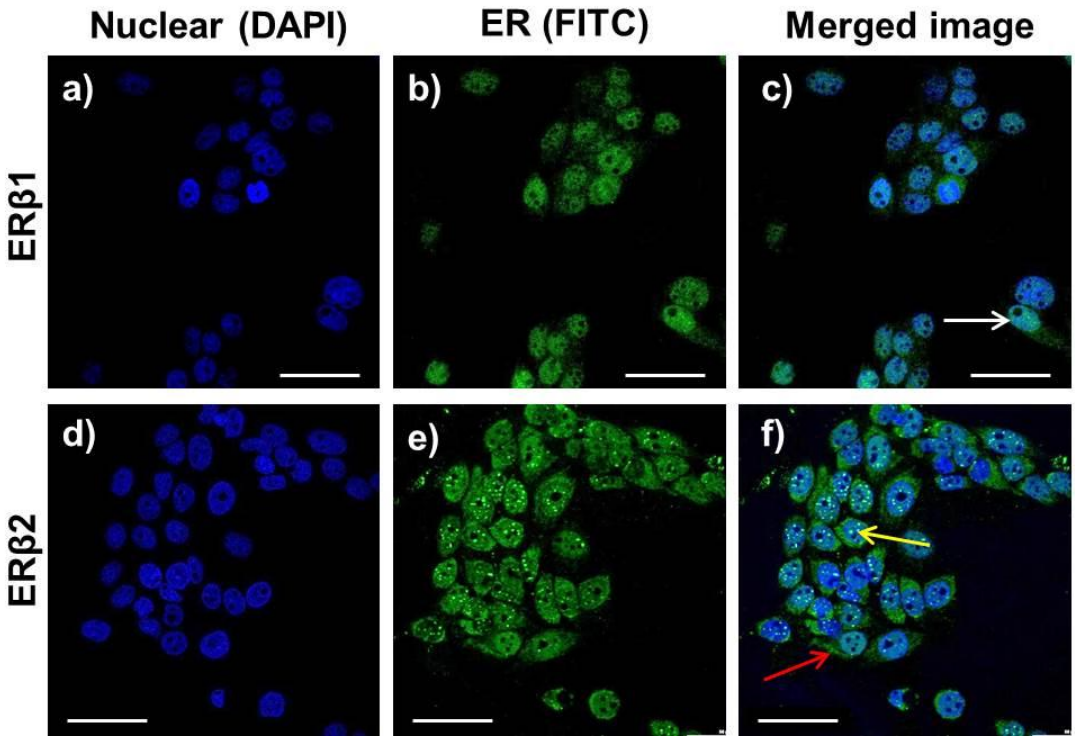

Figure 3.7. Immunofluorescence images of ERβ1 and ERβ2 expression patterns in the basal cell line BT20
(a & d) Cell nuclei were labelled with DAPI (blue), (b & e) ER proteins are visualised in green (FITC), (c & f) Merge image; DAPI and FITC overlaid
ERβ1 expression in BT-20 cells was entirely located to the nucleus (white arrow, c). ERβ2 expression in BT-20 cells was present in both the cytoplasm (red arrow, f) and in the nucleus, which was also expressed as ERβ2 nuclear speckles (yellow arrow, f).
60 x magnification. Scale bars =50µm.

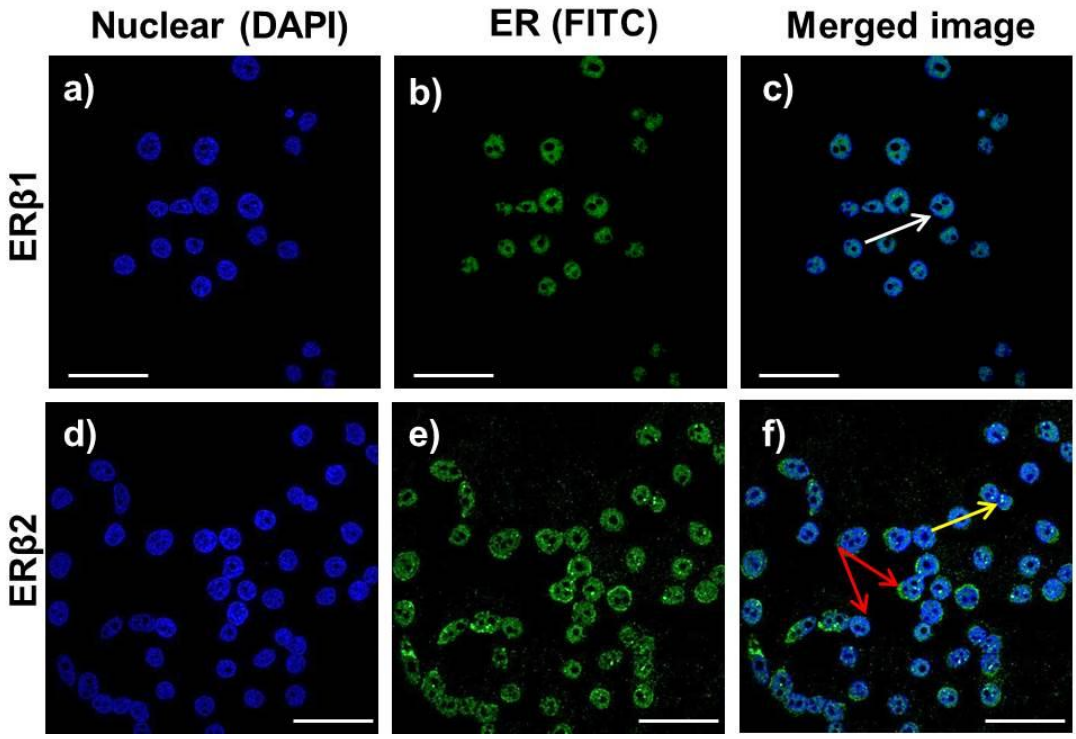

Figure 3.8. Immunofluorescence images of ERβ1 and ERβ2 expression patterns in the basal cell line MDA-MB-468
(a & d) Cell nuclei were labelled with DAPI (blue), (b & e) ER proteins are visualised in green (FITC), (c & f) Merge image; DAPI and FITC overlaid
ERβ1 expression in MDA-MB-468 cells was entirely located to the nucleus (white arrow, c). ERβ2 expression in MDA-MB-468 cells was present in both the cytoplasm (red arrow, f) and in the nucleus, which was also expressed as ERβ2 nuclear speckles (yellow arrow, f).
60x magnification. Scale bars =50µm.

3.4.1.5 Claudin-Low Cell Lines

Figure 3.9 and 3.10 illustrate the ERβ1 and ERβ2 expression patterns in MDA-MB-231 and MDA-MB-436 cells representing Claudin-low subtypes. All cell lines were negative for ERα staining (data not shown).

Expression patterns of ERβ1 and ERβ2 in MDA-MB-231 cells is displayed in Figure 3.9. ERβ1 expression was both nuclear and cytoplasmic. The staining intensity appeared weaker in the cytoplasmic compartment. Image (c) illustrates this with cytoplasmic staining indicated by the red arrow and nuclear by the yellow arrow. Cytoplasmic expression was polar. Nuclear expression was stronger than cytoplasmic and was regular in intensity between individual cells. MDA-MB-231 cells had comparable amounts of ERβ2 in both the nucleus and cytoplasm, demonstrated by the equal staining intensities. Again as with ERβ1, cytoplasmic ERβ2 seemed to localise to one side of the cell, indicated by the red arrow in image (f). This phenomenon was not been seen in any other cell type. ERβ2 nuclear speckles were present in around half of the cells (yellow arrow, f).

Figure 3.10 displays expression patterns of ERβ1and ERβ2 in MDA-MB-436 cells. ERβ1 expression was entirely nuclear indicated by the white arrow in the merge image (c).ERβ2 expression was both nuclear and cytoplasmic. Cytoplasmic staining was slightly weaker than in the nucleus pointed out on the merge image (f) by the red arrow, and was present in all cells. Nuclear staining was stronger indicating increased expression in this compartment. ERβ2 nuclear speckles were very few in number and were only present in a small amount of the cells indicated by the yellow arrow on merge image (f).

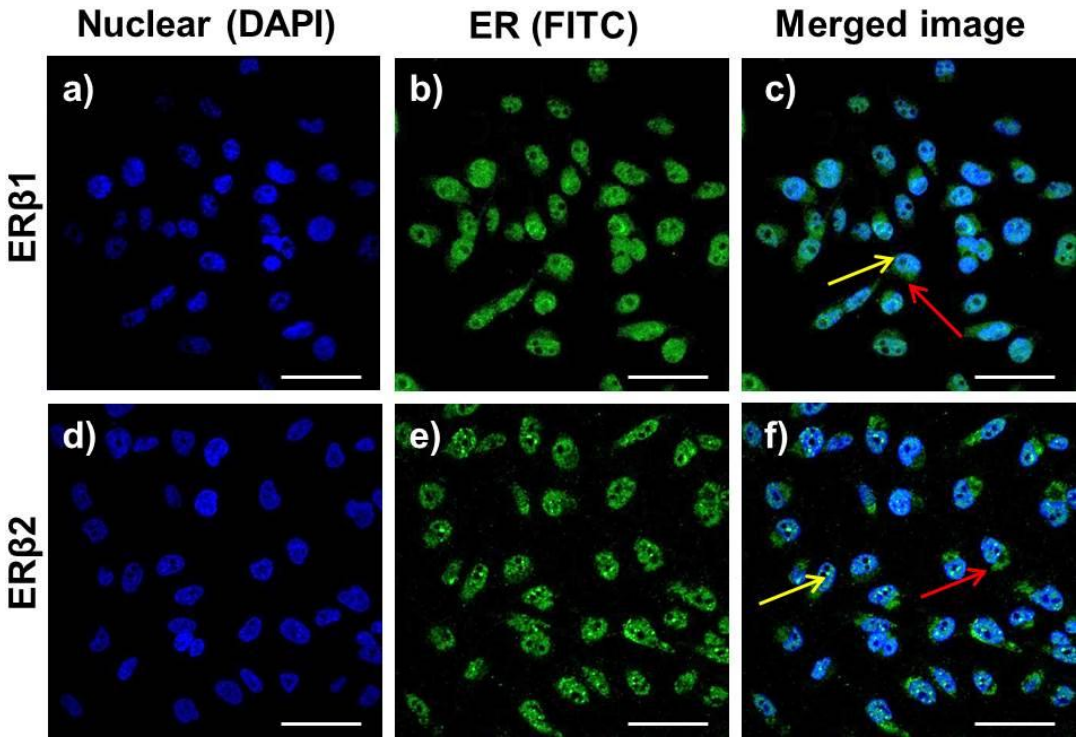

Figure 3.9. Immunofluorescence images of ERβ1 and ERβ2 expression patterns in the basal cell line MDA-MB-231
(a & d) Cell nuclei were labelled with DAPI (blue), (b & e) ER proteins are visualised in green (FITC), (c & f) Merge image; DAPI and FITC overlaid
ERβ1expression in MDA-MB-231 cells was present in the nucleus (yellow arrow, c) and cytoplasm (red arrow, c).
ERβ2 expression in MDA-MB-231 cells was present in the cytoplasm (red arrow, f) and in the nucleus, which was also expressed as ERβ2 nuclear speckles (yellow arrow, f).
60x magnification. Scale bars =50µm.

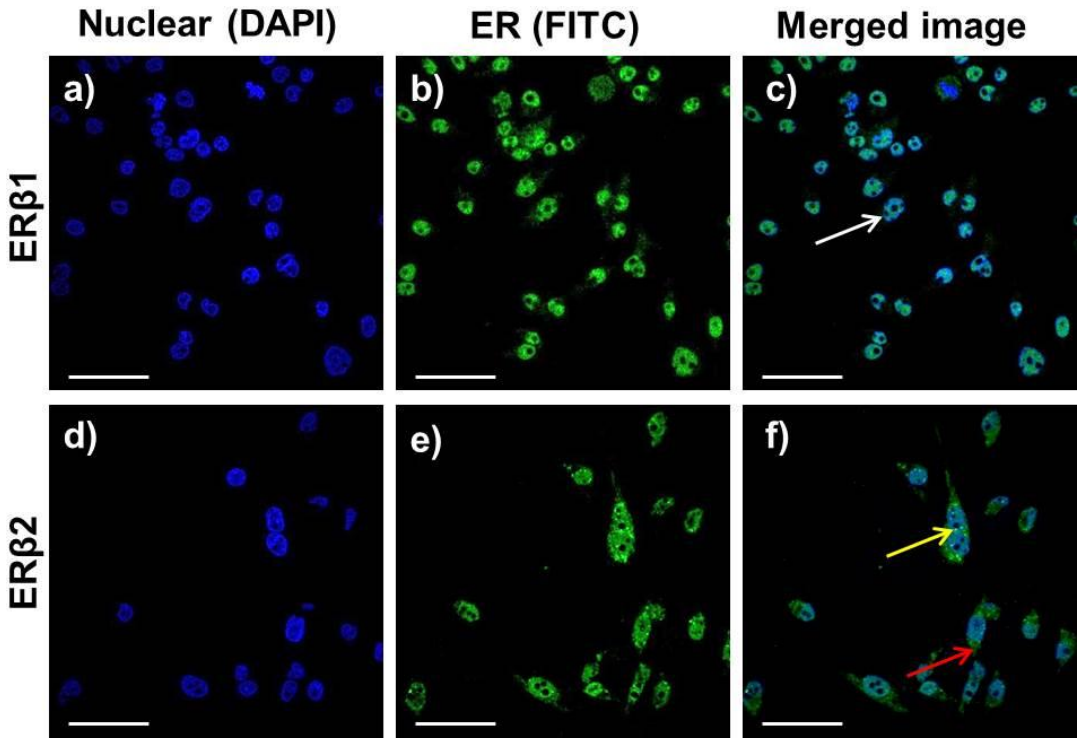

Figure 3.10. Immunofluorescence images of ERβ1 and ERβ2 expression patterns in the basal cell line MDA-MB-436
(a & d) Cell nuclei were labelled with DAPI (blue), (b & e) ER proteins are visualised in green (FITC), (c & f) Merge image; DAPI and FITC overlaid
ERβ1expression in MDA-MB-436 cells was entirely nuclear located (white arrow, c). ERβ2 expression in MDA-MB-436 cells was present in both the cytoplasm (red arrow, f) and in the nucleus, which was also expressed as ERβ2 nuclear speckles (yellow arrow, f).
60 x magnification. Scale bars =50µm.

To summarise the above data, ERα and ERβ1 expression was nuclear except in BT474 and MDA-MB-231 cells where ERβ1 was also detected in the cytoplasm. ERβ2 expression was detected in both the nucleus and cytoplasm in all cell lines. All cell lines exhibited ERβ2 nuclear speckles, however these varied in number and size with the greatest number consistently identified in T47D cells.

3.4.2 Quantification of mRNA expression of ERα, ERβ1 and ERβ2 in breast cancer cell lines

The relative mRNA expression levels of ERα, ERβ1 and ERβ2 were investigated in all 9 cell lines used in this study, and results are presented in Figure 3.11. The aim was to assess the relative amounts of each receptor between the different cell lines, in order to provide more comprehensive information on ER expression patterns in each molecular subgroup. Expression was normalised to the RPLP0 reference gene, which has been validated as a suitable reference gene in breast cancer samples as expression remains stable (162).

As expected from Luminal cell lines, which are inherently defined by their expression of ERα, MCF-7, T47D and BT474 cells all expressed ERα at high levels (Figure 3.11 a). Relative expression levels of ERα in MCF-7 cells were comparable to those of the reference gene RPLP0.

ERβ1 mRNA expression was low across all cell lines. ERβ2 mRNA expression levels was also low, but varied between cell lines. Lowest levels were present in the HER2, Basal and claudin-low cell lines. ERβ2 mRNA levels were greater in the luminal cell lines.

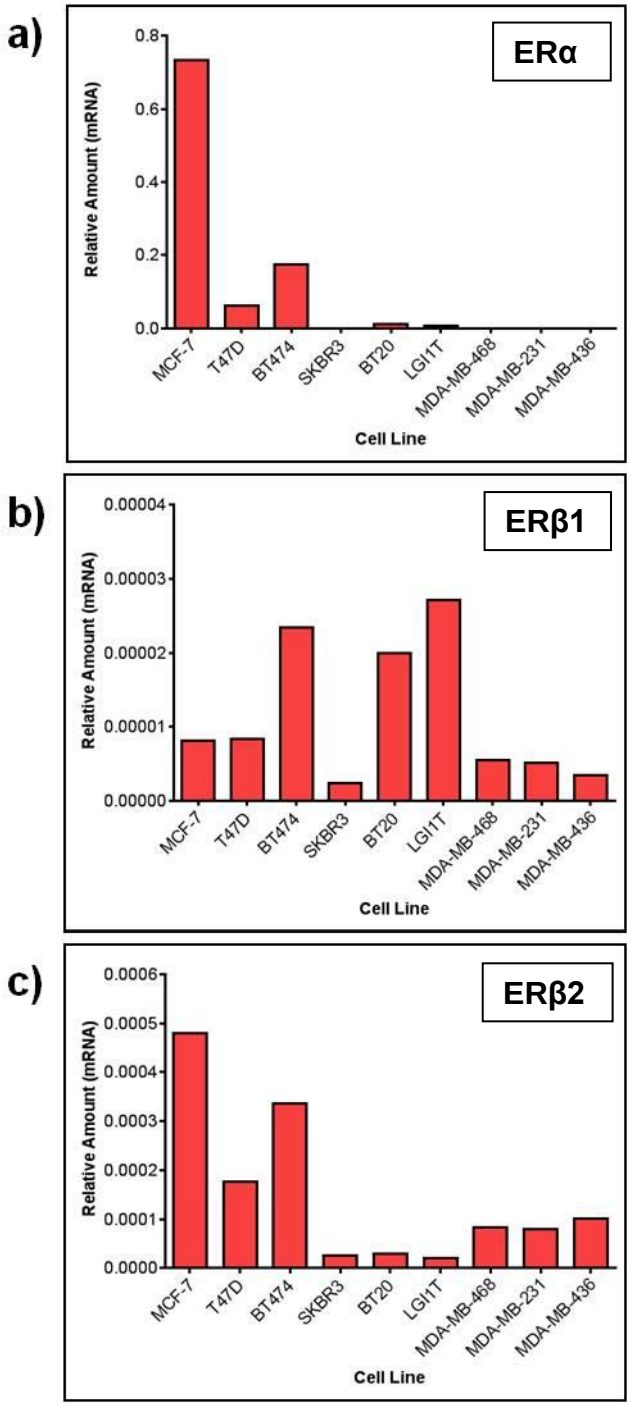

Figure 3.11. mRNA relative expression data of ERs in 9 breast cancer cell lines

Relative mRNA amounts normalised to the mRNA levels in the reference gene RPLP0, which was given the value 1

Relative mRNA expression of (a) ERα, (b) ERβ1 and (c) ERβ2, in breast cancer cell lines

3.4.3 Colocalisation of mitochondria and ERβ2 protein in breast cancer cells lines

As cytoplasmic ERβ2 expression was demonstrated in all cells lines examined except T47D, co-labelling of mitochondria (mitotracker dye) and ERβ2 protein (immunofluorescence) was performed, to determine whether there was any potential colocalisation. All cell lines examined demonstrated colocalisation of the mitochondria and ERβ2 protein. This was quantified in each cell as the degree of red/green channel overlap in the cytoplasm of each cell using Pearson's correlation coefficient which was generated for every cell analysed. Control samples were run by calculating colocalisation of the cytoplasmic protein cyclophilin A with mitochondria to test the robustness of our analysis.

The control antibody cyclophilin A, a protein specifically located in the cytoplasm, was used to determine the levels of colocalisation that would occur by chance. This protein is highly abundant and ubiquitously expressed in the cytoplasm of all cells but importantly not within the mitochondria. Colocalisation values obtained using cyclophilin A antibody likely represent colocalisation by chance and can suggest a cut-off value for true colocalisation allowing better interpretation of results. Figure 3.12 displays the colocalisation results for the controls. The merge images for MCF-7 illustrates no visible signs of yellow staining which suggests there is no colocalisation of cyclophilin A and the mitochondria. This is confirmed when examining the frequency distribution graph, where the graph is skewed to the left and the Pearson's values are low ranging from 0 to 0.3. In MDA-MB-231 cells there initially appears to be some colocalisation of cyclophilin A and mitochondria as parts of the cytoplasm appear yellow in the merge image signified by the white arrow. However upon quantification analysis, it is clear this is not the case, with Pearson's values ranging from 0.1-0.3 shown on the frequency distribution graph.

This further emphasises the importance of eliminating subjectivity and analysing images with a robust and accurate technique to determine true colocalisation. These figures for colocalisation suggest that 0.3 or lower may represent the colocalisation that occurs by chance, where pixels just happen to overlap in an unrelated manner.

The results obtained from the control samples indicated that the observations made in this experiment are robust and that colocalisation of ERβ2 with the mitochondria is occurring, at varying levels, in all cell lines suggesting the protein's presence within this organelle.

The luminal cell lines, MCF-7 (row a) and BT474 (row b), demonstrated some ERβ2 and mitochondrial colocalisation (Figure 3.13, white arrows). These yellow regions are more obvious in BT474 cells possibly due to more intense cytoplasmic ERβ2 staining observed in the FITC image. The quantity of colocalisation for these cell lines is shown in the frequency distribution graphs displaying the Pearson's correlation coefficient values for each cell analysed. The values indicate colocalisation between ERβ2 and mitochondria, which supports the observations made in the image interpretation. The values are skewed to the right in both cell lines, more so in BT474 cells, indicating greater colocalisation as the values increase. The spread of data is greater in BT474 cells with values ranging from 0.1-0.8 whereas values of 0.3-0.8 are observed in MCF-7 cells. This illustrates variability in the extent of colocalisation between individual cells.

In SKBR3 cells, colocalisation of ERβ2 and mitochondria seems apparent in the merged image (Figure 3.14). The white arrows indicate possible colocalisation. Upon quantification, Pearson's correlation coefficient values displayed in the frequency distribution graph indicate true colocalisation, ranging from 0.3-0.8, with a median value of 0.59. As before, this indicates a high degree of variability in the amount of colocalisation between individual cells.

In the basal cell lines illustrated in Figure 3.15, BT20 (row a), LGI1T (row b) and MDAMB-468 (row c) all appeared to display areas of colocalisation (white arrows). This is particularly obvious visually in some MDA-MB-468 cells (row c), where areas of ERβ2 (blue arrow) are also strongly stained with mitotracker dye (yellow arrow), resulting in an intense yellow area on the merged image (white arrow). Although again, the frequency distribution graphs were skewed to the right indicating colocalisation, this was much more apparent for MDA-MB-468 cells, which displayed higher values (0.5 to 0.9), than LGI1T (0.3 to 0.7) and BT20 (0.3 to 0.8). The median Pearson's correlation coefficient values were 0.59 and 0.63 for BT20 and LGI1T respectively, however this average was higher for MDAMB468 at 0.67. MDA-MB-468 cells produced correlation values of 0.5 or above, suggesting these cells displayed some level of colocalisation of mitochondria and ERβ2.

The claudin low cell lines demonstrated the highest levels of colocalisation among all cell lines examined, with the exception of MDA-MB-468 cells. Figure 3.16 illustrates ERβ2 and mitochondria staining in MDA-MB-231 cells (row a) and MDA-MB-436 cells (row b). Both demonstrate very strong areas of yellow staining which are obvious to the eye on the merge (white arrows). As in MDA-MB-468 cells, MDA-MB-436 cells show very intense staining in identical areas on the FITC and Mitotracker image (blue arrows), which when observed in the merged image appears considerably yellow (white arrows). Observations from both merged images suggest a large amount of colocalisation in these cell lines. The frequency distribution graphs confirm this as both are skewed to the right indicating colocalisation, with MDA-MB-436 values ranging from 0.6-0.9, the highest values observed for all cell lines. This also illustrates every cell analysed exhibits colocalisation of ERβ2 and the mitochondria. In MDAMB231 cells the values ranged from 0.2-0.9, which unlike MDAMB436, indicates that not every cell displayed colocalisation of ERβ2 with the mitochondria. The median Pearson's value for MDA-MB-231 and MDA-MB-436 cells was 0.68 and 0.74 respectively.

These are among the highest values demonstrated for all cell lines examined, along those for MDA-MB-468 cells. Median Pearson's values for each cell line is summarised in Table 3.1.

Cell Line	Molecular subgroup	Median colocalisation Pearson's value
MCF-7	Luminal A	0.55
BT474	Luminal B	0.54
SKBR3	HER2	0.59
BT20	Basal	0.59
LGI1T	Basal	0.63
MDA-MB-468	Basal	0.67
MDA-MB-231	Claudin-low	0.68
MDA-MB-436	Claudin-low	0.74

Table 3.1. Summary of the median Pearson's correlation coefficient values for each cell line as a measure of colocalisation quantity, and its relation to molecular subtype.

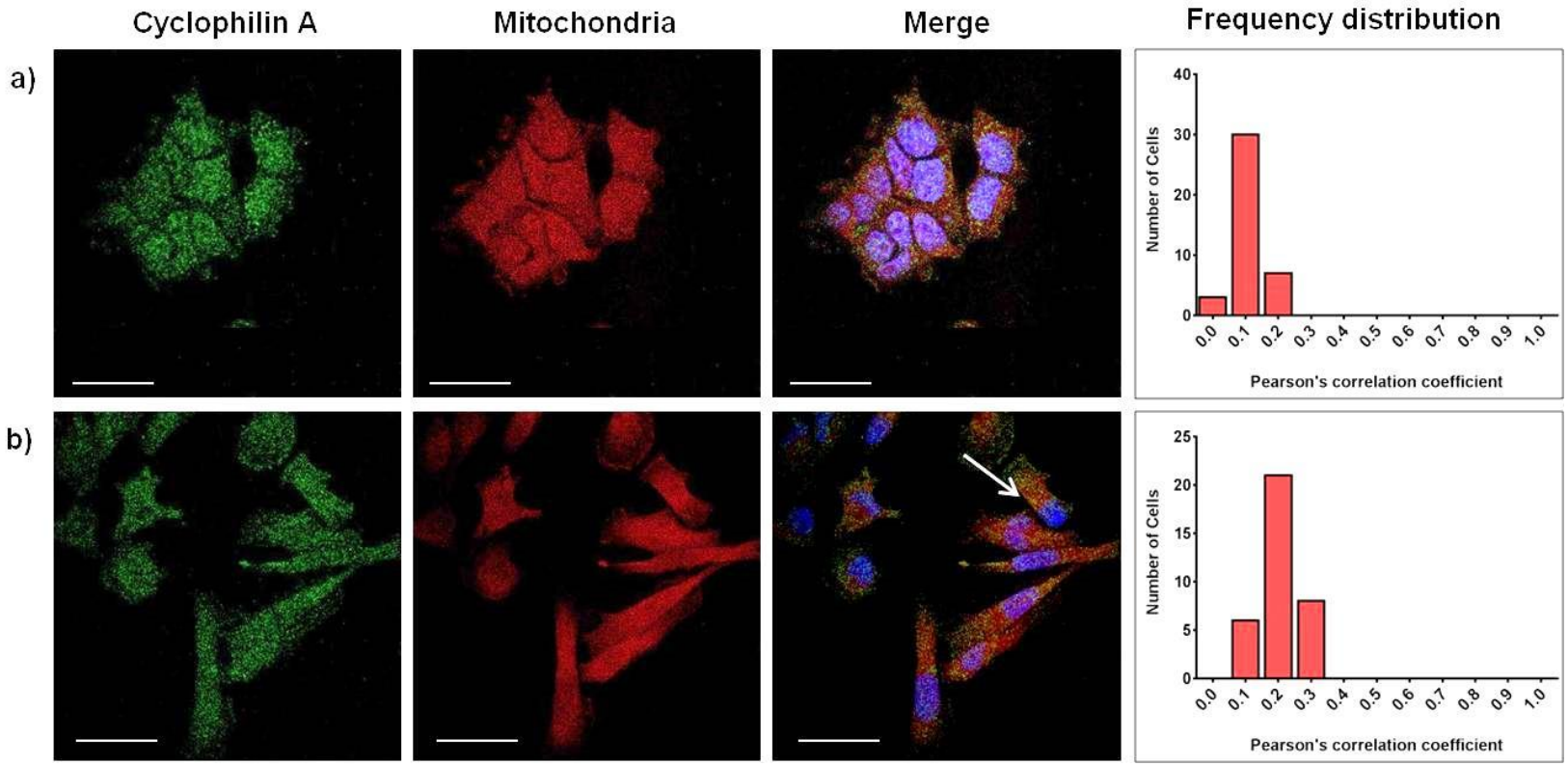

Figure 3.12. Analysis of colocalisation in controls using immunofluorescence of cyclophilin A with the mitochondria in MCF-7 and MDA-MB-231 cell lines, and subsequent generation of colocalisation coefficients for quantification
(a) MCF-7 (b) MDA-MB-231 cells stained with; Cyclophilin A antibody (FITC, green), fluorescent mitotracker® dye (Texas Red, red), and DAPI nuclear stain (blue). A Merge image (overlapped red and green channels) was generated for colocalisation quantification analysis. Areas of visible colocalisation are indicated by the white arrows. Colocalisation was quantified by generation of Pearson's value for each cell and plotted Values plotted on the frequency distribution graph. Pearson's values range from 0, which represents no colocalisation, to 1, complete colocalisation. Images acquired at 60x magnification. Scale bars= 50µm.

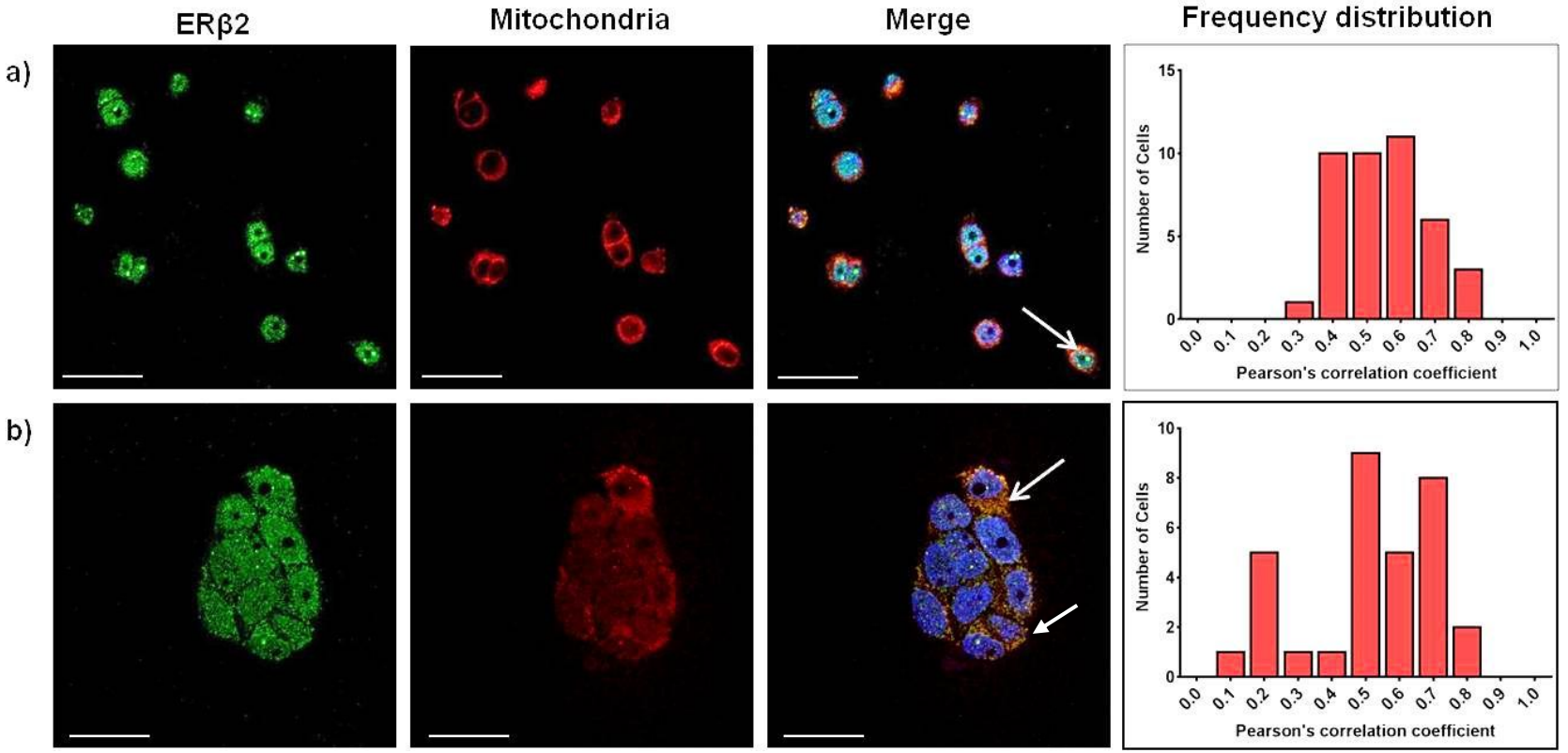

Figure 3.13. Analysis of colocalisation using immunofluorescence of ERβ2 with the mitochondria in Luminal cell lines, and subsequent generation of colocalisation coefficients for quantification

(a) MCF-7 (b) BT474 cells stained with; ERβ2 antibody (FITC, green), fluorescent mitotracker® dye (Texas Red, red), and DAPI nuclear stain (blue). A Merge image (overlapped red and green channels) was generated for colocalisation quantification analysis. Areas of visible colocalisation are indicated by the white arrows. Colocalisation was quantified by generation of Pearson's value for each cell and plotted Values plotted on the frequency distribution graph. Pearson's values range from 0, which represents no colocalisation, to 1, complete colocalisation. Images acquired at 60x magnification. Scale bars= 50µm.

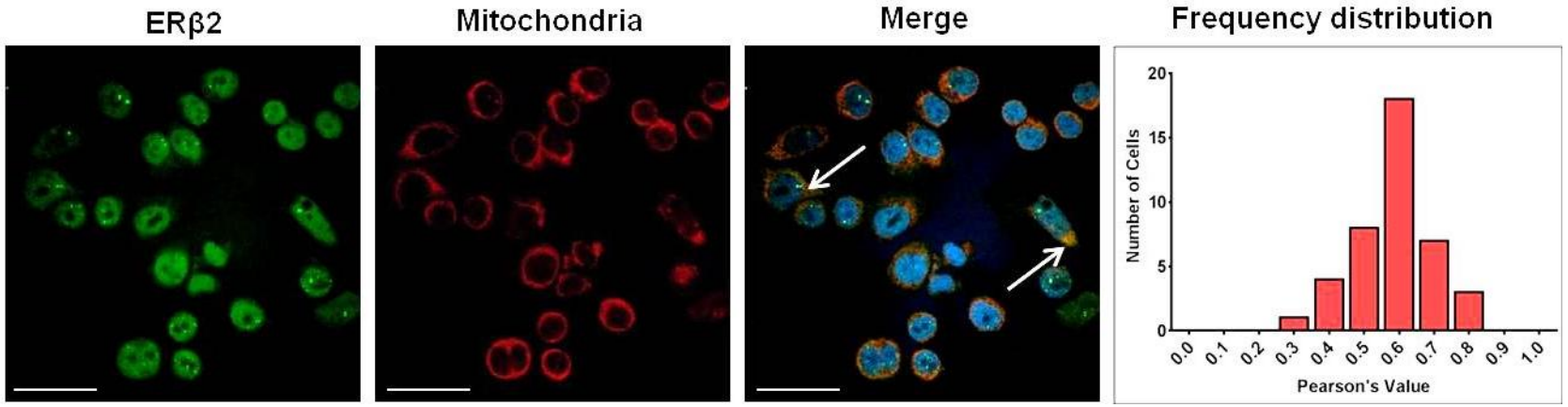

Figure 3.14. Analysis of colocalisation using immunofluorescence of ERβ2 with the mitochondria in a HER2+ cell line, and subsequent generation of colocalisation coefficients for quantification

SKBR3 cells stained with; ERβ2 antibody (FITC, green), fluorescent mitotracker® dye (Texas Red, red), and DAPI nuclear stain (blue). A Merge image (overlapped red and green channels) was generated for colocalisation quantification analysis. Areas of visible colocalisation are indicated by the white arrows. Colocalisation was quantified by generation of Pearson's value for each cell and plotted Values plotted on the frequency distribution graph. Pearson's values range from 0, which represents no colocalisation, to 1, complete colocalisation.
Images acquired at 60x magnification. Scale bars= 50µm.

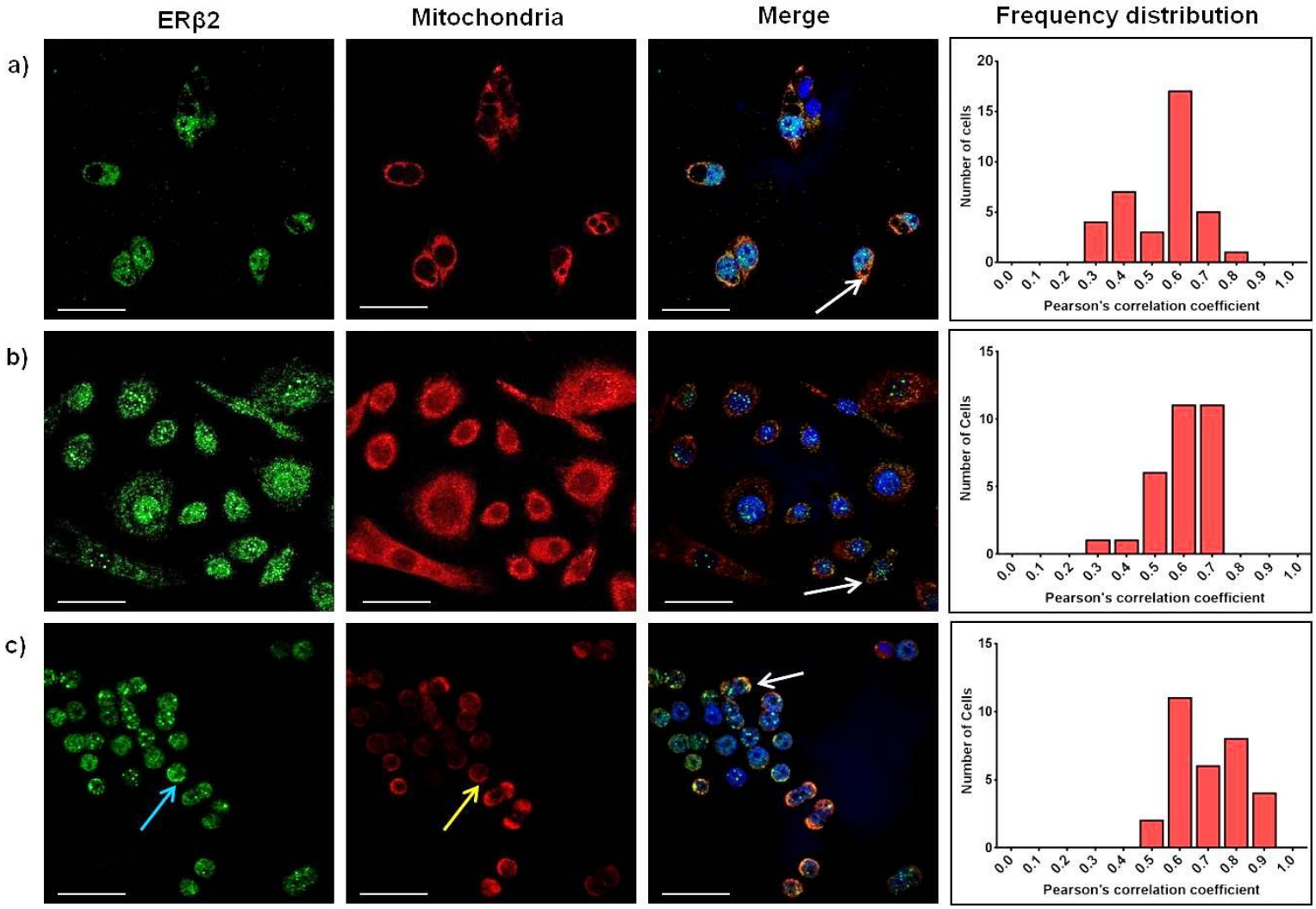
ERβ2
Mitochondria
Merge
Frequency distribution
a)
b)
c)
Number of cells
Number of Cells
Pearson's correlation coefficient
0.0
0.1
0.2
0.3
0.4
0.5
0.6
0.7
0.8
0.9
1.0

Figure 3.15. Analysis of colocalisation using immunofluorescence of ERβ2 with the mitochondria in basal cell lines, and subsequent generation of colocalisation coefficients for quantification

(a) BT-20 (b) LGI1T (c) MDA-MB-468 cells stained with; ERβ2 antibody (FITC, green), fluorescent mitotracker® dye (Texas Red, red), and DAPI nuclear stain (blue). A Merge image (overlapped red and green channels) was generated for colocalisation quantification analysis. Areas of visible colocalisation are indicated by the white arrows. Colocalisation was quantified by generation of Pearson's value for each cell and plotted Values plotted on the frequency distribution graph. Pearson's values range from 0, which represents no colocalisation, to 1, complete colocalisation.

Images acquired at 60x magnification. Scale bars= 50µm.

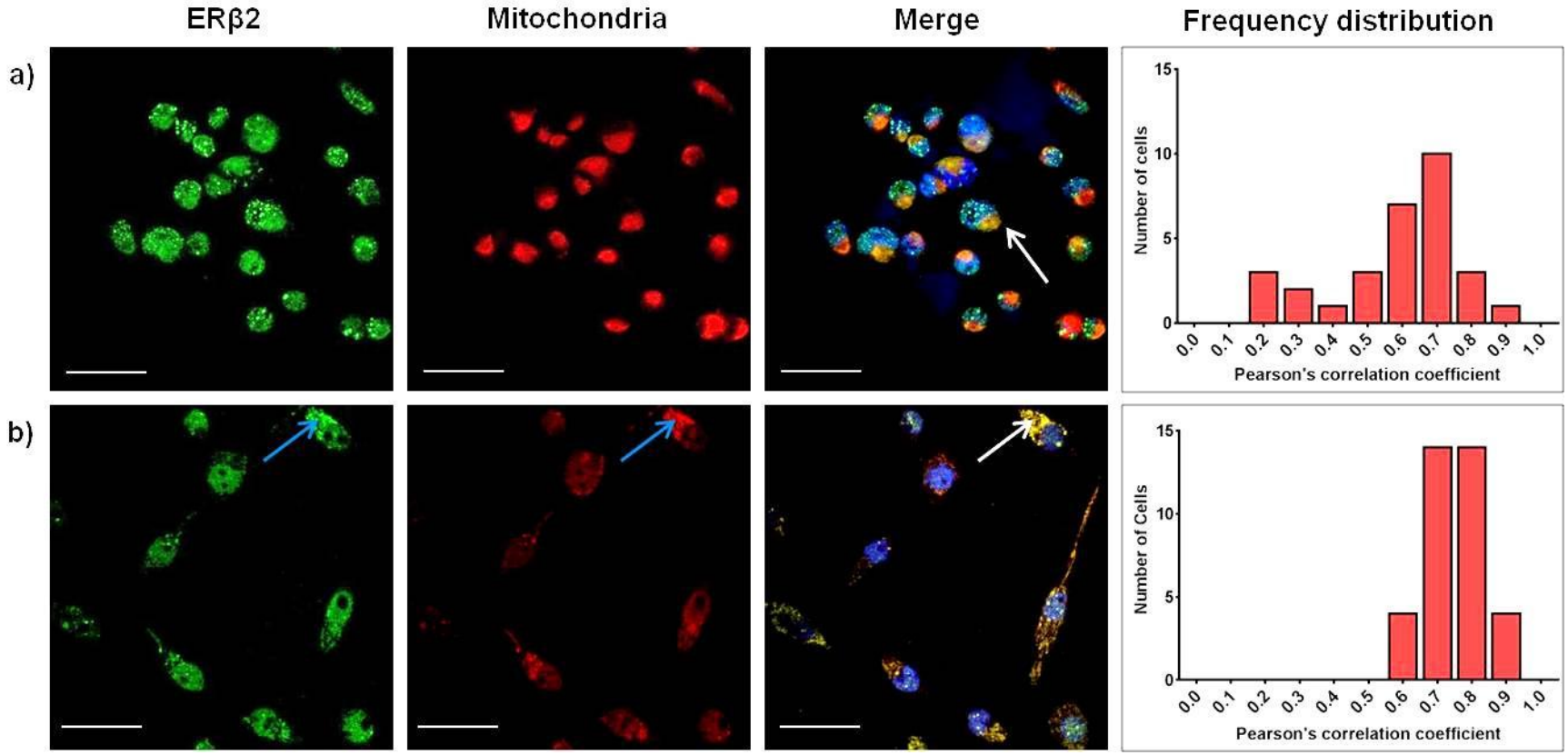

Figure 3.16. Analysis of colocalisation using immunofluorescence of ERβ2 with the mitochondria in claudin-low cell lines, and subsequent generation of colocalisation coefficients for quantification

(a) MDA-MB-231 (b) MDA-MB-436 cells stained with; ERβ2 antibody (FITC, green), fluorescent mitotracker® dye (Texas Red, red), and DAPI nuclear stain (blue). A Merge image (overlapped red and green channels) was generated for colocalisation quantification analysis. Areas of visible colocalisation are indicated by the white arrows. Colocalisation was quantified by generation of Pearson's value for each cell and plotted Values plotted on the frequency distribution graph. Pearson's values range from 0, which represents no colocalisation, to 1, complete colocalisation.

Images acquired at 60x magnification. Scale bars= 50µm.

3.5 Discussion

The results from this chapter have illustrated that ERβ2 is present in both the nucleus and cytoplasm of breast cancer cell lines, whereas ERα and ERβ1 are predominantly expressed in the nucleus. Cytoplasmic ERβ2 colocalised with the mitochondria, suggesting it may be present in this compartment. Nuclear ERβ2 is predominantly expressed as punctate speckled structures.

It is recognised that inactivated ERs reside in the cytoplasm of cells. Ligand activation or trans-activation signalling from other pathways results in activation of the ERs, translocation to the nucleus and dimerisation with other activated ERs to control gene regulation. This would imply nuclear ER is activated whereas cytoplasmic ER is inactive. However, ERs may also have an alternative function in the cytoplasm. ERβ has been implicated in cytoplasmic signalling pathways e.g. p38 MAPK and PI3K/AKT (163-166). ERβ has been identified in the mitochondria of breast cancer cells with levels increasing under E2 stimulation (122) and it is hypothesised that ERβ may contribute to mtDNA gene transcription (122, 123). This suggests ER can be active in the nucleus, cytoplasm and mitochondria, and therefore its presence in each of these compartments may indicate a function. It may therefore be important to examine the subcellular location of ERs in order to determine its function and potential influence on prognosis. We examined ER expression patterns in breast cancer cells and identified their presence in these compartments.

3.5.1 ERβ2 was detected in the nucleus and cytoplasm of breast cancer cell lines

Immunofluorescent examination of the nine cell lines used in this study, which are representative of five major molecular subgroups (36) with the addition of the claudin-low group (37), revealed expression of ERα was observed only in the

luminal A cells, MCF-7 and T47D, and luminal B cells, BT474. The luminal breast cancers are partly defined by their expression of ERα so these results were as expected. Expression of ERβ1 protein was present in all cell lines, and similarly in the literature ERβ1 is present across all molecular subgroups (74, 87). Expression was predominantly confined to the nucleus and again this was also reflected in the literature (75, 86, 87). This suggests the cell lines used are representative of the ERβ1 expression patterns seen in patient tumours (74, 94).

ERβ2 exhibited both nuclear and cytoplasmic staining in all cell lines. Expression in both cellular compartments has also been reported in the literature, and location is demonstrated to affect prognosis. Nuclear ERβ2 is associated with good prognosis and overall survival whereas cytoplasmic is poor prognostically (94, 100). The same prognostic capacity has been observed in ovarian cancer, with cytoplasmic expression correlated with a poor prognosis (102). In addition cytoplasmic ERβ2 expression has been demonstrated to correlate with poor response to chemotherapy compared to nuclear ERβ2 (167). These prognostic differences suggest this receptor may have alternate function depending upon its location in the cell. This potential double edged functionality may explain some of the controversy in the literature regarding whether ERβ2 is ‘good or bad’. Some studies report ERβ2 presence to be associated with a good clinical outcome (75, 90, 96), whereas others report ERβ2 presence is associated with poor outcome (152). There are also studies that have made no correlation between ERβ2 presence and clinical outcome (91, 99, 168). It is only when its subcellular location is examined that these controversies may become resolved. My results also reveal that ERβ2 expression was observed across all molecular subgroups and in both the cytoplasm and nucleus. Expression in both compartments may suggest a function for ERβ2 in each. In T47D cells cytoplasmic staining was weaker. This may be due to the high

intensity of nuclear staining, specifically the speckles, and therefore requiring the images for this cell line to be acquired at lower gain settings.

An interesting observation was made concerning ERβ2 and ERβ1 expression patterns in MDA-MB-231 cells. Cytoplasmic expression appeared to be located on one side of the cell nucleus in the majority of cells, and when we stained the mitochondria, they too were observed on the same side of the cell nucleus. MDA-MB-231 is an aggressive cell line known for its invasive capacity (169). It has been described in the literature that the mitochondria regulate invasion and migration in breast cancer cells (170). A correlation has been observed between mitochondria localisation to the anterior leading edge of the cell and faster migration (171). We have observed that, not only do the mitochondria localise to one side in some MDA-MB-231 cells, but this colocalises with ERβ2, also on the same side of the cell. This may suggest that ERβ2 is involved in migration/invasion processes when located in the mitochondria.

3.5.2 ERβ2 nuclear speckles were detected in the nucleus of breast cancer cell lines

All cell lines exhibited a speckled pattern of ERβ2 expression in the cell nucleus, which was not observed when cells were stained using ERα or ERβ1 antibodies. These speckles varied in number and size. T47D cells demonstrated the most and largest ERβ2 speckles, present in every cell. Some cell line such as MDA-MB-436, MDA-MB-468 and LGI1T had very few speckles and not every cell possessed them. Speckles were also entirely nuclear located. Z-stack images for each cell line were done and a 3D reconstruction of the cells performed. This 3D reconstruction could be manoeuvred in the Elements software in order to inspect each cell in detail, and we found that no speckles were located outside the blue DAPI stained nucleus (data not shown). No correlations have been made between speckle numbers and molecular subgroup; however it did appear that there may be fewer

ERβ2 nuclear speckles in triple negative cell lines compared to ERα or HER2 positive cells.

Nuclear ERβ2 is suggested to be good prognostically (94, 100), however it is unknown whether presence of ERβ2 nuclear speckles is also indicative of good clinical outcome. Reduction in nuclear ERβ2 speckles in TNBC cells could indicate poorer outcome which correlates with the more aggressive nature of this molecular group.

ERβ2 nuclear speckles are an observation made in this study and in previous work within the Breast Research Group at Leeds. In a related study by our group nuclear speckles were also observed using an antibody that detects ERβ1 phosphorylated at serine 105. These correlated with better survival and with ERβ1 and ERβ2 expression (172). ERβ2 speckles will be further investigated in chapter 5.

3.5.3 mRNA expression of estrogen receptors in breast cancer cell lines

As immunofluorescence does not give an accurate measure of relative expression, we were unable to compare the levels of ERs between cell lines, only its presence and location within the cell. We performed qRT-PCR analysis of ERα, ERβ1 and ERβ2 expression levels (Figure 3.11) to quantify the amount of ER transcripts in each cell line. This is not a measure of protein expression but it does give an indication of what it may be if mRNA is translated. Although there are some incidences where mRNA does not correlate with protein (88, 90, 173) likely due to post-transcriptional regulation, in most cases positive correlation is observed. Investigation of ERβ1 and ERβ2 protein and mRNA levels in 150 breast tumours, found protein levels significantly correlated with mRNA levels (75). Only the luminal cell lines, MCF-7, T47D and BT474 expressed ERα mRNA. ERβ2 mRNA expression was greatest in these three cell lines suggesting the two receptors may correlate. Other studies have described a significant correlation between protein levels of ERβ2 compared to ERα (75, 94), which corroborates out data. The HER2,

Basal and claudin-low cell lines all demonstrated lower levels of ERβ2 expression with only small variation between cell lines, but at these very low endogenous levels these changes are difficult to interpret. ERβ1 mRNA expression levels were variable across all cell lines with no apparent association with molecular subgroup. This is comparable with data presented in the literature, which examined ERβ1 protein expression between molecular groups (74, 87).

3.5.4 ERβ2 colocalised with the mitochondria in breast cancer cell lines

It has been established in the literature that ERβ does have a presence and potential function in the mitochondria (121, 122, 174). Currently, only ERβ1 or total ERβ, where specific isoform involvement was not specified, has been studied in relation to a potential activity within mitochondria. As we observed that ERβ1 was not expressed in the cytoplasm of most of our cell lines, but ERβ2 was, we wanted to investigate if this cytoplasmically located ERβ2 colocalised with the mitochondria and if there was an association between the amount of colocalisation and the molecular subgroup. This not only indicated ERβ2 was present in the mitochondria, but may suggest ERβ2 has a potential function within this organelle.

All cell lines examined displayed some ERβ2 and mitochondria colocalisation. This was more obvious in some cell lines where regions of yellow could be visualised on the merge immunofluorescent images. In some cases however, colocalisation was only identified after automated quantification such as in LGI1T where a yellow colour in the merge image was less visible. The median values of colocalisation for each cell line summarised in Table 3.1, demonstrates that the basal cell lines display the highest levels of colocalisation with MDA-MB-436 displaying the highest level.

The triple negative phenotype is generally representative of a more aggressive breast cancer cell with a poorer prognosis and outcome (27-29). Cytoplasmic ERβ2

has also been linked to poorer prognosis and outcome (100, 102). This may suggest mitochondrial ERβ2 is implicated in these poorer outcome tumours.

3.5.5 Interpretation of colocalisation

One major pitfall of colocalisation experiments is the interpretation of colocalisation itself. Most studies rely on interpretation of this by eye as yellow regions (if proteins are labelled with green and red fluorophores). However this is extremely subjective and consistency between images is not guaranteed. Misinterpretation of colocalisation or subjective inaccuracies adds to the importance of automated quantification.

As already mentioned in 3.1.4, colocalisation described the spatial overlap of the signal of two labelled proteins (157), and does not provide proof that the two interact. However by taking into consideration of colocalisation that occurs by chance, whereby pixel signal overlaps without there being a true relationship between the two, we can say interaction is likely. Interpretation of our results relied on taking this into account, and by generating Pearson's values, which can describe the degree of correlation between the two proteins. Our measure of colocalisation by chance by staining cyclophilin A and mitochondria did not exceed a value of 0.3, suggesting little correlation. This validated our method for calculating colocalisation by chance and strengthens our true colocalisation data, as median values for each cell line ranged from 0.54-0.74, suggesting spatial overlap was more than by chance occurrence and suggesting possible interaction between ERβ2 and the mitochondria. Another more complex method described in the literature to take into account the occurrence of colocalisation by chance during colocalisation experiments is referred to the Costes method (175) . This method is a complex but very accurate way to eliminate by chance colocalisation for each individual image or even cell negating the need to run separate control samples. Images are divided into small squares them randomly scrambled and colocalisation measured. This is

done numerous times and images ‘pass’ if 90% of the Pearson’s values are lower in the scrambled images than the real image. As each image is its own control it also improves accuracy. Other methods aside from image scrambling include one described by Babbey et al (2006) (176). The method involves acquiring the image and then rotating either the green or red image 90 degrees. This leads to random placement of the pixels from one channel on top of the other and then enables generation of a colocalisation by chance value for that particular image. Ideally image scrambling methods could have been employed in this study as they are widely regarded as efficient ways of measuring true colocalisation; however the resources and technology to carry this out were not available to us. The large number of cells analysed demonstrating reproducibility and the use of our two unrelated probes to measure colocalisation by chance does provide an accurate alternative approach to these methods.

3.5.6 Coefficient selection

For this experiment, where the red/green pixel intensity data was demonstrated to be linear, the Pearson’s coefficient correlation was deemed the most suitable metric to use to measure colocalisation. The robust nature and simplicity of the Pearson’s correlation coefficient and its negation of user bias and image pre-processing and differences in acquisition settings as experiments were performed at different times, meant it was the more appropriate coefficient to use. For this experiment the information gained from generation of Pearson’s values enabled us to ascertain that a true interaction between ERβ2 and mitochondria was likely.

3.6 Summary

Immunofluorescent analysis has demonstrated that ERs are differentially expressed across molecular subgroups of breast cancer cells. ERα is expressed

predominantly in the nucleus of luminal cell lines. ERβ1 is expressed in cells across all molecular subgroups and is generally located in the nucleus; however some cell lines do demonstrate weak cytoplasmic staining. ERβ2 has been observed in both the nucleus and cytoplasm of all cell lines examined. Intensity of staining varies in both compartments, but generally stronger cytoplasmic expression was observed in the triple negative cell lines. Increased expression of ERβ2 in the cytoplasm in the more aggressive triple negative cell lines, correlates with the observation that cytoplasmic ERβ2 is a poor prognostic marker, as triple negative cancers usually have the worst prognosis. Colocalisation immunofluorescence studies have also identified that cytoplasmic ERβ2 does colocalise with the mitochondria, with the highest levels correlated with the triple negative phenotype. This may point towards a function for cytoplasmic ERβ2 within the mitochondria. The mitochondria are the powerhouse of cells and a large number of processes are associated with this organelle e.g. migration, proliferation, apoptosis. The suggestion of a functional role for ERβ2 in the mitochondria certainly deserves further study. A speckled pattern of nuclear ERβ2 expression was observed in all cell lines. These speckles varied in number and size; the luminal A cell line T47D contained the most, whereas the fewest were detected in triple negative cell lines. The significance of these speckles is as yet unknown, but will be further investigated in chapter 5.

4.0 Chapter 4: Generation of ERβ2 overexpressing cell lines for functional analysis of ERβ2 in breast cancer

4.1 Introduction

4.1.1 ERβ2 overexpression studies

Only a handful of studies have examined the functional effect of ERβ2 by overexpression in breast cancer. Omoto et al (2003) (104) stably expressed ERβ2 in MCF-7 cells. They examined the effect on growth using serum starvation to initiate G1/0 arrest and analysed the cell cycle distribution. ERβ2 overexpression resulted in a reduced S-phase population. Also to assess growth, an anchorage-independent colony formation assay was performed. Fewer colonies were formed under E2 exposure and none formed without E2 in the ERβ2 overexpressing cells, compared with control cell lines where colonies formed in both, suggesting ERβ2 impairs growth in MCF-7 cells. They also reported that ERβ2 oppositely regulated a subset of genes compared to ERβ1. This suggests ERβ2 has a distinct function from ERβ1 in MCF-7 cells. Zhao et al, 2007 (95) stably overexpressed ERβ2 using an inducible expression system where ERβ2 was overexpressed in MCF-7 cells upon doxycycline treatment. The authors reported that ERβ2 induced proteasome-dependent degradation of ERα by forming a heterodimer with ERα. They also noted that expression of ERβ2 inhibited recruitment of ERα to the ERE's, resulting in suppression of ERα-regulated genes.

Despite this suggested tumour suppressive nature of ERβ2, studies examining the effect of ERβ2 over-expression on ERα negative cell lines in breast are lacking. The function of ERβ2 has been investigated in prostate cancer cell lines, which are inherently ERα negative. In this setting ERβ2 increased proliferation and was demonstrated to upregulate c-myc, which promotes proliferation. It was also

revealed to upregulate factors involved in bone metastasis (106). This data suggests that ERβ2 may be oncogenic in prostate cancer.

4.1.2 ERβ2 target genes

Very few ERβ2 target genes have been identified partly due to the lack of ERβ2 functional studies. ChIP-Seq and RNA-Seq studies have identified ERβ1 gene targets. ERβ2 regulates nuclear genes by heterodimerisation with ERβ1 or ERα; consequently many of these genes identified may also be regulated by ERβ2. However it is unclear what affect ERβ2 has on gene targets when dimerisation occurs especially with ERβ1. Omoto et al (2003) (104) performed microarray analysis on a subset of genes and compared their regulation in ERβ2 overexpressing cells to ERβ1 overexpressing cells and wild-type cells. They discovered that there were a number of genes that were differentially regulated when ERβ2 was overexpressed compared to ERβ1 overexpressing cells and wild type cells. These included some that were down-regulated such as histone deacetylase 6 (*HDAC6*), cell division cycle 6 homolog (*CDC6*) and retinoblastoma binding protein 8 (*RBBP8*), and some genes that were up-regulated e.g. ERα and aconitase 2 mitochondrial (*ACO2*). The regulation of these genes by ERβ2 could indicate tumourigenic or tumour suppressive effects on the cells, indicating the complexity of ERβ2 and its function in breast cancer cells. In addition, ERβ2 differentially regulates c-myc and cyclin E in prostate cancer cells (106) compared to ERβ1 overexpressing cells. It therefore appears ERβ2 may oppose the action of ERβ1.

4.1.3 Mitochondrially transcribed genes and ERβ

Mitochondria contain small circular genomes containing genetic information for components involved in oxidative phosphorylation. This mitochondrial DNA (mtDNA) is around 16500 base pairs in size and encodes 13 protein coding genes, 22 transfer RNA (tRNA) genes, 2 ribosomal RNA (rRNA) genes (177) and a more recently identified peptide coding gene humanin (178). The proteins coded for by mtDNA are all involved oxidative phosphorylation, a process whereby the cell can produce ATP or energy. mtDNA has a D-loop region, which contains the promoters for gene transcription and also controls mtDNA copy number. As previously identified in chapter 3, ERβ2 localises to the mitochondria. This suggests that ERβ2 may have a function within this organelle. As discussed in chapter 1, an ERβ binding site has been identified in the D-loop of mtDNA by Grober et al (2007) (47); suggesting ERβ may be involved in the regulation of mtDNA gene transcription. However ChIP-Seq analysis of ERα binding sites did not identify one in the mtDNA suggesting ER mediated mtDNA transcription is regulated by ERβ isoforms only. A study in normal breast epithelial cells revealed the expression of the mtDNA transcribed genes *CO1*, *CO2* and *ND1* increased upon ERβ1 activation, suggesting ERβ1 has a role in regulation of some mtDNA genes (122). Similarity, upregulation of mitochondrial respiratory complex IV genes was reported in cardiac tissue of rats following trauma when mitochondrial ERβ levels rose (123). None of these studies have investigated ERβ2's role in the mitochondria. However, in ovarian cancer ERβ2 has been demonstrated to locate to the mitochondria where it interacts with BAD, resulting in inhibition of BAX oligomerization and subsequent apoptosis inhibition (153). This demonstrates one role for ERβ2 in the mitochondria, but its involvement in mtDNA gene transcription is as yet unknown.

4.2 Aims

This chapter aimed to investigate the functional role of ERβ2 in ERα positive and negative breast cancer cell lines by examination of:

- the effect of ERβ2 overexpression on cell growth, cell cycle distribution and migration
- expression levels of potential nuclear target genes that may be regulated by ERβ2
- expression levels of mitochondrially transcribed genes involved in the electron transport chain in ERβ2 overexpressing cells
- the effect of estrogenic ligands on ERβ2 protein levels in the cytoplasm, nucleus and mitochondria

4.3 Results

The protein coding sequence for ERβ2 was cloned into a retroviral overexpression vector and four breast cancer cell lines were transduced to overexpress ERβ2 using this vector. These cell lines were examined for functional changes compared to control cell counterparts, to investigate the role ERβ2 plays in breast tumourigenesis.

4.3.1 Generation of ERβ2 overexpressing cell lines

Although the cloning and transfection/transduction processes were part of the methodology to generate ERβ2 overexpressing cells, which are detailed in section 2.15, the results from each step are described below.

4.3.1.1 Recombination cloning

ERβ2 fragments were amplified from a pcDNA-ERβ2 vector from 4 PCR reactions each using different annealing temperatures in order to obtain optimal amplified fragment yield, and the PCR products were visualised on an agarose gel displayed in Figure 4.1a. All reactions produced a clean band at an expected 1.5kb, so were combined, purified and used in the recombination reaction. Fragments were inserted into the cut pFB-NeoFLAG3 vector, and transformed into DHα E. coli. Sixteen positive colonies were picked and grown up in LB broth containing ampicillin, purified and digested with EcoR1. Figure 4.1c1 illustrates the EcoR1 sites in the construct. Figure 4.1b represents the 16 digested colonies run on an agarose gel labelled 1-8 and 10-17, with a 10kb ladder for size reference. Samples 9 and 18 were the original pCDNA3-ERβ2 vector also cut with EcoR1 for comparison. This vector is smaller so leftover template DNA from the reaction that may have been taken up by the competent DHα E coli produced bands of approximately 1.1kb and 6kb. Clones positive for ERβ2 incorporation into the vector produced 2 bands, one at ~7kb and another at 1.1kb. Clones displaying a smaller

molecular weight first band of ~6kb were potentially template DNA. Potential positive clones were identified (8 and 11) and together with a possible template DNA clone (5) were diluted and run out on agarose again to produce clearer bands in order to determine the molecular weight more accurately, illustrated in Figure 4.1c2. Sample 5 was discarded as a potential pCDNA3 ERβ2 template clone as the largest band was smaller at around 6kb. Samples 8 and 11 were believed to be possible positive pFB-NeoFLAG3-ERβ2 clones. To further confirm positive clones, a digest using EcoRV was performed and Figure 4.1d1 depicts where the cutting sites are in the construct. Three bands were visualised when the samples were run on agarose for both clones at the predicted sizes of 2150bp, 2800bp and 3050bp displayed in Figure 4.1d2, suggesting the ERβ2 coding sequence had been successfully incorporated into the retroviral vector. DNA from clones 8 and 11 was purified and sequenced to confirm the presence of ERβ2 coding region in the pFB-NeoFLAG3 vector. Alignment of the sequence from the clones to the ERβ2 coding sequence from the BLAST database confirmed 100% similarity and confirmed the insertion was in frame after the FLAG epitope. Clone 8 was used in this study. The DNA was transfected in phoenix A packaging cell lines, which produced virus particles containing the vector DNA. These viral particles once harvested, were transduced into MCF-7, T47D, MDA-MB-231 and MDA-MB-468 cells. Separate 'negative' counterparts were also made using the pFB-NeoFLAG3 vector only transduced into these 4 cell lines in the same way, which did not express ERβ2. Selection based on antibiotic resistance for cells that had successfully incorporated the pFB-NeoFLAG3-ERβ2 DNA or the vector only (pFB-NeoFLAG3) into their genome was performed using geneticin (G418).

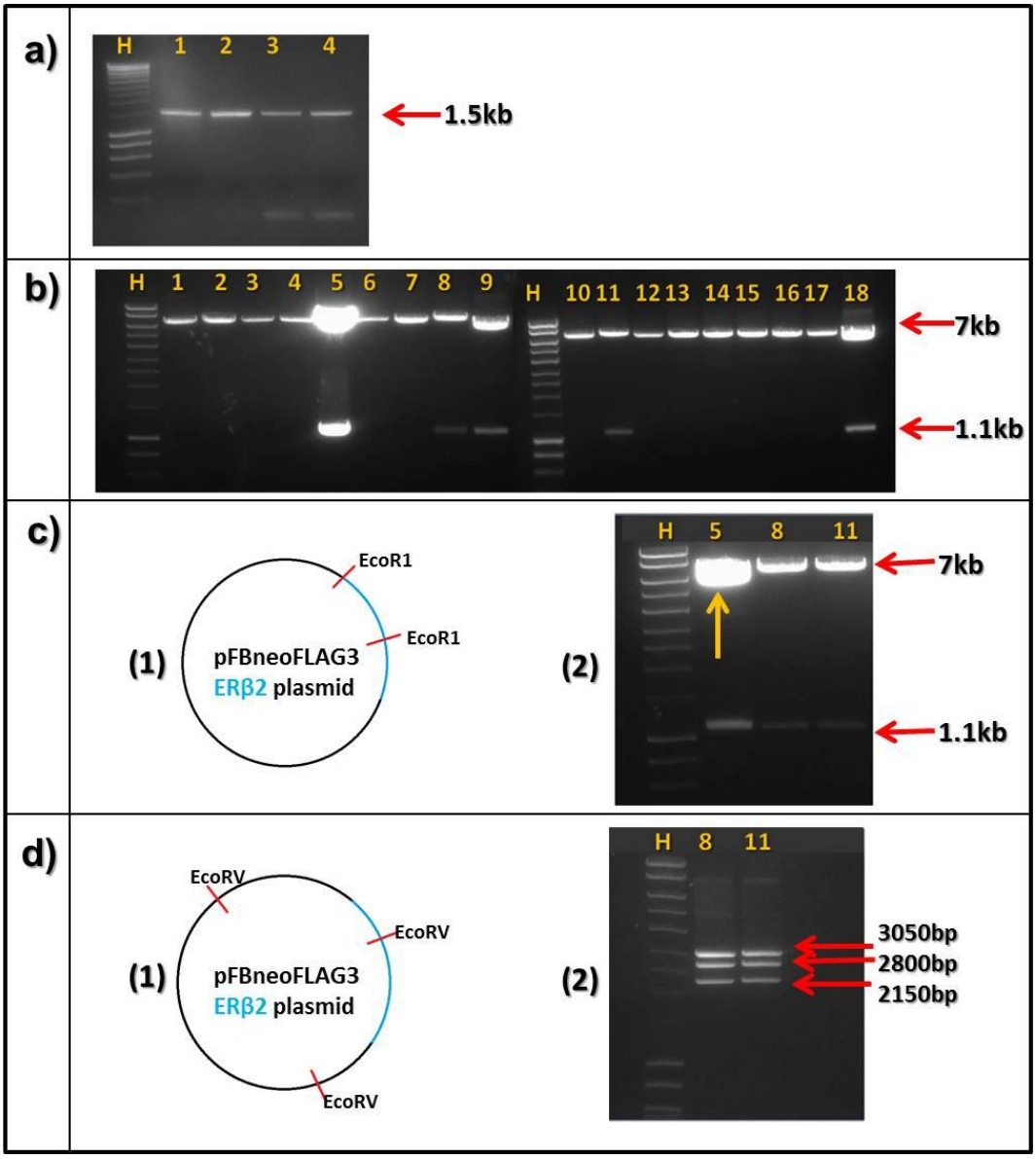

Figure 4.1. Amplification and recombination of an ERβ2 fragment into the retroviral vector pFB-NeoFLAG3, and subsequent restriction digests for confirmation of successful recombination.
(a) Four amplified ERβ2 fragments produced at 4 annealing temperatures containing homologous ends to the cut pFB-NeoFLAG3 vector. 1- 53°C, 2- 58°C, 3- 63°C, 4- 68°C.
(b) DNA from sixteen colonies picked from the ERβ2 "positive" plate. 1-8, 10-17; EcoR1 digested DNA from 16 ERβ2 "positive" colonies. 9, 18; pcDNA3 ERβ2 vector. Expected band sizes: ~7 kb and ~1.1kb.
(c1) schematic on the pRBneoFLAG3 ERβ2 recombined plasmid showing position of EcoR1 cutting site
(c2) Three potential positive clones, 5, 8 and 11
(d1) schematic on the pRBneoFLAG3 ERβ2 recombined plasmid showing position of EcoRV cutting sites
(d2) EcoRV digests of the two samples from colonies 8 and 11. Expected band sizes 3050bp, 2800bp, and 2150bp.

4.3.2 Geneticin (G418) dose optimisation

Geneticin (G418) is a commonly utilised antibiotic used to select for cells which have taken up recombinant DNA plasmid containing a neomycin resistance gene. To choose the correct dose of geneticin to select for cells transduced with the ERβ2 vector, an antibiotic kill assay was performed on wild type cells. MCF-7, T47D, MDA-MB-468 and MDA-MB-231 cells were exposed to varying doses of geneticin over 10 days. Figure 4.2 illustrates images of the cells incubated with the lowest dose of geneticin needed to kill all cells by the end of the selection period. MCF-7, T47D and MDA-MB-231 cells required a geneticin dose of 500µg/ml and MDA-MB-468 cells required a dose of 200µg/ml in order to kill all cells during selection. By day 9 of selection no viable cells were present, only cell debris. These doses were used under the same experimental conditions to select cells transduced with the pFB-neoFLAG3 ERβ2 vector or the empty vector control cells containing pFB-NeoFLAG3 vector. Cells that survived after 10 days of selection were considered positive for the recombinant DNA vector or empty vector.

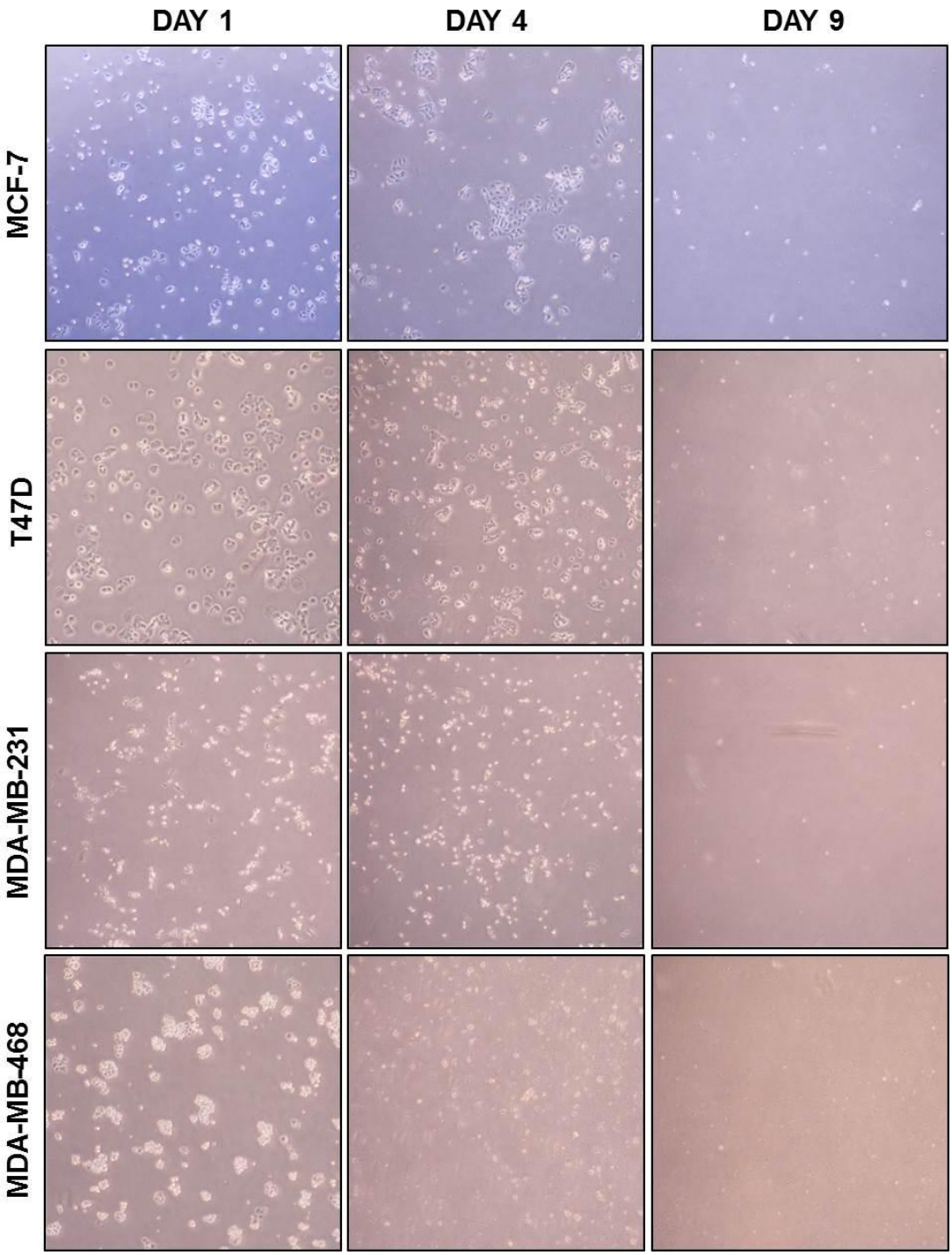

Figure 4.2. Geneticin dose optimisation for the selection of pFB-NeoFLAG3-ERβ2 positive clones.
MCF-7, T47D, and MDA-MB-231 cell selected with 500 µg/ml of geneticin, MDA-MB-468 selected with 200 µg/ml. Images presented taken on day1, 4 and 9 of selection. Images taken at 4x magnification

4.3.3 Confirmation of ERβ2 overexpression expression in cell lines

Once ERβ2 overexpressing cell lines had been established, ERβ2 expression was confirmed by measuring both mRNA and protein levels compared to the vector only control cell lines and wild type cell lines. qRT-PCR data for quantification of ERβ2 mRNA in wild type, empty vector control and ERβ2 overexpressing cells is summarised in Figure 4.3. MCF-7, T47D, MDA-MB-231 and MDA-MB-468 cells all demonstrated a statistically significant increase in ERβ2 mRNA levels compared to both wild type and empty vector control counterparts. MCF-7 overexpressing cells displayed around a 1000 fold increased in ERβ2 expression compared to the empty vector transduced control MCF-7 cells. T47D ERβ2 overexpressing cells exhibited the lowest expression fold increase of all the cell lines with around a 140 fold increase in ERβ2 mRNA compared to the control cells. Over a 2200 fold increase in ERβ2 mRNA was seen in MDA-MB-231ERβ2 overexpressing cells compared to the empty vector control cells. This was the highest fold increase observed over all the cell lines. MDA-MKB-468 ERβ2 overexpressing cells exhibited a1500 fold increase in ERβ2 mRNA compared to the control cells.

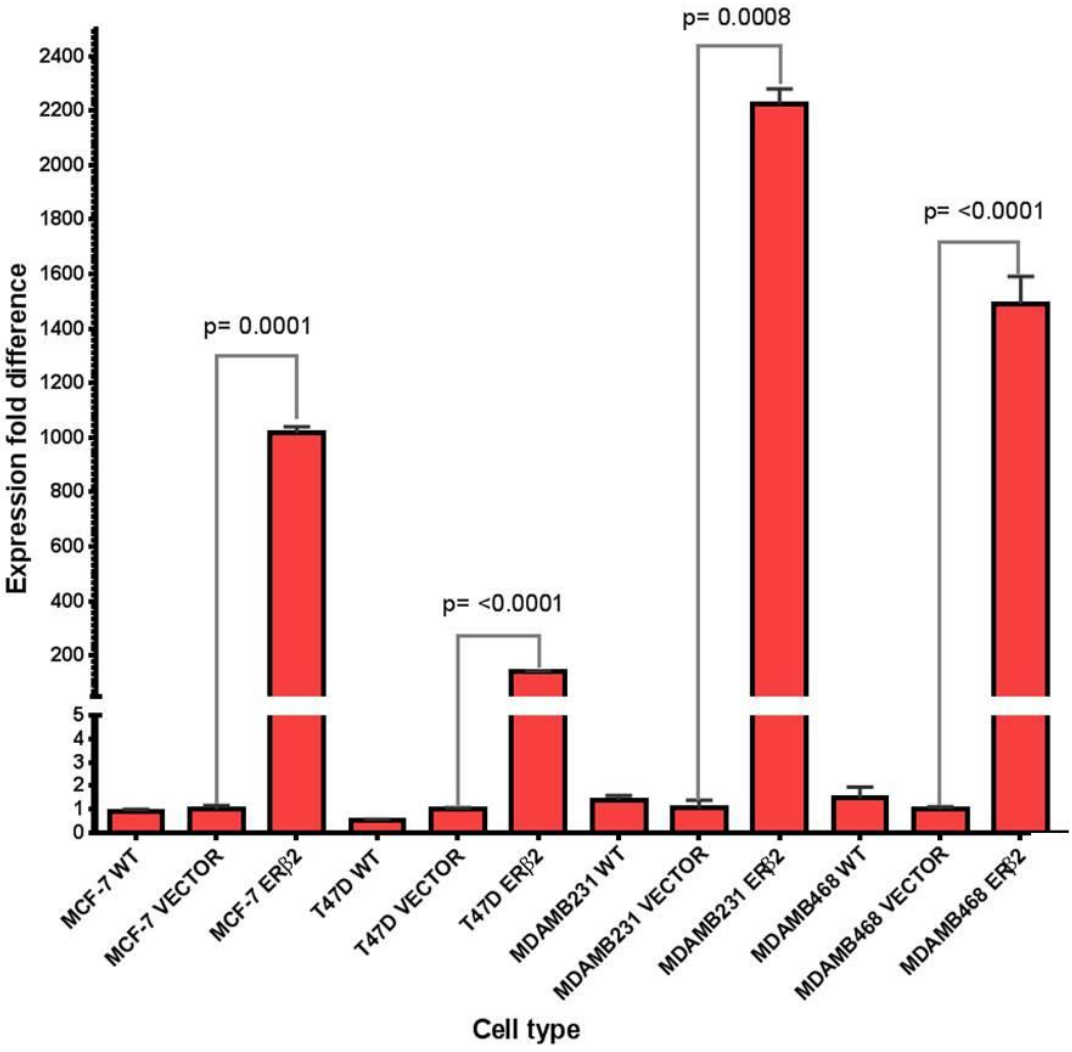

Figure 4.3. qRT-PCR quantification of ERβ2 mRNA in wild type (WT), vector control and ERβ2 overexpressing cell lines
mRNA levels of ERβ2 expressed as a fold difference normalised to the vector control cells with a value of 1.
Error bars represent ± SEM for n=3 (technical replicates). Statistically significant fold changes between vector control cells and ERβ2 overexpressing cells (*) and p-values, measured using a student's t-test, are displayed.

ERβ2 overexpression was also confirmed at the protein level, as mRNA levels do not always correlate with protein levels (90). Western blot was used for quantification of ERβ2 protein in the transduced cell lines, using an antibody to the FLAG epitope attached to the N-terminus of the protein. Quantification of total ERβ protein using an ERβ antibody that measures all isoforms was performed on MDA-MB-231 cells only. This data is summarised in Figure 4.4. Figure 4.4a illustrates the ERβ2 protein levels, characterised using the FLAG M2 antibody, in wild type (WT), empty vector control (V) and ERβ2 overexpressing (ERβ2) cell lines. Bands representing protein levels were present only in the ERβ2 overexpressing cells. MDA-MB-231 cells appeared to contain the largest amount of ERβ2 protein withT47D containing the least. These bands were all detected at the expected size of 58kDa, slightly larger than native ERβ2 at 55.5Kda due to the presence of the FLAG3 tag (~2.5kDa). No bands were present in the wild-type or empty vector controls. β-actin was used as a loading control, and was consistent between samples. Figure 4.4b represents total ERβ (all isoforms) levels in MDA-MB-231 cells. This antibody was used to detect ERβ2 overexpression only in MDA-MB-231 cells as these had the highest level of overexpression. Expression levels in the other cell lines were not high enough to be detected. A band was present only in the overexpressing cell lines at the expected size of around 58kDa. Absence of a band in wild type and control vector only cells suggests that ERβ2 protein is being detected, not other isoforms. Endogenous protein would be identified in all samples if levels were high enough for detection. Again, β-actin was used as a loading control.

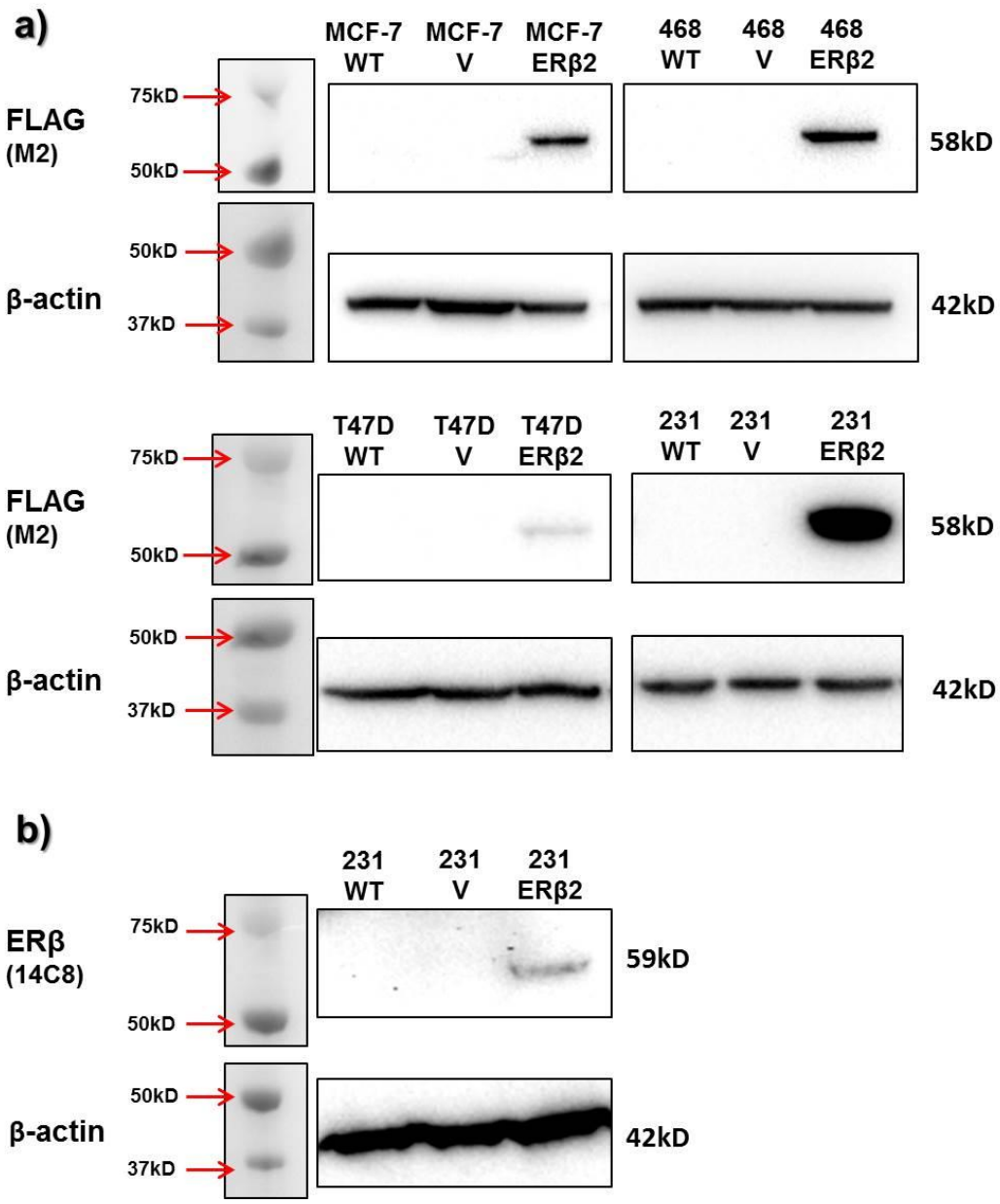

Figure 4.4. Western blot for ERβ2 detection in cell lines; wild type, pFB-NeoFLAG3 and pFB-NeoFLAG3-ERβ2 transduced cells using FLAG M2 or ERβ (14C8) antibodies.

a) FLAG M2 antibody was used to detect ERβ2 protein in MCF-7, T47D, MDA-MB-231 and MDA-MB-468 ERβ2 overexpressing cells. Wildtype and empty vector cells were also analysed to show specificity for FLAG epitope. bands of 58kDa were detected in all ERβ2 overexpressing cells. B-actin antibody was used as a loading control and bands were observed at 42kDa

b) Total ERβ antibody (14C8) was used to detect ERβ protein in MDA-MB-231 ERβ2 overexpressing cells, where a band was observed at 59kDa. No ERβ protein was detected in wild type and vector only control cells. B-actin antibody was used as a loading control and bands were observed at 42kDa

Results suggest that ERβ2 was successfully overexpressed in the 4 cell lines, MCF-7, T47D, MDA-MB-231 and MDA-MB-468. qRT-PCR data, measuring specifically ERβ2 mRNA and western blot data measuring protein using the FLAG M2 antibody to the N terminal epitope attached to the recombinant ERβ2 protein, show increased ERβ2 expression only in the pFB-NeoFLAG3-ERβ2 vector transduced cell lines. Band intensity differences in protein are correlated with the differences in mRNA. MDA-MB-231 cells demonstrate the highest expression fold increase in ERβ2 mRNA levels and also demonstrate the most intense band on the western blot, potentially signifying increased protein levels. T47D cells displayed the lowest expression fold increase in ERβ2 mRNA compared to its control. They also exhibited the faintest band on the western blot, indicating the least protein. As exposure times were kept constant between cell lines, experimental conditions were identical as samples were all assayed together and loading controls appear even, we were confident that the differences in band intensity correlated with their protein levels. Expression of ERβ2 between wild-type cells and empty vector control cells was comparable with very little, but nevertheless analogous, mRNA signal detected by qRT-PCR and no protein detected by western blot. In forthcoming experiments the empty vector control cells were used to represent the control cell line as an equivalent to wild-type cells.

4.3.4 Investigating the effect of ERβ2 overexpression on cellular proliferation

Cell proliferation was measured between the empty vector control cells and the ERβ2 overexpressing cells to investigate whether ERβ2 affects cell growth. Cell counts were performed over a 120 hour period, with both ERβ2 overexpressing and empty vector control cells counted at 48, 72, 96 and 120 hours after seeding. Figure 4.5 illustrates the growth curve data. MCF-7 and T47D cell lines are categorised as luminal A, and express ERα. ERβ2 overexpression in both of these cell lines resulted in a decrease in cellular proliferation rate indicated by consistently reduced cell numbers, signifying ERβ2 induced growth suppression. In T47D cells, increased separation of the lines indicates the suppressive effect of ERβ2 was greater than in MCF-7 cells. By 120 hours cell numbers in the empty vector control cell line was around 1.5 million whereas in the ERβ2 overexpressing cell line it was only around 320,000. MDA-MB-231 cells and MDA-MB-468 cell lines have a triple negative phenotype. In MDA-MB-231 cells, ERβ2 overexpression resulted in an increase in proliferation, and by 120 hour average cell numbers reached 830,000 compared with 650,000 in the control cells, suggesting ERβ2 promotes growth in this cell line. Conversely, ERβ2 overexpression decreased cellular proliferation in MDA-MB-468 cells, suggesting ERβ2 differentially regulates growth in these cell lines.

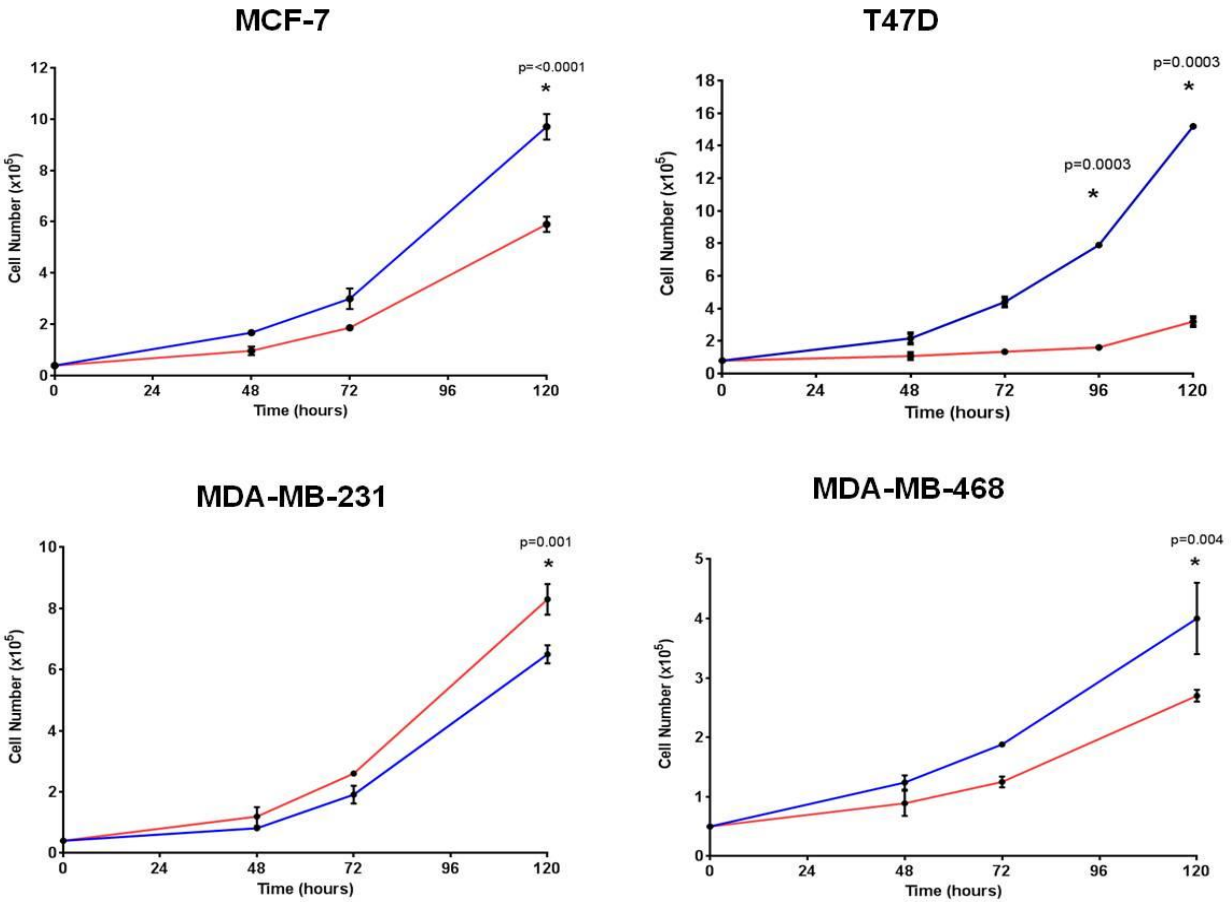

Figure 4.5. Proliferation analysis of ERβ2 overexpressing versus vector control MCF-7, T47D, MDA-MB-231 and MDA-MB-468 cells. ERβ2 overexpression (red line) resulted in growth suppression in MCF-7, T47D and MDA-MB-468 cells, and growth promotion is MDA-MB-231 cells, compared to their vector control counterparts (blue line). Error bars represent ± SEM for n=2 (technical replicates). Statistically significant changes in cell number (*) and p-values, measured using a multiple student's t-tests with Holm-Sidak correction, are displayed.

4.3.5 Cell cycle distribution

Vector control cells and ERβ2 overexpressing cells were analysed using flow cytometry to determine whether the overexpression of ERβ2 protein affected their cell cycle distribution. Figure 4.6 illustrates the cell cycle distribution in MCF-7 and MDA-MB-231 vector control and ERβ2 overexpressing cells. These histograms show the percentage of cells in a population that are in G1/0, S or G2/M phase. There was no notable difference in cell cycle distribution between both MCF-7 and MDA-MB-231 control cells and their ERβ2 overexpressing counterparts, suggesting ERβ2 overexpression does not affect the percentage of cells in each phase of the cell cycle. This data suggests cell cycle distribution was unaffected by an increase in ERβ2 protein and the changes observed in proliferation rate may not be due to cell cycle regulation.

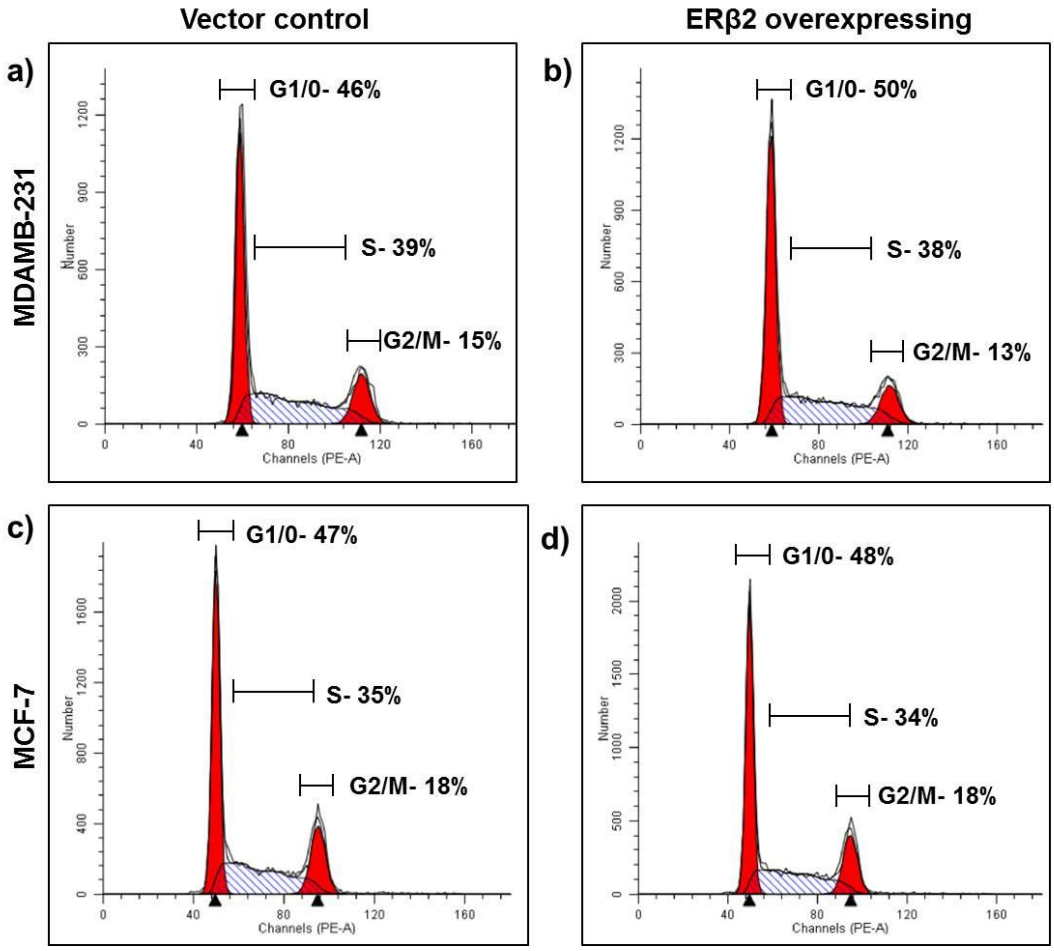

Figure 4.6. Cell cycle distribution of MDA-MB-231 and MCF-7 ERβ2 overexpressing compared and vector control cells

Cells were incubated with the fluorescent dye propidium iodide (PI) and analysed by flow cytometry. The average percentage of cells in G1/0, S and G2/M phase is shown above their respective peaks on the graphs.

a) MDA-MB-231 vector control cell cycle distribution

b) MDA-MB-231 ERβ2 overexpressing cell cycle distribution

c) MCF-7 vector control cell cycle distribution

d) MCF-7 ERβ2 overexpressing cell cycle distribution

4.3.6 Cell migration

Cell migration was measured in ERβ2 overexpressing MCF-7, T47D, MDA-MB-231 and MDA-MB-468 cells and their respective control cell lines to investigate whether overexpression of ERβ2 protein affected cell migration rates. Data from one representative replicate is displayed in Figure 4.7. The graphs display the relative wound density (RWD), a metric that measures cell density in the wound area expressed relative to the cell density outside of the wound area. This allows a more accurate calculation of migration as it normalises for changes in cell density in the wound caused by proliferation. All cell lines overexpressing ERβ2 demonstrated a decrease in migration. MCF-7 and MDA-MB-468 ERβ2 overexpressing cells had a RWD of around 10% less than the control cells at 20 and 60 hours post wounding respectively, illustrated by the dotted black lines in Figure 4.7 a and d. MDA-MB-468 cells did not to completely fill the wound over the course of the experiment, and by 140 hours, the RWD was only around 40%, suggesting these cells are not inherently migratory. In MDA-MB-231 cells the RWD was around 12% less in the ERβ2 overexpressing cells than the control cells at 10 hours depicted by the black dotted line in Figure 4.7c. T47D ERβ2 overexpressing cells had a RWD of around 12% less than in the control cells by 100 hours, illustrated by the dotted line in Figure 4.7b.

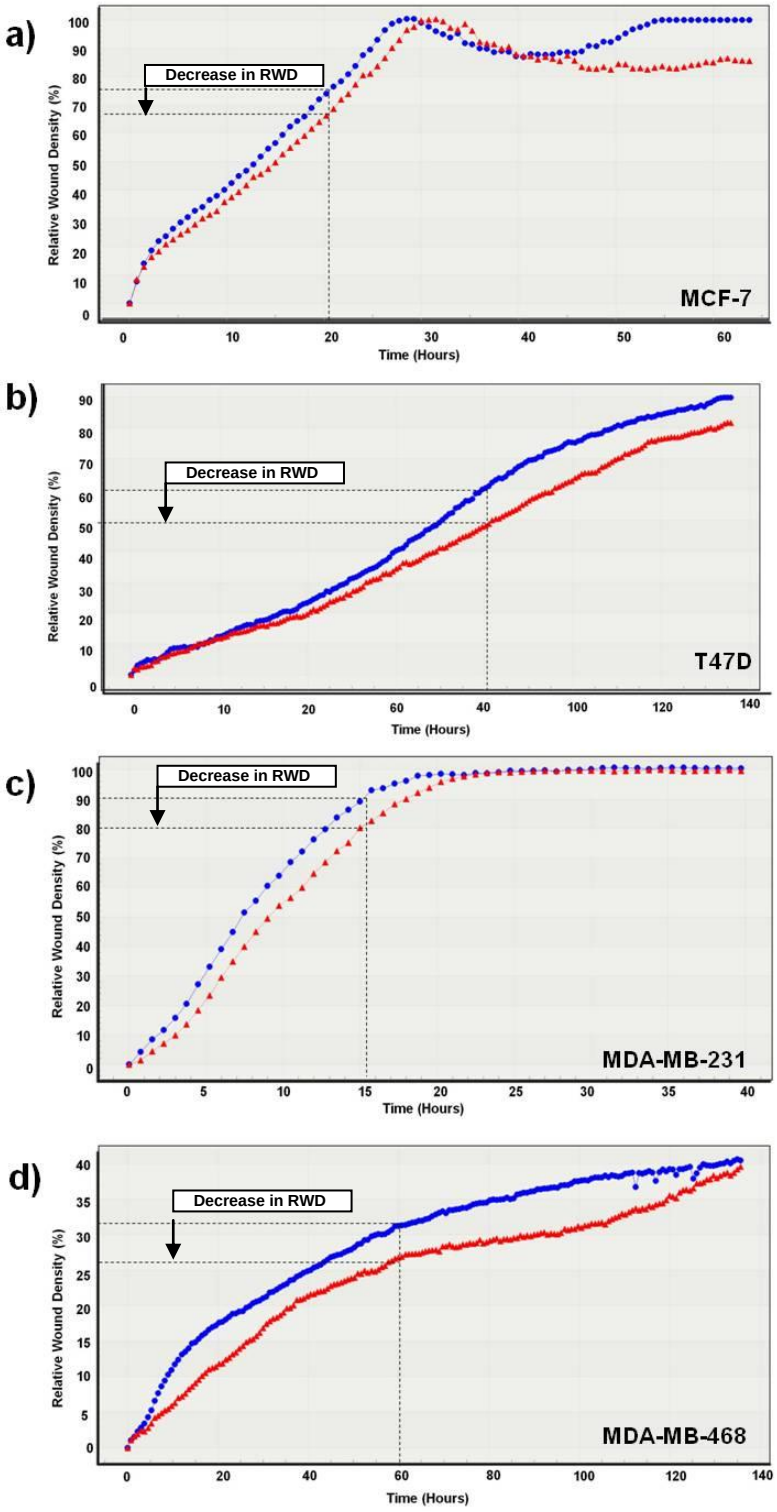

Figure 4.7. Migration wound healing assay performed on ERβ2 overexpressing cells.
Migration is measured as the relative wound density (RWD) % over time. Migration was decreased in all ERβ2 overexpressing cells (red line) compared to their control counterparts (blue line), illustrated by the dotted lines indicating different RWDs at a single time point. a) MCF-7 cells, b) T47D cells, c) MDA-MB-231 cells, d) MDA-MB-468 cells. Significance was not tested as only one replicate was performed.

4.3.7 Target gene validation

Four genes were selected for ERβ2 target gene qRT-PCR validation, all of which had been demonstrated to be regulated by ERβ. Candidates *CDK6*, *BCL-2* and *RIP140* were identified from a list of genes demonstrated to be directly regulated by ERβ from ChIP-Seq analysis of ERβ binding sites (47). *S100A7* was demonstrated to be a target for ERβ1 in the triple negative cell line MDA-MB-468, and was upregulated by E2 treatment in ERβ overexpressing cells (115), and was found to be associated with ERβ2 by the Breast Research Group in Leeds (179). The mRNA levels of these genes were examined in empty vector control and ERβ2 overexpressing cells and were either untreated or treated with E2 (ERα and ERβ agonist) or DPN (ERβ agonist). The mRNA levels of the target genes were measured with the aim to elucidate whether the ERβ2 isoform had involvement in their transcriptional regulation. Results are illustrated in Figure 4.8 (MCF-7 cells) and 4.9 (MDA-MB-231 cells) where the black bars represent the vector control cells and the red bars represent the ERβ2 overexpressing cells.

qRT-PCR expression data from each gene investigated was normalised to the vector control cells for each treatment, which was given an expression fold change of 1 i.e. E2 treated ERβ2 overexpressing cells were normalised to E2 treated vector control cells. This was done to concentrate the findings on the effect of ERβ2 overexpression and not the effect of the ligands alone. However the ligands did alter gene expression in just the control vector cells, so mRNA expression that has been normalised to only the untreated control is displayed in appendix 7.5

ERβ2 overexpression and subsequent ligand treatment had little effect on *BCL-2* or *CDK6* mRNA expression in MCF-7 cells, (Figure 4.8a and 4.8b respectively). The minor increases in expression observed with DPN treatment are beyond the sensitivity of the assay and therefore cannot be interpreted as a real fold change. *S100A7* expression was upregulated in MCF-7 cells, which overexpressed ERβ2 (Figure 4.8c). In the untreated cells more than a 2 fold increase in *S100A7* mRNA was observed, and this increased to around 5 fold when cells were treated with E2 and DPN. Although *RIP140* mRNA expression marginally decreased in untreated ERβ2 overexpressing cells (Figure 4.8d), this was negated when cells were treated with E2 and DPN.

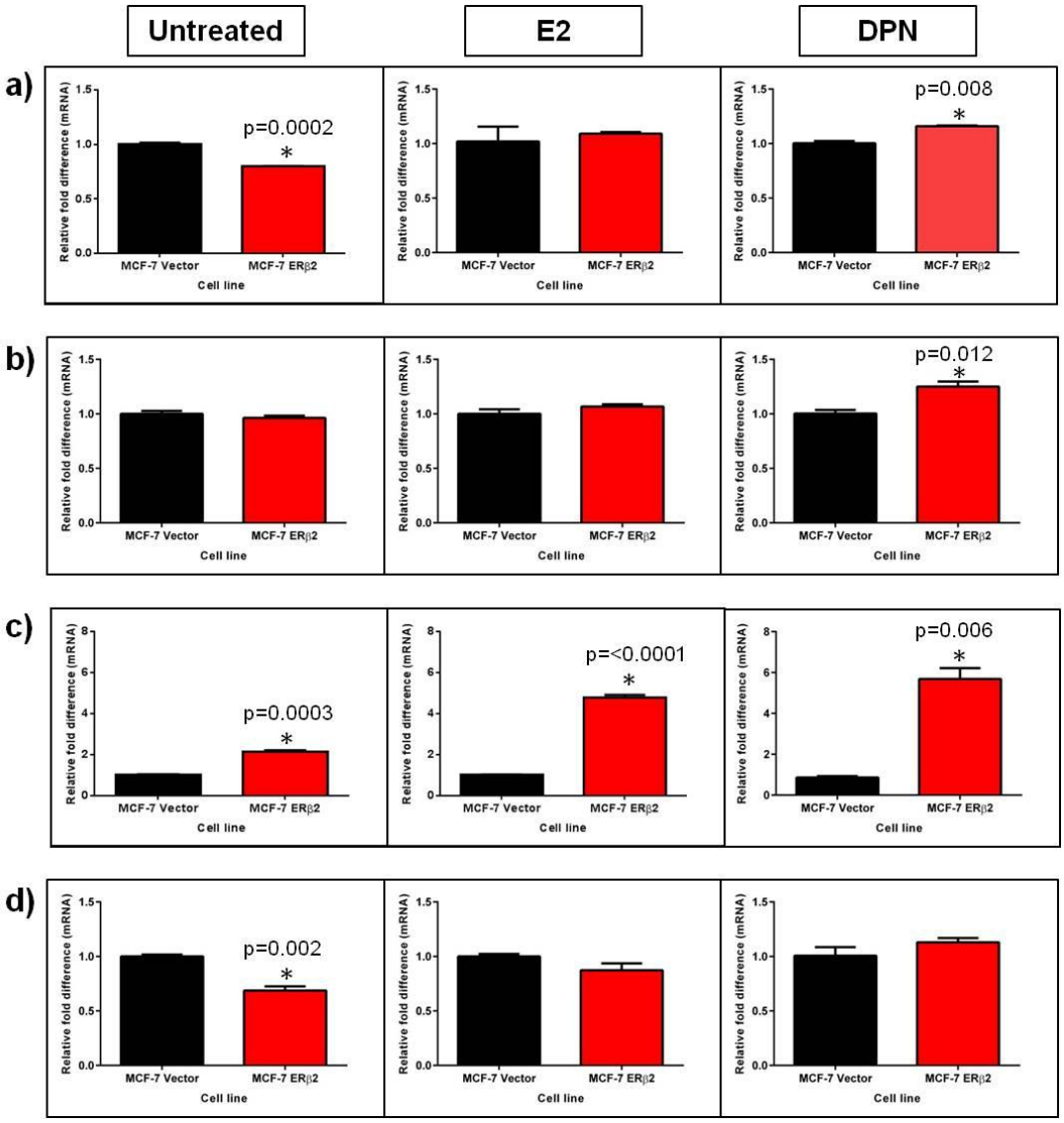

Figure 4.8. qRT-PCR quantification of the mRNA expression levels of BCL-2 CDK6, S100A7 and RIP140 in ERβ2 overexpressing and vector control MCF-7 cells treated with E2 (1nM) or DPN (10nM) for 24 hours

mRNA is expressed as a relative fold difference normalised to the vector control cell expression, which was given a value of 1. Relative fold expression difference of *BCL-2* (a), *CDK6* (b), *S100A7* (c), and *RIP140* (d)

Error bars represent ± SEM for n=3 (technical replicates). Statistically significant fold changes (*) and p-values, measured using a student's t-test, are displayed.

Contrary to MCF-7 cells, ERβ2 overexpression influenced *BCL-2* expression in MDA-MB-231 cells (Figure 4.9a). In untreated MDA-MB-231 cells, *BCL-2* mRNA was downregulated approximately 1.7 fold in ERβ2 overexpressing cells compared to the control cells. However when treated with E2 or DPN, *BCL-2* expression was increased, suggesting opposing regulation with and without ligand presence. A similar finding was observed with *CDK6* mRNA expression (Figure 4.9b). In untreated cells *CDK6* expression was marginally reduced, however upon E2 and DPN treatment expression of *CDK6* was increased up to 2.5 fold compared to control cells. *S100A7* mRNA expression is illustrated in Figure 4.9c. Expression remained unchanged in the absence of ligand treatment, however in the presence of E2 and DPN, expression increased by approximately 2 fold, however this was less pronounced than the increase observed in MCF-7 ERβ2 overexpressing cells. *RIP140* mRNA expression is illustrated in Figure 4.9d. Expression decreased in ERβ2 overexpressing MDA-MB-231 cells with a decrease of over 2 fold in untreated and DPN treated cells and approximately 1.7 fold in E2 treated cells.

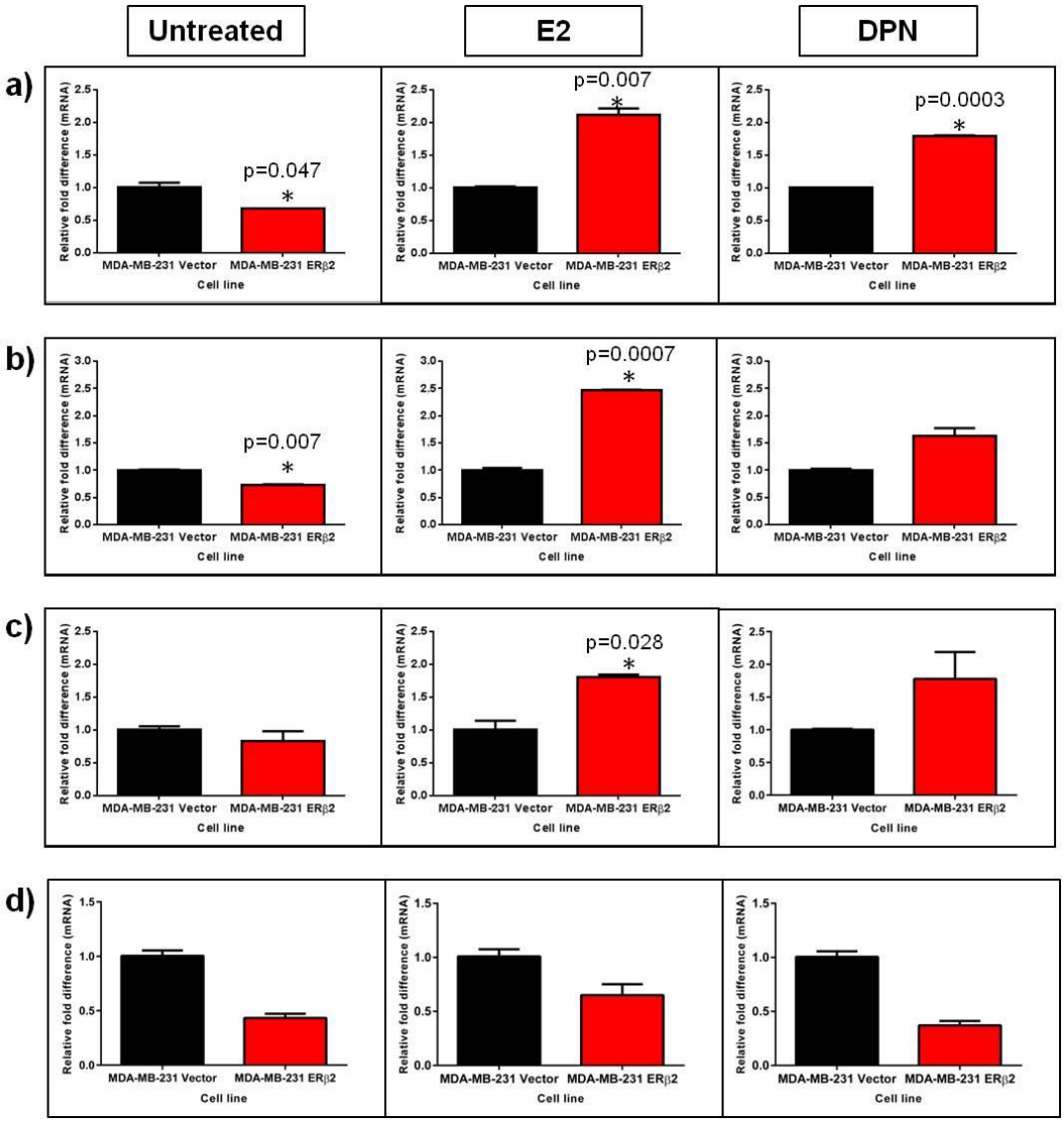

Figure 4.9. qRT-PCR quantification of the mRNA expression levels of BCL-2 CDK6, S100A7 and RIP140 in ERβ2 overexpressing and vector control MDA-MB-231 cells treated with E2 (1nM) or DPN (10nM) for 24 hours

mRNA is expressed as a relative fold difference normalised to the vector control cell expression, which was given a value of 1. Relative fold expression difference of *BCL-2* (a), *CDK6* (b), *S100A7* (c), and *RIP140* (d)

Error bars represent ± SEM for n=3 (technical replicates). Statistically significant fold changes (*) and p-values, measured using a student's t-test, are displayed.

4.3.8 Mitochondrially transcribed genes

A number of mtDNA transcribed genes were also investigated with respect to ERβ2 overexpression, as ERβ2 was found to colocalise with the mitochondria, detailed in chapter 3.5. *ND1*, *ND2*, *ATP6* and *CYB* mRNA expression was investigated in MCF-7 and MDA-MB-231 cells, both in ERβ2 overexpressing cells and their empty vector control counterparts. Again, qRT-PCR expression data from each gene investigated was normalised to the vector control cells (given an expression fold change of 1) for each treatment, Results are shown in Figure 4.10 (MCF-7 cells) and 4.11 (MDA-MB-231 cells) where the black bars represent the vector control cells and the red bars represent the ERβ2 overexpressing cells. Gene expression normalised to the untreated empty vector control cells only are displayed in appendix 7.6, to illustrate gene expression changes as a result of ligand treatment only.

mtDNA gene expression data for MCF-7 cells are displayed in Figure 4.10. ERβ2 overexpression had no effect on *ND1* expression levels without ligand treatment, or with DPN treatment. However, upon incubation with E2, expression of *ND1* decreased 2 fold compared to the control cells (Figure 4.10a). *ND2* mRNA levels were again unaffected by ERβ2 overexpression without the presence of a ligand, whereas E2 treatment decreased *ND2* levels by around 1.8 fold and DPN treatment only marginally increased expression by approximately 1.3 fold (Figure 4.10b). In ERβ2 overexpressing cells without treatment *ATP6* and *CYB* levels were both increased 1.4 fold illustrated in Figure 4.10c and 4.10d respectively. E2 had little effect on expression levels of ATP6 and CYB and DPN treatment only marginally increased their expression.

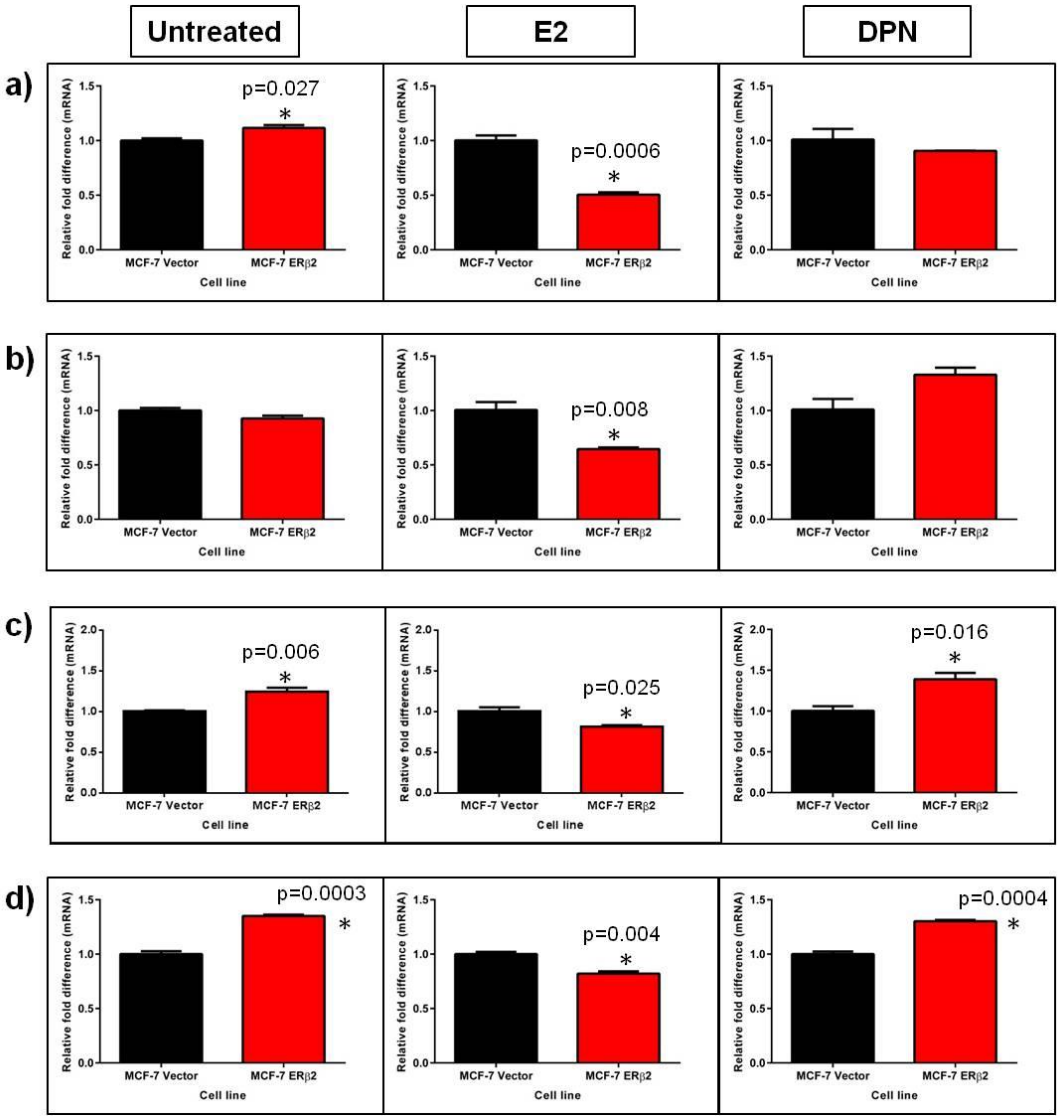

Figure 4.10. qRT-PCR quantification of the mRNA expression levels of ND1, ND2, ATP6 and CYB in ERβ2 overexpressing MCF-7cells treated with E2 (1nM) or DPN (10nM) for 24 hours

mRNA is expressed as a relative fold difference normalised to the vector control cell expression, which was given a value of 1. Relative fold expression difference of *ND1* (a), *ND2* (b), *ATP6* (c), *CYB* (d)

Error bars represent ± SEM for n=3 (technical replicates). Statistically significant fold changes (*) and p-values, measured using a student's t-test, are displayed.

In contrast to MCF-7 cells, ERβ2 overexpression in MDA-MB-231 cells had a more pronounced effect on gene transcription of mtDNA transcribed genes, when exposed to E2 and DPN. *ND1* expression levels in ERβ2 overexpressing cells were unchanged with no ligand treatment compared to the vector control cells (Figure 4.11a); however upon E2 and DPN treatment, mRNA expression increased 2 fold and 1.5 fold respectively in the ERβ2 overexpressing cells compared to their control counterparts. *ND2* mRNA expression increased 1.5 fold in untreated ERβ2 overexpressing cells (Figure 4.11b). E2 treatment resulted in almost a 4 fold increase in *ND2* mRNA levels in ERβ2 overexpressing cells, whereas *ND2* mRNA levels only marginally increased with DPN treatment. Figure 4.11c illustrates *ATP6* mRNA levels in response to ERβ2 overexpression. No ligand treatment resulted in a marginal increase in *APT6* mRNA. E2 treatment produced a more marked 2 fold increase in *ATP6* expression whereas in response to DPN treatment only a slight increase in mRNA levels was observed. ERβ2 overexpression resulted in a 2 fold increase in *CYB* mRNA compared to control cells and as with the other mtDNA genes, DPN treatment only marginally increased mRNA levels. ERβ2 overexpression with no ligand treatment did not affect *CYB* mRNA expression (Figure 4.11d).

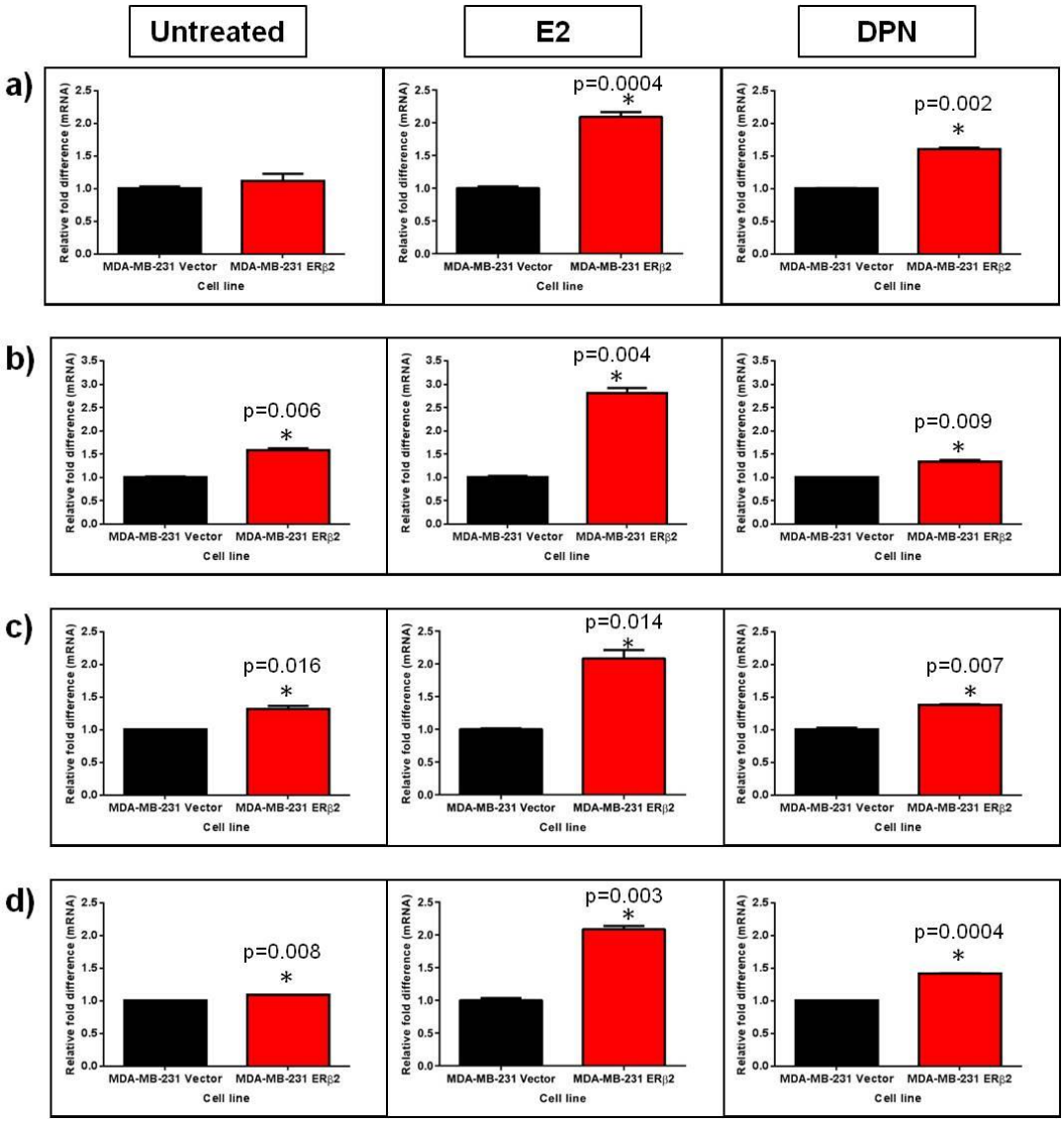

Figure 4.11. qRT-PCR quantification of the mRNA expression levels of ND1, ND2, ATP6 and CYB in ERβ2 overexpressing MDA-MB-231cells treated with E2 (1nM) or DPN (10nM) for 24 hours

mRNA is expressed as a relative fold difference normalised to the vector control cell expression, which was given a value of 1. Relative fold expression difference of *ND1* (a), *ND2* (b), *ATP6* (c), *CYB* (d)

Error bars represent ± SEM for n=3 (technical replicates). Statistically significant fold changes (*) and p-values, measured using a student's t-test, are displayed.

4.3.9 Subcellular fractionation

As demonstrated in section 3.2, it was possible to detect ERβ2 at the protein level in the transduced cell lines using the FLAG M2 antibody raised to the 5' epitope of the ERβ2 protein. Subcellular fractionation allowed us to examine ERβ2 protein levels in the different cellular compartments; the nucleus, mitochondria and cytoplasm. Cells were then stimulated with various estrogenic ligands targeted to ERα and ERβ1, in order to study how these drugs may affect ERβ2 cellular distribution. Information gathered from this experiment could suggest where in the cell ERβ2 may be most functional, and whether estrogenic ligands effect this distribution. Figure 4.12 illustrates the distribution of ERβ2 protein in subcellular compartments (Nuclear, cytoplasmic and mitochondrial) in ERβ2 overexpressing MCF-7 and MDA-MB-231 cells. Different loading controls were used for the nuclear, cytoplasmic and mitochondrial fractions; TATA binding protein, cyclophilin A and cytochrome C respectively. These antibodies were applied to each fraction to check enrichment as indicated by the red arrows in Figure 4.12.

In MDA-MB-231 cells almost all ERβ2 protein was observed in the cytoplasmic and mitochondrial fractions. Lower levels of ERβ2 in comparison were detected in the nuclear fraction as only a very faint band was observed. The nuclear fraction was enriched as a band was only observed with the nuclear marker (TATA-BP). Likewise the cytoplasmic fraction was also enriched as only a band appeared with cyclophilin A incubation. Some contamination of the mitochondrial fraction with cytoplasm was observed as a band was detected on the blot with cyclophilin A incubation; however a more robust band was present under cytochrome C incubation demonstrating the fraction was likely enriched for mitochondria.
In MCF-7 cells, ERβ2 was present at increased levels in the mitochondria and lower levels were detected in the cytoplasmic demonstrated by a fainter band in this

fraction. No protein was detected in the nuclear fraction and the absence of a band may be due to low undetectable protein levels. Again fractions were examined for enrichment. The nuclear fraction was enriched demonstrated by the band present under TATA BP incubation. Some contamination with cytoplasmic proteins was also detected in this fraction; however the band was fainter, indicating the fraction was likely to be predominantly nuclear enriched. The mitochondrial fraction demonstrated enrichment, but with a small amount of nuclear protein present in this fraction indicated by a faint band when probed with TATA-BP antibody. The cytoplasmic fraction was enriched, with a band present under cyclophilin A incubation, and no nuclear or mitochondrial cross contamination was observed. All fractions demonstrated enrichment, and thus the method was deemed suitable and robust for the fractionation of subcellular compartments.

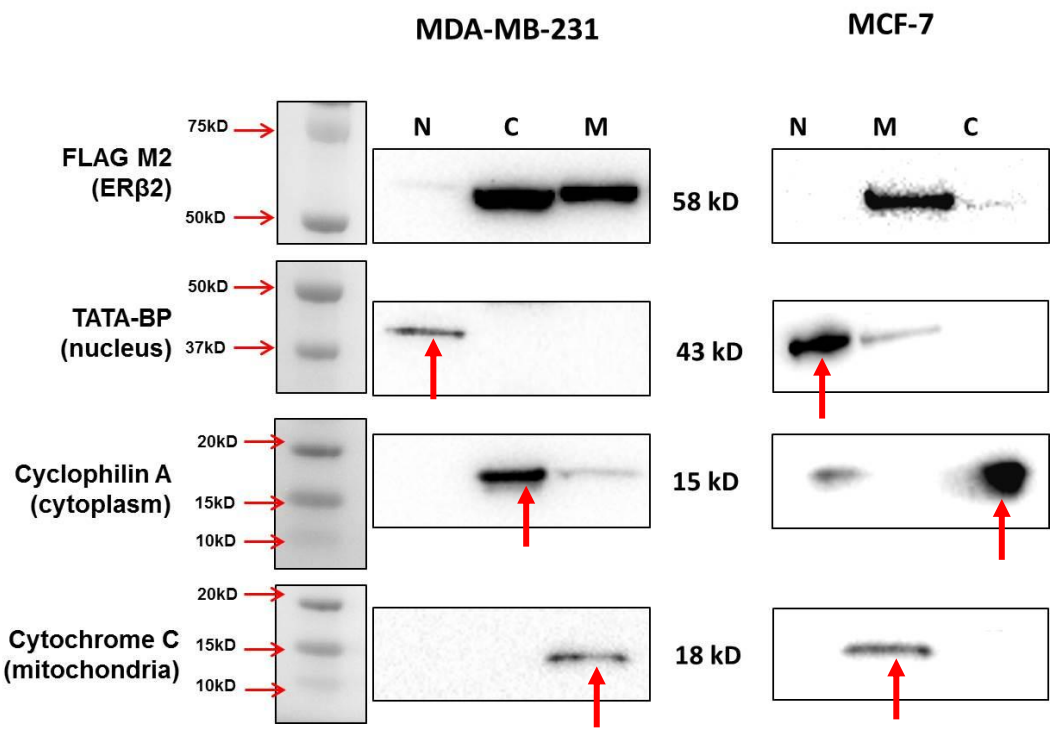

Figure 4.12. Western blot of ERβ2 in nuclear, cytoplasmic and mitochondrial compartments in pFB-NeoFLAG3-ERβ2 transduced cell lines.
FLAG M2 antibody was used to detect ERβ2 protein in nuclear cytoplasmic and mitochondrial cellular fractions. Bands were detected in all fractions in MDA-MB-231 cells and in the mitochondrial and cytoplasmic fractions of MCF-7 cells at 58kDa. TATA-BP, Cyclophilin A and cytochrome C were used as markers for the nucleus, cytoplasmic and mitochondria respectively to show enrichment and purity of each fraction (red arrows).

MCF-7 and MDA-MB-231 ERβ2 overexpressing cells were incubated with E2, 4-OHT, DPN or genistein to investigate whether these ligands would alter the cellular distribution of ERβ2 between the subcellular compartments. ERβ2 protein was detected using the FLAG M2 antibody. Whole protein extracts were also prepared to evaluate the effect of the ligands on total cellular ERβ2 protein levels. We used TATA-BP, cyclophilin A and cytochrome C as controls for equal loading for the nuclear, cytoplasmic and mitochondrial fractions respectively in the following experiment, rather than to demonstrate enrichment.

Figure 4.13a illustrates levels of ERβ2 in whole cell extracts of MCF-7 cells in response to estrogenic ligands or no ligand stimulation (control). In the presence of E2, DPN and genistein, ERβ2 protein levels appeared reduced, indicated by the fainter bands compared to the untreated controls. Genistein treatment resulted in no detectable ERβ2 protein. The β-actin loading control for the genistein treated sample indicated less total protein was loaded, which may have contributed to this lack of detection. The effect of the ligands on mitochondrial ERβ2 (Figure 4.13b) mirrored whole cell ERβ2 levels. E2, DPN and genistein treatment resulted in decreased ERβ2 protein levels demonstrated by the fainter bands compared to the untreated control, whereas 4-OHT treatment produced no apparent change in ERβ2 protein levels. In the cytoplasmic fractions (Figure 4.13c), E2 genistein and 4-OHT resulted in reduction of ERβ2 protein in the cytoplasm and this was more pronounced in response to E2 and genistein. Again this reduction is similar to that seen in the whole cell extracts. When comparing ERβ2 levels in the cytoplasm upon DPN treatment to untreated cells, protein levels appear unchanged. However ERβ2 protein appears to be reduced in whole cell extracts upon DPN treatment suggesting ERβ2 levels are actually increased in the cytoplasm as a result of DPN stimulation. Nuclear ERβ2 (Figure 4.13d) mirrored whole cell ERβ2 protein levels. 4-OHT treatment resulted in unchanged ERβ2 protein levels and DPN treatment

reduced ERβ2 nuclear protein compared to untreated cells. Upon E2 and genistein treatment we were unable to detect any ERβ2 protein in the nuclear fraction, possibly due to protein levels being out of the range of detection for this assay.

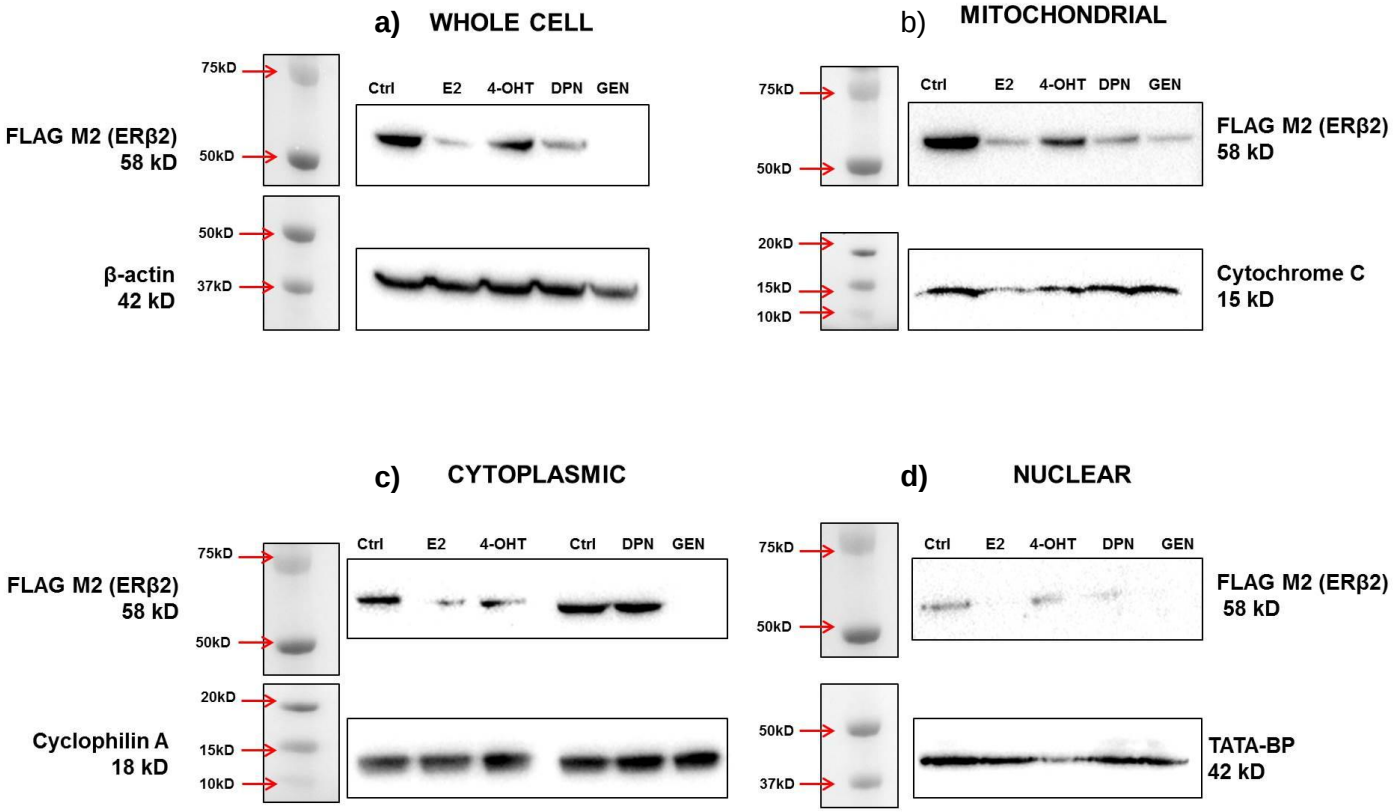

Figure 4.13. Western blot of ERβ2 in whole cells, nuclear, cytoplasmic and mitochondrial fractions in MCF-7 ERβ2 overexpressing cells treated with E2, 4-OHT, DPN or genistein.
FLAG M2 antibody was used to detect ERβ2 in nuclear cytoplasmic and mitochondrial cellular fractions. Bands were present at 58kDa. β-actin (42kDa), TATA-BP (42kDa), Cyclophilin A (18kDa) and cytochrome C (15kDa) were used as loading controls for the whole cell fraction, nucleus, cytoplasm and mitochondria respectively.

Figure 4.14 illustrates the effect of E2, 4-OHT, DPN and genistein on ERβ2 protein distribution between cellular compartments in MDA-MB-231 cells. Whole cell ERβ2 levels were measured and displayed in Figure 4.14a. ERβ2 protein levels were unchanged by treatment with E2, 4-OHT and DPN treatment. Genistein treatment resulted in a reduction of ERβ2 protein in MDA-MB-231 cells. In the mitochondrial fractions, ERβ2 protein levels were unchanged upon E2 and 4-OHT treatment (Figure 4.14b). Due to the fainter band in the loading control, DPN treatment may reduce ERβ2 protein levels in this fraction, despite no apparent change observed with FLAG M2 incubation. ERβ2 protein levels were increased in the mitochondria upon genistein treatment. Figure 4.14c demonstrates estrogenic ligand treatment effects on ERβ2 levels in the cytoplasm. With the exception of DPN, none of the ligands changed ERβ2 protein levels in the cytoplasmic compartment. As in MCF-7 cells, ERβ2 protein levels in the cytoplasm are increased in response to DPN treatment. In the nuclear fractions ERβ2 protein levels were decreased in response to DPN treatment (Figure 4.14d). The loading control band is also fainter suggesting less cellular protein was loaded in this sample which may mean ERβ2 protein levels are lower.

.

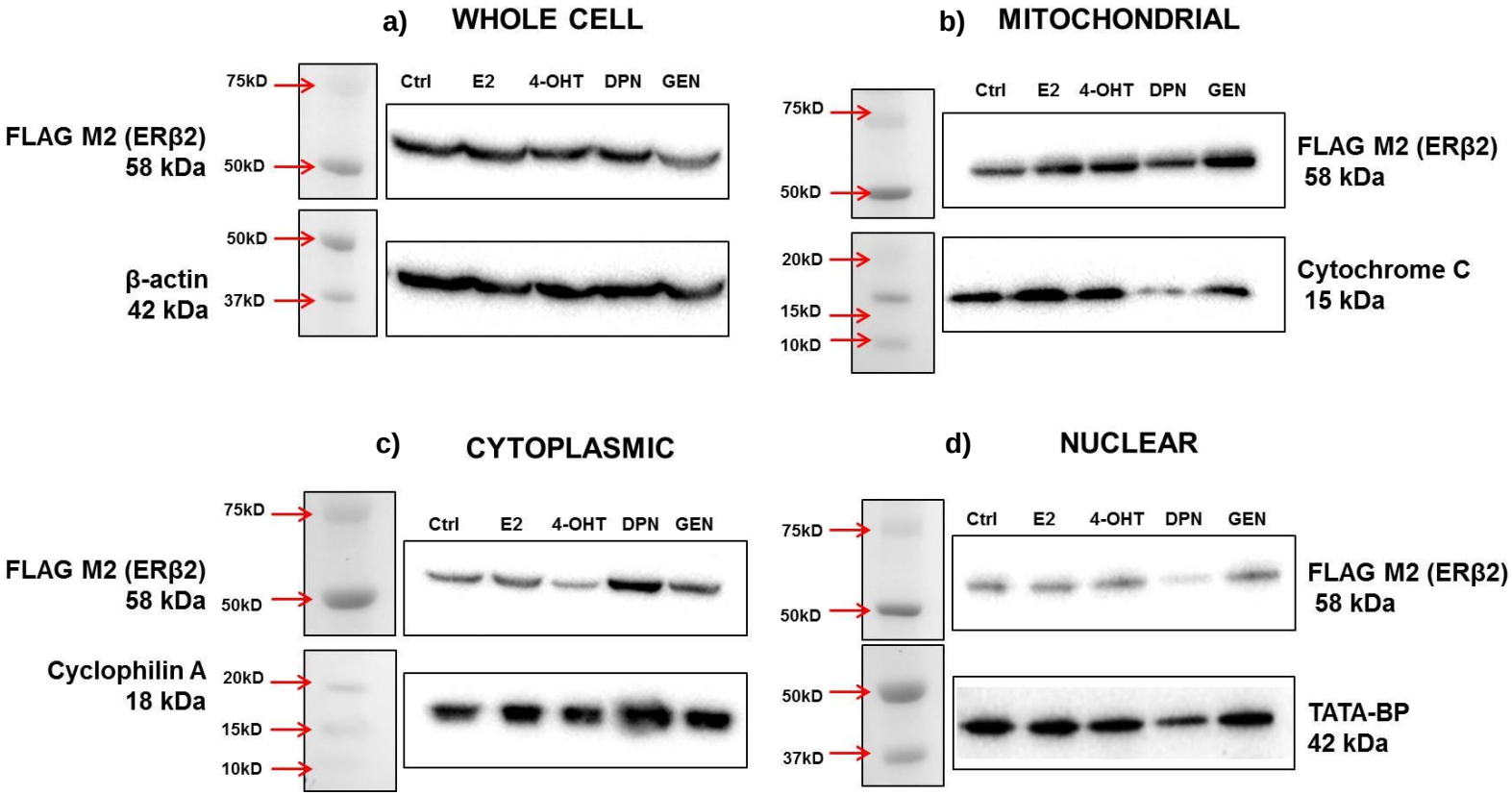

Figure 4.14. Western blot of ERβ2 in whole cells, nuclear, cytoplasmic and mitochondrial fractions in MDA-MB-231 ERβ2 overexpressing cells treated with E2, 4-OHT, DPN or genistein.

FLAG M2 antibody was used to detect ERβ2 in nuclear cytoplasmic and mitochondrial cellular fractions. Bands were present at 58kDa. β-actin (42kDa), TATA-BP (42kDa), Cyclophilin A (18kDa) and cytochrome C (15kDa) were used as loading controls for the whole cell fraction, nucleus, cytoplasm and mitochondria respectively.

4.4 Discussion

There is limited literature regarding the function of ERβ2 in breast cancer especially outside of the ERα positive setting. To address this, ERβ2 protein was overexpressed in ERα positive MCF-7 and T47D cells and ERα negative MDA-MB-231 and MDA-MB-468 cells to begin to explore the function of ERβ2.

4.4.1 A need for the FLAG epitope on the ERβ2 protein

There is only one commercially available ERβ2 antibody, the 57/3 clone, produced by Serotec. It has been validated for use in IHC, however other applications have been either untested or the antibody is considered unsuitable. The antibody's specificity has been validated and confirmed in the literature using peptide blocking assays (94, 153).

We have used it successfully for immunofluorescence in this project; however other antibody based assays have been difficult. The antibody has repeatedly failed to detect endogenous ERβ2 on western blot. Studies concerning the detection of ERβ2 protein by western blot in cell line overexpression experiments have all either used an in-house antibody (61, 101), which lacks external validation, a protein tag to demonstrate protein quantification (95), or used antibodies to detect total ERβ and determined ERβ2 expression based on molecular weight (146, 180). None have used the 57/3 ERβ2 antibody. This antibody was however capable of detecting ERβ2 by western blot in lysed tissue samples (94). It is yet to successfully detect ERβ2 protein by western blot in cell line lysates. To overcome this obstacle, we used a FLAG-tag attached to the N-terminus of the ERβ2 protein. The flag epitope should not interfere with protein function and provides a target for an antibody. The FLAG M2 antibody used in this study has been well validated in over-expression studies (181-184) and has been used to specifically detect ERβ over-expression (47, 95, 184, 185). The FLAG epitope allowed us to confirm ERβ2

overexpression in our engineered cell lines and to perform functional assays, which would otherwise be problematic, in order to study ERβ2.

4.4.2 Confirmation of ERβ2 overexpression

Overexpression of ERβ2 mRNA and protein was demonstrated in the cell lines transduced with the ERβ2 overexpression vector. Overexpression was confirmed at both the mRNA and protein levels as post-transcriptional modifications can alter expression of a protein by processes such as mRNA degradation or silencing. This can lead to discordant levels of mRNA and protein, as mRNA is not always translated into protein. This has specifically been reported for ERβ isoforms in breast (88, 90, 186). The absence of UTRs in the mRNA from the overexpressed ERβ2, as only the coding sequence was present in the overexpression vector, would mean it would be unlikely that mRNA and protein levels would not be concordant; however both qRT-PCR and western blots were performed to confirm this. qRT-PCR indicated that wild type and the vector only transduced control cell lines expressed comparable levels of ERβ2 mRNA. Our results did show that there was variability between the levels of ERβ2 expressed between cell lines. This may be explained partly by transduction efficiency. Often it is assumed that during transduction cells will incorporate one retroviral vector containing the gene of interest into their genome; however in practice some cells will incorporate numerous vectors, leading to variability in overexpression levels. Cells with higher transduction efficiency will often incorporate increased copy numbers of vector DNA into their genome leading to increased expression of the protein (187). The transduction efficiency between different breast cancer cell lines has been explored by Hines et al, 2015 (188). They determined that luminal breast cancer cell lines had much lower transductional efficiencies than basal cell lines, with MCF-7 and T47D cells demonstrating lower levels of transduction and MDA-MB-231 and MDA-MB-468 cell lines demonstrating the highest transduction efficiency. This was

explained by the capability of the cell to bind the virus, with luminal cells more deficient in binding capacity, which was suggested to be due to the expression of glycans on the outside of these cells. These can function to protect cells from infection (189), thus resulting in increased resistance of luminal cells to viral transduction.

To support ERβ2 overexpression detected by the FLAG M2 antibody, a total ERβ antibody, 14C8, was used to detect ERβ in MDA-MB-231 cells, which expressed the highest levels of ERβ2. Skliris et al, 2002 reviewed 7 ERβ antibodies for various protocols specifically for breast tissue (190). Of these, D7N and 8D5 produced the strongest and most specific bands (specificity determined by expected band size), while 14C8 produced weaker bands at the expected size. We used D7N initially to validate ERβ2 overexpression in the cell lines. However, this antibody detected ERβ protein in the wild type, vector control and ERβ2 overexpressing cells at equal levels indicated by bands of similar intensity, despite ERβ2 being overexpressed up to 2200 fold at the mRNA level. This antibody was therefore discarded due to concerns about specificity. The 14C8 antibody, although signal detection was weaker, had been well validated by others (100, 191, 192). ERβ expression was confirmed in the ERβ2 overexpressing MDA-MB-231 cells but not in the wild type or vector only control cells, suggesting the antibody is detecting the high levels of ERβ2 rather than any low levels of endogenous ERβ. The antibody was only capable of detecting ERβ2 in the MDA-MB-231 cells, suggesting this antibody is only capable of detecting high levels of ERβ. This is recognised in the literature with its use in ERβ overexpression studies but not to detect endogenous ERβ in breast.

4.4.3 The physiological effect of ERβ2 overexpression on breast cancer cell lines

ERβ2 overexpression studies in breast have only been performed in MCF-7 cells. These give a limited view on the function of ERβ2 in breast cancer and convey its function only in the presence of ERα. We know from the literature that ERβ2 represses the function of ERα (95). This was confirmed with our growth curve data where ERβ2 overexpression caused growth suppression in ERα positive MCF-7 and T47D cells. This is likely due to prevention of ERα binding to EREs and increased degradation of ERα protein described previously, resulting in a reduction in transcription of ERα regulated genes, which have been shown to promote proliferation.

In ERα negative cells lines, the growth suppression mechanism previously described by Zhao et al, 2007 (95) is unfeasible. The effect of overexpression of ERβ2 in triple negative cell lines on growth was more complex not only in our cell lines but also in the literature. In the MDA-MB-231 cells proliferation rate increased, however in MDA-MB-468 cells, also a triple negative phenotype, cell proliferation decreased. In the literature, overexpression of ERβ2 in the triple negative cell line HS578T had no effect on growth (105) and observations made by Murphy et a (193) found no effect on growth in ERβ2 overexpressing MDA-MB-231 cells. In prostate cancer cells, which are ERα negative, ERβ2 overexpression resulted in increased expression of proliferative genes such as *c-myc* and downregulation of the cell cycle inhibitor *p21*, leading to an increase in proliferation (106). This was opposite to the effect that ERβ1 had on the cells. Variability of the effect of ERβ2 on proliferation in the literature and in our cell lines demonstrates the complexity of ERβ2's action.

Surprisingly cell cycle distribution was unchanged upon ERβ2 overexpression in our cell lines. The overexpression of ERβ2 protein appears to alter proliferation of cells without altering their cell cycle distribution. Others have also reported that ERβ2 overexpression also resulted in proliferation but with no change in the cell cycle distribution (194).This may suggest ERβ2 controls proliferation by mechanisms other than regulation of various cell cycle proteins.

A possible mechanism, by which ERβ2 may affect proliferation or changes in cell number, could be by an increase/decrease in cell death. ERβ2 has also been implicated in apoptosis in ovarian cancer. ERβ2 expression correlated with apoptosis, and inhibited BAX oligomerisation and cytochrome C release, which ultimately inhibited apoptosis (153). A decrease in apoptosis could explain increased cell numbers in ERβ2 overexpressing MDA-MB-231 cells. An effect on apoptosis is supported by our gene expression data. *BCL-2* expression was increased in this cell line when ERβ2 was overexpressed. *BCL-2* is an anti-apoptotic protein therefore increased levels could inhibit apoptosis, leading to increased cell numbers. This effect on apoptosis could explain why no change in cell cycle distribution is seen in MCF-7 and MDA-MB-231 cells. Although ERβ1 appears to inhibit proliferation by inducing G2/M arrest by downregulation of cyclin D1, cyclin A, CDK1 and c-myc and the upregulation of p21 and p27 (80, 81), ERβ2 may not affect proliferation in this way via the direct regulation of cell cycle proteins.

It is unclear why the two cell lines, both triple negative phenotypes, may behave in opposite ways in terms of growth. Both cell lines have similar expression patterns of marker proteins; both are negative for expression of ERα, PR and HER2 and positive for expression of AR, Ki67, and low levels of HER3, however, these cell lines differ in their expression of EGFR (195). MDA-MB-468 cells express very high levels of EGFR, however MDA-MB-231 cells express only faint, barely perceptible levels of EGFR, which was deemed negative when analysed using the HER2

scoring system. The growth suppression seen in MDA-MB-468 cells may be explained by ERβ2 interference with EGFR signalling. There is evidence for crosstalk between ER and EGFR signalling (165, 196). Overexpression of ERβ1 in triple negative breast cancer cell lines is demonstrated to cause an increase in ubiquitinated EGFR, thus increasing EGFR degradation, and inhibiting downstream proliferative signalling. As it has been hypothesised that ERβ2 can enhance the transactivation of ERβ1, overexpression of ERβ2 may enhance ERβ1's inhibitory action on EGFR resulting in a decrease in cellular proliferation due to suppression of downstream signalling e.g. PI3K/AKT and MAPK/ERK pathway (196). Inhibition of EGFR has also been demonstrated to increase apoptosis (197), which could also contribute to reduced cell numbers. Interaction with EGFR could explain the differences in proliferation between MDA-MB-231 and MDA-MB-468 cells, as only MDA-MB-468 express EGFR at high levels. Use of siRNAs or shRNAs to silence the expression of EGFR in MDA-MB-468 cells could be performed to confirm this potential involvement of EFGR. Measurement of a downstream gene target of EGFR could also be compared between the control and ERβ2 overexpressing cells to examine whether EGFR signalling pathways are inhibited in ERβ2 overexpressing cells.

Despite variation in proliferation regulation, the effect of ERβ2 overexpression on migration was consistent, decreasing it across all cell lines. Proliferation and migration often positively correlate, despite both being mutually exclusive. The 'go or grow' theory (198) suggests while a cell is moving or migrating it is not dividing. In wound healing experiments, proliferation may also affect the wound closure and be misinterpreted as migration. In MCF-7, T47D and MDA-MB-468 cells the decrease in migration rate could be due to the decrease in proliferation rates. However the RWD metric takes into consideration proliferation by calculating the density of cells inside and outside the wound. To confirm that proliferation has no influence on migration, inhibition of proliferation during wound healing with

chemicals such as actinomycin D or mitomycin C, could be employed. In MDA-MB-231 cells proliferation and migration were inversely correlated, suggesting for these cells both biological processes are independent of each other. The effect of ERβ2 on migration, invasion and metastasis has not been widely studied in breast but has been explored in other cancers. Clinical data suggests ERβ2 is inversely correlated with invasion and metastasis in breast cancer, which supports our data (94). This is also the case in lung cancer where ERβ2 expression correlated with interleukin-12 receptorβ2 (IL-12Rβ2). ERβ2 was demonstrated to upregulate IL-12Rβ2 via interaction with p38MAPK resulting in a decrease in cellular invasion (199), suggesting a possible mechanism by which ERβ2 can regulate invasion. Although not all studies are in breast cancer, IL-12 has been demonstrated to induce interferon gamma (IFN-γ) production triggering the production of anti-angiogenic chemokines (200). Inhibition of angiogenesis is one mechanism proposed to reduce cell migration and invasion. Expression levels of IL-12Rβ2 could be investigated in our ERβ2 overexpressing versus the control cells in order to examine whether this effect is also seen in breast. Contrary to these studies, in prostate cancer ERβ2 expression was associated with increased invasion, but with no effect on migration (101). Given the differing results linking ERβ2 to migration and invasion between cancer types, cellular context appears to be important when considering the role of ERβ2 on cell migration and invasion. The effect of ERβ1 overexpression on migration has been investigated in more detail in breast cancer, and may suggest ways in which ERβ2 can affect cellular migration. Phosphorylation of ERβ1 has been linked to migration regulation. A number of residues mostly in the AF-1 domain of the ERβ protein have been identified as sites of phosphorylation by intracellular kinases (201). EGF and Ras are both able to phosphorylate and activate ERβ by MAPK activation. EGF treatment in cells overexpressing ERβ resulted in a decrease in migration; suggesting phosphorylation of ERβ and subsequent regulation of target genes may regulate migration. It has been demonstrated that phosphorylation of serine 105 on ERβ results in migration inhibition (202). ERβ2 only varies from ERβ1 in its AF-2 domain, and has the same AF-1 domain as ERβ. As the majority of phosphorylation sites are contained within

the AF-1 domain on ERβ1, it is possible ERβ2 is also capable of being phosphorylated in the same way, potentially contributing to regulation of migration. This could account for the decrease in migration observed with overexpression of ERβ2 as with ERβ1.

4.4.4 The effect of ERβ2 overexpression on nuclear gene transcription

Expression of possible ERβ2 target genes was investigated in ERβ2 overexpressing and control cells. A lack of literature regarding ERβ2's function in TNBC, meant it was important to investigate target gene regulation in both ERα positive (MCF-7) and ERα negative (MDA-MB-231) cells. As it is demonstrated that ERβ2 functions by heterodimerising with ERα or ERβ1, ligands targeted to both of these receptors were used to gain insight into which receptor mediates ERβ2 function.

ERβ2 overexpression had very little effect on *BCL-2* and *CDK6* levels in MCF-7. Although ERβ2 decreased proliferation in MCF-7 cells demonstrated in section 3.6, it is likely this is through suppression of ERα signalling rather than regulation of cell cycle proteins, supported by our finding that no change in *CDK6* expression or cell cycle distribution was observed. It is common that with direct regulation of cell cycle proteins, the cell cycle will arrest and this has been observed with ERβ1 overexpression (80, 84). It is not known whether ERβ2 regulates other cell cycle proteins e.g. c-Myc (106) or apoptotic proteins (153) as is the case in other cancers, therefore regulation of the cell cycle or apoptosis via other proteins cannot be ruled out. *S100A7* mRNA levels were dramatically increased in MCF-7 cells overexpressing ERβ2, with the greatest increase in *S100A7* levels observed with ligand treatment. *S100A7* is thought to be tumourigenic when expressed in ERα negative breast .It is associated with poorer outcome in these ERα negative tumours (203). Its function in ERα positive tumours is relatively unknown. Both E2

and DPN upregulated *S100A7* to similar levels in the ERβ2 overexpressing MCF-7 cells suggesting the effect is mediated through interaction with ERβ1. Others have reported that ERβ specifically, but not ERα regulates *S100A7* expression (204), which supports this observation. Although linked to a more invasive phenotype, its overexpression in MCF-7 cells has been demonstrated to reduce proliferation and migration, suggesting it could also function as a tumour suppressor. Specifically, *S100A7* overexpression in MCF-7 and T47D cells downregulated β-catenin, cyclin D1, and c-myc, which code for proteins involved in cell adhesion and proliferation respectively (205). Upregulation of *S100A7* by ERβ2 could contribute to the reduced proliferation and migration seen in our ERβ2 overexpressing MCF-7 and T47D cells by regulating these downstream genes.

As with MCF-7 cells very little change in gene expression was observed with no treatment between MDA-MB-231 control and ERβ2 overexpressing cells. Expression levels of *BCL-2* in the ERβ2 overexpressing cells increased upon ligand treatment compared to their respective control cells. This suggests a possible anti-apoptotic role for ERβ2 in this ERα negative cell line. As previously discussed the increase in proliferation in these cells may be due to a decrease in apoptosis. Increasing *BCL-2* levels supports this theory. In order to confirm a physiological effect on apoptosis, flow cytometry could be utilised to measure the level of cell death in our ERβ2 overexpressing cells versus the control cell lines, using annexin V stain, which detects the externalization of phosphatidylserine from the cell membrane (206). In the literature ERβ has been described as a protective protein, reducing apoptosis to preserve the cell. In the brain tissue ERβ enhanced *BCL-2* expression upon DPN stimulation resulting in neuroprotection (207). Similar finding was observed in cardiac tissue (208). By upregulation of *BCL-2*, ERβ2 may also adopt a cell protective role; however this may only be applicable in an ERα negative setting upon stimulation with a ligand. In MDA-MB-231 cells, *CDK6* mRNA

expression increased with ligand treatment, suggesting ERβ2 may further enhance cell proliferation in MDA-MB-231 cells by promoting G1 to S phase transition. Analysis of cell cycle distribution and proliferation upon ligand treatment could confirm whether this was the case as we currently only investigated these without ligand treatment. As CDK6 was unaltered without treatment yet proliferation was still increased, ERβ2 may act both ligand dependently and independently to regulate proliferation in this cell line. When analysed by Grober et al (47), ERβ1 was demonstrated to downregulate *CDK6* around 2 fold. As ERβ2 appears to have the opposite effect on both *CDK6* expression and proliferation in this cell line, ERβ2 may act to dominantly repress the transcriptional action of ERβ1 in a ligand-dependant manner. ERβ2 could also influence *CDK6* expression from a cytoplasmic location. AKT/PI3K activation is known to upregulate *CDK6* expression (209). ERβ1 has been reported to increase activation of the AKT/PI3K pathway in cardiac tissue (208). However in breast, ERβ1 has been demonstrated to suppress this pathway in ERα positive MCF-7 and T47D cells (116). Whether this suppression extends to ERα negative cells remains to be seen. *S100A7* mRNA expression was upregulated by ERβ2 overexpression in MDA-MB-231 cells with ligand treatment, but to a lesser extent than in MCF-7 cells. As previously discussed, *S100A7* upregulation may contribute to the reduced migration observed in this cell line, however other factors such as upregulation of cell cycle proteins e.g. *CDK6*, may also contribute. In MDA-MB-231 cells *RIP140* was downregulated with and without ligand stimulation, suggesting ERβ2 may regulate its expression ligand independently. *RIP140* is a co regulator of ERs (210). It is required for the downregulation of a number of target genes by ERα and ERβ, and functions as a co-repressor of both receptors (211). As these receptors have been implicated in tumourigenesis and tumour suppression respectively, it is unclear whether *RIP140* expression is favourable or unfavourable in breast cancer. In a recent study, knockdown of *RIP140* prevented an E2 mediated increase in proliferation and G2/M

population in MCF-7 cells. In ERβ overexpressing MCF-7 cells *RIP140* knockdown increased the number of cells in S-phase (212). This suggests *RIP140* can modulate both tumourigenic and tumour suppressive effects depending on ER status.

4.4.5 The effect of ERβ2 overexpression on mitochondrial gene transcription

With cytoplasmic ERβ2, potentially encompassing mitochondrial ERβ2, established as a marker for poor prognosis (94, 100, 102), the function of ERβ2 in this cellular compartment may be tumourigenic. Mitochondrial genes code for proteins involved in oxidative phosphorylation, which make up the various components of this pathway required to produce ATP molecules. ATP is used by the cell as energy for numerous processes such as protein or RNA/DNA synthesis, active transport, structural regulation (assembly/disassembly of the cytoskeleton) and cell movement/migration. Despite some studies demonstrating a decrease in oxidative phosphorylation in cancers due to the reliance on glycolysis for energy (Warburg effect) (213), there are others that have established cancers can increase oxidative phosphorylation and ATP production, during tumourigenesis (214, 215). As ERβ2 was demonstrated to colocalise with the mitochondria in this study, suggesting it may be localised to this compartment, it's potential as a transcriptional regulator of mtDNA coded genes was investigated.

In MCF-7 cells, ERβ2 overexpression resulted in a decrease in expression of *ND1* and *ND2* upon E2 treatment, suggesting regulation is ligand dependent in this cell line. Only a small downregulation of *ATP6* and *CYB* was observed. DPN treatment had little effect on mtDNA gene regulation, suggesting changes observed result from an interaction with ERα and not ERβ1. As no binding site was detected for ERα in the mitochondrial genome in previous studies (47), it is possible E2

treatment results in heterodimerisation of ERα/ ERβ2, and directs its function outside of the mitochondria. ERα has been reported to regulate nuclear transcribed genes involved in mtDNA transcription. Upregulation of NRF-1 and subsequent upregulation of TFAM by ERα upon E2 treatment from its nuclear location has been reported in MCF-7 cells (216-218). TFAM is required for mtDNA transcription, and functions as a key activator of mitochondrial transcription. Its upregulation was followed by an increase in COX1 and *ND1* transcription, two mtDNA transcribed genes. This indirect regulation of mtDNA encoded genes could explain the decrease in mtDNA transcription of the genes examined in this study. As ERβ2 is known to inhibit the action of ERα (95), it is possible ERβ2 may suppress transcription of NRF-1 and TFAM by heterodimerisation with ERα upon E2 activation, thus suppressing mtDNA gene transcription. To confirm this hypothesis, mRNA and protein levels of both TFAM and NRF-1 could be investigated by qRT-PCR and western blot in ERβ2 overexpressing cells compared to the control cells.

In MDA-MB-231 cells, ERβ2 overexpression caused increased mtDNA gene transcription for all genes investigated upon ligand treatment, opposite to the effect observed in MCF-7 cells. The effect was more pronounced upon E2 stimulation than DPN. E2 is a more potent ligand with a lower EC50 (219) value and a higher ligand binding affinity (5.5 fold higher) for ERβ than DPN (220), which may explain why the effect in response to E2 is more discernible. In MDA-MB-231 mtDNA gene regulation by ERβ2 appears to be ligand dependent, as little change was observed without treatment. ChIP-Seq analysis has identified an ERβ1 binding site in the D-loop region of the mitochondrial genome, the region that controls mtDNA gene transcription (47), suggesting a function for ERβ in the regulation of mtDNA coded genes. In the absence of ERα in this cell line, gene transcription is likely mediated through ERβ2/ERβ1 heterodimers, and is likely to be as a result of direct regulation on mtDNA. This direct regulation of mtDNA coded genes has been described in the

literature for ERβ. It was demonstrated to be localised to the mitochondria, and upon E2 stimulation, it drove the transcription of some mtDNA encoded genes, for example in breast, COX1, COXII and *ND1* were all upregulated upon DPN (ERβ agonist) treatment (122). Similarly, in cardiac tissue ERβ caused up-regulation of proteins making up complex IV, the last enzyme in the respiratory electron transport chain, following tissue trauma. This was coupled with an increase in ATP production and apoptosis suppression, suggesting a cardio protective role for ERβ in the mitochondria (123). As ERβ2 overexpression resulted in increased expression of components of the respiratory chain complex, which would presumably drive oxidative phosphorylation, an increase in ATP synthesis may ensue. Driving proliferation and cell growth may provide a possible explanation for upregulation of mtDNA transcribed genes. Cellular ATP production can be measured by way of a colorimetric micro-plate assay, where conversion of ATP to ADP by ATP synthase can be measured in both the control and ERβ2 overexpressing cells, and would give an indication as to the downstream physiological effect of increased mtDNA gene transcription. In contrast to this there is literature that implicates ERβ1 in the suppression of oxidative phosphorylation (124). However, it is important to note that this is through the regulation of nuclear encoded genes that are involved in oxidative phosphorylation e.g. inhibition of succinate dehydrogenase B transcription, a protein involved in oxidative phosphorylation. The subsequent reduced ATP production and cellular proliferation is not mediated through mitochondrial ERβ. In contrast, ERβ2 may be acting from a mitochondrial location, which appears to result in the opposite effect potentially resulting in tumourigenesis. This would strengthen the link between cytoplasmic ERβ and poorer prognosis especially if a downstream increase in cellular energy production and suppression of apoptosis, characteristic of tumourigenesis, is observed as in cardiac tissue (123).

4.4.6 Subcellular fractionation

In chapter 3, ERβ2 expression in the nucleus, cytoplasm and the mitochondria was identified by immunofluorescence. We sought to demonstrate this ERβ2 protein expression in each of these compartments, and investigate whether various estrogenic ligands would affect ERβ2 cellular distribution. Western blot analysis of ERβ2 protein distribution established that the highest levels of ERβ2 protein were detected in the mitochondria of MCF-7 cells and in the cytoplasm and mitochondria of MDA-MB-231 cells. This suggests a function for ERβ2 in these compartments which is contrasting to its suggested function as a nuclear transcription factor.

Mitochondrial ERβ has been described in the literature in various tissues including breast, uterine and cardiac (121, 123, 221). We have demonstrated ERβ2 colocalisation and now presence of the protein in the mitochondria of breast cancer cells. As previously discussed in section 4.4.5, some mtDNA genes have been demonstrated to be regulated by ERβ and we demonstrated that ERβ2 overexpression both upregulated and downregulated some mtDNA genes, suggesting it functions as a transcription factor within the mitochondria, and may have a role in oxidative phosphorylation. Others have identified ERβ1 to be anti-apoptotic when located within the mitochondria, due to upregulation of manganese superoxide dismutase, preventing reactive oxygen species forming (124). This has also been observed in prostate, where ERβ activation by E2 causes a decrease in ROS (222). Aside from a possible involvement of ERβ2 in oxidative phosphorylation, ERβ2 may also have involvement in apoptosis. When located in the mitochondria of ovarian cancer tissue interaction of ERβ2 with the pro-apoptotic protein BAD has been identified, which occurred ligand independently. The study went on to demonstrate that in the cells with the BAD/ERβ2 complexes, Bcl-xL/BAX complexes were also evident which led to the inhibition of the release of

cytochrome C from the mitochondria, a phenomenon preceding apoptosis (153). The abundance of ERβ2 in the mitochondria of MDA-MB-231 and MCF-7 cells may function in a similar manner. As in this study, using a proximity ligation assay, protein-protein interaction between ERβ2 and BAD could be investigated in breast cancer cells. We have already identified *BCL-2* upregulation by ERβ2 in MDA-MB-231 cells and other apoptotic proteins could also be investigated in the same way to further confirm involvement.

The presence of ERβ2 in the cytoplasm is often associated with inactivity prior to activation and phosphorylation with a ligand. However there is evidence for a non-genomic role for ERβ suggesting a function for ERβ in the cytoplasm. Cytoplasmic ERβ signalling has been demonstrated to activate AP-1 sites in target gene promotes. When MAPK was inhibited, AP-1 was not activated, suggesting promoter activation occurs via the MAPK pathway (223). In lung cancer cells, where ERβ expression was cytoplasmic, activation with estrogen caused activation of cAMP, Akt and MAPK signalling, without translocation of ERβ to the nucleus suggesting, in these cells, ERβ functions to regulate target genes cytoplasmically (166). This in turn may actually increase proliferation, which is contrary to the tumour suppressive role ERβ is described as having. Clearly there is evidence for a cytoplasmic function of ERβ, but whether this extends to ERβ2 remains to be seen. Measuring downstream target gene levels known to be regulated by MAPK signalling or measurement of phosphorylated (activated) MAPK pathway components in cells overexpressing ERβ2 versus control cells would enable us to determine whether ERβ2 has any involvement in the activation/inhibition of this pathway.

4.4.6.1 The effect of ligands on ERβ2 subcellular localisation

ERβ functions both ligand-dependently and ligand-independently. The effect of various estrogenic ligands on distribution of ERβ2 within each cellular compartment was examined, to observe whether ligands influence the cellular localisation of ERβ2. In MCF-7 cells, with the exception of DPN treatment, ERβ2 protein levels mirrored those in the whole cell extracts

These data suggests the ligands do not influence mitochondrial or nuclear ERβ2 levels and the changes seen are attributed to whole cell changes possibly caused by up or down-regulation of the protein. In both MCF-7 and MDA-MB-231 cells DPN treatment resulted in increased cytoplasmic ERβ2 compared to the untreated cells. DPN is an ERβ agonist, targeting the only ligand binding isoform, ERβ1. A potential role for ERβ has been suggested in section 4.6, where regulation of MAPK signalling has been evidenced. In addition, DPN has been reported to decrease MAKP phosphorylation levels in breast tumours (224). An association with MAPK signalling has also been reported in lung cancer cells, where a 3.7 fold increase of MAPK phosphorylation was observed upon DPN treatment (166). These effects are likely mediated through ERβ1 as DPN is its agonist. This literature indicates evidence for a non-genomic role for ligand activated cytoplasmic ERβ in cancer, where ERβ2 may also have some involvement in kinase signalling pathways in view of the increased cytoplasmic ERβ2 levels stimulated by DPN. Whether the effect is stimulatory or inhibitory would require further study; however measurement of either MAPK target genes, phosphorylated MAPK signalling components or use of a MAPK reporter assay could indicate signalling activation in ERβ2 overexpressing cells compared to control cells upon DPN treatment.

Genistein treatment resulted in increased mitochondrial ERβ2 in both cell lines compared to untreated control cells. Genistein is also an ERβ1 agonist but can act as a weaker agonist of ERα (225).

A potential role for ERβ2 in the mitochondria has been suggested and discussed previously in section 4.5. We have demonstrated that ERβ2 overexpression results in changes in mitochondrial respiratory chain proteins upon ligand treatment. It is possible genistein may also regulate ERβ2 mediated mitochondrial gene transcription through activation of ERβ1. As genistein had a more profound effect on ERβ2 mitochondrial localisation, regulation of mtDNA transcribed genes by ERβ2 demonstrated in 4.3.8, may be further enhanced by genistein treatment therefore re-analysis of mtDNA transcribed genes upon genistein treatment could address this speculation.

4.5 Summary

The series of experiments performed in this chapter portray ERβ2 as both tumourigenic and tumour suppressive. ERβ2 overexpression both suppresses and promotes proliferation in different cell lines. Interestingly in two different cell lines with the triple negative phenotype, ERβ2 overexpression has opposing effects on proliferation. Consideration of potential crosstalk with other cytoplasmic signalling pathways may explain this effect. ERβ2 also reduces cell migration in all cell lines studied; however it is unclear how ERβ2 influences this process. Examination of the proteins involved in migration and invasion that have been linked to ERβ in the literature could however give an indication.

ERβ2 appears to suppress and enhance mitochondrial DNA gene transcription in ERα positive and negative cells respectively, suggesting opposing functions on cellular energy production dependant on ERα status. Similarly ERβ2 appears to differentially regulate some of its target genes between different cell lines suggesting more than one mechanism for target regulation. ERβ2 may regulate target genes non-genomically via crosstalk with other signalling pathways e.g. MAPK/ERK, PI3K/AKT. In prostate cancer cells, ERβ2 has opposing actions to ERβ1, thought to be mediated by its effect on cytoplasmic signalling pathways. Multiple potential mechanisms for target gene regulation could explain the differential physiological effects ERβ2 has on different cell types. In MDA-MB-231 cells, ERβ2 regulated target genes in a way that may promote tumourigenesis, with upregulation of *BCL-2, CDK6* and mitochondrially transcribed genes potentially promoting cellular energy production, possibly explaining the increased proliferation observed in these cell lines with ERβ2 overexpression. This is very different to the role it has in ERα positive cells, where ERβ2 is seen to be tumour suppressive. As these target genes were differentially regulated only upon ligand treatment, it would be interesting to re-consider proliferation and cell cycle distribution upon ligand treatment. Upregulation of *BCL-2* and *CDK6* in MDA-MB-231 ERβ2 overexpressing

cells upon treatment could mean these processes will be further enhanced and changes in cell cycle distribution may occur.

The identification that most ERβ2 is expressed in the cytoplasm of MDA-MB-231 cells in the fractionation experiments gives weight to the observation that cytoplasmic ERβ2 is a poor prognostic marker in various cancers including ovarian, prostate and breast. As two opposing roles for ERβ2 are emerging, it is clear further investigation needs to be done taking into consideration multiple signalling pathways other than estrogen signalling. These results underline the complexity of ERβ2 functionality.

5.0 Chapter 5: Characterisation of ERβ2 nuclear speckles in breast cancer cell lines

5.1 Introduction

In Chapter 3 the observation was made that ERβ2 was expressed as speckles in the nucleus of all breast cancer cell lines examined. To understand the potential function of these speckles we must first consider the function of nucleus itself and some of its similarly speckled proteins.

5.1.1 The cell nucleus

The cell nucleus is a membrane enclosed organelle found within eukaryote cells. Each cell contains around 2 meters of DNA, which comprises the entire organism's genetic material, excluding the small number of genes (38) contained in the mitochondrial genome. This is tightly wrapped around proteins, primarily histones, to form chromatin. Chromatin is organised into euchromatin; a relaxed structure allowing transcription, and heterochromatin, a tightly compacted transcriptionally inactive complex. Euchromatin contains the genes that are frequently expressed and therefore regularly transcribed in that particular cell. Chromatin is further packaged and condensed forming chromosomes, which reside in specific regions of the cell nucleus. The major function of the cell nucleus is to regulate gene transcription and mediate DNA replication during the cell cycle. Additional nuclear structures aid transcription by harbouring proteins such as splicing factors or those involved in transcription.

5.1.2 Nuclear structures

There are a number of bodies within the nucleus containing proteins that function to aid in transcription and post-transcriptional modifications. They are observed as speckled structures containing defining sets of marker proteins.
They include promyelocytic leukemia (PML) nuclear bodies, nuclear speckles, paraspeckles, cajal bodies and nucleoli. A diagram of the cell nucleus containing these nuclear structures is displayed in Figure 5.1.It is also suggested that transcription occurs at specific sites in the nucleus rather than homogenously, which have been termed transcription factories (226).

5.1.2.1 Nucleolus

The nucleolus is made up of three components; the granular component (GC), the dense fibrillar component (DFC) and the fibrillar centre (FC). Pre-RNA synthesis and early rRNA processing occurs within the DFC while late rRNA processing events and assembly of ribosomal proteins occurs in the GC. Nucleoli function as the site for ribosome synthesis and assembly. They contain the genes required for biogenesis of ribosomal RNA (rRNA) and the 40S and 60S ribosomal subunits. Transcription of rRNA requires both RNA pol I and III (227).

5.1.2.2 PML bodies

PML bodies are around 0.1-1 μm in diameter and are found in the nucleus of higher eukaryotes. They are named after their major component, PML. PML bodies were first identified at the site of a translocation associated with promyelocytic leukemia where the PML gene becomes fused in a chromosomal translocation with the retinoic acid receptor alpha (RARα) on chromosome 17 resulting in the creation of an oncogene. PML bodies associate with the nuclear matrix, a dynamic network of fibres that play a role in anchorage and regulation of many nuclear functions e.g. DNA replication, gene silencing and transcription (228). They recruit numerous

proteins and are proposed to facilitate their posttranslational modifications (namely sumoylation), then sequester, modify or degrade these proteins (229). The PML protein itself has been associated with DNA repair and apoptosis control (230, 231).

5.1.2.3 Cajal bodies

Cajal bodies are another nuclear sub-domain that forms speckled structures of around 0.1-2.0 µm. They are found in the nuclei of proliferating cells and are commonly observed in tumour cells. A major component of cajal bodies is the protein coilin, which anchors them to the nucleolus, and coilin P-80 is a widely used marker for these structures (232). Their number and size varies during progression of the cell cycle with the most found at G1 phase and fewer larger bodies observed in G2. They are believed to function as posttranscriptional modifiers and contain large amounts of splicing small nuclear ribonucleoproteins (snRNPs)(233, 234)

5.1.2.4 Nuclear speckles

Nuclear speckles are interchromatin granule clusters enriched in pre-mRNA splicing factors. These are dynamic structures of variable shape and size, which act as storage/assembly compartments that can supply splicing factors to active transcription sites. Pre-mRNA structures are often located on the periphery of nuclear speckles. Nuclear speckles have been observed to increase in size upon transcriptional inhibition (234, 235) suggesting speckles are not the direct site of splicing but are involved in storage, assembly or modification of splicing factors.

5.1.2.5 Paraspeckles

Paraspeckles, like nuclear speckles, are found in the interchromatin space and are around 0.5-1µm in diameter (236). They are widespread within mammalian cells. Their name comes from the fact that they are located in parallel or adjacent to nuclear speckles. Their function is currently speculative; however they are believed to contribute to transcriptional regulation by nuclear retention of RNA (237).

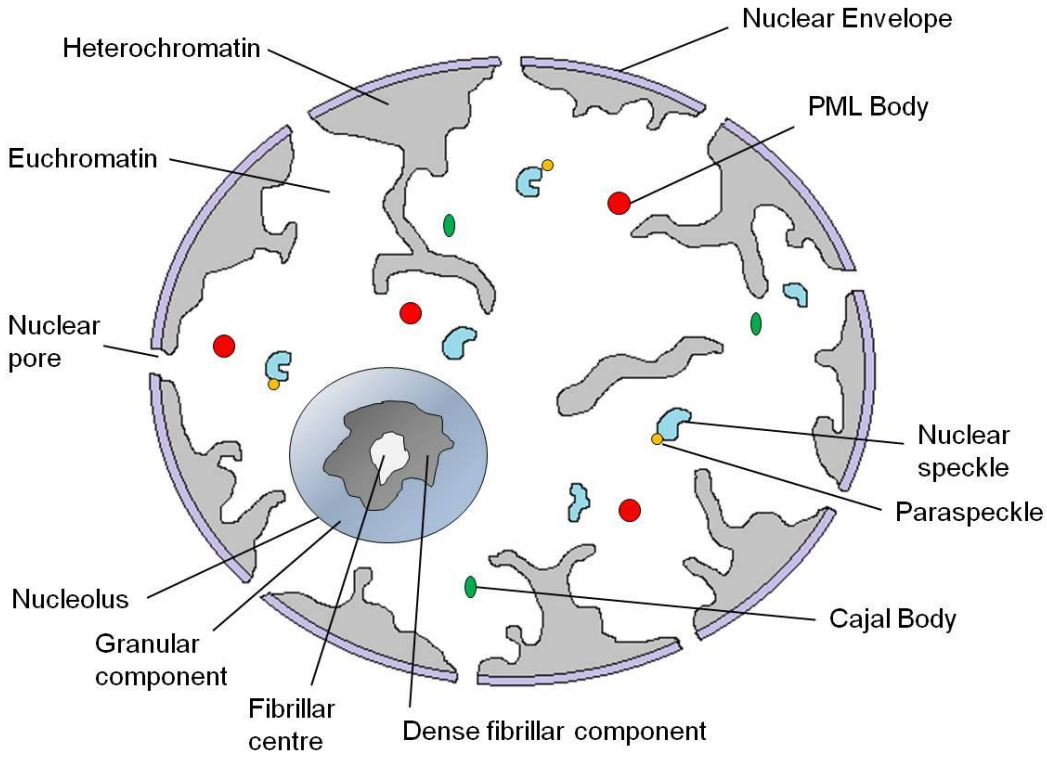

Figure 5.1. The structure of a nucleus depicting the sub-nuclear structures present in eukaryote cells.

5.1.3 Nuclear structures and cancer

Some of the nuclear sub-domains mentioned above have been linked to cancer. PML is believed to be tumour suppressive due to its function in mediating cell death. Reduced PML levels are observed in solid tumours compared to normal tissue. PML bodies have been associated with cell cycle regulation, by interaction with p53 and the Bloom syndrome protein (BLM), DNA damage (238), apoptosis (239) and senescence (240).

The nucleolus has been linked to tumourigenesis as proliferating cancer cells often have increased demand for ribosome biogenesis. Loss of function of the tumour suppressive proteins pRB and p53 cause an up-regulation of ribosome biogenesis in cancer tissues (241). The nucleolus contains a number of proteins implicated in cancer. Nucleostemin can both activate and suppress p53 as can nucleophosmin (242-245). Nucleolin can also be tumour suppressive or oncogenic through its association with RNA I and II polymerase and by telomere association. It can also activate p53 tumour suppressor by preventing its ubiquitination and therefore degradation (246).

5.1.4 Nuclear speckled ER

ERβ2 has been identified by a previous PhD student in the Breast Research Group at Leeds to be expressed in distinct speckle like structures in the cell nucleus in MCF-7 cells and primary breast cancer tissue samples (C.A. Green, unpublished observation). A similar expression pattern has been identified when examining the expression of ERβ phosphorylated at serine-105 (172). Expression of this speckled activated ERβ protein was associated with higher grade tumours in a cohort of 108 tamoxifen-resistant and 351 tamoxifen-sensitive breast cancer cases that were examined. Speckles were also observed in MCF-7 cells and upon E2 and DPN treatment, numbers significantly increased. In addition to ERβ, ERα has also been

observed as speckled nuclear structures when phosphorylated at ser118 upon co-expression with SOX2, a transcriptional regulator (247).

Our previous observations detailed in chapter 3, have established that ERβ2 is expressed as distinct speckles localised in the nucleus of 9 breast cancer cell lines. It is unclear as to their function and whether they are associated with other nuclear proteins and therefore warrants further investigation

5.2 Aims

The aims of this chapter were to examine the function and characteristics of ERβ2 nuclear speckles by investigating:

- if ERβ2 speckles colocalise with other nuclear proteins expressed as speckled structures
- ERβ2 speckle dynamics in response to estrogenic ligands
- whether speckles are associated with phases of the cell cycle
- whether speckles are influenced by transcriptional or translational inhibition

5.3 Methods

This section outlines the development, optimisation and validation of the ERβ2 speckle counting method used in the experiments presented in this chapter. The optimised parameters were then applied to all images where counting of ERβ2 speckles was required. This allowed increased accuracy and reproducibility of results when comparing different images, and dismissed any user bias in the counting process.

5.3.1 Development of ERβ2 speckle analysis methodology

ERβ2 speckles are easily identifiable on the confocal microscope looking down the eyepiece, but the resolution of the images acquired means identifying them by eye from these images becomes more difficult. Looking down the microscope for long periods of time in an attempt to count the speckles manually is not feasible as the constant excitation of the fluorophores attached to the protein of interest leads to bleaching. To overcome these difficulties an automated method for speckle counting was developed. Image (1) in Figure 5.2 represents the stages of image processing in order to ultimately count 'objects' (speckles) within the cells. Briefly the cell nucleus was identified (a) and a DAPI mask was overlaid (b). Each nucleus was converted to an ROI (region of interest) and numbered by the software shown in image (c). Objects were counted in each ROI using a FITC intensity threshold and pixel exclusion to isolate speckles based on intensity and size respectively, and the software counted these objects. The white arrows in Figure 5.2d point to objects counted as speckles highlighted in pink.

5.3.2 Validation of ERβ2 speckle analysis methodology

MCF-7 cells stained with ERβ2 antibody were used for validation purposes of the automated speckle counting protocol. ERβ2 speckles were only present in a proportion of the cells, and those without speckles were easily identified by eye and marked for analysis on the image acquired. Six images from six separate slides were examined using the above methodology (examples in appendix 7.2). To determine the minimum size that a speckle would be to be counted as such, a size exclusion method was adopted. This excluded objects based on the number of pixels that made them up. In the subset of negative images, where no visible speckles were present, analysis was performed for **≤** 1, **≤** 2, **≤** 3 then **≤** 4 pixel exclusion, using the FITC intensity threshold of 1200. Only upon 4 or fewer pixel exclusion were no objects recorded in the 'negative' images, and therefore we were satisfied that the algorithm would not detect smaller intensely stained 'objects' that were not considered speckles when visualised down the eyepiece of the microscope. The object counts for the pixel exclusion settings can be found in appendix 7.3. The principle of this pixel exclusion is illustrated in Figure 5.3, where without size thresholding single pixels would be counted as objects (a), but with pixel exclusion applied only objects or 5 pixels or more are counted (b).
The optimised final settings; 1200 FITC threshold with 4 pixels or less exclusion, were used to analyse all images which required ERβ2 speckle counting.

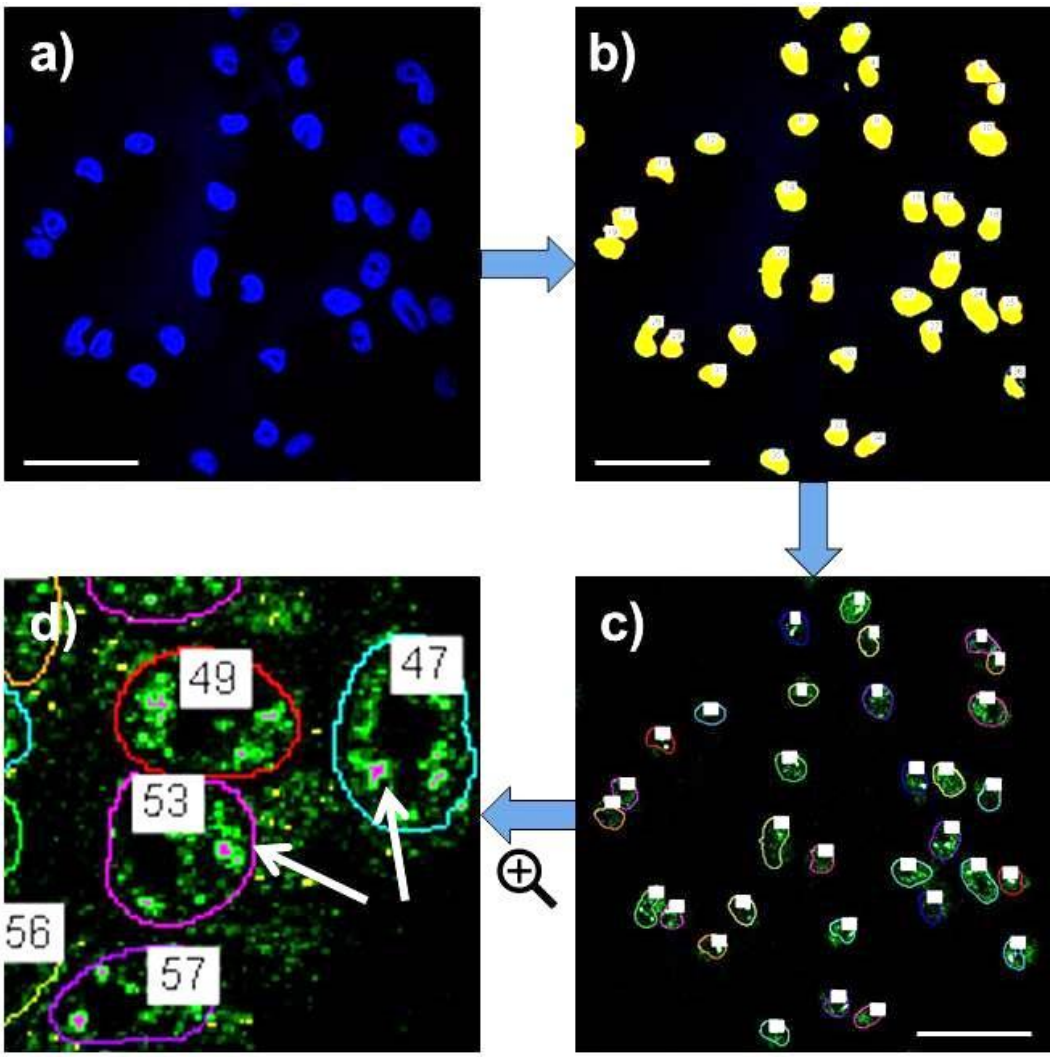

Figure 5.2. Images representing the steps required for speckle counting
a) The cell nucleus was identified
b) A DAPI mask was overlaid
c) The DAPI mask was converted to ROIs (regions of interest), one for each nuclei, and numbered
d) FITC thresholding of 1200 was applied and speckles of 5 pixels or more were highlighted in pink, indicated by the white arrows

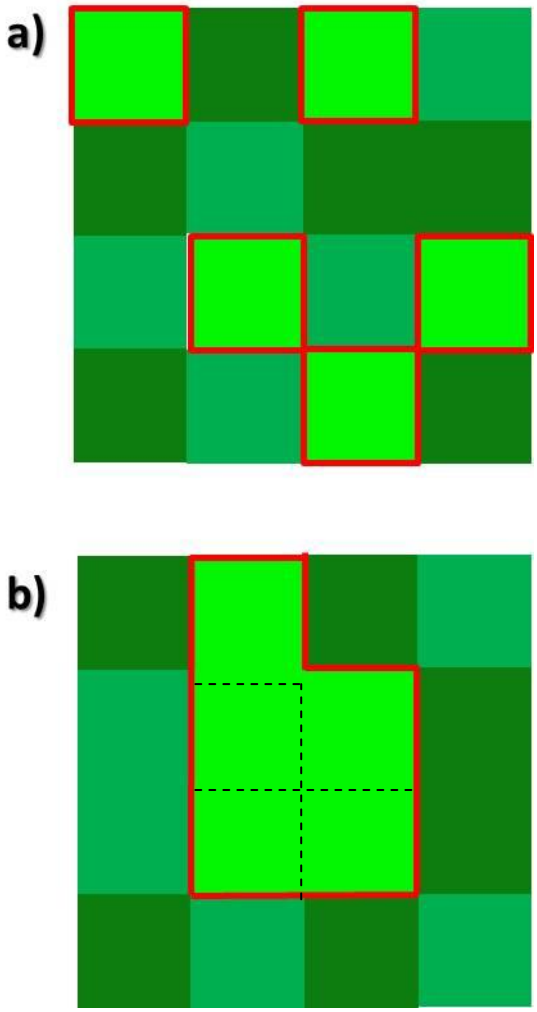

Figure 5.3. Illustration of the principle of size thresholding for identification of ERβ2 nuclear speckles.
a) No pixel exclusion applied to size thresholding. Single pixels are recognised by the software as objects or 'speckles', highlighted in red
b) 4 pixel or less exclusion applied to size thresholding. Only objects of 5 pixels or more, highlighted in red, or more are recognised as an object or 'speckle'.

5.4 Results

5.4.1 Colocalisation investigation of ERβ2 with other known nuclear speckled proteins

An interesting observation made in chapter 3 was that ERβ2 is often expressed as speckles in the nucleus of breast cancer cell lines. In order to elucidate their potential function, colocalisation of ERβ2 speckles with other nuclear speckled proteins was considered using immunofluorescence. ERβ2 was labelled along with co-staining with coilin (a marker for cajal bodies), PML, or SC-35 (a marker for nuclear speckles) antibodies (Figure 5.4). The top row represents ERβ2 (green) and coilin (red) staining. On the merged image ERβ2 speckles are indicated by the white arrow and coilin staining cajal bodies by the yellow arrows. The magnified cell on the bottom right corner of this image shows the location of the some of the speckles more clearly. There was no overlap (colocalisation) of coilin (thus cajal bodies) with ERβ2 speckles. In the middle row colocalisation of ERβ2 (green) with PML (red) was investigated. Speckled expression of both proteins is shown in the merged image with ERβ2 indicated by the white arrow and PML with the yellow arrow. No colocalisation was observed with ERβ2 and PML staining and the magnified cell in the merged image illustrated this in an individual cell. The bottom row demonstrated dual staining with ERβ2 and SC-35 antibodies. In the merged image, ERβ2 speckles (green) and nuclear speckles (red) can be seen. Again there was little overlap in their staining and the two appear not to colocalise. However, ERβ2 speckles did often appear adjacent to SC-35 nuclear speckles. An example of this is shown clearly in the magnified cell at the bottom right of the merged image with ERβ2 speckles pointed out by the white arrow and nuclear speckles denoted by the yellow arrow.

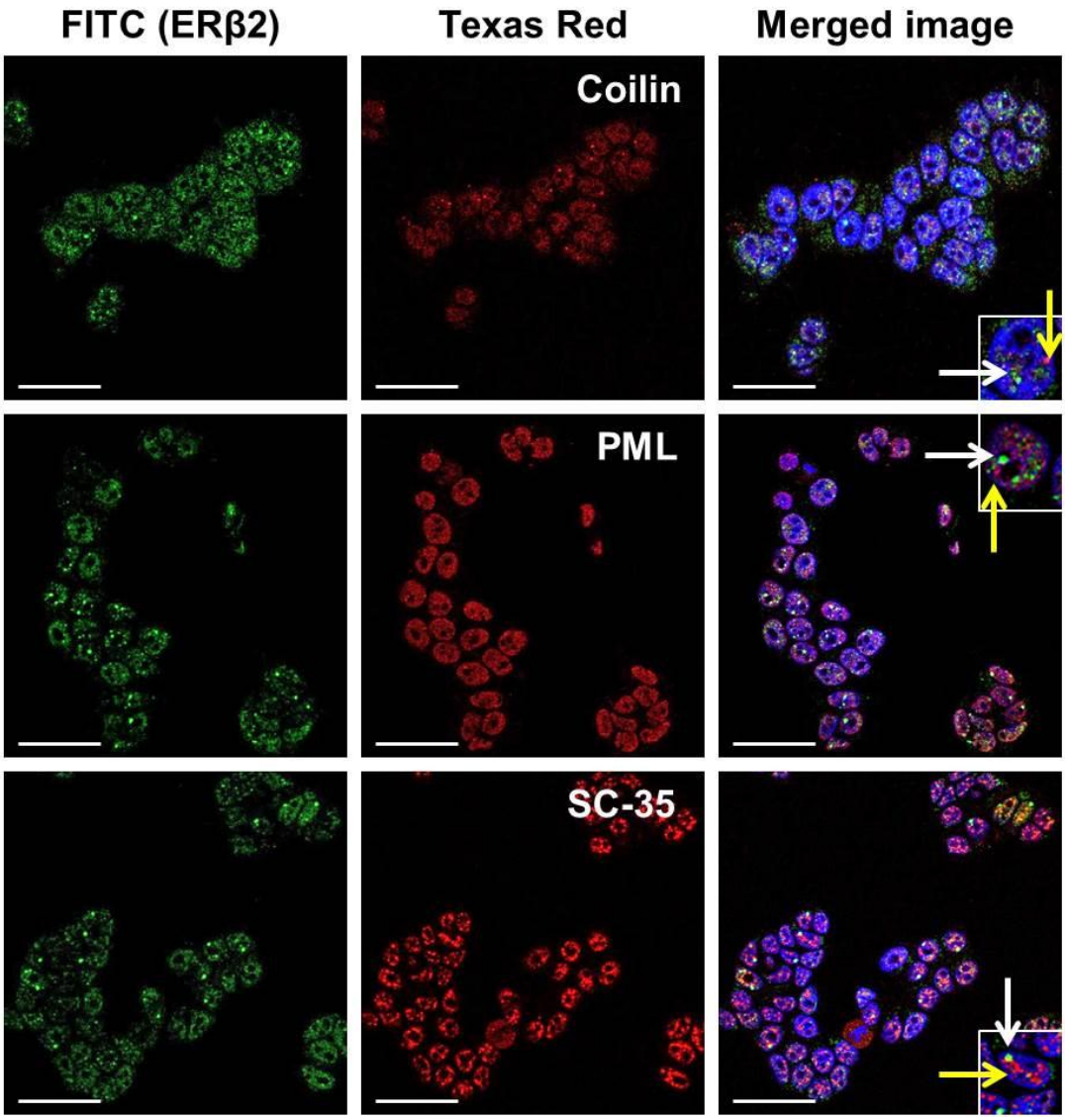

Figure 5.4. Co-staining of MCF-7 cells with ERβ2 and other nuclear speckled proteins.
ERβ2 stained images are presented on the left and Coilin, PML and SC-35 staining are displayed in the middle column. Merged image indicates green (ERβ2) and red (coilin, PML, SC-35) co-staining.
The yellow arrow on the magnified cells indicates coilin, PML or SC-35 speckles and the white arrow ERβ2 speckles.
Images acquired at 60x magnification and scale bars represent 50µm.

Colocalisation with the nucleolus was also considered, results of which are presented in Figure 5.5. Two slides of MCF-7 cells were analysed and presented at 60x magnification (left). A group of cells from each image were enlarged to illustrate features in the nucleus, presented on the right. Due to the detailed resolution of the images gained using the Nikon A1R confocal microscope, the nucleolus can be seen without using an antibody. These are pointed out as dark spots, unstained by DAPI, by the red arrows in the magnified images. ERβ2 speckles are indicated by the white arrows in these images, and no overlap between the two was observed, signifying no colocalisation. ERβ2 speckles were consistently absent from the nucleolus throughout this project.

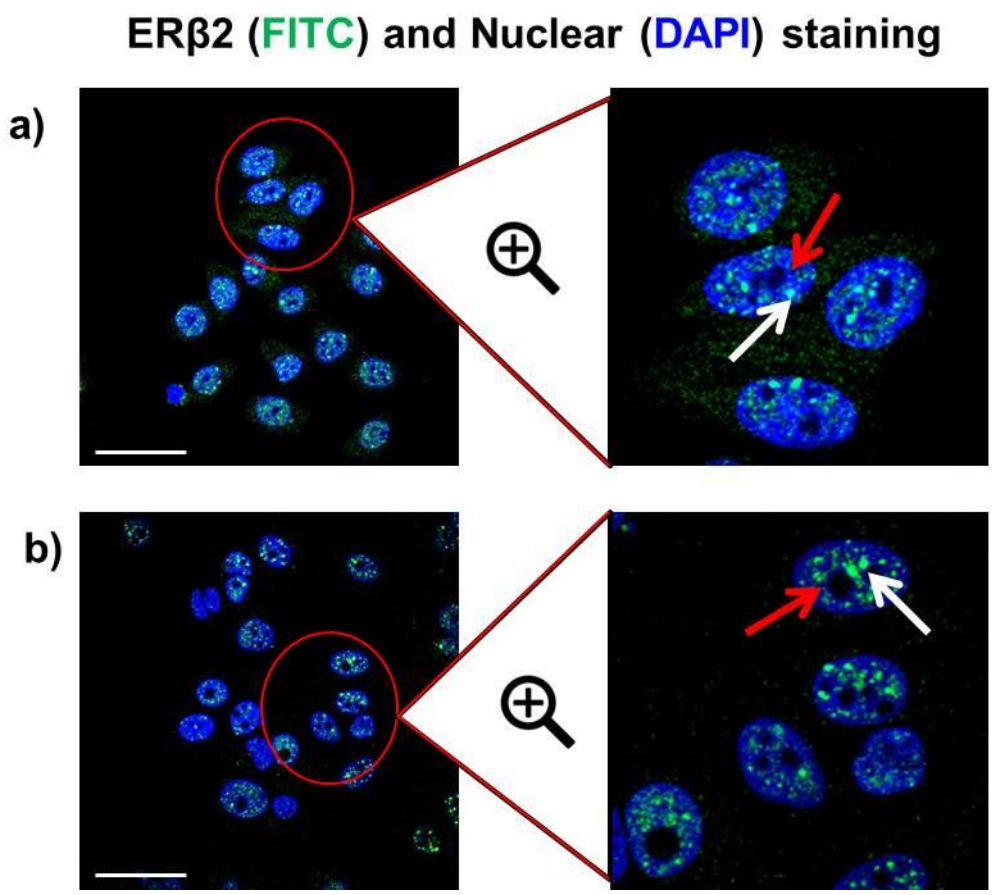

Figure 5.5. MCF-7 cells illustrating the location of the nucleolus and ERβ2 nuclear speckles.
Two examples of ERβ2 staining (green) and nuclear DAPI staining (blue) illustrating the location of ERβ2 speckles in relation to the nucleoli. Circled are groups of cells magnified on the right hand images, which illustrate the nucleolus, indicated by the red arrows, and ERβ2 speckles, by the white arrows. Scale bars represent 50µ.Images on the left were taken at 60x magnification.

5.4.2 Examination of ERβ2 nuclear speckle number in response to estrogenic ligand treatment

ERβ2 is not known to function as a homodimer, and is instead thought to exert its effects by heterodimerisation with other ERs. As it is a non-ligand binding isoform, its ligand dependent transcriptional effects are mediated by binding to either ERα or ERβ1. Estrogenic ligands targeted to ERα and/or ERβ1 were used to investigate whether ERβ2 speckle numbers would change in response to ligand activation, which may suggest involvement in ER transcription. MCF-7 and MDA-MB-231 cells were incubated with E2 (ERα/β agonist), 4-OHT (ERα/β antagonist), DPN (ERβ agonist) and genistein (ERβ > ERα agonist) and ERβ2 immunofluorescence was performed then ERβ2 speckles counted. Cell proliferation and ERβ2 mRNA levels were also measured in parallel. In order to establish an effective working concentration that stimulated a physiological effect, cell proliferation dose response assays were initially performed on MCF-7 cells while incubated with the various ligands (appendix 7.7).

Figure 5.6 displays MCF-7 growth curves using the effective ligand concentrations previously determined, and cell numbers measured every 24 hours from 48 hours to 120 hours. As expected 1nM E2 increased growth of MCF-7 cells (a), while 4-OHT at 50nM (b), DPN at 10nM (c) and genistein at 30μM (d) all resulted in growth suppression.

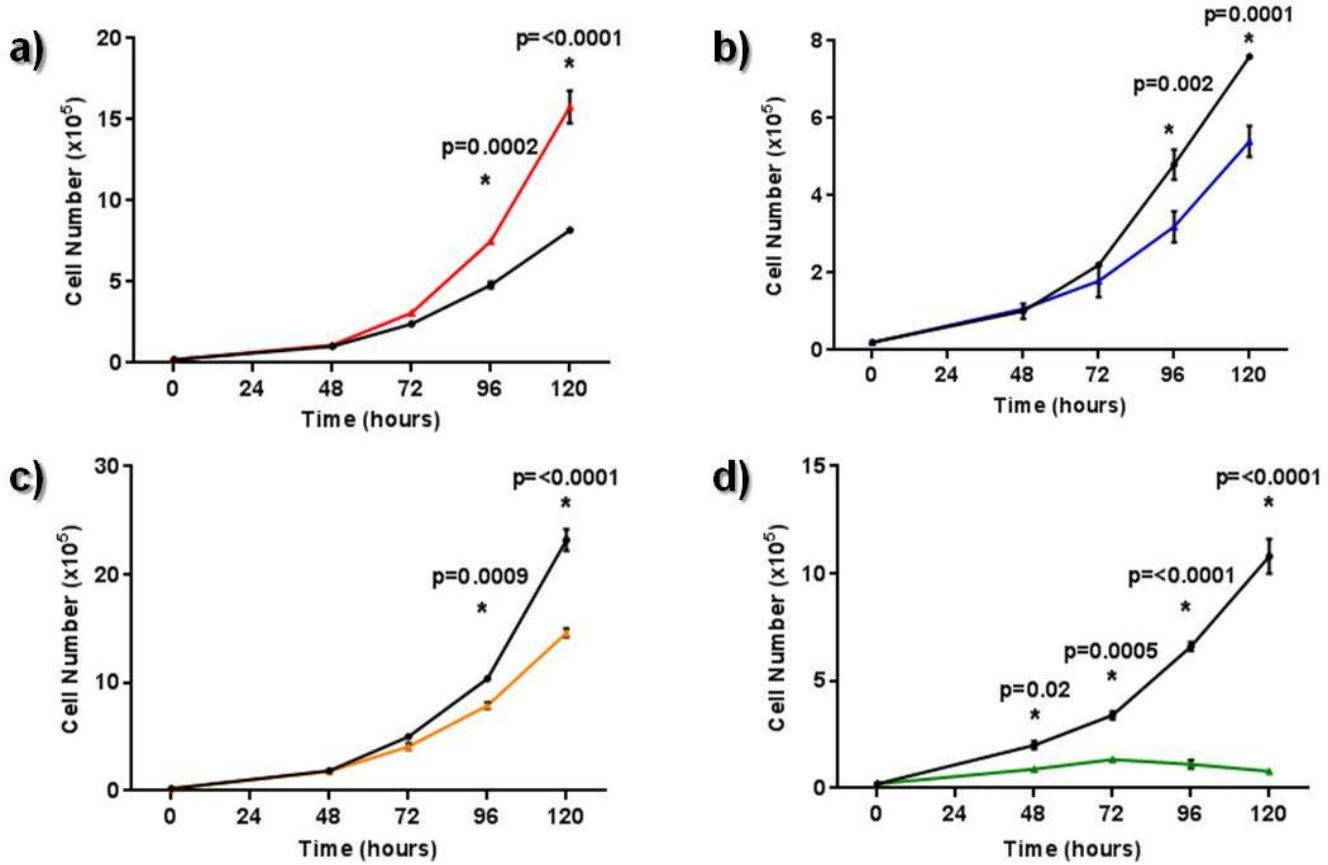

Figure 5.6. MCF-7 growth curves in response to estrogenic ligands.
Cell counts were performed at 48, 72, 96 and 120 hours and cell number plotted. a) E2 (1nM), red line), b) 4-OHT (50nM), blue line, c) DPN (10nM), yellow line, d) genistein (30uM), green line. The black lines on all graphs represent untreated control cells. Error bars represent ± SEM for n=2 (technical replicates). Statistically significant changes in cell number (*) and p-values, measured using a multiple student's t-tests with Holm-Sidak correction, are displayed.

Figure 5.7 demonstrates the ERβ2 nuclear speckle patterns seen in MCF-7 cells after incubation with estrogenic ligands. The red arrows point to visible speckles on the images. There is an increase in the number of speckles after incubation with 4-OHT and genistein.

Figure 5.8a illustrates the results of the automated counting of the ERβ2 speckles. The difference between the control cells and those treated with E2 was not statistically significant suggesting E2 does not affect ERβ2 speckle number. However 4-OHT, DPN and genistein all resulted in a significant increase in ERβ2 speckles.

Figure 5.8b illustrates the levels of total cellular ERβ2 mRNA in the cells in response to the same ligands. This data demonstrated that exposure to E2 resulted in a decrease in ERβ2 mRNA, however speckle number remained unchanged. 4-OHT caused an increase in ERβ2 mRNA, which was mirrored in the increase in ERβ2 speckle number. mRNA levels in response to DPN remained unchanged. Interestingly, despite genistein causing a significant increase in ERβ2 speckles, a significant decrease of ERβ2 mRNA was observed.

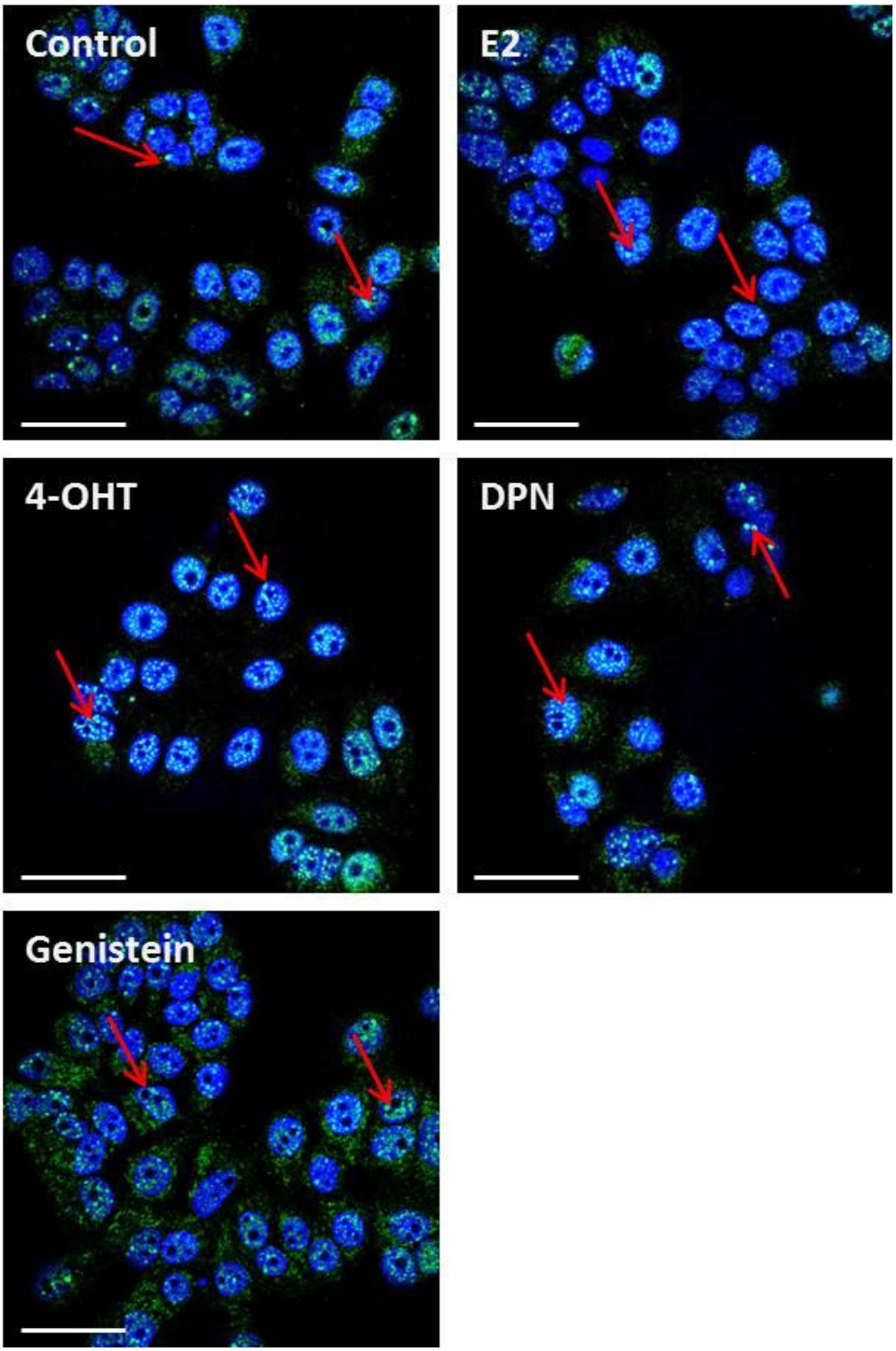

Figure 5.7. Immunofluorescence analysis of ERβ2 speckle expression pattern in MCF-7 cells in response to the estrogenic ligands E2, 4-OHT, DPN and genistein.
The control image represents untreated cells. The red arrows indicate ERβ2 nuclear speckles. Images taken at 60x magnification and scale bars represent 50µm.

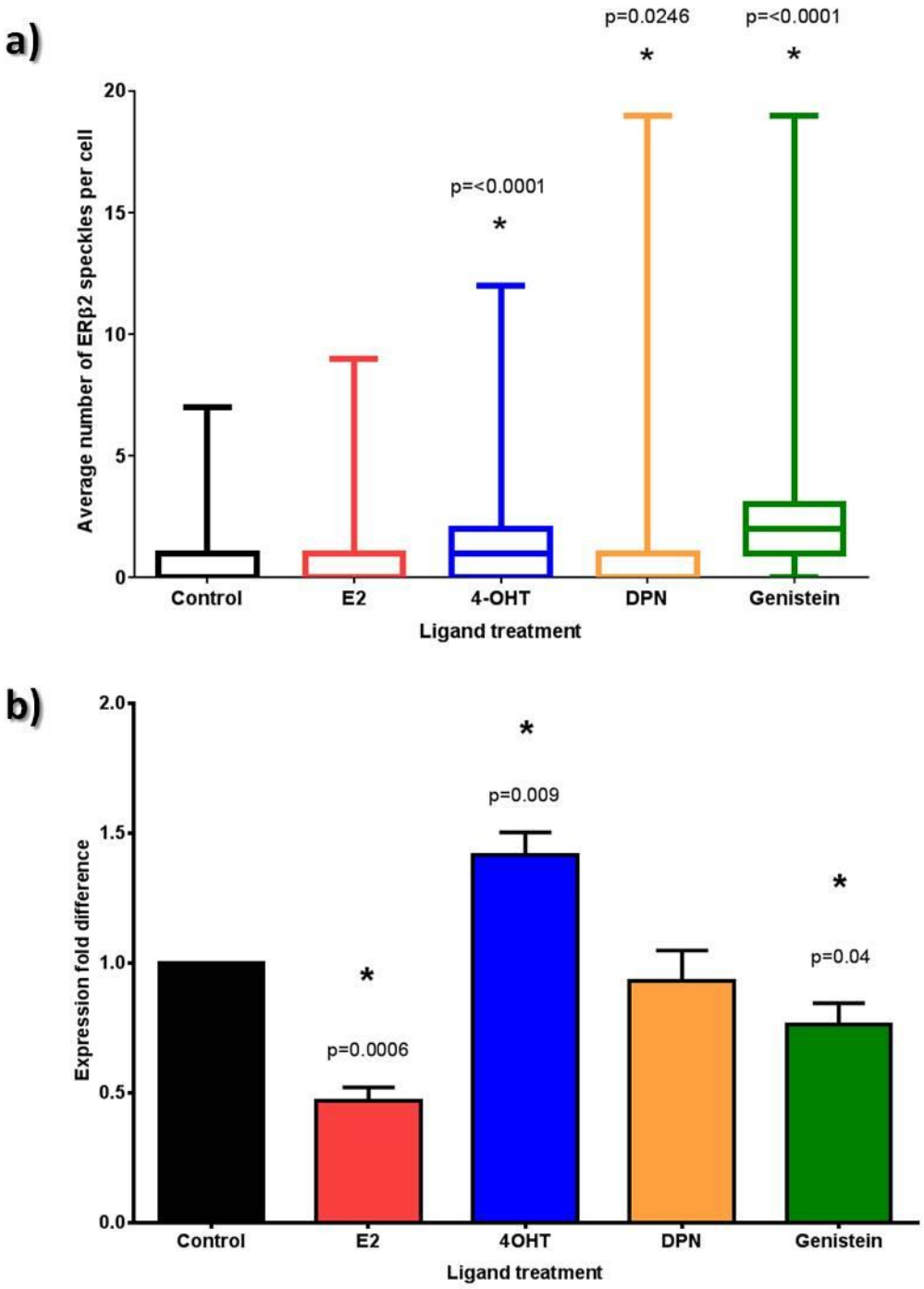

Figure 5.8. Analysis of ERβ2 nuclear speckle number and mRNA levels in MCF-7 cells in response to estrogenic ligands.

a) Box and Whiskers plot displaying the average ERβ2 speckle number per cell in response to E2, 4-OHT, DPN and genistein. The box represents the interquartile range (50% of the data) and whiskers are the upper and lower quartiles (25% of data each) extending to the extreme values. Absence of a lower whisker indicates lower quartile is equal to the minimum value. Statistically significant speckle number changes compared to control untreated cells(*) and p-values, measured using a student's t-test are displayed.

b) ERβ2 mRNA levels in response to E2, 4-OHT, DPN and genistein. Error bars represent ± SEM for n=3 (technical replicates). Statistically significant fold changes compared to control untreated cells (*) and p-values, measured using a multiple student's t-tests with Holm-Sidak correction, are displayed.

Growth curves of MDA-MB-231 in response to the various estrogenic ligands are displayed in Figure 5.9, which was again performed to check the concentration has a physiological effect on the cells. The black line on each of the graphs represents the control ‘untreated’ cells, which were grown and counted in parallel to the treated cells. The growth of E2 (red line), 4-OHT (blue line), DPN (yellow line) and genistein (green line) treated MDA-MB-231 cells are displayed in Figure 5.9. Both E2 (a) and 4-OHT (b) treatment had little effect on growth compared to the control cells. However DPN treatment (c) resulted in a marked increase in cell growth displayed by the separation of the yellow and black (untreated cells) lines of the graph. Genistein treatment resulted in a more pronounced suppression of cell growth and at 72 hours cell numbers began to decrease suggesting induction of cell death.

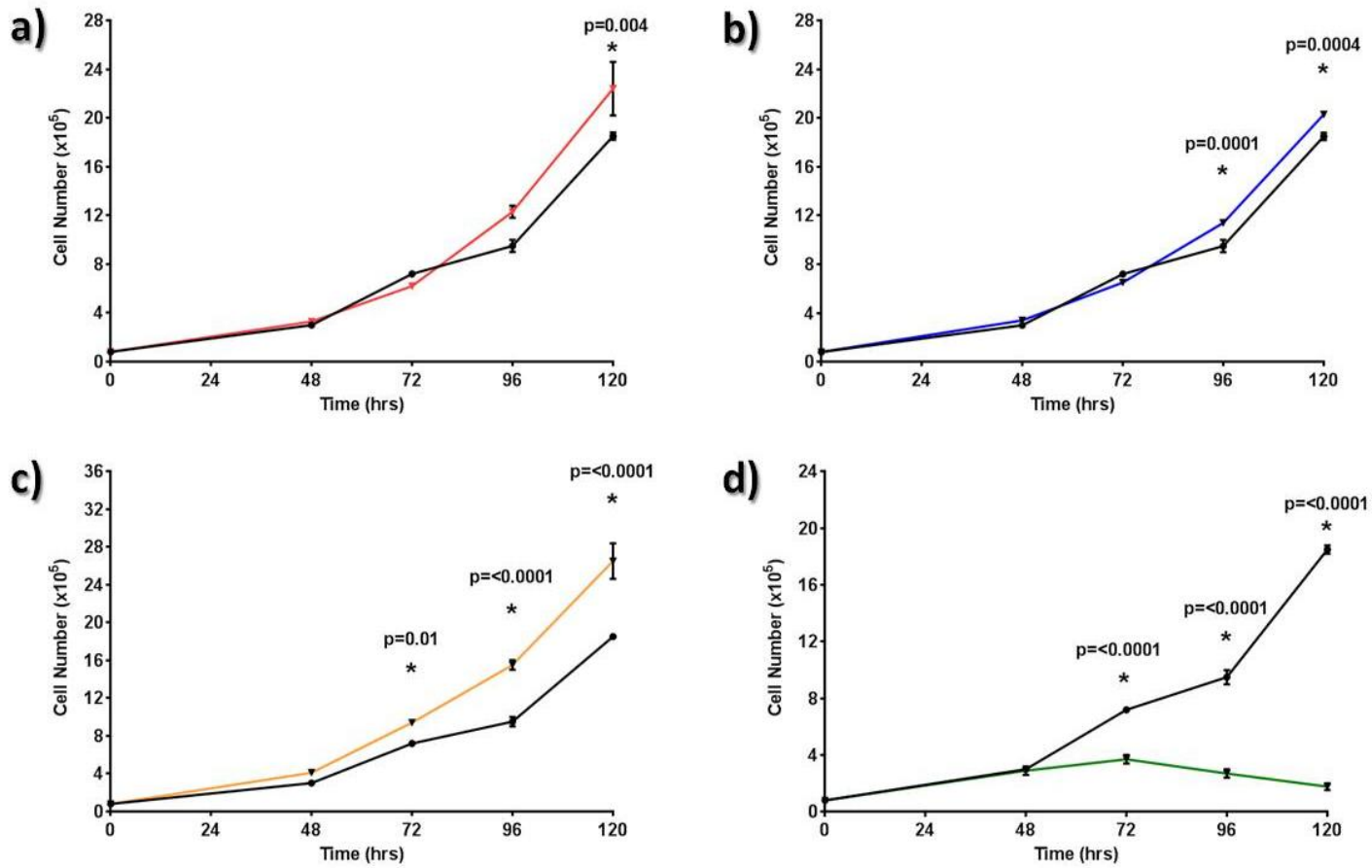

Figure 5.9. MDA-MB-231 growth curves in response to estrogenic ligands.
Cell counts were performed at 48, 72, 96 and 120 hours and cell number plotted. a) E2 (1nM), red line), b) 4-OHT (50nM), blue line, c) DPN (10nM), yellow line, d) genistein (30uM), green line. The black lines on all graphs represent untreated control cells. Error bars represent ± SEM for n=2 (technical replicates). Statistically significant changes in cell number (*) and p-values, measured using a multiple student's t-tests with Holm-Sidak correction, are displayed.

Figure 5.10 represents expression patterns of ERβ2 by immunofluorescence after MDA-MB-231 cells were treated with E2, 4-OHT, DPN or genistein. An untreated control image is also presented. The red arrows indicate visible ERβ2 speckles. Visual examination of the images revealed no obvious difference in ERβ2 speckle number compared to the control image when cells were treated with E2, 4-OHT and DPN. However, upon genistein treatment ERβ2 speckles appeared to increase noticeably in number compared to the control.

When ERβ2 speckles were counted using the automated method, this observation was confirmed and only genistein resulted in a statistically significant increase in average number of ERβ2 speckles in each cell. This is illustrated in Figure 5.11a. As previously described, genistein was the only ligand from the panel that resulted in anti-proliferation. When examining the mRNA data illustrated in Figure 5.11b, E2, 4-OHT and DPN treatment, did not affect overall ERβ2 mRNA levels in the cells. As observed in MCF-7 cells, genistein did result in a significant decrease in ERβ2 mRNA, despite causing an increase in the number of ERβ2 speckles.

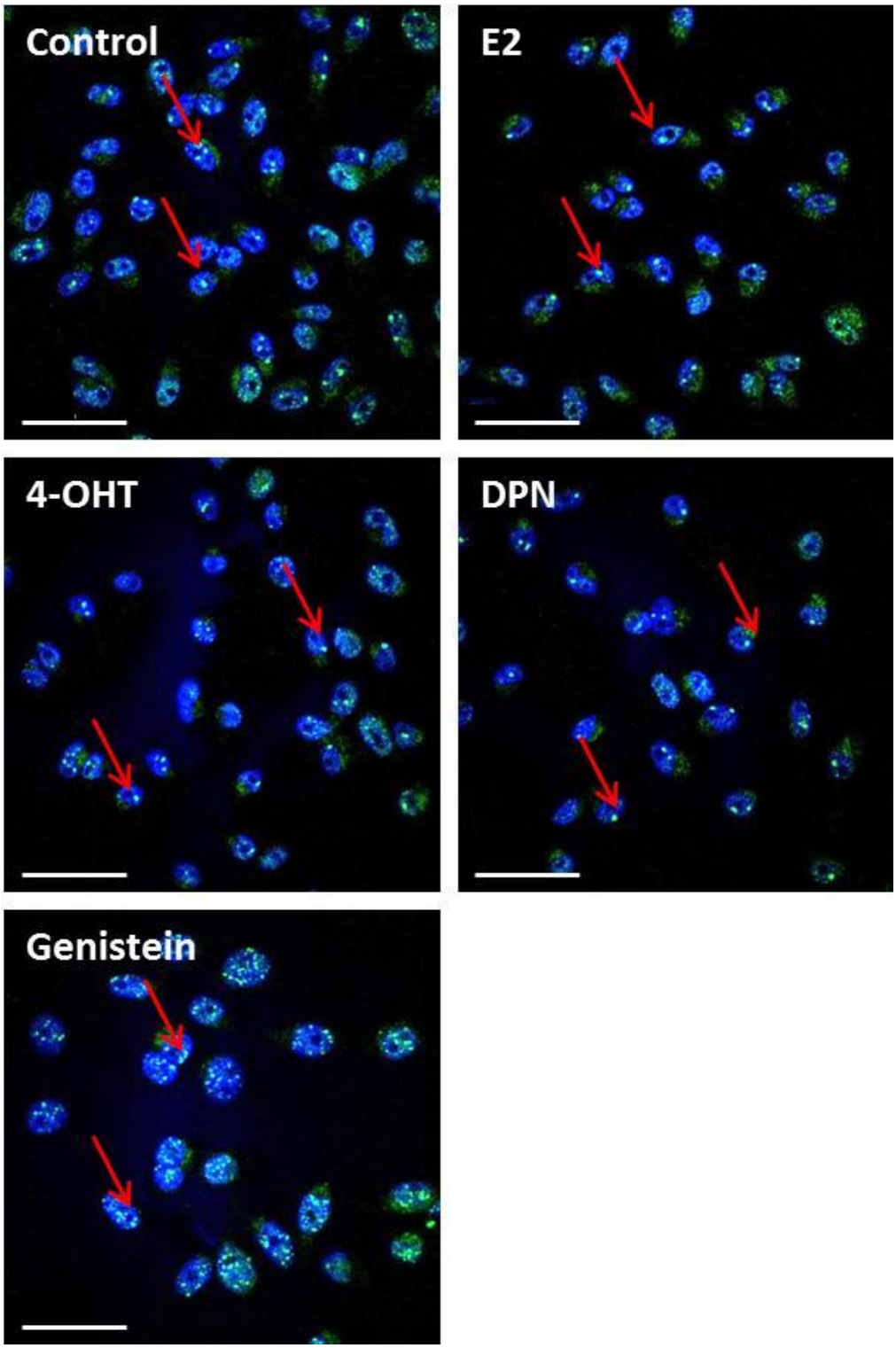

Figure 5.10. Immunofluorescence analysis of ERβ2 speckle expression pattern in MDA-MB-231 cells in response to the estrogenic ligands E2, 4-OHT, DPN and genistein.
The control image represents untreated cells. The red arrows indicate ERβ2 nuclear speckles. Images taken at 60x magnification and scale bars represent 50µm.

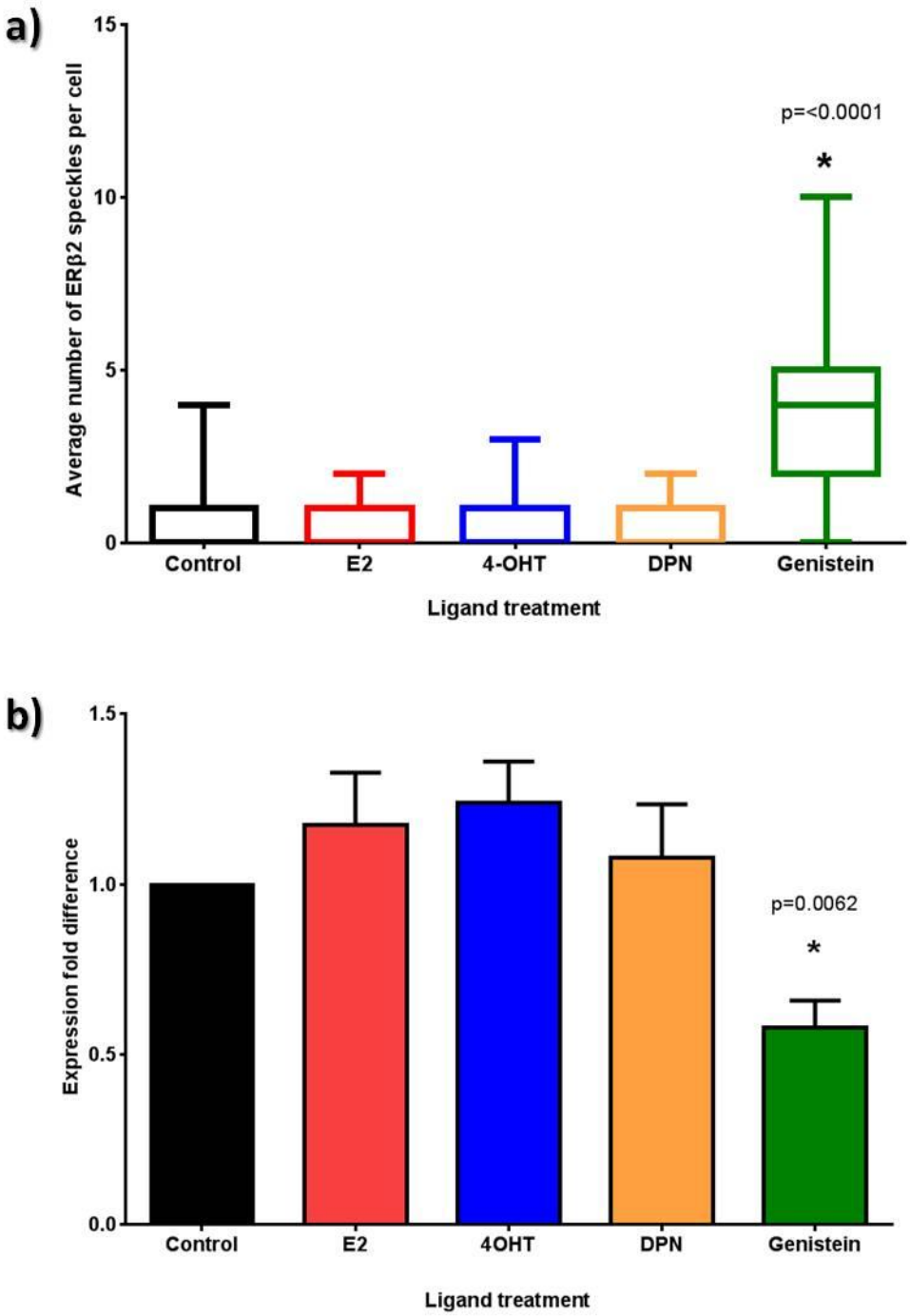

Figure 5.11. Analysis of ERβ2 nuclear speckle number and mRNA levels in MDA-MB-231 cells in response to estrogenic ligands.
a) Box and Whiskers plot displaying the average ERβ2 speckle number per cell in response to E2, 4-OHT, DPN and genistein. The box represents the interquartile range (50% of the data) and whiskers are the upper and lower quartiles (25% of data each) extending to the extreme values. Absence of a lower whisker indicates lower quartile is equal to the minimum value. Statistically significant speckle number changes compared to control untreated cells(*) and p-values, measured using a student's t-test are displayed.
b) ERβ2 mRNA levels in response to E2, 4-OHT, DPN and genistein. Error bars represent ± SEM for n=3 (technical replicates). Statistically significant fold changes

compared to control untreated cells (*) and p-values, measured using a multiple student's t-tests with Holm-Sidak correction, are displayed.

5.4.3 An investigation of the cell cycle distribution of ERβ2 nuclear speckles

Work up to this point suggests that ERβ2 speckles are rarely present in every cell. They have been demonstrated to be dynamic and more abundant when proliferation is suppressed in response to estrogenic ligands. This led to the hypothesis that ERβ2 speckles could be related to specific phases of the cell cycle. To investigate this further we examined ERβ2 speckles in relation to stages of the cell cycle. The doubling time of MCF-7 cells was initially determined by measuring proliferation, and the growth curve is displayed in Figure 5.12. Doubling time was calculated to be 19.7 hours using the following doubling time equation where Td= Doubling time, t= time, q= cell number (248):

$$T_d = (t_2 - t_1) * \frac{\log(2)}{\log(\frac{q_2}{q_1})}.$$

Time point 24 and 48 were used as this represented linear exponential part of the curve (T1=48, T2= 24, q1= 296,800, q2= 690,000). Doubling time was rounded up to 20 hours for the purpose of this experiment, and estimation of time spent in each portion of the cell cycle is displayed in Figure 5.13.

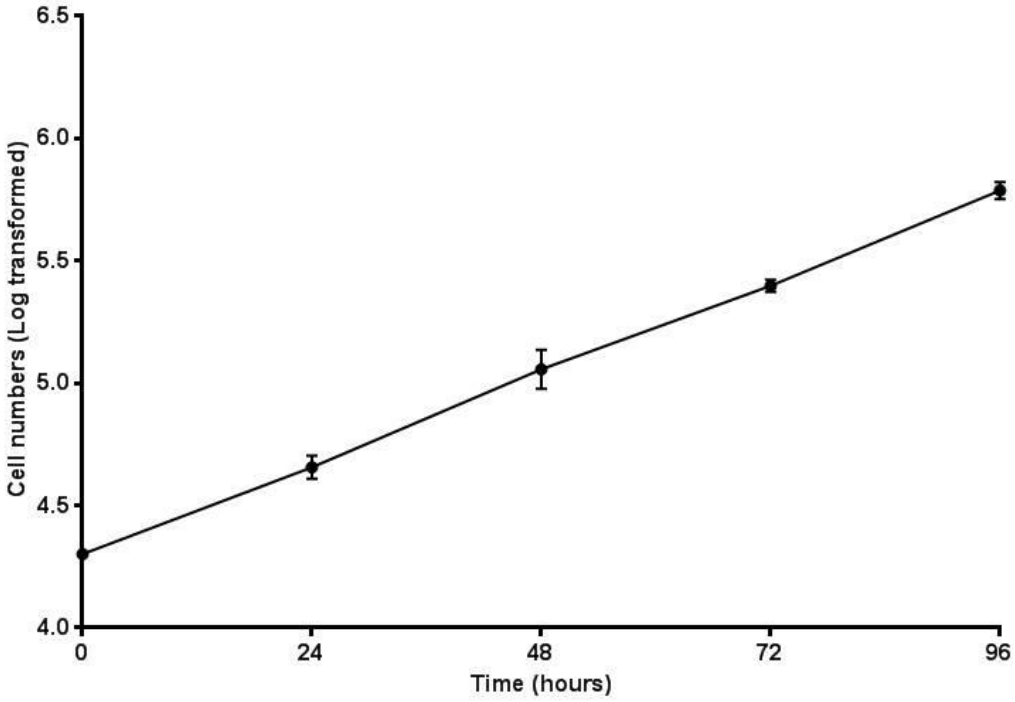

Figure 5.12. Log transformed growth curve for wild type MCF-7 cells for calculation of doubling time

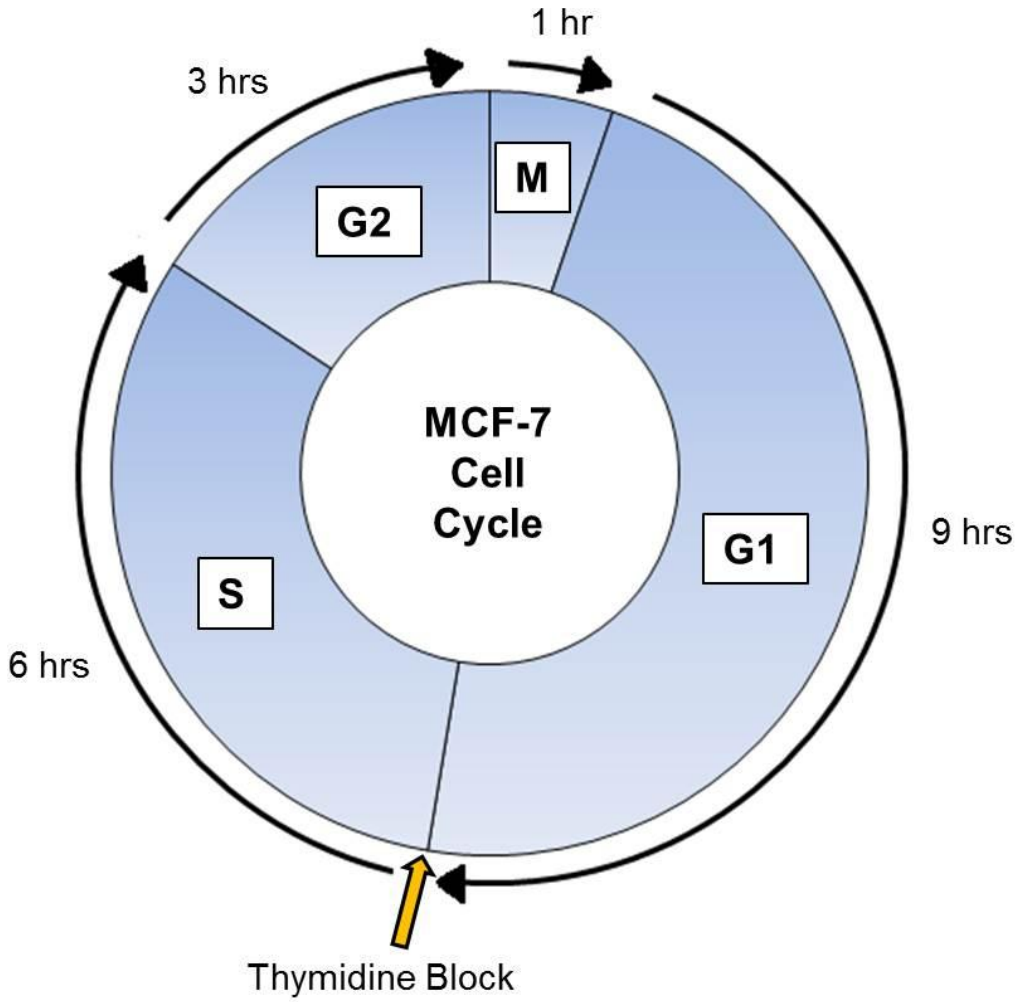

Figure 5.13. A Diagrammatic representation of the length of time MCF-7 cells remains in each phase of the cell cycle.
MCF-7 cells were calculated to have a doubling time of 19 hours and this was used to calculate time spent in each cell cycle phase. The point at which thymidine blocks cell cycle progression is indicated at the G1-S-phase border.

MCF-7 cells were synchronised using a double thymidine block then released and ERβ2 speckle number measured at 0, 8, 10 and 12 hours post release. In parallel flow cytometric analysis at each time point allowed determination of the percentage of cells in each phase of the cell cycle. These time points were determined using the doubling time and estimated time spent in each cell cycle phase, calculated previously.

Figure 5.14 illustrates ERβ2 expression patterns in synchronised MCF-7 cells analysed after 0, 8, 10 and 12 hours after thymidine release. A control image was also acquired from unsynchronised untreated MCF-7 cells. The red arrows on the images indicate visible ERβ2 nuclear speckles. These were present in the control, 0 and 8 hours post thymidine release cells, but disappeared completely at 10 and 12 hours after thymidine release.

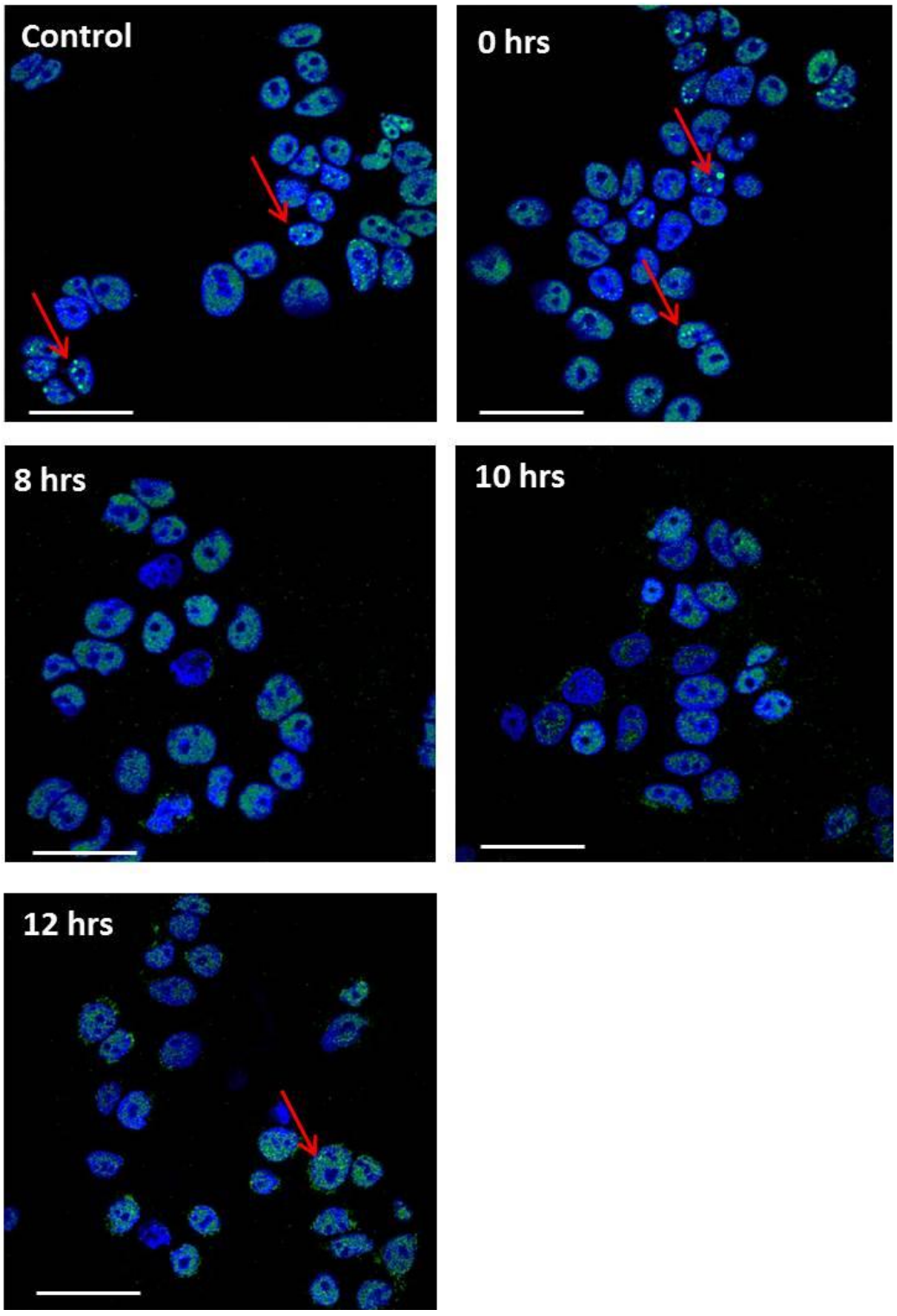

Figure 5.14. Immunofluorescence analysis of ERβ2 speckle expression pattern in MCF-7 cells at 0, 8, 10 and 12 hours after release of a thymidine block.
The control image represents untreated cells. The red arrows indicate ERβ2 nuclear speckles. Images taken at 60x magnification and scale bars represent 50µm.

Pie charts in Figure 5.15a illustrate the cell cycle distribution at each time point, and results demonstrate that synchronisation was achieved and enrichment of cells at S-phase was observed. 77% of the cell population was in S-phase before release of the thymidine block. Upon release, cells appeared to move into G2/M and G1 phase verified by the increased percentage of cells in G2/M and G1 phases at 8 and 10 hours post release. By 12 hours the majority of cells were still in G2/M phase with G1 percentage only increasing to 31%. A large proportion of cells remained in S-phase, suggesting cells were moving through the cell cycle at a slower rate than expected. The automated speckle counts confirmed the observation made from images, that a reduction in speckle number was observed at 8, 10 and 12 hours post release, displayed in the graph in Figure 5.15a. Upon comparison to the cell cycle distribution, it appears there was a decrease in speckles when the majority of cells are in G2/M-phase at time points 8, 10 and 12. At 10 and 12 hours this reduction of speckle number was deemed statistically significant.

Figure 5.15b illustrates ERβ2 mRNA expression levels at each time point post thymidine release, normalised to the control (=1). At time point 8 and 10 mRNA was significantly decreased. The majority of ERβ2 mRNA levels did not appear to correlate with speckle number changes, however at time point 10 mRNA was significantly decreased, as was speckle number.

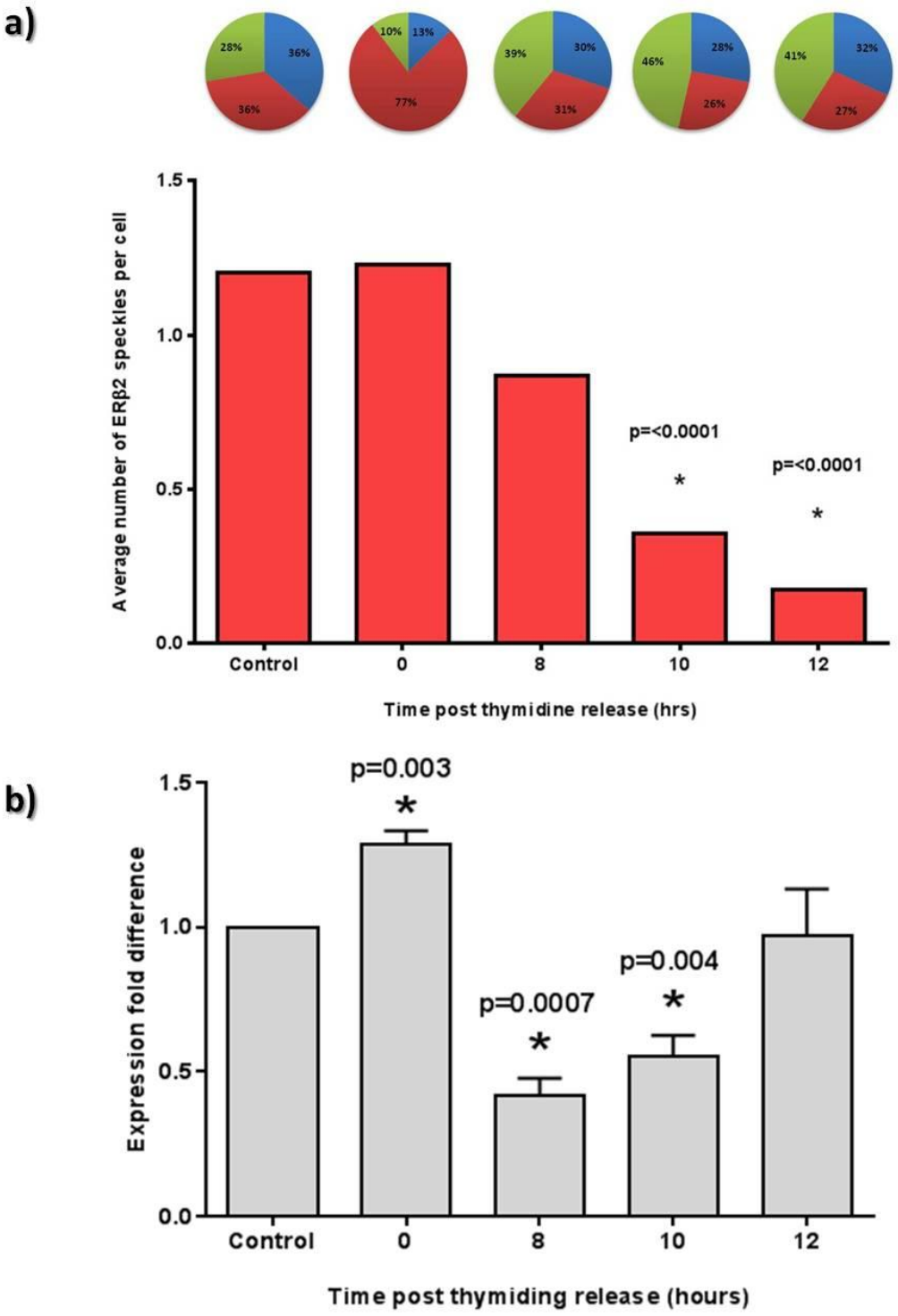

Figure 5.15. Analysis of ERβ2 speckle number after S-phase cell synchronisation in MCF-7 cells

a) Pie charts represent cell cycle distribution 0,8,10 and 12 hours after removal of S-phase blockade (green= G2/M phase, red= S-phase, blue= G1/0 phase). Graph displays ERβ2 speckle number 0,8,10 and 12 hours after removal of S-phase blockade. Control represents unsynchronised untreated cells.

b) ERβ2 mRNA levels at each time point post thymidine release, normalised to the control sample.

Student's t-tests were performed and p-values are displayed on statistically significant changes (*) compared to controls.

5.4.4 Investigation of transcriptional and translational inhibition on ERβ2 nuclear speckles

Previous experiments have demonstrated ERβ2 nuclear speckles to be dynamic structures, their numbers being changeable dependent on cell type or external stimulus and potentially inversely related to the G2/M phase of the cell cycle. The principle of ER signalling maintains that upon activation ERs travel from the cytoplasm to the nucleus when they exert transcriptional effects. As these speckles were dynamic and had a nuclear location we hypothesised that ERβ2 speckles may be involved in transcription or translation, with speckles representing areas of active transcription. MCF-7 cells were incubated with a transcriptional inhibitor actinomycin D (ActD) or with cyclohexamide (CHX) to investigate whether the number of speckles would change upon transcriptional or translational inhibition respectively. As ERβ2 protein was only detectable on a western blot while using the FLAG M2 antibody (illustrated in chapter 4.3.3) we used MCF-7 ERβ2 overexpressing cells to enable us to confirm inhibition of transcription and translation using qRT-PCR and western blot techniques. To confirm that the effect of these compounds on ERβ2 speckle number was also applicable to endogenous ERβ2 protein levels, ERβ2 immunofluorescence and qRT-PCR assays were also performed on the empty vector control MCF-7 cells. Expression patterns of ERβ2 were comparable in both cell lines upon ActD and CHX treatment.

The effect of ActD treatment for 30 minutes, 1, 2, 4, and 24 hours on ERβ2 speckle expression is shown in Figure 5.16a. The red arrows indicate visible ERβ2 speckles. These speckles are present in the cells of the control sample and after 30 minutes and 1 hour of treatment (red arrows). After 2 hours post ActD treatment speckles became difficult to distinguish with notably fewer present in the image. Using the automated speckle counting methodology described in 5.3.1, speckles

were counted and average number of speckles per cell is displayed in Figure 5.16b. As ActD treatment time increased, fewer ERβ2 speckles were present in the cells. After 2 hours nearly all ERβ2 speckles had been eliminated and at 4 hours, no speckles were present suggesting complete inhibition of ERβ2 speckle transcription. Despite the disappearance of ERβ2 speckles at 4 hours of transcriptional inhibition, homogenously expressed ERβ2 in the cytoplasm was still present and expression appeared unaffected by the transcriptional inhibition, illustrated by the white arrows, suggesting cytoplasmic ERβ2 protein may not be a result of active transcription.

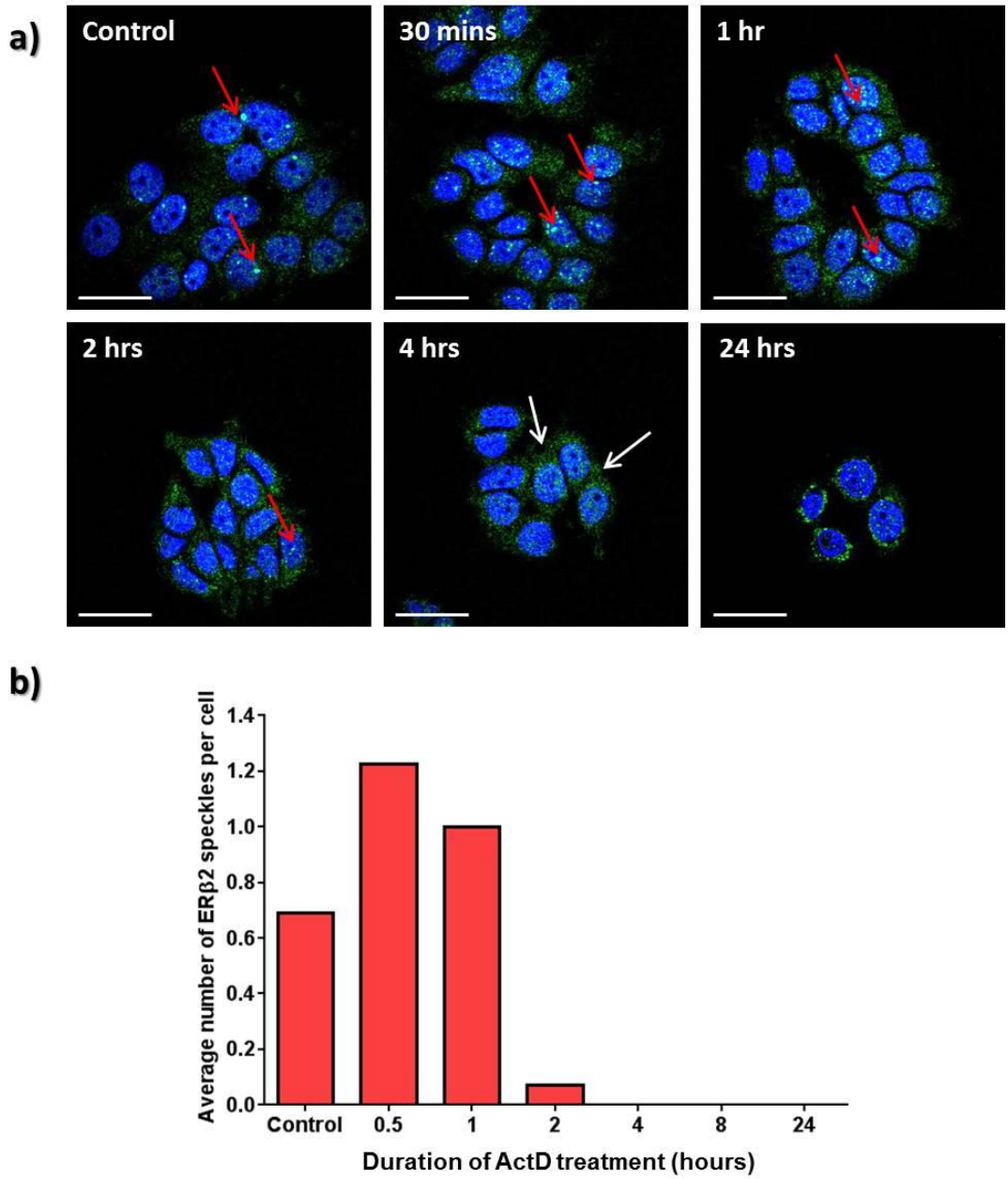

Figure 5.16. Analysis of ERβ2 speckles in response to actinomycin (ActD) in MCF-7 cells.
a) Immunofluorescence analysis of ERβ2 speckle expression after 0.5, 1, 2, 4 and 24 hours of ActD treatment. Red arrows indicate visible ERβ2 speckles. White arrows indicate cytoplasmic ERβ2.
b) Average number of ERβ2 speckles per cell after 0.5, 1, 2, 4 and 24 hours of ActD treatment
Images acquired at 60x magnification and scale bars represent 50µm. Control represents untreated cells.

Cells were then treated with CHX for 30minutes, 1, 2, 4, and 24 hours and ERβ2 speckles analysed. Visible ERβ2 speckles were present in the cells up to 2 hours of CHX treatment indicated by the red arrows in Figure 5.17a. At 2 hours however, speckles reduced in number and by 4 hours of treatment, no speckles were visible. ERβ2 nuclear speckle numbers were counted from two biological replicates and average speckle numbers plotted on the graph shown in Figure 5.17b. Again this demonstrated concordance with the visual results; fewer speckles were observed with 2 hours of CHX treatment and complete disappearance of the ERβ2 nuclear speckles was observed at four hours of treatment. As with ActD, CHX treatment did not seem to affect expression patterns of homogenously expressed ERβ2 in the nucleus or cytoplasm (indicated by the white arrows in Figure 5.17a), with expression remaining unchanged after translational inhibition.

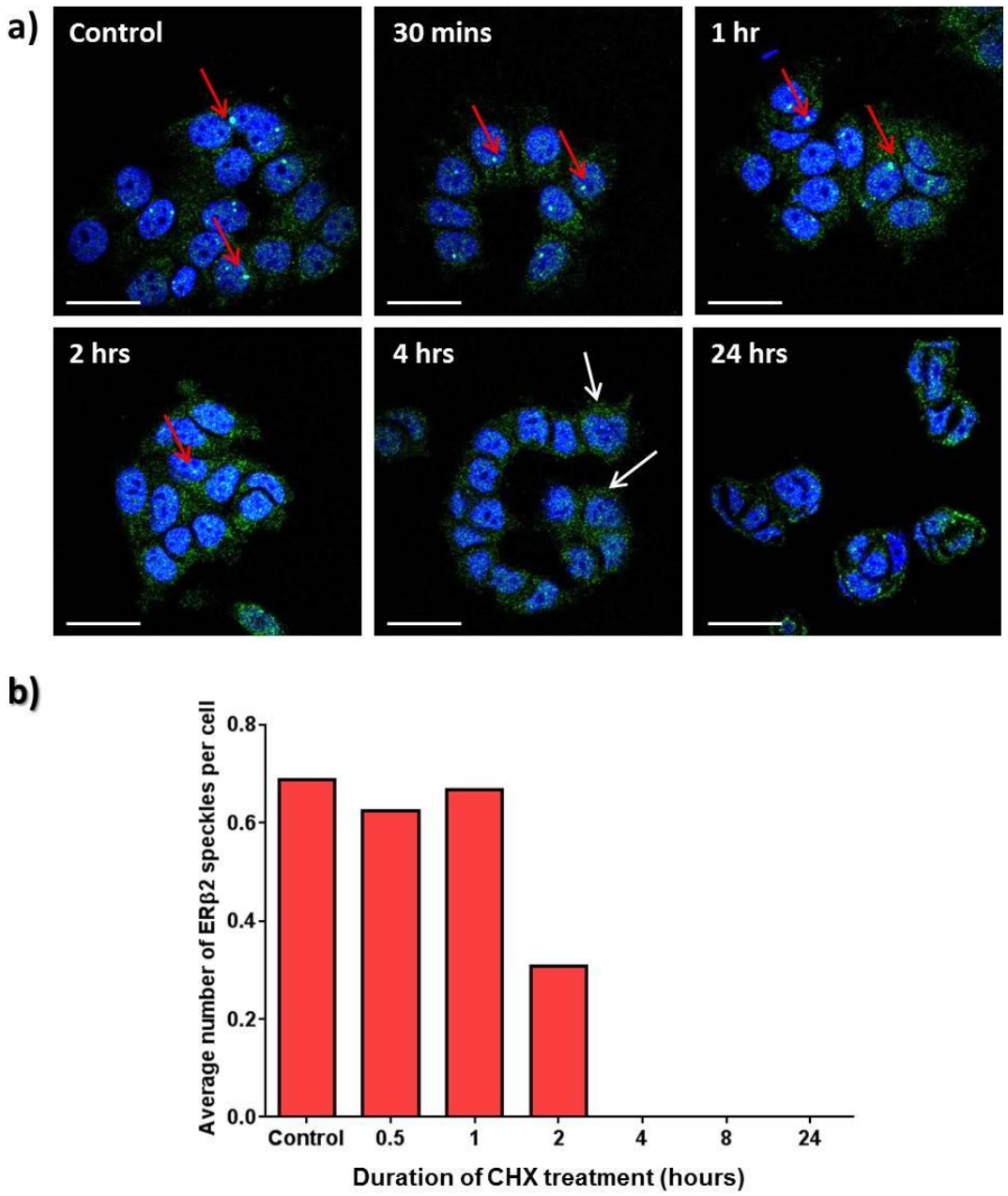

Figure 5.17. Analysis of ERβ2 speckles in response to cyclohexamide (CHX) treatment in MCF-7 cells.
a) Immunofluorescence analysis of ERβ2 speckle expression after 0.5, 1, 2, 4 and 24 hours of CHX treatment. Red arrows indicate visible ERβ2 speckles. White arrows indicate cytoplasmic ERβ2.
b) Average number of ERβ2 speckles per cell after 0.5, 1, 2, 4 and 24 hours of CHX treatment
Images acquired at 60x magnification and scale bars represent 50µm. Control represents untreated cells.

Despite the fact that ActD and CHX are known inhibitors of transcription and translation respectively, we wanted to be able to prove this inhibition with the concentration used in this experiment. In parallel to immunofluorescence, flasks of MCF-7 cells were treated with ActD and CHX for 30 minutes, 1, 2, 4 and 24 hours and cells were harvested for RNA (ActD) or protein (CHX) extraction. Transcriptional inhibition was measured by calculating ERβ2 mRNA levels and translational inhibition was measured by western blot of ERβ2 protein. Figure 5.18a depicts ERβ2 mRNA levels upon ActD treatment for 30 minutes, 1, 2, 4, 8 and 24 hours. Levels were normalised to the no treatment control (=1). The graph demonstrated a decrease in ERβ2 mRNA as time increased; confirming ERβ2 transcription was inhibited by the concentration used. Figure 5.18b depicts the protein levels of ERβ2 upon CHX treatment for 30 minutes, 1,2,4,8 and 24 hours. ERβ2 was measured using the FLAG M2 antibody directed towards the FLAG3 epitope on the aberrantly expressed ERβ2 protein and β-actin was used as a control for equal loading. The level of ERβ2 protein decreased as treatment time increases, and protein became undetectable at 24 hours. This confirmed inhibition of protein synthesis occurred at the CHX concentration used for this experiment.

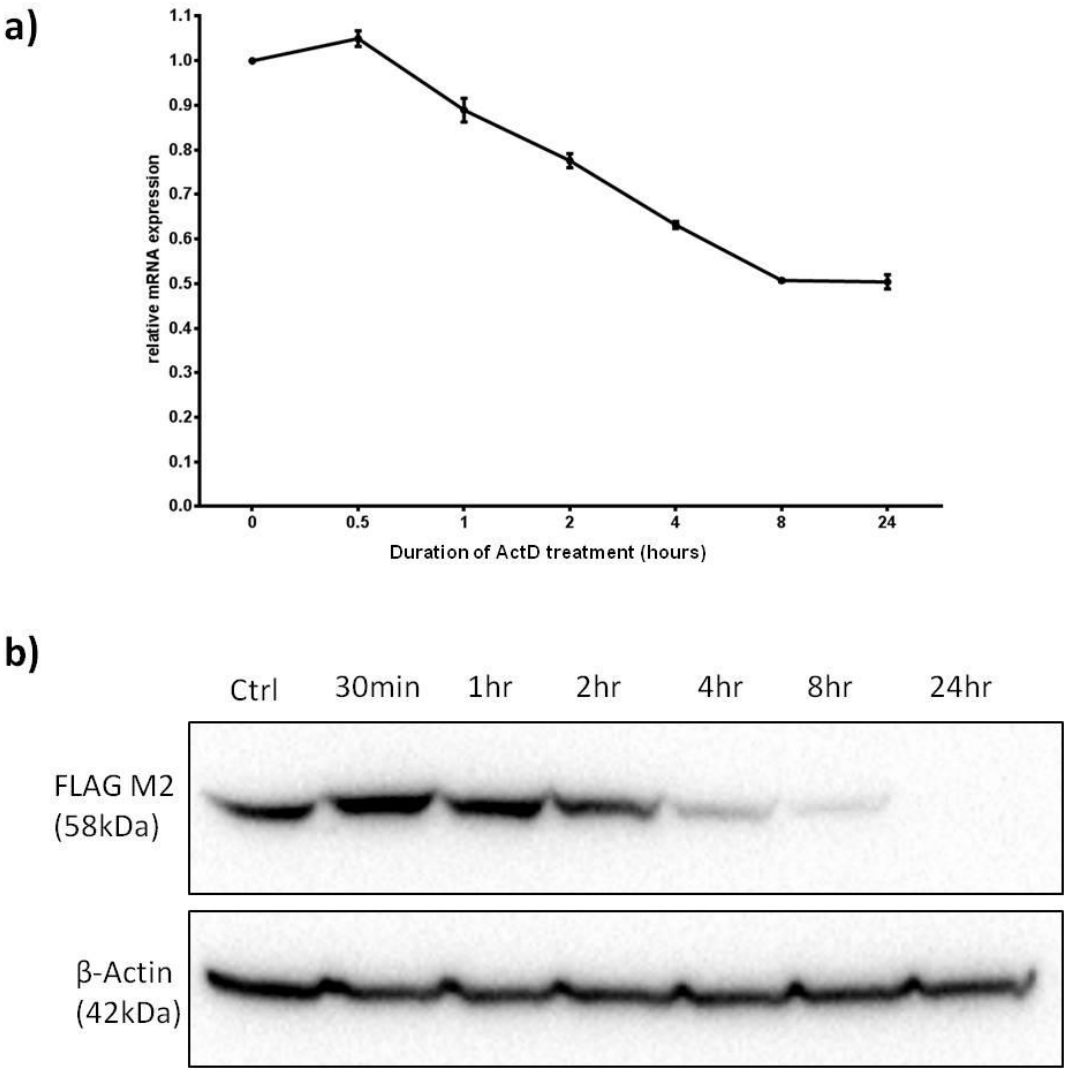

Figure 5.18. ERβ2 mRNA and protein expression in ERβ2 overexpressing MCF-7 cells after ActD and CHX treatment respectively.
a) ERβ2 mRNA quantification demonstrated by qRT-PCR at 0.5, 1, 2, 4, 8 and 24 hours after ActD treatment, normalised to the untreated control.
b) ERβ2 protein quantification demonstrated by western blot using FLAG M2 antibody, at 0.5, 1, 2, 4, 8 and 24 hours CHX treatment. Untreated control sample also analysed. β-actin was used as a control for equal loading.

5.5 Discussion

ERβ2 speckles had been identified in chapter 3 when ERβ2 expression patterns were examined in nine breast cancer cell lines. This speckled expression was unique to ERβ2 and was not observed with ERα or ERβ1. This finding led to the implication that these speckles may have alternative function to homogenously expressed ERβ2. This chapter intended to discover more about these speckles and their possible function.

5.5.1 Automation of ERβ2 speckle counting

In order to accurately investigate ERβ2 speckles an automated speckle counting method was required for both consistency and to eliminate the subjectivity that manual counting might generate. ERβ2 speckles were defined as consistently distinct, intense areas of ERβ2 expression located in the nucleus and fluorescence was frequently saturated. For this reason they could be distinguished by the software by intensity thresholding. A threshold of 1200 in the FITC channel (used to detect ERβ2 expression) excluded pixels with an intensity of below that value, which omitted most homogenously expressed ERβ2 from being analysed. However, using FITC thresholding alone did not eliminate all staining that was not ERβ2 speckles. To discriminate between single or small clusters of intensely stained pixels and ERβ2 speckles, exclusion based on the size was also employed along with FITC thresholding, with objects larger than 4 pixels defined as a speckle. Attempting this manually, by assessing the size of the speckles by eye, could be problematic with the major pitfall being subjectivity. Automation reduced error and enabled accurate comparisons between images.

5.5.2 ERβ2 does not colocalise with other known nuclear speckled proteins

Many nuclear proteins are expressed in a speckled pattern in the cell nucleus and have been demonstrated to have a distinct function. Many of these e.g. PML bodies and nuclear speckles, function in pre-mRNA splicing or other post-transcriptional modifications (228, 235). As ERβ2 is expressed in the nucleus of breast cancer cells in a similar pattern, we investigated whether ERβ2 speckles colocalised with these other speckled proteins. This may indicate a similar role for ERβ2 speckles and potential involvement in transcriptional regulation. Interestingly, ERβ2 nuclear speckles did not colocalise with coilin (a marker of cajal bodies), PML or nuclear speckles, neither did they localise to the nucleoli. However, ERβ2 speckles appeared to be located adjacent to nuclear speckles labelled with SC-35 antibody. It has been reported that rather than being sites of active transcription, nuclear speckles, which contain splicing factors required for mRNA processing, are located adjacent to areas of active transcription (235). Subunits of RNA pol II have been also associated with nuclear speckles (249, 250).This could indicate ERβ2 speckles may also localise close to areas of active transcription. This observation was made for expression of the androgen receptor (AR), another member of the nuclear receptor superfamily The group measured BrUTP incorporation by immunofluorescence, which marked sites of active transcription in cells expressing GFR-AR. AR speckles only partially overlapped with active sites of transcription but was observed to be adjacent to nuclear speckles (251).

Performing colocalisation experiments of ERβ2 speckles with RNA pol II by immunofluorescence could be performed, potentially indicating the involvement of ERβ2 speckles in transcription if they are found to be located at active sites. Alternatively BrUTP incorporation could be measured as performed by Royan et al (2007) (251).

5.5.3 ERβ2 speckles dynamically respond to external stimuli

The mechanism of action for ERβ2 proposes that upon activation it translocates to the nucleus and dimerises with other ERs. This ER complex then recruits co-regulators and controls gene transcription (49). ERβ2 is not capable of effectively binding a ligand due to differences in protein folding compared with other ERs, which results in a smaller ligand binding pocket. Its activation therefore depends on dimerisation with other ligand binding ERs (ERα and ERβ1) (146). We examined the effect of various estrogenic ligands targeted to ERα and/or ERβ1 on the number of ERβ2 nuclear speckles present in MCF-7 (ERα positive, ERβ1 positive) and MDA-MB-231 (ERα negative, ERβ1 positive) cells. In MCF-7 cells 4-OHT, DPN and genistein treatment resulted in a significant increase in speckle numbers. In MDA-MB-231 cell only genistein resulted in a significant increase in ERβ2 speckles. Hamilton-Burke et al (172) demonstrated E2 and DPN increased speckle number and size detected by ERβ phosphorylated at ser105, supporting our observation that stimulation with particular ligands resulted in increased numbers of ERβ2 speckles. Interestingly ligands that triggered anti-proliferation in MCF-7 and MDA-MB-231 cells were also those that resulted in a significant increase in ERβ2 speckle number. This may signify that speckles are involved in suppression of the cell cycle, and if they are transcriptionally active, may enhance the transcription of genes that suppress the cell cycle e.g. p21,p27 or repress those that drive proliferation. In the overexpression experiments detailed in chapter 4.3.4, ERβ2 resulted in an increase in proliferation in MDA-MB-231 cells, whereas ERβ2 speckles in this cell line are associated with anti-proliferation. This could indicate distinct function for ERβ2 speckles, and deserves further exploration.

mRNA levels only partially correlated with speckle number. In MCF-7 cells only 4-OHT resulted in a concomitant increase in speckles and mRNA. With all other ligands no correlations were observed. Surprisingly genistein treatment resulted in a significant decrease in ERβ2 mRNA levels in both MCF-7 and MDA-MB-231cells,

but speckle number significantly increased. This may suggest an increase in speckle numbers could be independent from ERβ2 transcription. This contradicts our findings that a reduction in ERβ2 mRNA by transcriptional inhibition resulted in the disappearance of speckles, suggesting they are actively synthesised. If formation of speckles in this case is not a direct result of increased transcription, it could be possible that some of ligands may stimulate the formation of speckles from ERβ2 protein already residing in the cell.

Ligand activation of ERs results in downstream dimerisation and gene regulation. Increased speckle number in response to ligands may suggest they are transcriptionally active. To investigate the possibility that ERβ2 speckles may be associated with transcription, Act D and CHX was used to inhibit transcription and translation respectively and the effect on speckle number was assessed. Actinomycin D is an antibiotic and chemotherapy medication often used to as a useful tool in molecular biology to inhibit transcription. It acts by binding DNA at the transcription initiation complex forming a stable complex that inhibits RNA synthesis (252). Cyclohexamide is an antibiotic agent that prevents protein synthesis occurring within cells. It is believed to prevent the translation elongation step in protein synthesis through binding to the E-site of the 60S ribosomal unit and blocks tRNA translocation (253). Both compounds resulted in the disappearance of ERβ2 nuclear speckles. The disappearance with both transcription and protein synthesis inhibition suggests the turnover of ERβ2 in the speckles is faster than homogenously expressed ERβ2, which was still present in the cells after all speckles had disappeared, and therefore may represent an active pool of ERβ2 protein. ERβ2 speckle protein appears to be actively transcribed and translated in the cell. Speckle turnover appears to be around 2-4 hours, as by this point they disappear under transcriptional/translational inhibition. Either ERβ2 speckle formation is dependent on high turnover proteins, which when their transcription is

halted by ActD and CHX, transcription of ERβ2 also stops, or speckles themselves have a rapid turnover and inhibition of ERβ2 transcription and translation results in speckle disappearance.

Speckled expression of ERs has been described in the literature. ERα has demonstrated a speckled pattern of expression, when *SOX2* was overexpressed. *SOX2* is a protein that functions as an activator or suppressor of gene transcription and has been associated with the initial stages of tumourigenesis in breast. Authors reported that ERα phosphorylated at ser118 was elevated and expressed as numerous speckles in the nucleus upon SOX2 overexpression. This suggests SOX2 has some involvement in formation of ERα speckles possibly co-regulating transcription within these sites (247). As discussed earlier ERβ phosphorylated at ser105 formed speckles in the nucleus of MCF-7 cells (172). Phosphorylated ERβ is characteristic of activated ERβ, potentially regulating transcription of its target genes. We have established in our cell lines that some estrogenic ligands resulted in an increase in ERβ2 speckle number a similar finding to the results in the phospho-ERβ study. Using colocalisation immunofluorescence with a phospho-ERβ and ERβ2 antibody may indicate whether ERβ2 is likely phosphorylated at these sites. Phospho-ERβ antibodies are not isoform specific as many of the phosphorylation sites identified on the ERβ protein are within the AF-1 domain (165, 254, 255) therefore they may detect phosphorylation sites in all ERβ isoforms as this domain is homologous to all. If colocalisation reveals overlap of phospho-ERβ speckles and ERβ2 speckles, it could be that, due to the commonality of phosphorylation sites between ERβ isoforms, it is ERβ2 that becomes activated, which may suggest ERβ2 speckles are transcriptionally active. There are additional phospho-ERβ antibodies targeted to phosphorylation sites other than the ser105 antibody described by Hamilton-Burke et al (172), for example phospho-ERβ at ser87, which may also need careful consideration. Evidence from the literature

regarding speckled expression of ERs, suggests ERα and phospho- ERβ speckles are areas of transcriptionally active protein and may function to regulate target genes. This may suggest ERβ2 speckles are similar in function, but whether they regulate transcription themselves remains to be seen.

5.5.4 ERβ2 speckles and the cell cycle

The correlation of ERβ2 speckles with anti-proliferation may indicate an association with the cell cycle. MCF-7 cells were synchronised at the G1/0 to S-phase checkpoint then allowed to move through the cell cycle as a synchronous population. Speckle numbers were examined as cells moved through each phase. Cell synchronisation is an effective way of studying protein expression at various stages of the cell cycle, as well as investigation of cell cycle events. Theoretically once synchronised, cells should move through stages of cell cycle homogenously, however they may only remain synchronised for a short period of time often for only one or two rounds of cell division. However in fast proliferating cancer cells it is likely to be less. As cell progress to G1, due to the high degree of variability in time spent in this phase, cells can quickly become unsynchronised. Here MCF-7 cells were synchronised at the boundary between G1 and S-phase. MCF-7 cells have a short doubling time. In the literature this varies, but is thought to be around 24 hours (256), but when growth curve analysis was performed on our MCF-7 cells, doubling time was around 20 hours. Time points for speckle number analysis were based on a doubling time of 20 hours. As the length of time spent in S, G2 and M phase rarely change at around 6, 3-4 hours and 1 hour respectively (257), the variable G1 phase length was then calculated to be around 9 hours. Our results did not suggest speckles were associated with a particular phase of the cell cycle as they were present throughout. However there did appear to be a trend where speckle number was decreased in G2/M phase. Although previous experiments suggested ERβ2 speckles may be associated with anti-proliferation, the lack of association with a

particular phase of the cell cycle may indicate growth suppression is not mediated via cell cycle proteins. The decrease in speckle number at G2/M phase may be explained by the increased proportion of cells undergoing mitosis. In mitosis the nuclear membrane breaks down and nuclear proteins are released into the cytosol. Nuclear transcription is repressed during this time (258, 259) and no ERβ2 speckles were visible. This observation was confirmed when cells were synchronised with nocodazole, an M-phase blocker, in preliminary work (data not shown). No ERβ2 speckles were visible in any cells during M-phase. Therefore in G2/M phase, the proportion of cells undergoing mitosis would be increased, reducing the number of ERβ2 speckles in the cell population.

Although cells were successfully synchronised at the start of S-phase they quickly lost synchrony and did not always move through homogenously. This appears to be a pitfall of using chemical synchronisation in fast proliferating cancer cell lines. Preliminary experiments using nocodazole for synchronisation of cells in M-phase proved difficult, as not only did cells fail to move through the cell cycle synchronously, high doses of the chemical proved toxic, something that has been described in the literature (260). An effective dose for synchronisation also appeared to damage some of the cells so recovery time from synchronisation was varied in the cell population. This ultimately led to non-synchronous movement through the cell cycle as some cells took longer to recover.

Alternative methods to analyse ERβ2 speckles in relation to the cell cycle may prove more effective, and could resolve some of the pitfalls of this experiment. The use of markers for cell cycle phases may be more applicable. Co-staining cells for ERβ2 and cell cycle proteins specific to each phase could be achieved by immunofluorescence, enabling correlations to be made between the two. This still poses problems, as the most obvious cell cycle phase markers are the cyclins. However their expression crosses over into multiple phases so using these for

immunofluorescence analysis is not ideal. Anti-BrdU antibodies may be more suitable for successfully marking S-phase, however finding markers for other phases may be more challenging. An alternative approach involving more sophisticated technology could greatly improve this experiment. The ImageStreamX imaging flow cytometer (Merck Millipore) combines immunofluorescent imaging with flow cytometry, the two major aspects of this assay. This platform would negate the need for cell synchronisation as cell phase would be detected during processing. In parallel with the determination of cell cycle phase, immunofluorescent imaging on the cell could detect ERβ2 speckles and using the IDEAS® software and quantify speckle numbers for each cell cycle phase. This technology has the capacity to analyse thousands of cells, generating multiple experimental replicates in a short space of time and would increase the reliability, accuracy and reproducibility of results.

5.5.5 Summary

Experiments in this chapter have identified ERβ2 nuclear speckles may be

- associated with anti-proliferation
- sites of active gene expression

- representative of a pool of differentially regulated ERβ2 when compared to homogenously expressed ERβ2.
- adjacent to sites of post-transcriptional modification

As ERβ2 speckles are actively transcribed and translated and upon specific ligand activation they increase in number, they may represent a pool of ERβ2 involved in transcriptional regulation. The association with anti-proliferation may suggest regulation of target genes that are involved in suppression of cell proliferation; however this may not be due to suppression of specific cell cycle proteins that govern progression through each phase as ERβ2 speckle appeared to be constrictively expressed in all phases of the cell cycle. The link to anti-proliferation may suggest presence of speckles is associated with tumour suppression, even in cells (MDA-MB-231) where ERβ2 overexpression appeared to result in tumourigenesis. This may indicate ERβ2 speckles have alternate function to homogenously expressed ERβ2.

6.0 Final Discussion

There is currently a lack of knowledge regarding ERβ2 and its role in both normal breast tissue and breast cancer. Clinical data has suggested ERβ2 presence can

be both good and bad prognostically. This mixed prognostic ability may be due to the fact that ERβ2 differs in cellular location between studies. When both nuclear and cytoplasmic expression has been examined, cytoplasmic expression was linked to poor prognosis and poor survival and nuclear expression had been linked with a better outcome (94, 100). This differential prognostic ability dependent on subcellular location has also been reported in other cancer types such as ovarian (102) and prostate cancers (101). Building on this observation, it is possible that ERβ2 could have differing functions dependent upon where it is located in the cell, which may account for the varied prognosis.

We hypothesised that ERβ2 may have alternate functions when expressed with or without ERα. This appeared to be the case as ERβ2 overexpression resulted in suppression of proliferation in MCF-7 cells, in concordance with the literature (95, 104), but increased proliferation in triple negative MDA-MB-231 cells. In MDA-MB-468 cells, also triple negative, proliferation decreased. Clearly the action of ERβ2 is far more complex than just its interaction with ERα. To our knowledge only one study has investigated the function of ERβ2 outside of an ERα positive environment in breast where its expression in the triple negative cell line HS578T revealed no effect on proliferation (105). In other cancers such as prostate and ovarian, which do not express ERα, an association with tumourigenesis has emerged (106, 153). However in lung cancer ERβ2 appears to be tumour suppressive (199). These contradictory findings may be due to the cellular location of ERβ2.

We proposed ERβ2 has a different function when located in the cytoplasm compared to its function in the nucleus as a transcription factor. This hypothesis was based on the different prognostic ability of ERβ2 in the nucleus, as a marker of good prognosis, and the cytoplasm, as a marker of poor prognosis. We investigated the presence of ERβ2 protein in the nucleus, cytoplasm and mitochondria, and

explored a possible function in these compartments. Nuclear ERβ2 expression was observed predominantly as 'nuclear speckles' in all breast cancer cell lines examined. These presented as intense areas of ERβ2 staining under immunofluorescence analysis confined to dots or speckles in the cell nucleus varying in number and size between cell lines. It was revealed speckles were actively synthesised as inhibition of transcription and translation resulted in their disappearance, suggesting ERβ2 speckles are areas of unstable ERβ2. They were also associated with anti-proliferation regardless of cell type. As ERβ2 speckles in MDA-MB-231 cells were associated with anti-proliferation, however ERβ2 overexpression was associated with proliferation; it appears ERβ2 may have multiple functions. ERβ2 may be both tumourigenic and tumour suppressive in the same cell line depending on its cellular location. Others who have investigated overexpression of ERβ2 have suggested its oncogenic role may be due to regulation of cytoplasmic signalling pathways (106). In addition we have uncovered a potentially tumourigenic role for ERβ2 in the mitochondria of MDA-MB-231 cells, via upregulation of genes associated with oxidative phosphorylation. Upregulation of mtDNA encoded genes and subsequent activation of oxidative phosphorylation may result in increased energy production which could drive cell growth. Although it is proposed cancer cells switch to glycolysis as a preferred source of energy, oxidative phosphorylation still provides most of the cell's ATP (261) , and remains vital as a source of energy. Mitochondrial ERβ2 has also been linked to suppression of apoptosis (153), contributing to an overall tumourigenic effect.

The link to tumourigenesis and poor prognosis doesn't stop at the ERβ2 isoform. Despite its widely accepted tumour suppressor function, ERβ1 has been associated with tumourigenesis when it is located in the cytoplasm. Cytoplasmic ERβ1 expression is rare in the literature, but has been located in the cytoplasm of ovarian (262), vulval (263) and lung (166) cancers. Here it appears to be a poor prognostic factor; a contradiction to its reported tumour suppressive function. Mitochondrially

located ERβ1 has been associated with cell survival. This provides substantiation that ERβ1 may have opposing functions when located in the nucleus as opposed to the cytoplasm.

This evidence suggests that a tumourigenic function for ERβ2 and ERβ1 may be due to a cytoplasmic location. Nuclear located ERβ2 in the form of speckles may be tumour suppressive, similarly to the nuclear function of ERβ1. This finding correlates with the clinical observation that nuclear ERβ2 is a marker of good prognosis whereas cytoplasmic expression is associated with poor prognosis.

6.1 Limitations and Solutions

One major challenge encountered during this project stemmed from the ERβ2 protein itself. This is a less well studied isoform of ERβ and as such, one way in which our work became limited was in terms of antibodies available. Only one

commercially available antibody exists, which has been successfully used for immunofluorescence throughout this project. It was however unsuitable for protein detection via western blot despite numerous attempts. Endogenous levels of ERβ2 in breast cancer cell lines were low as demonstrated by qRT-PCR in chapter 3. This presented a challenge to the project as endogenous ERβ2 protein was undetectable by western blot, a useful and crucial tool in protein expression studies. However, the use of overexpression vectors and protein tags enabled us to investigate a functional aspect of ERβ2 action. The FLAG M2 antibody permitted us to use western blots for confirmation of ERβ2 overexpression and investigation of ERβ2 protein distribution in cellular compartments, the basis of the subcellular fractionation experiments.

Another limitation regarding the detection of ERβ2 was the examination of ERβ2 speckles. This was limited to immunofluorescence as speckles were a visual phenomenon and appeared to be a separate entity from homogenously expressed ERβ2. The use of confocal microscopy allowed us to scrutinize these speckles in detail to accurately measure changes in size and number in response to external stimuli as well as utilising colocalisation immunofluorescence to study possible interactions. Other groups that have undertaken investigation of speckled structures have also focused experimental attention towards immunofluorescence. A study that investigated the speckled expression of S1-1 nuclear domains performed similar experiments to this study. S1-1 speckles were found to be dynamic and upon transcriptional inhibition speckles decreased in number (264). ERβ2 speckle behaved in the same way. The authors proposed that these S1-1 speckles are sites of active gene expression, something we have alluded to but not confirmed. Similarly to our results, they also found that S1-1 speckles were located adjacent to nuclear speckles. It appears immunofluorescent based experiments are common when investigating speckle like structures in cells, and much information can be gained from them. However another study used whole genome screening

techniques to identify proteins that localise to nuclear bodies, something that could be applied to ERβ2 speckle investigations to glean more information about these structures. Currently it is unknown if ERβ2 speckles interact with other proteins and although we performed colocalisation with PML, nuclear speckles and cajal bodies, there are numerous other proteins that form or interact with speckle structures in the nucleus. This study identified 325 proteins that localise to distinct nuclear bodies (265). A similar approach could identify ERβ2 speckle interactions and enhance our current knowledge.

One issue encountered during the subcellular fractionation experiments was that despite clear differences observed in ERβ2 expression in different cell compartments, upon ligand treatment the changes were more subtle. This experiment may have therefore benefitted from quantification to detect differences in ERβ2 protein levels between compartments.
Licor offer an alternative to traditional western blots with their In-Cell Western™, which measures cellular protein in an automated quantitative approach using fluorescence measurement, thus reducing potential experimental human error. With the ability to measure protein *in-situ,* this technique may be able to detect ERβ2 protein in each cellular compartment. With this assay based on immunofluorescence, we could use the ERβ2 antibody and measure endogenous ERβ2 rather than only detecting overexpressed FLAG tagged ERβ2.

Another potential issue with the fractionation westerns was the loading controls used. Each fraction required a different loading control, a protein located only in that particular compartment. However the use of cytochrome C as a marker for the mitochondria could prove unreliable if any of the ligands tested caused changes in apoptosis. The release of cytochrome C from the mitochondria to the cytoplasm is a

significant step in the induction of apoptosis. We did not measure apoptosis in response to estrogenic ligands used in this study or in ERβ2 overexpressing cells. This could be done in future work to confirm whether apoptosis is affected and outline the suitability of cytochrome C as a loading control. Genistein has also been shown to induce ROS in the literature (266). ROS generation results in cytochrome C release from the mitochondria and ultimately apoptosis. If densitometry was used to normalise the band intensities to the loading control in the mitochondrial fractions, results could therefore be skewed. Use of another mitochondrial marker i.e. for proteins involvement in oxidative phosphorylation e.g. COX IV could overcome this, however given that we have shown ERβ2 interferes with mtDNA transcription this may not be plausible. The use of the Licor technology would negate the need for specific cellular compartment loading controls and ultimately may be a better alternative if quantification of ERβ2 is required.

6.2 Future work

The work carried out in this project has begun to clarify the function of ERβ2 and its potential implications in breast cancer. We suggest multiple functions for ERβ2 which may depend on cellular location.

To build on the ERβ2 speckle work, it would be useful to investigate speckles as sites of active transcription. Although speckles responded to transcriptional and translational inhibition, it is unclear if they are transcriptionally active. Moving forward it would be useful to perform further colocalisation analysis using techniques already been established in chapter 3, with a further subset of proteins. The techniques used by Fong et al, 2013 (265) could be applied to ERβ2 speckles. Authors sub-cloned the Human ORFeome v5.1 Library containing open reading frames of over 12,700 genes into a Flag tagged vector then transfected into HeLa cells. Proteins were detected by immunofluorescence and those that formed nuclear foci were investigated by colocalisation with distinct nuclear bodies.
The same techniques could be applied to ERβ2 speckles to identify possible protein interactions with ERβ2 speckles. In addition colocalisation of ERβ2 speckles with RNA Polymerase II may indicate if these speckles are at sites of active transcription. It would also be interesting to investigate whether the phospho-ERβ speckles described in the literature (172) colocalise with ERβ2 speckles, which may also indicate ERβ2 speckle as active. If transcriptionally active, speckles could represent an important pool of ERβ2 which regardless of the molecular phenotype of the cell could indicate a tumour suppressive function through target gene regulation, at least in terms of cellular proliferation. One important consideration in the speckle work is whether other ERs play a role in speckle formation and activity. As ERβ2 is believed to have little function alone, but instead exerts its action through ERβ1 or ERα heterodimerisation (54) it is feasible that ERβ2 speckles formation may rely on interaction with other ERs. By using siRNAs or shRNAs to knockdown the expression of ERα or ERβ1 could suggest whether these proteins are required for speckle formation. This knockdown could also be of use in other assays. Measurement of proliferation and migration under knockdown conditions

could suggest whether these other ER's are involved in mediating ERβ2's effects on these processes.

We hypothesised that ERβ2's cytoplasmic function may mediate tumourigenesis as demonstrated by its effects on gene expression and proliferation in ERβ2 overexpressing MDA-MB-231 cells. As already discussed in previous chapters, examination of downstream target genes to cytoplasmic kinase signalling pathways or kinase signalling reporter assays in the ERβ2 overexpressing cells could verify whether cytoplasmic ERβ2 plays a role in the regulation of these pathways. The use of phospho-kinase antibody arrays to measure activated components of kinase signalling could be useful to indicate whether these pathways are activated. We have alluded to a possible function in the mitochondria in regulation of mtDNA transcribed genes which code for proteins involved in oxidative phosphorylation. To further support this observation; firstly all 13 mtDNA coded genes could be investigated by qRT-PCR in the overexpressing ERβ2 cells to complete the panel of mtDNA protein coding genes. It may also be advantageous to confirm protein expression of these genes too. Leading on from this, oxidative phosphorylation in the ERβ2 overexpressing cell lines and ATP levels could be measured to confirm whether upregulation of mtDNA genes does lead to increased cellular energy production. In addition, as others have suggested ERβ2 may be involved in apoptosis regulation (153), measurement of apoptosis could be carried out in ERβ2 overexpressing cells. If apoptosis is affected, interaction of ERβ2 with the proteins involved could be measured for example BAX, as ERβ2 has been demonstrated to interact with this protein in ovarian cancer.

In this project we briefly investigated some potential ERβ2 target genes in chapter 3. We found differential gene expression between ERα positive and ERα negative cell lines suggesting differential gene expression dependent on molecular profile of the tumour. Global analysis of gene regulation has been performed for ERβ1 (47)

using ChIP-Seq technology to identify DNA binding sites on ERβ1 target gene promoters in MCF-7 (ERα positive) cells, and genes identified were involved in processes such as cell cycle progression, apoptosis and adhesion.

RNA-Seq is a similar technique but measures RNA transcripts, and has been utilised to detect ERβ gene targets in the triple negative breast cancer cell line MDA-MB-468 (115). Again gene ontology analysis revealed genes regulated were involved in cell proliferation, differentiation and cell cycle. RNA-Seq gives the added advantage of quantification, so up or down-regulation of the target genes can be measured. Both of these techniques would be a useful tool to investigate ERβ2 target genes and would give a much more comprehensive view of the genes regulated by ERβ2. These experiments are complex however, and require a great deal of expertise, time and financial support so this type of technique may be more applicable to post-doctoral study. These experiments would however be the first genome wide study of ERβ2 target genes and greatly improve our understanding of this protein, potentially providing answers as to how ERβ2 mediates proliferation and migration, demonstrated in chapter 4.

Despite the evidence around the role of ERβ in breast cancer since its discovery in 1996 and the initial excitement in the scientific community as to its potential as a therapeutic target, almost 20 years later its function still remains unclear. The contradictory data around its role in breast cancer means targeting ERβ therapeutically is not yet viable. Many factors would need consideration before ERβ could be used clinically. A suitable ERβ antibody for clinical use may be difficult to select, since many are demonstrated to be ineffective or non-specific. Further complexity is brought about by the presence of 3 ERβ isoforms in breast tissue, ERβ1, ERβ2 and ERβ5. Many studies focus on ERβ1 expression and function but ERβ2 has also been shown to be a strong prognostic marker. Just focussing on one or not distinguishing between isoforms may hinder potential treatment, especially as only ERβ1 is the ligand binding isoform and therefore a potential

direct target for therapy. Another consideration would be the location of ERβ within the cell. It has become apparent that ERβ may have alternative function outside the nucleus. Targeting ERβ with therapy agonistically when it is cytoplasmically located may be worse for the patient, especially when mitochondrially localised and this may drive cellular energy production promoting growth and migration. Because the nature of ERβ action is so complex, it might be some time before this receptor is utilised therapeutically.

7.0 Appendix

7.1 Blast data from pFB-NeoFLAG3-ERβ2 vector

Homo sapiens estrogen nuclear receptor beta variant b (NR3A2) mRNA, complete cds

ID: gb|HQ692821.1|Length: 1488Number of Matches: 1

Score	Expect	Identities	Gaps	Strand
2748 bits(1488)	0.0	1488/1488(100%)	0/1488(0%)	Plus/Plus

Related Information

Gene-associated gene details
UniGene-clustered expressed sequence tags
Map Viewer-aligned genomic context
Range 1: 1 to 1488GenBankGraphics

```
Query  1     ATGGATATAAAAAACTCACCATCTAGCCTTAATTCTCCTTCCTCCTACAACTGCAGTCAA  60
             ||||||||||||||||||||||||||||||||||||||||||||||||||||||||||||
Sbjct  1     ATGGATATAAAAAACTCACCATCTAGCCTTAATTCTCCTTCCTCCTACAACTGCAGTCAA  60
Query  61    TCCATCTTACCCCTGGAGCACGGCTCCATATACATACCTTCCTCCTATGTAGACAGCCAC  120
             ||||||||||||||||||||||||||||||||||||||||||||||||||||||||||||
Sbjct  61    TCCATCTTACCCCTGGAGCACGGCTCCATATACATACCTTCCTCCTATGTAGACAGCCAC  120
Query  121   CATGAATATCCAGCCATGACATTCTATAGCCCTGCTGTGATGAATTACAGCATTCCCAGC  180
             ||||||||||||||||||||||||||||||||||||||||||||||||||||||||||||
Sbjct  121   CATGAATATCCAGCCATGACATTCTATAGCCCTGCTGTGATGAATTACAGCATTCCCAGC  180
Query  181   AATGTCACTAACTTGGAAGGTGGGCCTGGTCGGCAGACCACAAGCCCAAATGTGTTGTGG  240
             ||||||||||||||||||||||||||||||||||||||||||||||||||||||||||||
Sbjct  181   AATGTCACTAACTTGGAAGGTGGGCCTGGTCGGCAGACCACAAGCCCAAATGTGTTGTGG  240
Query  241   CCAACACCTGGGCACCTTTCTCCTTTAGTGGTCCATCGCCAGTTATCACATCTGTATGCG  300
             ||||||||||||||||||||||||||||||||||||||||||||||||||||||||||||
Sbjct  241   CCAACACCTGGGCACCTTTCTCCTTTAGTGGTCCATCGCCAGTTATCACATCTGTATGCG  300
Query  301   GAACCTCAAAAGAGTCCCTGGTGTGAAGCAAGATCGCTAGAACACACCTTACCTGTAAAC  360
             ||||||||||||||||||||||||||||||||||||||||||||||||||||||||||||
Sbjct  301   GAACCTCAAAAGAGTCCCTGGTGTGAAGCAAGATCGCTAGAACACACCTTACCTGTAAAC  360
Query  361   AGAGAGACACTGAAAAGGAAGGTTAGTGGGAACCGTTGCGCCAGCCCTGTTACTGGTCCA  420
             ||||||||||||||||||||||||||||||||||||||||||||||||||||||||||||
Sbjct  361   AGAGAGACACTGAAAAGGAAGGTTAGTGGGAACCGTTGCGCCAGCCCTGTTACTGGTCCA  420
Query  421   GGTTCAAAGAGGGATGCTCACTTCTGCGCTGTCTGCAGCGATTACGCATCGGGATATCAC  480
             ||||||||||||||||||||||||||||||||||||||||||||||||||||||||||||
Sbjct  421   GGTTCAAAGAGGGATGCTCACTTCTGCGCTGTCTGCAGCGATTACGCATCGGGATATCAC  480
Query  481   TATGGAGTCTGGTCGTGTGAAGGATGTAAGGCCTTTTTTAAAAGAAGCATTCAAGGACAT  540
             ||||||||||||||||||||||||||||||||||||||||||||||||||||||||||||
Sbjct  481   TATGGAGTCTGGTCGTGTGAAGGATGTAAGGCCTTTTTTAAAAGAAGCATTCAAGGACAT  540
Query  541   AATGATTATATTTGTCCAGCTACAAATCAGTGTACAATCGATAAAAACCGGCGCAAGAGC  600
             ||||||||||||||||||||||||||||||||||||||||||||||||||||||||||||
Sbjct  541   AATGATTATATTTGTCCAGCTACAAATCAGTGTACAATCGATAAAAACCGGCGCAAGAGC  600
Query  601   TGCCAGGCCTGCCGACTTCGGAAGTGTTACGAAGTGGGAATGGTGAAGTGTGGCTCCCGG  660
             ||||||||||||||||||||||||||||||||||||||||||||||||||||||||||||
Sbjct  601   TGCCAGGCCTGCCGACTTCGGAAGTGTTACGAAGTGGGAATGGTGAAGTGTGGCTCCCGG  660
Query  661   AGAGAGAGATGTGGGTACCGCCTTGTGCGGAGACAGAGAAGTGCCGACGAGCAGCTGCAC  720
             ||||||||||||||||||||||||||||||||||||||||||||||||||||||||||||
Sbjct  661   AGAGAGAGATGTGGGTACCGCCTTGTGCGGAGACAGAGAAGTGCCGACGAGCAGCTGCAC  720

Query  721   TGTGCCGGCAAGGCCAAGAGAAGTGGCGGCCACGCGCCCCGAGTGCGGGAGCTGCTGCTG  780
             ||||||||||||||||||||||||||||||||||||||||||||||||||||||||||||
Sbjct  721   TGTGCCGGCAAGGCCAAGAGAAGTGGCGGCCACGCGCCCCGAGTGCGGGAGCTGCTGCTG  780
Query  781   GACGCCCTGAGCCCCGAGCAGCTAGTGCTCACCCTCCTGGAGGCTGAGCCGCCCCATGTG  840
             ||||||||||||||||||||||||||||||||||||||||||||||||||||||||||||
Sbjct  781   GACGCCCTGAGCCCCGAGCAGCTAGTGCTCACCCTCCTGGAGGCTGAGCCGCCCCATGTG  840
Query  841   CTGATCAGCCGCCCCAGTGCGCCCTTCACCGAGGCCTCCATGATGATGTCCCTGACCAAG  900
             ||||||||||||||||||||||||||||||||||||||||||||||||||||||||||||
Sbjct  841   CTGATCAGCCGCCCCAGTGCGCCCTTCACCGAGGCCTCCATGATGATGTCCCTGACCAAG  900
Query  901   TTGGCCGACAAGGAGTTGGTACACATGATCAGCTGGGCCAAGAAGATTCCCGGCTTTGTG  960
             ||||||||||||||||||||||||||||||||||||||||||||||||||||||||||||
Sbjct  901   TTGGCCGACAAGGAGTTGGTACACATGATCAGCTGGGCCAAGAAGATTCCCGGCTTTGTG  960
Query  961   GAGCTCAGCCTGTTCGACCAAGTGCGGCTCTTGGAGAGCTGTTGGATGGAGGTGTTAATG  1020
             ||||||||||||||||||||||||||||||||||||||||||||||||||||||||||||
```

```
Sbjct  961   GAGCTCAGCCTGTTCGACCAAGTGCGGCTCTTGGAGAGCTGTTGGATGGAGGTGTTAATG  1020
Query  1021  ATGGGGCTGATGTGGCGCTCAATTGACCACCCCGGCAAGCTCATCTTTGCTCCAGATCTT  1080
              ||||||||||||||||||||||||||||||||||||||||||||||||||||||||||||
Sbjct  1021  ATGGGGCTGATGTGGCGCTCAATTGACCACCCCGGCAAGCTCATCTTTGCTCCAGATCTT  1080
Query  1081  GTTCTGGACAGGGATGAGGGGAAATGCGTAGAAGGAATTCTGGAAATCTTTGACATGCTC  1140
              ||||||||||||||||||||||||||||||||||||||||||||||||||||||||||||
Sbjct  1081  GTTCTGGACAGGGATGAGGGGAAATGCGTAGAAGGAATTCTGGAAATCTTTGACATGCTC  1140
Query  1141  CTGGCAACTACTTCAAGGTTTCGAGAGTTAAAACTCCAACACAAAGAATATCTCTGTGTC  1200
              ||||||||||||||||||||||||||||||||||||||||||||||||||||||||||||
Sbjct  1141  CTGGCAACTACTTCAAGGTTTCGAGAGTTAAAACTCCAACACAAAGAATATCTCTGTGTC  1200
Query  1201  AAGGCCATGATCCTGCTCAATTCCAGTATGTACCCTCTGGTCACAGCGACCCAGGATGCT  1260
              ||||||||||||||||||||||||||||||||||||||||||||||||||||||||||||
Sbjct  1201  AAGGCCATGATCCTGCTCAATTCCAGTATGTACCCTCTGGTCACAGCGACCCAGGATGCT  1260
Query  1261  GACAGCAGCCGGAAGCTGGCTCACTTGCTGAACGCCGTGACCGATGCTTTGGTTTGGGTG  1320
              ||||||||||||||||||||||||||||||||||||||||||||||||||||||||||||
Sbjct  1261  GACAGCAGCCGGAAGCTGGCTCACTTGCTGAACGCCGTGACCGATGCTTTGGTTTGGGTG  1320
Query  1321  ATTGCCAAGAGCGGCATCTCCTCCCAGCAGCAATCCATGCGCCTGGCTAACCTCCTGATG  1380
              ||||||||||||||||||||||||||||||||||||||||||||||||||||||||||||
Sbjct  1321  ATTGCCAAGAGCGGCATCTCCTCCCAGCAGCAATCCATGCGCCTGGCTAACCTCCTGATG  1380
Query  1381  CTCCTGTCCCACGTCAGGCATGCGAGGGCAGAAAAGGCCTCTCAAACACTCACCTCATTT  1440
              ||||||||||||||||||||||||||||||||||||||||||||||||||||||||||||
Sbjct  1381  CTCCTGTCCCACGTCAGGCATGCGAGGGCAGAAAAGGCCTCTCAAACACTCACCTCATTT  1440
Query  1441  GGAATGAAGATGGAGACTCTTTTGCCTGAAGCAACGATGGAGCAGTGA  1488
              ||||||||||||||||||||||||||||||||||||||||||||||
Sbjct  1441  GGAATGAAGATGGAGACTCTTTTGCCTGAAGCAACGATGGAGCAGTGA  1488
```

7.2 Images used for speckle algorithm validation

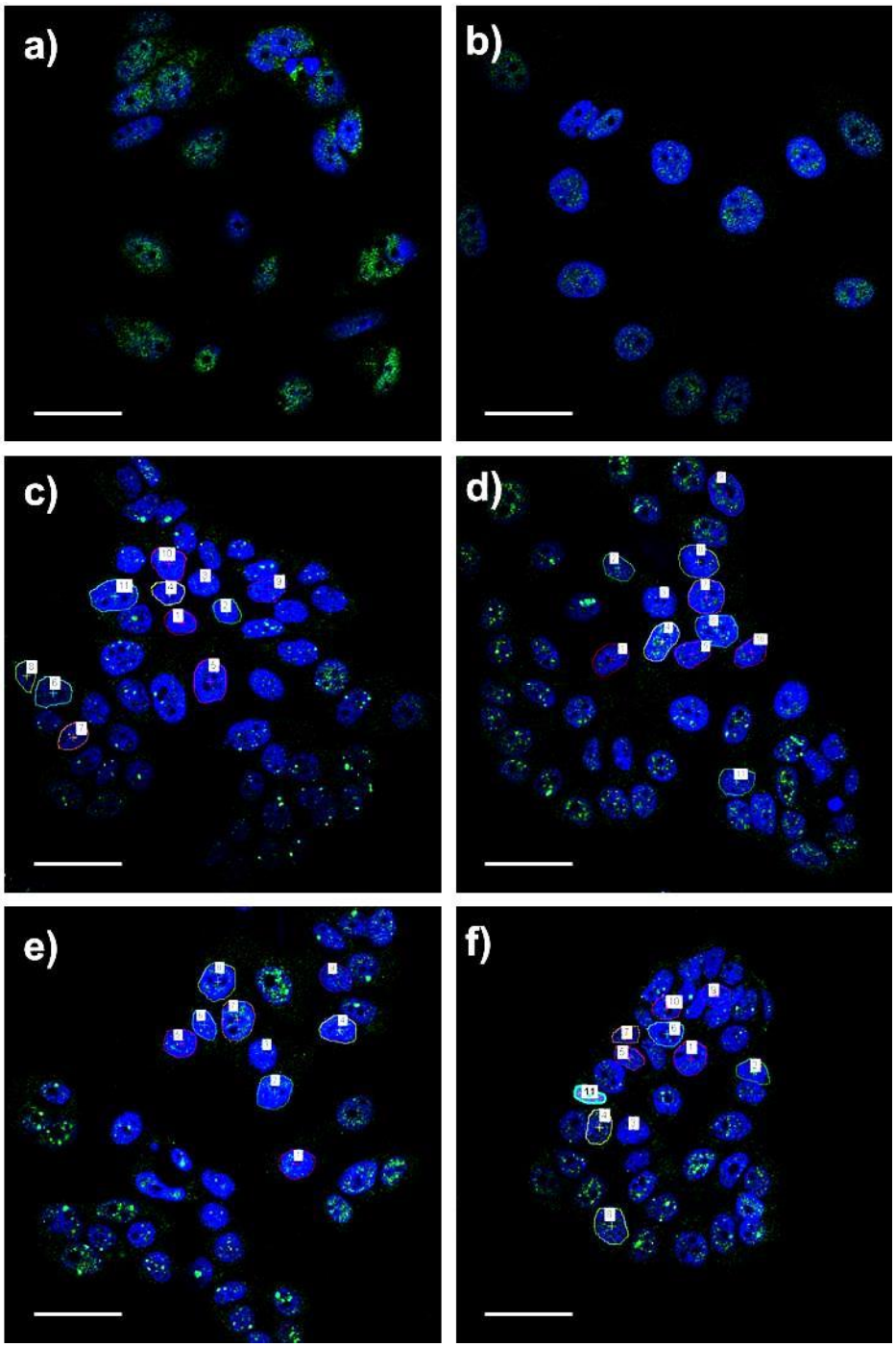

MCF-7 cells stained with ERβ2 antibody (green) and the nuclear DAPI stain (blue) were used for validation of speckle counting algorithm.
a-b) No speckles were identified in whole images so all cells were used for the algorithm validation c-f) Cells without speckles were identified down the eyepiece of the microscope and marked for use in the algorithm validation.

7.3 Speckle number data after pixel exclusion from images used for speckle algorithm validation

Validation image	Number of speckles				
	No pixel exclusion	≤ 1 pixel exclusion	≤ 2 pixel exclusion	≤ 3 pixel exclusion	≤ 4 pixel exclusion
Negative validation_1	62	20	6	3	0
Negative validation_2	42	6	0	0	0
Negative validation_3	19	3	0	0	0
Negative validation_4	73	18	3	1	0
Negative validation_5	103	28	6	2	0
Negative validation_6	25	3	0	0	0

Pixel exclusion data upon analysis of negative images displayed in 7.2. The number of speckles were counted after exclusion based on the number of pixels that made up the speckle.

7.4 Cumulative analysis of cells analysed for ERβ2 and mitochodnronda colocalisation to determine the number required to stabilise the histogram shape

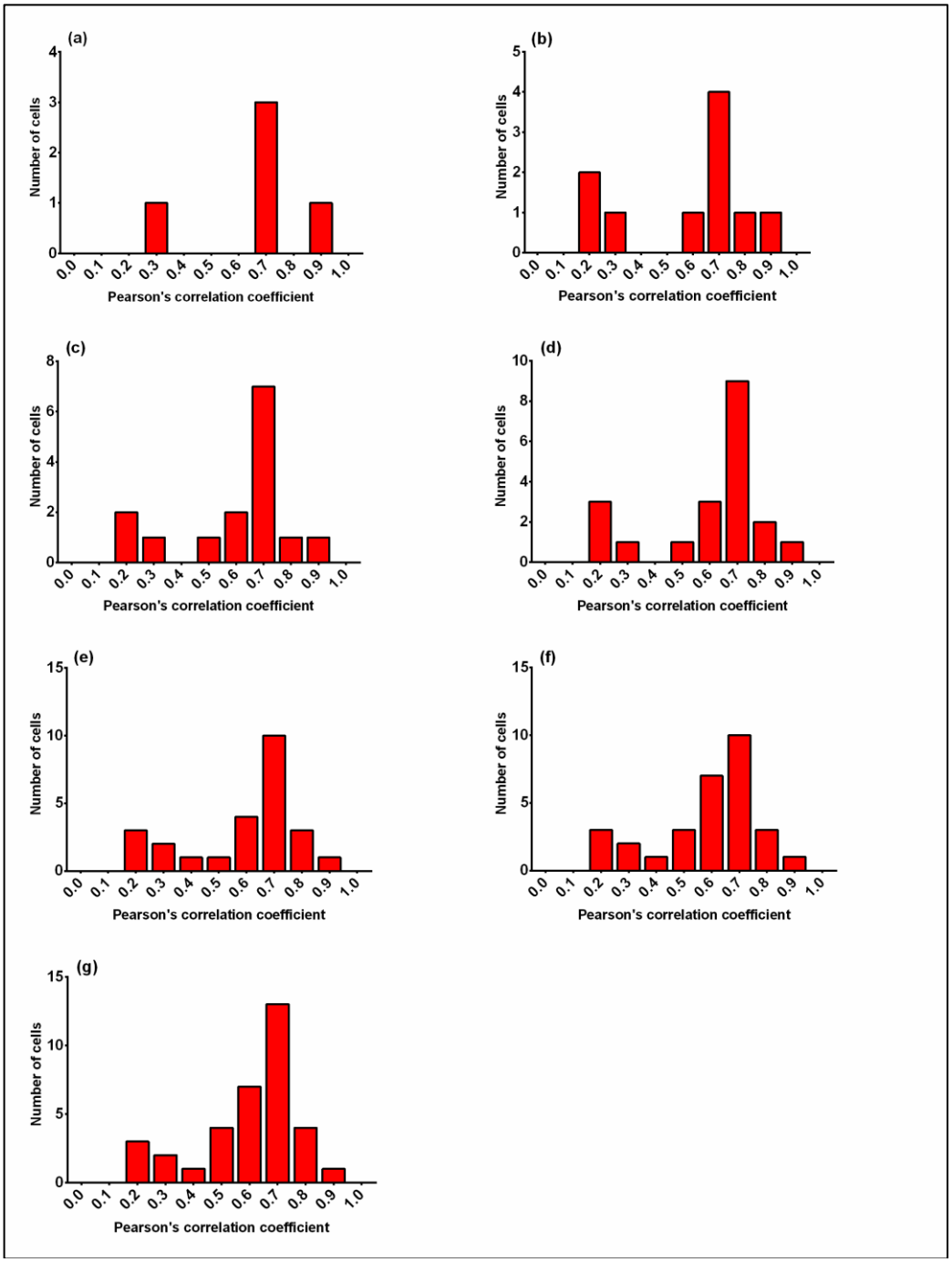

Cumulative analysis of the colocalisation of ERβ2 and mitochondria in MDA-MB-231 cells
a) 5 cells analysed b) 10 cells analysed c) 15 cells analysed d) 20 cells analysed e) 25 cells analysed f) 30 cells analysed g) 35 cells analysed

7.5 Nuclear target gene expression in ERβ2 overexpressing cells compared to control

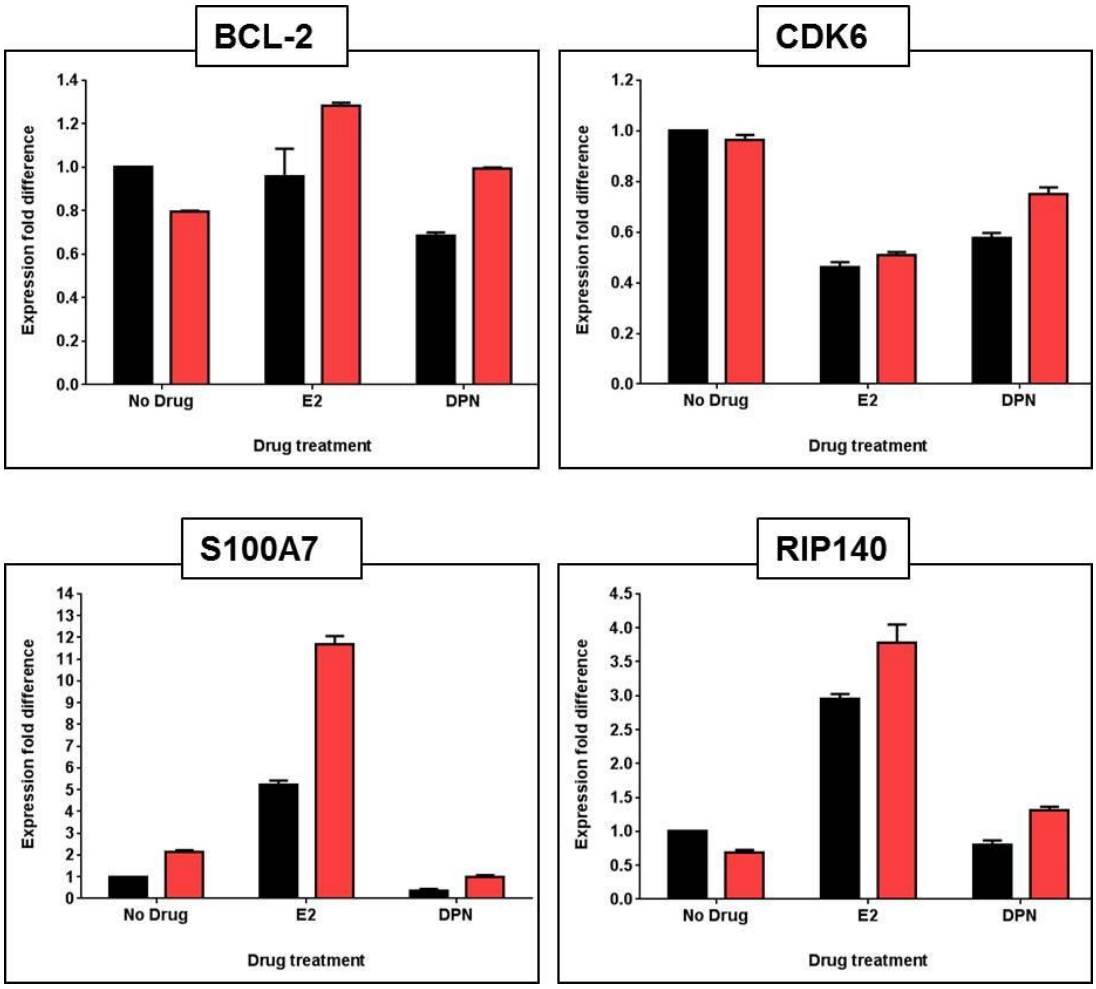

qRT-PCR quantification of the mRNA expression levels of BCL-2 CDK6, S100A7 and RIP140 in ERβ2 overexpressing and vector control MCF-7 cells treated with E2 (1nM) or DPN (10nM) for 24 hours

Red bars represent ERβ2 overexpressing cells. Black bars represent the empty vector control cells. Expression is normalised to the untreated empty vector control for each gene analysed, which was given the value of 1.

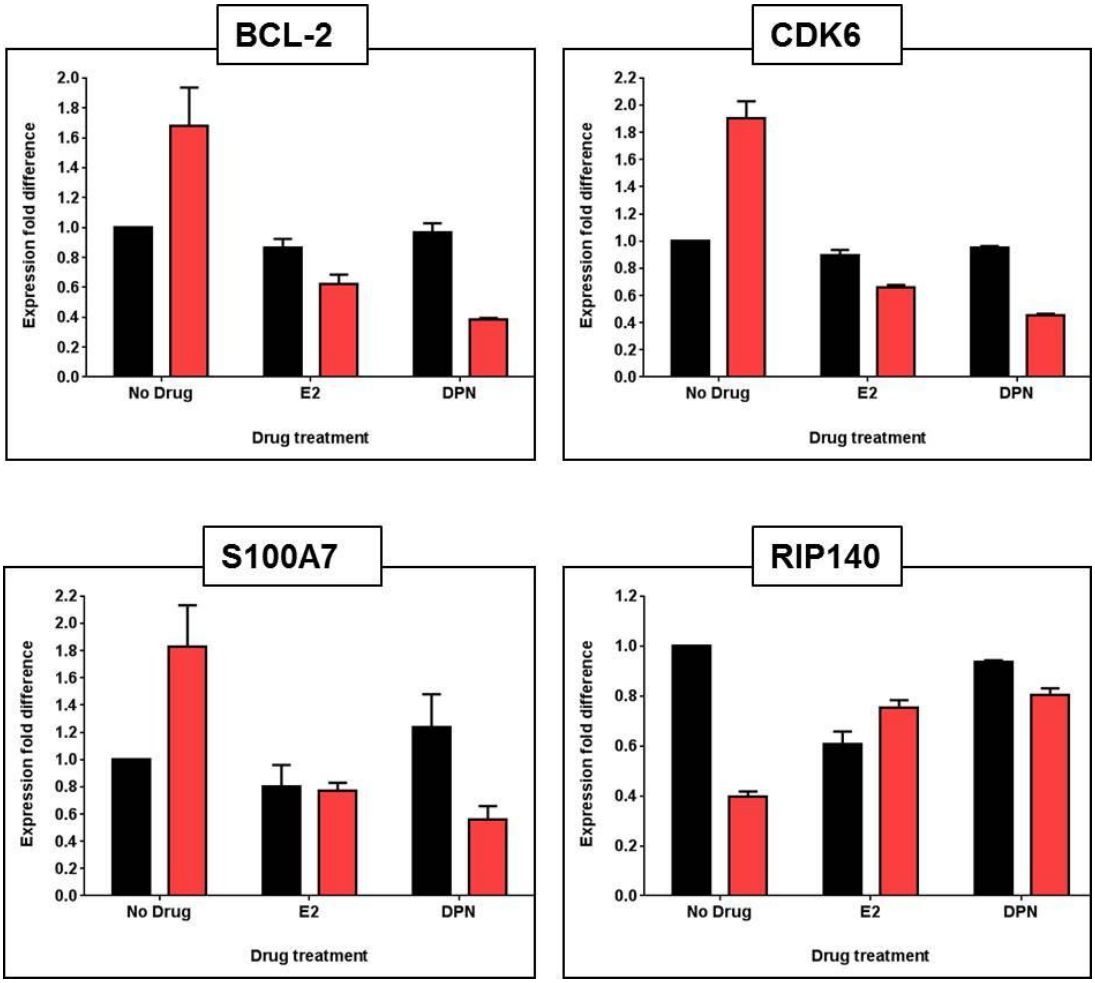

qRT-PCR quantification of the mRNA expression levels of BCL-2 CDK6, S100A7 and RIP140 in ERβ2 overexpressing and vector control MDA-MB-231 cells treated with E2 (1nM) or DPN (10nM) for 24 hours

Red bars represent ERβ2 overexpressing cells. Black bars represent the empty vector control cells. Expression is normalised to the untreated empty vector control for each gene analysed, which was given the value of 1.

7.6 Mitochondrial target gene expression in ERβ2 overexpressing cells compared to controls

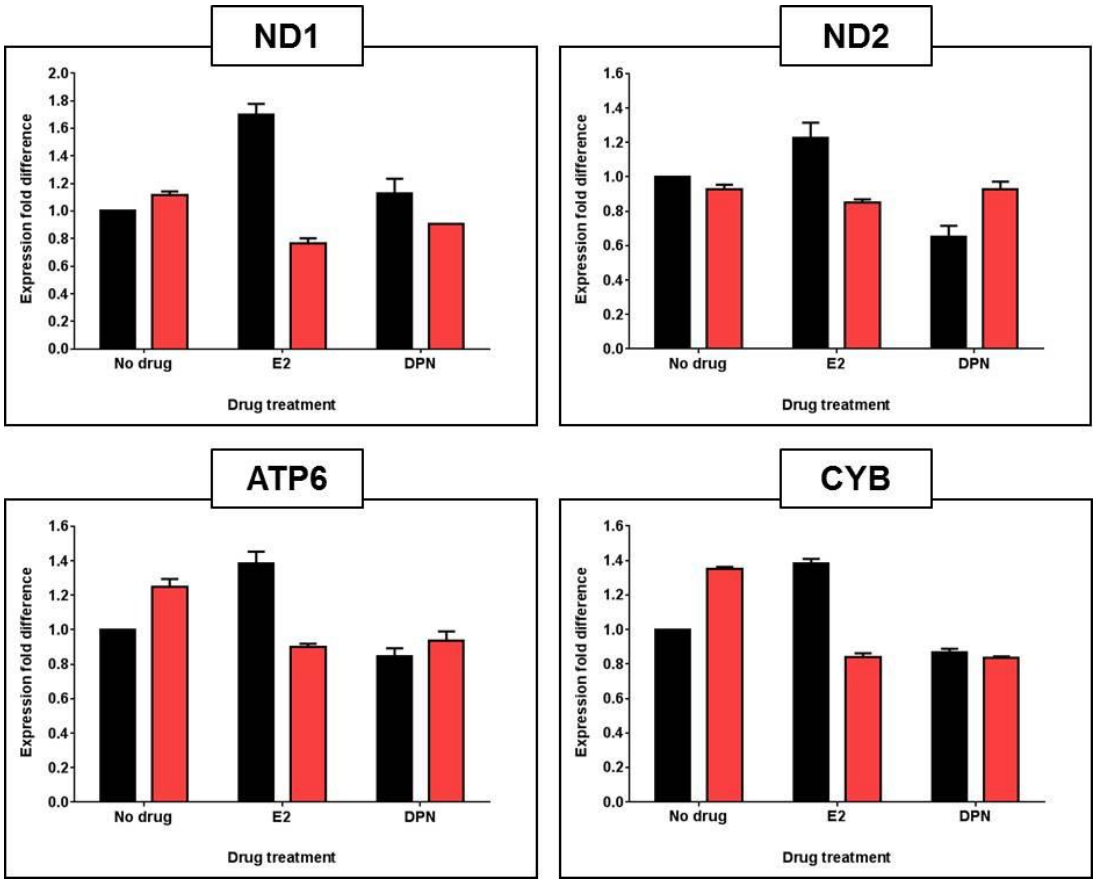

qRT-PCR quantification of the mRNA expression levels of ND1, ND2, ATP6 and CYB in ERβ2 overexpressing and vector control MCF-7cells treated with E2 (1nM) or DPN (10nM) for 24 hours

Red bars represent ERβ2 overexpressing cells. Black bars represent the empty vector control cells. Expression is normalised to the untreated empty vector control for each gene analysed, which was given the value of 1.

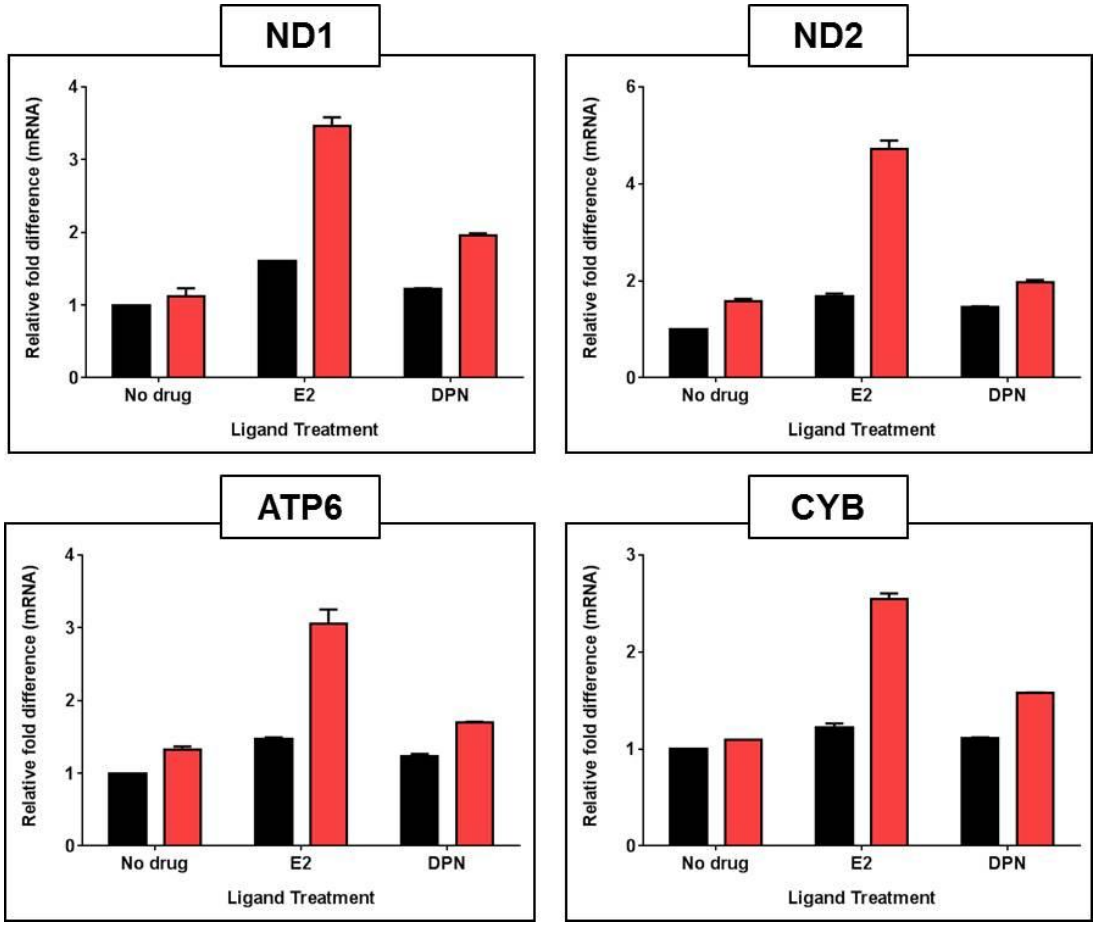

qRT-PCR quantification of the mRNA expression levels of ND1, ND2, ATP6 and CYB in ERβ2 overexpressing and vector control MDA-MB-231 cells treated with E2 (1nM) or DPN (10nM) for 24 hours

Red bars represent ERβ2 overexpressing cells. Black bars represent the empty vector control cells. Expression is normalised to the untreated empty vector control for each gene analysed, which was given the value of 1.

7.7 Estrogenic ligand dose response curves in MCF-7 cells

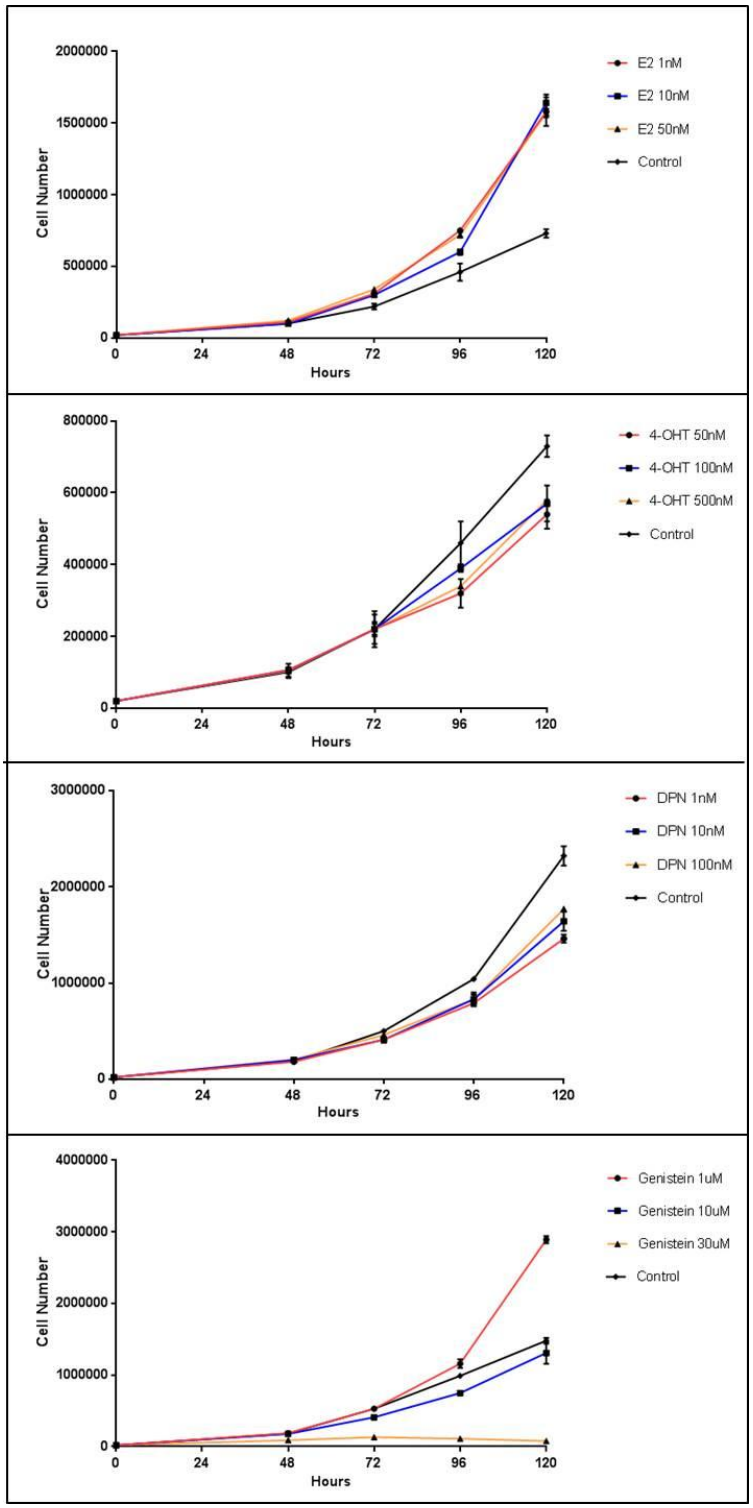

Dose response curves of MCF-7 cell proliferation in response to different doses of E2, 4-OHT, DPN and genistein

References

1. Mauvais-Jarvis P, Kuttenn F, Gompel A. Estradiol/progesterone interaction in normal and pathologic breast cells. Ann N Y Acad Sci. 1986;464:152-67.
2. Neville MC, McFadden TB, Forsyth I. Hormonal regulation of mammary differentiation and milk secretion. J Mammary Gland Biol Neoplasia. 2002 Jan;7(1):49-66.
3. Emerman JT, Vogl AW. Cell size and shape changes in the myoepithelium of the mammary gland during differentiation. Anat Rec. 1986 Nov;216(3):405-15.
4. J.C.E Underwood. General and Systematic Pathology: Elsevier; 2004.
5. Sadlonova A, Mukherjee S, Bowe DB, Gault SR, Dumas NA, Van Tine BA, Frolova N, Page GP, Welch DR, Novak L, Frost AR. Human Breast Fibroblasts Inhibit Growth of the MCF10AT Xenograft Model of Proliferative Breast Disease. The American Journal of Pathology. 2007;170(3):1064-76.
6. Jemal A, Bray F, Center MM, Ferlay J, Ward E, Forman D. Global cancer statistics. CA: A Cancer Journal for Clinicians. 2011;61(2):69-90.
7. Cancer Research UK. Cancer Research UK Press Release. [Press release] 2011 [16 July 2012]; Available from: http://info.cancerresearchuk.org/news/archive/pressrelease/2011-02-04-one-woman-in-eight-breast-cancer#2.
8. Cancer Research UK. Breast Cancer Statistics. [10/09/2015]; Available from: http://www.cancerresearchuk.org/health-professional/cancer-statistics/statistics-by-cancer-type/breast-cancer#heading-Two.
9. Polyak K, Hu M. Do myoepithelial cells hold the key for breast tumor progression? J Mammary Gland Biol Neoplasia. 2005 Jul;10(3):231-47.
10. Cancer Research UK. Breast Cancer Risk Factors. 2015 [cited 2015]; Available from: http://www.cancerresearchuk.org/health-professional/cancer-statistics/statistics-by-cancer-type/breast-cancer/risk-factors.
11. Easton D, Ford D, Peto J. Inherited susceptibility to breast cancer. Cancer Surv. 1993;18:95-113.
12. Walsh T, Casadei S, Coats KH, Swisher E, Stray SM, Higgins J, Roach KC, Mandell J, Lee MK, Ciernikova S, Foretova L, Soucek P, King MC. Spectrum of mutations in BRCA1, BRCA2, CHEK2, and TP53 in families at high risk of breast cancer. JAMA. 2006 Mar 22;295(12):1379-88.
13. Tan MH, Mester JL, Ngeow J, Rybicki LA, Orloff MS, Eng C. Lifetime cancer risks in individuals with germline PTEN mutations. Clin Cancer Res. 2012 Jan 15;18(2):400-7.
14. Ahmed M, Rahman N. ATM and breast cancer susceptibility. Oncogene. 2006 Sep 25;25(43):5906-11.
15. De Nicolo A, Tancredi M, Lombardi G, Flemma CC, Barbuti S, Di Cristofano C, Sobhian B, Bevilacqua G, Drapkin R, Caligo MA. A novel breast cancer-associated BRIP1 (FANCJ/BACH1) germ-line mutation impairs protein stability and function. Clin Cancer Res. 2008 Jul 15;14(14):4672-80.
16. Rahman N, Seal S, Thompson D, Kelly P, Renwick A, Elliott A, Reid S, Spanova K, Barfoot R, Chagtai T, Jayatilake H, McGuffog L, Hanks S, Evans DG, Eccles D, Easton DF, Stratton MR. PALB2, which encodes a BRCA2-interacting protein, is a breast cancer susceptibility gene. Nat Genet. 2007 Feb;39(2):165-7.
17. Cancer Research UK. Preventable cancer cases by cancer type. 2015 [cited 2015]; Available from: http://www.cancerresearchuk.org/health-professional/cancer-statistics/risk/preventable-cancers#heading-One.
18. Grann VR, Jacobson JS, Whang W, Hershman D, Heitjan DF, Antman KH, Neugut AI. Prevention with tamoxifen or other hormones versus prophylactic surgery in BRCA1/2-positive women: a decision analysis. Cancer J Sci Am. 2000 Jan-Feb;6(1):13-20.

19. Elston CW, Ellis IO. Pathological prognostic factors in breast cancer. I. The value of histological grade in breast cancer: experience from a large study with long-term follow-up. Histopathology. 1991 Nov;19(5):403-10.
20. Nieto MA. The ins and outs of the epithelial to mesenchymal transition in health and disease. Annu Rev Cell Dev Biol. 2011;27:347-76.
21. Schmalhofer O, Brabletz S, Brabletz T. E-cadherin, beta-catenin, and ZEB1 in malignant progression of cancer. Cancer Metastasis Rev. 2009 Jun;28(1-2):151-66.
22. Wang Y, Zhou BP. Epithelial-mesenchymal transition in breast cancer progression and metastasis. Chin J Cancer. 2011 Sep;30(9):603-11.
23. Fisher B, Redmond C, Fisher ER, Caplan R. Relative worth of estrogen or progesterone receptor and pathologic characteristics of differentiation as indicators of prognosis in node negative breast cancer patients: findings from National Surgical Adjuvant Breast and Bowel Project Protocol B-06. J Clin Oncol. 1988 Jul;6(7):1076-87.
24. Ali S, Coombes RC. Estrogen receptor alpha in human breast cancer: occurrence and significance. J Mammary Gland Biol Neoplasia. 2000 Jul;5(3):271-81.
25. Yu KD, Wu J, Shen ZZ, Shao ZM. Hazard of breast cancer-specific mortality among women with estrogen receptor-positive breast cancer after five years from diagnosis: implication for extended endocrine therapy. J Clin Endocrinol Metab. 2012 Dec;97(12):E2201-9.
26. Slamon DJ, Clark GM, Wong SG, Levin WJ, Ullrich A, McGuire WL. Human breast cancer: correlation of relapse and survival with amplification of the HER-2/neu oncogene. Science. 1987 Jan 9;235(4785):177-82.
27. Abd El-Rehim DM, Pinder SE, Paish CE, Bell J, Blamey RW, Robertson JF, Nicholson RI, Ellis IO. Expression of luminal and basal cytokeratins in human breast carcinoma. J Pathol. 2004 Jun;203(2):661-71.
28. Fan C, Oh DS, Wessels L, Weigelt B, Nuyten DS, Nobel AB, van't Veer LJ, Perou CM. Concordance among gene-expression-based predictors for breast cancer. N Engl J Med. 2006 Aug 10;355(6):560-9.
29. Nielsen TO, Hsu FD, Jensen K, Cheang M, Karaca G, Hu Z, Hernandez-Boussard T, Livasy C, Cowan D, Dressler L, Akslen LA, Ragaz J, Gown AM, Gilks CB, van de Rijn M, Perou CM. Immunohistochemical and clinical characterization of the basal-like subtype of invasive breast carcinoma. Clin Cancer Res. 2004;10(16):5367-74.
30. Dent R, Trudeau M, Pritchard KI, Hanna WM, Kahn HK, Sawka CA, Lickley LA, Rawlinson E, Sun P, Narod SA. Triple-negative breast cancer: clinical features and patterns of recurrence. Clin Cancer Res. 2007 Aug 1;13(15 Pt 1):4429-34.
31. Rakha EA, El-Sayed ME, Green AR, Lee AH, Robertson JF, Ellis IO. Prognostic markers in triple-negative breast cancer. Cancer. 2007;109(1):25-32.
32. Tischkowitz M, Brunet JS, Begin LR, Huntsman DG, Cheang MC, Akslen LA, Nielsen TO, Foulkes WD. Use of immunohistochemical markers can refine prognosis in triple negative breast cancer. BMC Cancer. 2007;7:134.
33. Bauer KR, Brown M, Cress RD, Parise CA, Caggiano V. Descriptive analysis of estrogen receptor (ER)-negative, progesterone receptor (PR)-negative, and HER2-negative invasive breast cancer, the so-called triple-negative phenotype: a population-based study from the California cancer Registry. Cancer. 2007 May 1;109(9):1721-8.
34. Dent R, Trudeau M, Pritchard KI, Hanna WM, Kahn HK, Sawka CA, Lickley LA, Rawlinson E, Sun P, Narod SA. Triple-Negative Breast Cancer: Clinical Features and Patterns of Recurrence. Clinical Cancer Research. 2007 August 1, 2007;13(15):4429-34.
35. Mitchell KW, Carey LA, Peppercorn J. Reporting of race and ethnicity in breast cancer research: room for improvement. Breast Cancer Res Treat. 2009 Dec;118(3):511-7.

36. Perou CM, Sorlie T, Eisen MB, van de Rijn M, Jeffrey SS, Rees CA, Pollack JR, Ross DT, Johnsen H, Akslen LA, Fluge O, Pergamenschikov A, Williams C, Zhu SX, Lonning PE, Borresen-Dale AL, Brown PO, Botstein D. Molecular portraits of human breast tumours. Nature. 2000;406(6797):747-52.
37. Prat A, Parker JS, Karginova O, Fan C, Livasy C, Herschkowitz JI, He X, Perou CM. Phenotypic and molecular characterization of the claudin-low intrinsic subtype of breast cancer. Breast Cancer Res. 2010;12(5).
38. Curtis C, Shah SP, Chin S-F, Turashvili G, Rueda OM, Dunning MJ, Speed D, Lynch AG, Samarajiwa S, Yuan Y, Graf S, Ha G, Haffari G, Bashashati A, Russell R, McKinney S, Langerod A, Green A, Provenzano E, Wishart G, Pinder S, Watson P, Markowetz F, Murphy L, Ellis I, Purushotham A, Borresen-Dale A-L, Brenton JD, Tavare S, Caldas C, Aparicio S. The genomic and transcriptomic architecture of 2,000 breast tumours reveals novel subgroups. Nature. [10.1038/nature10983]. 2012;advance online publication.
39. Lehmann BD, Bauer JA, Chen X, Sanders ME, Chakravarthy AB, Shyr Y, Pietenpol JA. Identification of human triple-negative breast cancer subtypes and preclinical models for selection of targeted therapies. J Clin Invest. 2011;121(7):2750-67.
40. Holliday D, Speirs V. Choosing the right cell line for breast cancer research. Breast Cancer Research. 2011;13(4):215.
41. Heldring N, Pike A, Andersson S, Matthews J, Cheng G, Hartman J, Tujague M, Strom A, Treuter E, Warner M, Gustafsson JA. Estrogen receptors: how do they signal and what are their targets. Physiol Rev. 2007;87(3):905-31.
42. Nelson LR, Bulun SE. Estrogen production and action. J Am Acad Dermatol. 2001 Sep;45(3 Suppl):S116-24.
43. Nilsson S, Makela S, Treuter E, Tujague M, Thomsen J, Andersson G, Enmark E, Pettersson K, Warner M, Gustafsson JA. Mechanisms of estrogen action. Physiol Rev. 2001 Oct;81(4):1535-65.
44. Zhao C, Dahlman-Wright K, Gustafsson JA. Estrogen receptor beta: an overview and update. Nucl Recept Signal. 2008;1(6).
45. Toft D, Gorski J. A receptor molecule for estrogens: isolation from the rat uterus and preliminary characterization. Proc Natl Acad Sci U S A. 1966;55(6):1574-81.
46. Kuiper GGJM, Enmark E, Pelto-Huikko M, Nilsson S, Gustafsson J-A. Cloning of a Novel Estrogen Receptor Expressed in Rat Prostate and Ovary. Proceedings of the National Academy of Sciences of the United States of America. 1996;93(12):5925-30.
47. Grober O, Mutarelli M, Giurato G, Ravo M, Cicatiello L, De Filippo M, Ferraro L, Nassa G, Papa M, Paris O, Tarallo R, Luo S, Schroth G, Benes V, Weisz A. Global analysis of estrogen receptor beta binding to breast cancer cell genome reveals an extensive interplay with estrogen receptor alpha for target gene regulation. BMC Genomics. 2011;12(1):36.
48. Hall JM, Couse JF, Korach KS. The multifaceted mechanisms of estradiol and estrogen receptor signaling. J Biol Chem. 2001 Oct 5;276(40):36869-72.
49. Leung YK, Lee MT, Lam HM, Tarapore P, Ho SM. Estrogen receptor-beta and breast cancer: translating biology into clinical practice. Steroids. 2012 Jun;77(7):727-37.
50. Heldring N, Pawson T, McDonnell D, Treuter E, Gustafsson JA, Pike AC. Structural insights into corepressor recognition by antagonist-bound estrogen receptors. J Biol Chem. 2007;282(14):10449-55.
51. Green KA, Carroll JS. Oestrogen-receptor-mediated transcription and the influence of co-factors and chromatin state. Nat Rev Cancer. 2007 Sep;7(9):713-22.
52. Klinge CM. Estrogen receptor interaction with co-activators and co-repressors. Steroids. 2000 May;65(5):227-51.
53. Matthews J, Gustafsson JA. Estrogen signaling: a subtle balance between ER alpha and ER beta. Mol Interv. 2003 Aug;3(5):281-92.

54. Leung YK, Mak P, Hassan S, Ho SM. Estrogen receptor (ER)-beta isoforms: a key to understanding ER-beta signaling. Proc Natl Acad Sci U S A. 2006;103(35):13162-7.
55. Leung Y-K, Lee M-T, Lam H-M, Tarapore P, Ho S-M. Estrogen receptor-beta and breast cancer: Translating biology into clinical practice. Steroids. 2012;77(7):727-37.
56. Menasce LP, White GR, Harrison CJ, Boyle JM. Localization of the estrogen receptor locus (ESR) to chromosome 6q25.1 by FISH and a simple post-FISH banding technique. Genomics. 1993 Jul;17(1):263-5.
57. Enmark E, Pelto-Huikko M, Grandien K, Lagercrantz S, Lagercrantz J, Fried G, Nordenskjold M, Gustafsson JA. Human estrogen receptor beta-gene structure, chromosomal localization, and expression pattern. J Clin Endocrinol Metab. 1997 Dec;82(12):4258-65.
58. Raj Kumar MNZ, Shagufta H. Khan, et al. The Dynamic Structure of the Estrogen Receptor. Journal of Amino Acids. 2011;2011.
59. Speirs V, Skliris GP, Burdall SE, Carder PJ. Distinct expression patterns of ER alpha and ER beta in normal human mammary gland. J Clin Pathol. 2002 May;55(5):371-4.
60. Huang B, Omoto Y, Iwase H, Yamashita H, Toyama T, Coombes RC, Filipovic A, Warner M, Gustafsson JA. Differential expression of estrogen receptor alpha, beta1, and beta2 in lobular and ductal breast cancer. Proc Natl Acad Sci U S A. 2014 Feb 4;111(5):1933-8.
61. Chi A, Chen X, Chirala M, Younes M. Differential expression of estrogen receptor beta isoforms in human breast cancer tissue. Anticancer Res. 2003 Jan-Feb;23(1A):211-6.
62. Markopoulos C, Berger U, Wilson P, Gazet JC, Coombes RC. Oestrogen receptor content of normal breast cells and breast carcinomas throughout the menstrual cycle. Br Med J (Clin Res Ed). 1988 May 14;296(6633):1349-51.
63. Krege JH, Hodgin JB, Couse JF, Enmark E, Warner M, Mahler JF, Sar M, Korach KS, Gustafsson JA, Smithies O. Generation and reproductive phenotypes of mice lacking estrogen receptor beta. Proc Natl Acad Sci U S A. 1998 Dec 22;95(26):15677-82.
64. Forster C, Makela S, Warri A, Kietz S, Becker D, Hultenby K, Warner M, Gustafsson JA. Involvement of estrogen receptor beta in terminal differentiation of mammary gland epithelium. Proc Natl Acad Sci U S A. 2002 Nov 26;99(24):15578-83.
65. Couse JF, Korach KS. Reproductive phenotypes in the estrogen receptor-alpha knockout mouse. Ann Endocrinol (Paris). 1999 Jul;60(2):143-8.
66. Lubahn DB, Moyer JS, Golding TS, Couse JF, Korach KS, Smithies O. Alteration of reproductive function but not prenatal sexual development after insertional disruption of the mouse estrogen receptor gene. Proc Natl Acad Sci U S A. 1993 Dec 1;90(23):11162-6.
67. Mueller SO, Clark JA, Myers PH, Korach KS. Mammary gland development in adult mice requires epithelial and stromal estrogen receptor alpha. Endocrinology. 2002 Jun;143(6):2357-65.
68. Le Romancer M, Poulard C, Cohen P, Sentis S, Renoir JM, Corbo L. Cracking the estrogen receptor's posttranslational code in breast tumors. Endocr Rev. 2011;32(5):597-622.
69. Liao XH, Lu DL, Wang N, Liu LY, Wang Y, Li YQ, Yan TB, Sun XG, Hu P, Zhang TC. Estrogen receptor alpha mediates proliferation of breast cancer MCF-7 cells via a p21/PCNA/E2F1-dependent pathway. FEBS J. 2014 Feb;281(3):927-42.
70. Sayeed A, Konduri SD, Liu W, Bansal S, Li F, Das GM. Estrogen receptor alpha inhibits p53-mediated transcriptional repression: implications for the regulation of apoptosis. Cancer Res. 2007 Aug 15;67(16):7746-55.

71. Roger P, Sahla ME, Makela S, Gustafsson JA, Baldet P, Rochefort H. Decreased expression of estrogen receptor beta protein in proliferative preinvasive mammary tumors. Cancer Res. 2001 Mar 15;61(6):2537-41.
72. Peng B, Lu B, Leygue E, Murphy LC. Putative functional characteristics of human estrogen receptor-beta isoforms. J Mol Endocrinol. 2003 Feb;30(1):13-29.
73. Smart E, Hughes T, Smith L, Speirs V. Estrogen receptor beta: putting a positive into triple negative breast cancer? Horm Mol Biol Clin Investig. 2013 Dec;16(3):117-23.
74. Marotti JD, Collins LC, Hu R, Tamimi RM. Estrogen receptor-beta expression in invasive breast cancer in relation to molecular phenotype: results from the Nurses' Health Study. Mod Pathol. 2010 Feb;23(2):197-204.
75. Sugiura H, Toyama T, Hara Y, Zhang Z, Kobayashi S, Fujii Y, Iwase H, Yamashita H. Expression of estrogen receptor beta wild-type and its variant ERbetacx/beta2 is correlated with better prognosis in breast cancer. Jpn J Clin Oncol. 2007 Nov;37(11):820-8.
76. Omoto Y, Kobayashi S, Inoue S, Ogawa S, Toyama T, Yamashita H, Muramatsu M, Gustafsson JA, Iwase H. Evaluation of oestrogen receptor beta wild-type and variant protein expression, and relationship with clinicopathological factors in breast cancers. Eur J Cancer. 2002 Feb;38(3):380-6.
77. Fleming FJ, Hill AD, McDermott EW, O'Higgins NJ, Young LS. Differential recruitment of coregulator proteins steroid receptor coactivator-1 and silencing mediator for retinoid and thyroid receptors to the estrogen receptor-estrogen response element by beta-estradiol and 4-hydroxytamoxifen in human breast cancer. J Clin Endocrinol Metab. 2004;89(1):375-83.
78. Myers E, Fleming FJ, Crotty TB, Kelly G, McDermott EW, O'Higgins N J, Hill AD, Young LS. Inverse relationship between ER-beta and SRC-1 predicts outcome in endocrine-resistant breast cancer. Br J Cancer. 2004 Nov 1;91(9):1687-93.
79. Rosin G, de Boniface J, Karthik GM, Frisell J, Bergh J, Hartman J. Oestrogen receptors beta1 and betacx have divergent roles in breast cancer survival and lymph node metastasis. Br J Cancer. 2014 Aug 26;111(5):918-26.
80. Paruthiyil S, Parmar H, Kerekatte V, Cunha GR, Firestone GL, Leitman DC. Estrogen Receptor β Inhibits Human Breast Cancer Cell Proliferation and Tumor Formation by Causing a G2 Cell Cycle Arrest. Cancer Research. 2004 January 1, 2004;64(1):423-8.
81. Paruthiyil S, Cvoro A, Tagliaferri M, Cohen I, Shtivelman E, Leitman DC. Estrogen receptor beta causes a G2 cell cycle arrest by inhibiting CDK1 activity through the regulation of cyclin B1, GADD45A, and BTG2. Breast Cancer Res Treat. 2011 Oct;129(3):777-84.
82. Strom A, Hartman J, Foster JS, Kietz S, Wimalasena J, Gustafsson JA. Estrogen receptor beta inhibits 17beta-estradiol-stimulated proliferation of the breast cancer cell line T47D. Proc Natl Acad Sci U S A. 2004;101(6):1566-71.
83. Murphy LC, Peng B, Lewis A, Davie JR, Leygue E, Kemp A, Ung K, Vendetti M, Shiu R. Inducible upregulation of oestrogen receptor-beta1 affects oestrogen and tamoxifen responsiveness in MCF7 human breast cancer cells. J Mol Endocrinol. 2005 Apr;34(2):553-66.
84. Hurtado A, Pinos T, Barbosa-Desongles A, Lopez-Aviles S, Barquinero J, Petriz J, Santamaria-Martinez A, Morote J, de Torres I, Bellmunt J, Reventos J, Munell F. Estrogen receptor beta displays cell cycle-dependent expression and regulates the G1 phase through a non-genomic mechanism in prostate carcinoma cells. Cell Oncol. 2008;30(4):349-65.
85. Iwase H, Zhang Z, Omoto Y, Sugiura H, Yamashita H, Toyama T, Iwata H, Kobayashi S. Clinical significance of the expression of estrogen receptors alpha and beta for endocrine therapy of breast cancer. Cancer Chemother Pharmacol. 2003;52(1):19.
86. Honma N, Horii R, Iwase T, Saji S, Younes M, Takubo K, Matsuura M, Ito Y, Akiyama F, Sakamoto G. Clinical importance of estrogen receptor-beta evaluation

in breast cancer patients treated with adjuvant tamoxifen therapy. J Clin Oncol. 2008;26(22):3727-34.
87. Novelli F, Milella M, Melucci E, Di Benedetto A, Sperduti I, Perrone-Donnorso R, Perracchio L, Venturo I, Nistico C, Fabi A, Buglioni S, Natali PG, Mottolese M. A divergent role for estrogen receptor-beta in node-positive and node-negative breast cancer classified according to molecular subtypes: an observational prospective study. Breast Cancer Res. 2008;10(5):4.
88. O'Neill PA, Davies MP, Shaaban AM, Innes H, Torevell A, Sibson DR, Foster CS. Wild-type oestrogen receptor beta (ERbeta1) mRNA and protein expression in Tamoxifen-treated post-menopausal breast cancers. Br J Cancer. 2004;91(9):1694-702.
89. Kim TJ, Lee A, Choi YJ, Song BJ, Yim HW, Kang CS. Prognostic Significance of High Expression of ER-beta in Surgically Treated ER-Positive Breast Cancer Following Endocrine Therapy. J Breast Cancer. 2012 Mar;15(1):79-86.
90. Vinayagam R, Sibson DR, Holcombe C, Aachi V, Davies MP. Association of oestrogen receptor beta 2 (ER beta 2/ER beta cx) with outcome of adjuvant endocrine treatment for primary breast cancer--a retrospective study. BMC Cancer. 2007;7:131.
91. Skliris GP, Leygue E, Curtis-Snell L, Watson PH, Murphy LC. Expression of oestrogen receptor-beta in oestrogen receptor-alpha negative human breast tumours. Br J Cancer. 2006;95(5):616-26.
92. Tonetti DA, Rubenstein R, DeLeon M, Zhao H, Pappas SG, Bentrem DJ, Chen B, Constantinou A, Craig Jordan V. Stable transfection of an estrogen receptor beta cDNA isoform into MDA-MB-231 breast cancer cells. J Steroid Biochem Mol Biol. 2003;87(1):47-55.
93. Hou YF, Yuan ST, Li HC, Wu J, Lu JS, Liu G, Lu LJ, Shen ZZ, Ding J, Shao ZM. ERbeta exerts multiple stimulative effects on human breast carcinoma cells. Oncogene. 2004;23(34):5799-806.
94. Shaaban AM, Green AR, Karthik S, Alizadeh Y, Hughes TA, Harkins L, Ellis IO, Robertson JF, Paish EC, Saunders PT, Groome NP, Speirs V. Nuclear and cytoplasmic expression of ERbeta1, ERbeta2, and ERbeta5 identifies distinct prognostic outcome for breast cancer patients. Clin Cancer Res. 2008;14(16):5228-35.
95. Zhao C, Matthews J, Tujague M, Wan J, Ström A, Toresson G, Lam EW-F, Cheng G, Gustafsson J-Å, Dahlman-Wright K. Estrogen Receptor β2 Negatively Regulates the Transactivation of Estrogen Receptor α in Human Breast Cancer Cells. Cancer Research. 2007 April 15, 2007;67(8):3955-62.
96. Palmieri C, Saji S, Sakaguchi H, Cheng G, Sunters A, O'Hare MJ, Warner M, Gustafsson JA, Coombes RC, Lam EW. The expression of oestrogen receptor (ER)-beta and its variants, but not ERalpha, in adult human mammary fibroblasts. J Mol Endocrinol. 2004 Aug;33(1):35-50.
97. Chantzi NI, Palaiologou M, Stylianidou A, Goutas N, Vassilaros S, Kourea HP, Dhimolea E, Mitsiou DJ, Tiniakos DG, Alexis MN. Estrogen receptor beta2 is inversely correlated with Ki-67 in hyperplastic and noninvasive neoplastic breast lesions. J Cancer Res Clin Oncol. 2014 Jun;140(6):1057-66.
98. Baek JM, Chae BJ, Song BJ, Jung SS. The potential role of estrogen receptor beta2 in breast cancer. Int J Surg. 2015 Feb;14:17-22.
99. Esslimani-Sahla M, Kramar A, Simony-Lafontaine J, Warner M, Gustafsson JA, Rochefort H. Increased estrogen receptor betacx expression during mammary carcinogenesis. Clin Cancer Res. 2005 May 1;11(9):3170-4.
100. Yan M, Rayoo M, Takano E, Investigators k, Fox S. Nuclear and cytoplasmic expressions of ERβ1 and ERβ2 are predictive of response to therapy and alters prognosis in familial breast cancers. Breast Cancer Research and Treatment. 2011;126(2):395-405.

101. Leung YK, Lam HM, Wu S, Song D, Levin L, Cheng L, Wu CL, Ho SM. Estrogen receptor β2 and β5 are associated with poor prognosis in prostate cancer, and promote cancer cell migration and invasion. Endocr Relat Cancer. 2010 Sep;17(3):675-89.
102. Ciucci A, Zannoni GF, Travaglia D, Petrillo M, Scambia G, Gallo D. Prognostic significance of the estrogen receptor beta (ERbeta) isoforms ERbeta1, ERbeta2, and ERbeta5 in advanced serous ovarian cancer. Gynecol Oncol. 2014 Feb;132(2):351-9.
103. Ogawa S, Inoue S, Watanabe T, Orimo A, Hosoi T, Ouchi Y, Muramatsu M. Molecular cloning and characterization of human estrogen receptor betacx: a potential inhibitor ofestrogen action in human. Nucleic Acids Res. 1998 Aug 1;26(15):3505-12.
104. Omoto Y, Eguchi H, Yamamoto-Yamaguchi Y, Hayashi S. Estrogen receptor (ER) beta1 and ERbetacx/beta2 inhibit ERalpha function differently in breast cancer cell line MCF7. Oncogene. 2003;22(32):5011-20.
105. Secreto FJ, Monroe DG, Dutta S, Ingle JN, Spelsberg TC. Estrogen receptor alpha/beta isoforms, but not betacx, modulate unique patterns of gene expression and cell proliferation in Hs578T cells. J Cell Biochem. 2007;101(5):1125-47.
106. Dey P, Jonsson P, Hartman J, Williams C, Strom A, Gustafsson JA. Estrogen receptors beta1 and beta2 have opposing roles in regulating proliferation and bone metastasis genes in the prostate cancer cell line PC3. Mol Endocrinol. 2012 Dec;26(12):1991-2003.
107. Lee MT, Ho SM, Tarapore P, Chung I, Leung YK. Estrogen Receptor β Isoform 5 Confers Sensitivity of Breast Cancer Cell Lines to Chemotherapeutic Agent-Induced Apoptosis through Interaction with Bcl2L12. Neoplasia. 2013 Nov;15(11):1262-71.
108. Hodges-Gallagher L, Valentine CD, El Bader S, Kushner PJ. Estrogen receptor beta increases the efficacy of antiestrogens by effects on apoptosis and cell cycling in breast cancer cells. Breast Cancer Res Treat. 2008 May;109(2):241-50.
109. Treeck O, Juhasz-Boess I, Lattrich C, Horn F, Goerse R, Ortmann O. Effects of exon-deleted estrogen receptor beta transcript variants on growth, apoptosis and gene expression of human breast cancer cell lines. Breast Cancer Res Treat. 2008 Aug;110(3):507-20.
110. Horimoto Y, Hartman J, Millour J, Pollock S, Olmos Y, Ho KK, Coombes RC, Poutanen M, Mäkelä SI, El-Bahrawy M, Speirs V, Lam EWF. ERβ1 Represses FOXM1 Expression through Targeting ERα to Control Cell Proliferation in Breast Cancer. Am J Pathol. 2011 Sep;179(3):1148-56.
111. Shanle EK, Hawse JR, Xu W. Generation of stable reporter breast cancer cell lines for the identification of ER subtype selective ligands. Biochem Pharmacol. 2011 Dec 15;82(12):1940-9.
112. Lazennec G, Bresson D, Lucas A, Chauveau C, Vignon F. ER beta inhibits proliferation and invasion of breast cancer cells. Endocrinology. 2001;142(9):4120-30.
113. Cammarata PR, Flynn J, Gottipati S, Chu S, Dimitrijevich S, Younes M, Skliris G, Murphy LC. Differential expression and comparative subcellular localization of estrogen receptor beta isoforms in virally transformed and normal cultured human lens epithelial cells. Experimental eye research. 2005;81(2):165-75.
114. Shaaban AM, Green AR, Karthik S, Alizadeh Y, Hughes TA, Harkins L, Ellis IO, Robertson JF, Paish EC, Saunders PTK, Groome NP, Speirs V. Nuclear and Cytoplasmic Expression of ERβ1, ERβ2, and ERβ5 Identifies Distinct Prognostic Outcome for Breast Cancer Patients. Clinical Cancer Research. 2008 August 15, 2008;14(16):5228-35.

115. Shanle EK, Zhao Z, Hawse J, Wisinski K, Keles S, Yuan M, Xu W. Research Resource: Global identification of estrogen receptor beta target genes in triple negative breast cancer cells. Molecular Endocrinology. 2013 August 26, 2013.
116. Lindberg K, Helguero LA, Omoto Y, Gustafsson JA, Haldosen LA. Estrogen receptor beta represses Akt signaling in breast cancer cells via downregulation of HER2/HER3 and upregulation of PTEN: implications for tamoxifen sensitivity. Breast Cancer Res. 2011;13(2):R43.
117. Chang EC, Frasor J, Komm B, Katzenellenbogen BS. Impact of estrogen receptor beta on gene networks regulated by estrogen receptor alpha in breast cancer cells. Endocrinology. 2006 Oct;147(10):4831-42.
118. Ruddy SC, Lau R, Cabrita MA, McGregor C, McKay BC, Murphy LC, Wright JS, Durst T, Pratt MA. Preferential estrogen receptor beta ligands reduce Bcl-2 expression in hormone-resistant breast cancer cells to increase autophagy. Mol Cancer Ther. 2014 Jul;13(7):1882-93.
119. Abeer M. Shaaban ARG, Suchita Karthik, et al. Nuclear and Cytoplasmic Expression of ERB1, ERB2, and ERB5 Identifies Distinct Prognostic Outcome for Breast Cancer Patients. Clinical Cancer Research. 2008.
120. Chen JQ, J. Russo. Mitochondrial oestrogen receptors and their potential implications in oestrogen carcinogenesis in human breast cancer. Journal of Nutritional and Environmental Medicine. 2008;17(1):76-89.
121. Chen JQ, Delannoy M, Cooke C, Yager JD. Mitochondrial localization of ERalpha and ERbeta in human MCF7 cells. Am J Physiol Endocrinol Metab. 2004;286(6):21.
122. Chen JQ, Russo PA, Cooke C, Russo IH, Russo J. ERbeta shifts from mitochondria to nucleus during estrogen-induced neoplastic transformation of human breast epithelial cells and is involved in estrogen-induced synthesis of mitochondrial respiratory chain proteins. Biochim Biophys Acta. 2007;12(46):29.
123. Hsieh YC, Yu HP, Suzuki T, Choudhry MA, Schwacha MG, Bland KI, Chaudry IH. Upregulation of mitochondrial respiratory complex IV by estrogen receptor-beta is critical for inhibiting mitochondrial apoptotic signaling and restoring cardiac functions following trauma-hemorrhage. J Mol Cell Cardiol. 2006 Sep;41(3):511-21.
124. Manente AG, Valenti D, Pinton G, Jithesh PV, Daga A, Rossi L, Gray SG, O'Byrne KJ, Fennell DA, Vacca RA, Nilsson S, Mutti L, Moro L. Estrogen receptor beta activation impairs mitochondrial oxidative metabolism and affects malignant mesothelioma cell growth in vitro and in vivo. Oncogenesis. 2013;2:e72.
125. Razandi M, Pedram A, Jordan VC, Fuqua S, Levin ER. Tamoxifen regulates cell fate through mitochondrial estrogen receptor beta in breast cancer. Oncogene. 2013 Jul 4;32(27):3274-85.
126. Levin ER, Pietras RJ. Estrogen receptors outside the nucleus in breast cancer. Breast Cancer Res Treat. 2008;108(3):351-61.
127. Xie W, Duan R, Safe S. Activation of adenosine deaminase in MCF-7 cells through IGF-estrogen receptor alpha crosstalk. J Mol Endocrinol. 2001 Jun;26(3):217-28.
128. Chimento A, Sirianni R, Delalande C, Silandre D, Bois C, Ando S, Maggiolini M, Carreau S, Pezzi V. 17 beta-estradiol activates rapid signaling pathways involved in rat pachytene spermatocytes apoptosis through GPR30 and ER alpha. Mol Cell Endocrinol. 2010 May 14;320(1-2):136-44.
129. Geraldes P, Sirois MG, Tanguay JF. Specific contribution of estrogen receptors on mitogen-activated protein kinase pathways and vascular cell activation. Circ Res. 2003 Sep 5;93(5):399-405.
130. Acconcia F, Totta P, Ogawa S, Cardillo I, Inoue S, Leone S, Trentalance A, Muramatsu M, Marino M. Survival versus apoptotic 17beta-estradiol effect: role of ER alpha and ER beta activated non-genomic signaling. J Cell Physiol. 2005 Apr;203(1):193-201.

131. Marino M, Ascenzi P. Membrane association of estrogen receptor alpha and beta influences 17beta-estradiol-mediated cancer cell proliferation. Steroids. 2008 Oct;73(9-10):853-8.
132. Vu T, Claret FX. Trastuzumab: Updated Mechanisms of Action and Resistance in Breast Cancer. Front Oncol. 2012;2.
133. Yan Y, Li X, Blanchard A, Bramwell VH, Pritchard KI, Tu D, Shepherd L, Myal Y, Penner C, Watson PH, Leygue E, Murphy LC. Expression of both Estrogen Receptor-beta 1 (ER-beta1) and its co-regulator Steroid Receptor RNA Activator Protein (SRAP) are predictive for benefit from tamoxifen therapy in patients with Estrogen Receptor-alpha (ER-alpha)-Negative Early Breast Cancer (EBC). Ann Oncol. 2013;11:11.
134. Phillips KA, Milne RL, Rookus MA, Daly MB, Antoniou AC, Peock S, Frost D, Easton DF, Ellis S, Friedlander ML, Buys SS, Andrieu N, Nogues C, Stoppa-Lyonnet D, Bonadona V, Pujol P, McLachlan SA, John EM, Hooning MJ, Seynaeve C, Tollenaar RA, Goldgar DE, Terry MB, Caldes T, Weideman PC, Andrulis IL, Singer CF, Birch K, Simard J, Southey MC, Olsson HL, Jakubowska A, Olah E, Gerdes AM, Foretova L, Hopper JL. Tamoxifen and risk of contralateral breast cancer for BRCA1 and BRCA2 mutation carriers. J Clin Oncol. 2013 Sep 1;31(25):3091-9.
135. Bartella V, Rizza P, Barone I, Zito D, Giordano F, Giordano C, Catalano S, Mauro L, Sisci D, Panno ML, Fuqua SA, Ando S. Estrogen receptor beta binds Sp1 and recruits a corepressor complex to the estrogen receptor alpha gene promoter. Breast Cancer Res Treat. 2012 Jul;134(2):569-81.
136. Fan P, Fan S, Wang H, Mao J, Shi Y, Ibrahim MM, Ma W, Yu X, Hou Z, Wang B, Li L. Genistein decreases the breast cancer stem-like cell population through Hedgehog pathway. Stem Cell Res Ther. 2013;4(6):146.
137. Zava DT, Duwe G. Estrogenic and antiproliferative properties of genistein and other flavonoids in human breast cancer cells in vitro. Nutr Cancer. 1997;27(1):31-40.
138. Hsieh CY, Santell RC, Haslam SZ, Helferich WG. Estrogenic effects of genistein on the growth of estrogen receptor-positive human breast cancer (MCF-7) cells in vitro and in vivo. Cancer Res. 1998 Sep 1;58(17):3833-8.
139. de Lemos ML. Effects of soy phytoestrogens genistein and daidzein on breast cancer growth. Ann Pharmacother. 2001 Sep;35(9):1118-21.
140. Ogasawara M, Matsunaga T, Suzuki H. Differential effects of antioxidants on the in vitro invasion, growth and lung metastasis of murine colon cancer cells. Biol Pharm Bull. 2007 Jan;30(1):200-4.
141. Buchler P, Gukovskaya AS, Mouria M, Buchler MC, Buchler MW, Friess H, Pandol SJ, Reber HA, Hines OJ. Prevention of metastatic pancreatic cancer growth in vivo by induction of apoptosis with genistein, a naturally occurring isoflavonoid. Pancreas. 2003 Apr;26(3):264-73.
142. Singh AV, Franke AA, Blackburn GL, Zhou JR. Soy phytochemicals prevent orthotopic growth and metastasis of bladder cancer in mice by alterations of cancer cell proliferation and apoptosis and tumor angiogenesis. Cancer Res. 2006 Feb 1;66(3):1851-8.
143. Shou J, Massarweh S, Osborne CK, Wakeling AE, Ali S, Weiss H, Schiff R. Mechanisms of tamoxifen resistance: increased estrogen receptor-HER2/neu cross-talk in ER/HER2-positive breast cancer. J Natl Cancer Inst. 2004 Jun 16;96(12):926-35.
144. Arpino G, Wiechmann L, Osborne CK, Schiff R. Crosstalk between the Estrogen Receptor and the HER Tyrosine Kinase Receptor Family: Molecular Mechanism and Clinical Implications for Endocrine Therapy Resistance. Endocr Rev. 2008 Apr;29(2):217-33.
145. Rizza P, Barone I, Zito D, Giordano F, Lanzino M, De Amicis F, Mauro L, Sisci D, Catalano S, Dahlman Wright K, Gustafsson JA, Ando S. Estrogen receptor

beta as a novel target of androgen receptor action in breast cancer cell lines. Breast Cancer Res. 2014;16(1):R21.
146. Leung Y-K, Mak P, Hassan S, Ho S-M. Estrogen receptor (ER)-β isoforms: A key to understanding ER-β signaling. Proceedings of the National Academy of Sciences. 2006 August 29, 2006;103(35):13162-7.
147. Neve et al. A collection of breast cancer cell lines for the study of functionally distinct cancer subtypes. Cancer Cell. 2006.
148. Prat A, Parker JS, Karginova O, Fan C, Livasy C, Herschkowitz JI, He X, Perou. CM. Phenotypic and molecular characterization of the claudin-low intrinsic subtype of breast cancer. Breast Cancer Research. 2010.
149. SEMIR VRANIC ZG, ZHAO-YI WANG. Update on the molecular profile of the MDA-MB-453 cell line as a model for apocrine breast carcinoma studies. Oncology Letters. 2011.
150. Speirs. DLHaV. Choosing the right cell line for breast cancer research. Breast Cancer Research. 2001.
151. Livak KJ, Schmittgen TD. Analysis of relative gene expression data using real-time quantitative PCR and the 2(-Delta Delta C(T)) Method. Methods. 2001 Dec;25(4):402-8.
152. Saji S, Omoto Y, Shimizu C, Horiguchi S, Watanabe T, Funata N, Hayash S, Gustafsson JA, Toi M. Clinical impact of assay of estrogen receptor beta cx in breast cancer. Breast Cancer. 2002;9(4):303-7.
153. Ciucci A, Zannoni GF, Travaglia D, Scambia G, Gallo D. Mitochondrial estrogen receptor beta2 drives antiapoptotic pathways in advanced serous ovarian cancer. Hum Pathol. 2015 Aug;46(8):1138-46.
154. Saunders PT, Millar MR, Macpherson S, Irvine DS, Groome NP, Evans LR, Sharpe RM, Scobie GA. ERbeta1 and the ERbeta2 splice variant (ERbetacx/beta2) are expressed in distinct cell populations in the adult human testis. J Clin Endocrinol Metab. 2002 Jun;87(6):2706-15.
155. Wimberly H, Han G, Pinnaduwage D, Murphy LC, Yang XR, Andrulis IL, Sherman M, Figueroa J, Rimm DL. ERbeta splice variant expression in four large cohorts of human breast cancer patient tumors. Breast Cancer Res Treat. 2014 Aug;146(3):657-67.
156. Wu W, Hodges E, Redelius J, Höög C. A novel approach for evaluating the efficiency of siRNAs on protein levels in cultured cells. Nucleic Acids Res. 2004;32(2):e17.
157. Dunn KW, Kamocka MM, McDonald JH. A practical guide to evaluating colocalization in biological microscopy. Am J Physiol Cell Physiol. 2011 Apr;300(4):C723-42.
158. Pearson K. Mathematical Contributions to the Theory of Evolution. III. Regression, Heredity, and Panmixia. Philosophical Transactions of the Royal Society of London A: Mathematical, Physical and Engineering Sciences. 1896 1896-01-01 00:00:00;187:253-318.
159. Manders EM, Stap J, Brakenhoff GJ, van Driel R, Aten JA. Dynamics of three-dimensional replication patterns during the S-phase, analysed by double labelling of DNA and confocal microscopy. J Cell Sci. 1992 Nov;103 (Pt 3):857-62.
160. Zinchuk V, Zinchuk O. Quantitative colocalization analysis of confocal fluorescence microscopy images. Curr Protoc Cell Biol. 2008 Jun;Chapter 4:Unit 4 19.
161. Manders EMM, Verbeek FJ, Aten JA. Measurement of co-localization of objects in dual-colour confocal images. Journal of Microscopy. 1993;169(3):375-82.
162. Shah KN, Faridi JS. Estrogen, tamoxifen, and Akt modulate expression of putative housekeeping genes in breast cancer cells. J Steroid Biochem Mol Biol. 2011 Jul;125(3-5):219-25.
163. Chen J, Hou R, Zhang X, Ye Y, Wang Y, Tian J. Calycosin suppresses breast cancer cell growth via ERbeta-dependent regulation of IGF-1R, p38 MAPK and PI3K/Akt pathways. PLoS One. 2014;9(3):e91245.

164. Klinge CM, Blankenship KA, Risinger KE, Bhatnagar S, Noisin EL, Sumanasekera WK, Zhao L, Brey DM, Keynton RS. Resveratrol and estradiol rapidly activate MAPK signaling through estrogen receptors alpha and beta in endothelial cells. J Biol Chem. 2005 Mar 4;280(9):7460-8.
165. Tremblay A, Tremblay GB, Labrie F, Giguere V. Ligand-independent recruitment of SRC-1 to estrogen receptor beta through phosphorylation of activation function AF-1. Mol Cell. 1999 Apr;3(4):513-9.
166. Hershberger PA, Stabile LP, Kanterewicz B, Rothstein ME, Gubish CT, Land S, Shuai Y, Siegfried JM, Nichols M. Estrogen receptor beta (ERbeta) subtype-specific ligands increase transcription, p44/p42 mitogen activated protein kinase (MAPK) activation and growth in human non-small cell lung cancer cells. J Steroid Biochem Mol Biol. 2009 Aug;116(1-2):102-9.
167. Thomas C, Gustafsson J-Å. The different roles of ER subtypes in cancer biology and therapy. Nat Rev Cancer. [10.1038/nrc3093]. 2011 08//print;11(8):597-608.
168. Miller WR, Anderson TJ, Dixon JM, Saunders PTK. Oestrogen receptor [beta] and neoadjuvant therapy with tamoxifen: prediction of response and effects of treatment. Br J Cancer. 2006 04/18/online;94(9):1333-8.
169. Neve RM, Chin K, Fridlyand J, Yeh J, Baehner FL, Fevr T, Clark L, Bayani N, Coppe JP, Tong F, Speed T, Spellman PT, DeVries S, Lapuk A, Wang NJ, Kuo WL, Stilwell JL, Pinkel D, Albertson DG, Waldman FM, McCormick F, Dickson RB, Johnson MD, Lippman M, Ethier S, Gazdar A, Gray JW. A collection of breast cancer cell lines for the study of functionally distinct cancer subtypes. Cancer Cell. 2006 Dec;10(6):515-27.
170. Zhao J, Zhang J, Yu M, Xie Y, Huang Y, Wolff DW, Abel PW, Tu Y. Mitochondrial dynamics regulates migration and invasion of breast cancer cells. Oncogene. 2013 Oct;32(40):4814-24.
171. Desai SP, Bhatia SN, Toner M, Irimia D. Mitochondrial localization and the persistent migration of epithelial cancer cells. Biophys J. 2013 May 7;104(9):2077-88.
172. Hamilton-Burke W, Coleman L, Cummings M, Green CA, Holliday DL, Horgan K, Maraqa L, Peter MB, Pollock S, Shaaban AM, Smith L, Speirs V. Phosphorylation of estrogen receptor beta at serine 105 is associated with good prognosis in breast cancer. Am J Pathol. 2010;177(3):1079-86.
173. Smith L, Brannan RA, Hanby AM, Shaaban AM, Verghese ET, Peter MB, Pollock S, Satheesha S, Szynkiewicz M, Speirs V, Hughes TA. Differential regulation of oestrogen receptor beta isoforms by 5' untranslated regions in cancer. J Cell Mol Med. 2010;14(8):2172-84.
174. Razandi M, Pedram A, Jordan VC, Fuqua S, Levin ER. Tamoxifen regulates cell fate through mitochondrial estrogen receptor beta in breast cancer. Oncogene. 2012;20(10):335.
175. Costes SV, Daelemans D, Cho EH, Dobbin Z, Pavlakis G, Lockett S. Automatic and Quantitative Measurement of Protein-Protein Colocalization in Live Cells. Biophys J. 2004 Jun;86(6):3993-4003.
176. Babbey CM, Ahktar N, Wang E, Chen CCH, Grant BD, Dunn KW. Rab10 Regulates Membrane Transport through Early Endosomes of Polarized Madin-Darby Canine Kidney Cells. Mol Biol Cell. 2006 Jul;17(7):3156-75.
177. Taanman JW. The mitochondrial genome: structure, transcription, translation and replication. Biochim Biophys Acta. 1999 Feb 9;1410(2):103-23.
178. Hashimoto Y, Niikura T, Tajima H, Yasukawa T, Sudo H, Ito Y, Kita Y, Kawasumi M, Kouyama K, Doyu M, Sobue G, Koide T, Tsuji S, Lang J, Kurokawa K, Nishimoto I. A rescue factor abolishing neuronal cell death by a wide spectrum. Proc Natl Acad Sci U S A. 2001 May 22;98(11):6336-41.
179. Hamilton-Burke W. The role of ERβ and ERβ associated proteins in breast carcinoma: The University of Leeds; 2014.

180. Fuqua SA, Schiff R, Parra I, Friedrichs WE, Su JL, McKee DD, Slentz-Kesler K, Moore LB, Willson TM, Moore JT. Expression of wild-type estrogen receptor beta and variant isoforms in human breast cancer. Cancer Res. 1999 Nov 1;59(21):5425-8.
181. Song EJ, Yim SH, Kim E, Kim NS, Lee KJ. Human Fas-Associated Factor 1, Interacting with Ubiquitinated Proteins and Valosin-Containing Protein, Is Involved in the Ubiquitin-Proteasome Pathway. Mol Cell Biol. 2005 Mar;25(6):2511-24.
182. Das S, Yeung KT, Mahajan MA, Samuels HH. Fas Activated Serine-Threonine Kinase Domains 2 (FASTKD2) mediates apoptosis of breast and prostate cancer cells through its novel FAST2 domain. BMC Cancer. 2014;14.
183. Lefevre L, Omeiri H, Drougat L, Hantel C, Giraud M, Val P, Rodriguez S, Perlemoine K, Blugeon C, Beuschlein F, de Reynies A, Rizk-Rabin M, Bertherat J, Ragazzon B. Combined transcriptome studies identify AFF3 as a mediator of the oncogenic effects of [beta]-catenin in adrenocortical carcinoma. Oncogenesis. [Original Article]. 2015 07/27/online;4:e161.
184. Wu X, Subramaniam M, Negron V, Cicek M, Reynolds C, Lingle WL, Goetz MP, Ingle JN, Spelsberg TC, Hawse JR. Development, Characterization, and Applications of a Novel Estrogen Receptor Beta Monoclonal Antibody. J Cell Biochem. 2012 Feb;113(2):711-23.
185. Badia E, Escande A, Balaguer P, Métivier R, Cavailles V. New stably transfected bioluminescent cells expressing FLAG epitope-tagged estrogen receptors to study their chromatin recruitment. BMC Biotechnol. 2009;9:77.
186. Shaw JA, Udokang K, Mosquera J-M, Chauhan H, Jones JL, Walker RA. Oestrogen receptors alpha and beta differ in normal human breast and breast carcinomas. The Journal of Pathology. 2002;198(4):450-7.
187. Kustikova OS, Wahlers A, Kuhlcke K, Stahle B, Zander AR, Baum C, Fehse B. Dose finding with retroviral vectors: correlation of retroviral vector copy numbers in single cells with gene transfer efficiency in a cell population. Blood. 2003 Dec 1;102(12):3934-7.
188. Hines WC, Yaswen P, Bissell MJ. Modelling breast cancer requires identification and correction of a critical cell lineage-dependent transduction bias. Nat Commun. [Article]. 2015 04/21/online;6.
189. Nizet V EJ. Bacterial and Viral Infections. Essentials of Glycobiology. Cold Spring Harbor (NY): Cold Spring Harbor Laboratory Press; 2009.
190. Skliris GP, Parkes AT, Limer JL, Burdall SE, Carder PJ, Speirs V. Evaluation of seven oestrogen receptor beta antibodies for immunohistochemistry, western blotting, and flow cytometry in human breast tissue. J Pathol. 2002 Jun;197(2):155-62.
191. Speirs V, Green CA, Shaaban AM. Oestrogen receptor beta immunohistochemistry: time to get it right? J Clin Pathol. 2008 Oct;61(10):1150-1; author reply 1-2.
192. Powell E, Shanle E, Brinkman A, Li J, Keles S, Wisinski KB, Huang W, Xu W. Identification of Estrogen Receptor Dimer Selective Ligands Reveals Growth-Inhibitory Effects on Cells That Co-Express ERα and ERβ. PLoS One. 2012;7(2).
193. Leygue E, Murphy LC. A bi-faceted role of estrogen receptor beta in breast cancer. Endocr Relat Cancer. 2013 Jun;20(3):R127-39.
194. Tang L, Wang Y, Strom A, Gustafsson J-Å, Guan X. Lapatinib induces p27Kip1-dependent G_1 arrest through both transcriptional and post-translational mechanisms. Cell Cycle. 2013 2013/08/15;12(16):2665-74.
195. Subik K, Lee JF, Baxter L, Strzepek T, Costello D, Crowley P, Xing L, Hung MC, Bonfiglio T, Hicks DG, Tang P. The Expression Patterns of ER, PR, HER2, CK5/6, EGFR, Ki-67 and AR by Immunohistochemical Analysis in Breast Cancer Cell Lines. Breast Cancer (Auckl). 2010;4:35-41.
196. Thomas C, Rajapaksa G, Nikolos F, Hao R, Katchy A, McCollum CW, Bondesson M, Quinlan P, Thompson A, Krishnamurthy S, Esteva FJ, Gustafsson

JA. ERbeta1 represses basal-like breast cancer epithelial to mesenchymal transition by destabilizing EGFR. Breast Cancer Res. 2012;14(6).
197. Goel S, Hidalgo M, Perez-Soler R. EGFR inhibitor-mediated apoptosis in solid tumors. J Exp Ther Oncol. 2007;6(4):305-20.
198. Hatzikirou H, Basanta D, Simon M, Schaller K, Deutsch A. 'Go or grow': the key to the emergence of invasion in tumour progression? Math Med Biol. 2012 Mar;29(1):49-65.
199. Liu ZG, Jiao XY, Chen ZG, Feng K, Luo HH. Estrogen receptorbeta2 regulates interlukin-12 receptorbeta2 expression via p38 mitogen-activated protein kinase signaling and inhibits non-small-cell lung cancer proliferation and invasion. Mol Med Rep. 2015 Jul;12(1):248-54.
200. Siddiqui F, Ehrhart EJ, Charles B, Chubb L, Li CY, Zhang X, Larue SM, Avery PR, Dewhirst MW, Ullrich RL. Anti-angiogenic effects of interleukin-12 delivered by a novel hyperthermia induced gene construct. Int J Hyperthermia. 2006 Nov;22(7):587-606.
201. Sanchez M, Picard N, Sauve K, Tremblay A. Challenging estrogen receptor beta with phosphorylation. Trends Endocrinol Metab. 2010 Feb;21(2):104-10.
202. .
203. Emberley ED, Niu Y, Njue C, Kliewer EV, Murphy LC, Watson PH. Psoriasin (S100A7) expression is associated with poor outcome in estrogen receptor-negative invasive breast cancer. Clin Cancer Res. 2003 Jul;9(7):2627-31.
204. Skliris GP, Lewis A, Emberley E, Peng B, Weebadda WK, Kemp A, Davie JR, Shiu RP, Watson PH, Murphy LC. Estrogen receptor-beta regulates psoriasin (S100A7) in human breast cancer. Breast Cancer Res Treat. 2007 Jul;104(1):75-85.
205. Deol YS, Nasser MW, Yu L, Zou X, Ganju RK. Tumor-suppressive effects of psoriasin (S100A7) are mediated through the beta-catenin/T cell factor 4 protein pathway in estrogen receptor-positive breast cancer cells. J Biol Chem. 2011 Dec 30;286(52):44845-54.
206. Vermes I, Haanen C, Steffens-Nakken H, Reutelingsperger C. A novel assay for apoptosis. Flow cytometric detection of phosphatidylserine expression on early apoptotic cells using fluorescein labelled Annexin V. J Immunol Methods. 1995 Jul 17;184(1):39-51.
207. Zhao L, Wu TW, Brinton RD. Estrogen receptor subtypes alpha and beta contribute to neuroprotection and increased Bcl-2 expression in primary hippocampal neurons. Brain Res. 2004 Jun 4;1010(1-2):22-34.
208. Wang M, Wang Y, Weil B, Abarbanell A, Herrmann J, Tan J, Kelly M, Meldrum DR. Estrogen receptor β mediates increased activation of PI3K/Akt signaling and improved myocardial function in female hearts following acute ischemia. Am J Physiol Regul Integr Comp Physiol. 2009 Apr;296(4):R972-8.
209. Gharibi B, Ghuman MS, Hughes FJ. Akt- and Erk-mediated regulation of proliferation and differentiation during PDGFRbeta-induced MSC self-renewal. J Cell Mol Med. 2012 Nov;16(11):2789-801.
210. White KA, Yore MM, Deng D, Spinella MJ. Limiting effects of RIP140 in estrogen signaling: potential mediation of anti-estrogenic effects of retinoic acid. J Biol Chem. 2005 Mar 4;280(9):7829-35.
211. Docquier A, Garcia A, Savatier J, Boulahtouf A, Bonnet S, Bellet V, Busson M, Margeat E, Jalaguier S, Royer C, Balaguer P, Cavailles V. Negative regulation of estrogen signaling by ERbeta and RIP140 in ovarian cancer cells. Mol Endocrinol. 2013 Sep;27(9):1429-41.
212. Madak-Erdogan Z, Charn TH, Jiang Y, Liu ET, Katzenellenbogen JA, Katzenellenbogen BS. Integrative genomics of gene and metabolic regulation by estrogen receptors alpha and beta, and their coregulators. Mol Syst Biol. 2013;9:676.
213. Warburg O. On the origin of cancer cells. Science. 1956 Feb 24;123(3191):309-14.

214. Guppy M, Leedman P, Zu XL, Russell V. Contribution by different fuels and metabolic pathways to the total ATP turnover of proliferating MCF-7 breast cancer cells. Biochem J. 2002 May 15;364(Pt 1):309-15.
215. Smolkova K, Bellance N, Scandurra F, Genot E, Gnaiger E, Plecita-Hlavata L, Jezek P, Rossignol R. Mitochondrial bioenergetic adaptations of breast cancer cells to aglycemia and hypoxia. J Bioenerg Biomembr. 2010 Feb;42(1):55-67.
216. Mattingly KA, Ivanova MM, Riggs KA, Wickramasinghe NS, Barch MJ, Klinge CM. Estradiol stimulates transcription of nuclear respiratory factor-1 and increases mitochondrial biogenesis. Mol Endocrinol. 2008 Mar;22(3):609-22.
217. Klinge CM. Estrogenic Control of Mitochondrial Function and Biogenesis. J Cell Biochem. 2008 Dec 15;105(6):1342-51.
218. O'Lone R, Knorr K, Jaffe IZ, Schaffer ME, Martini PG, Karas RH, Bienkowska J, Mendelsohn ME, Hansen U. Estrogen receptors alpha and beta mediate distinct pathways of vascular gene expression, including genes involved in mitochondrial electron transport and generation of reactive oxygen species. Mol Endocrinol. 2007 Jun;21(6):1281-96.
219. Sotoca AM, van den Berg H, Vervoort J, van der Saag P, Strom A, Gustafsson JA, Rietjens I, Murk AJ. Influence of cellular ERalpha/ERbeta ratio on the ERalpha-agonist induced proliferation of human T47D breast cancer cells. Toxicol Sci. 2008 Oct;105(2):303-11.
220. Stauffer SR, Coletta CJ, Tedesco R, Nishiguchi G, Carlson K, Sun J, Katzenellenbogen BS, Katzenellenbogen JA. Pyrazole ligands: structure-affinity/activity relationships and estrogen receptor-alpha-selective agonists. J Med Chem. 2000 Dec 28;43(26):4934-47.
221. Monje P, Zanello S, Holick M, Boland R. Differential cellular localization of estrogen receptor alpha in uterine and mammary cells. Mol Cell Endocrinol. 2001 Jul 5;181(1-2):117-29.
222. Miro AM, Sastre-Serra J, Pons DG, Valle A, Roca P, Oliver J. 17beta-Estradiol regulates oxidative stress in prostate cancer cell lines according to ERalpha/ERbeta ratio. J Steroid Biochem Mol Biol. 2011 Feb;123(3-5):133-9.
223. Karin M. The regulation of AP-1 activity by mitogen-activated protein kinases. J Biol Chem. 1995 Jul 14;270(28):16483-6.
224. Nair HB, Kirma NB, Ganapathy M, Vadlamudi RK, Tekmal RR. Estrogen receptor-beta activation in combination with letrozole blocks the growth of breast cancer tumors resistant to letrozole therapy. Steroids. 2011 Jul;76(8):792-6.
225. Barkhem T, Carlsson B, Nilsson Y, Enmark E, Gustafsson J, Nilsson S. Differential response of estrogen receptor alpha and estrogen receptor beta to partial estrogen agonists/antagonists. Mol Pharmacol. 1998 Jul;54(1):105-12.
226. Rieder D, Trajanoski Z, McNally JG. Transcription factories. Front Genet. 2012;3.
227. Olson MOJ. Nucleolus: Structure and Function. eLS: John Wiley & Sons, Ltd; 2001.
228. Stuurman N, Meijne AM, van der Pol AJ, de Jong L, van Driel R, van Renswoude J. The nuclear matrix from cells of different origin. Evidence for a common set of matrix proteins. J Biol Chem. 1990 Apr 5;265(10):5460-5.
229. Bernardi R, Pandolfi PP. Structure, dynamics and functions of promyelocytic leukaemia nuclear bodies. Nat Rev Mol Cell Biol. 2007 Dec;8(12):1006-16.
230. Dellaire G, Bazett-Jones DP. PML nuclear bodies: dynamic sensors of DNA damage and cellular stress. Bioessays. 2004 Sep;26(9):963-77.
231. Bernardi R, Papa A, Pandolfi PP. Regulation of apoptosis by PML and the PML-NBs. Oncogene. 0000 //print;27(48):6299-312.
232. Raska I, Ochs RL, Andrade LE, Chan EK, Burlingame R, Peebles C, Gruol D, Tan EM. Association between the nucleolus and the coiled body. J Struct Biol. 1990 Jul-Sep;104(1-3):120-7.
233. Morris GE. The Cajal body. Biochimica et Biophysica Acta (BBA) - Molecular Cell Research. 2008 11//;1783(11):2108-15.

234. Spector DL, Schrier WH, Busch H. Immunoelectron microscopic localization of snRNPs. Biol Cell. 1983;49(1):1-10.
235. Spector DL, Lamond AI. Nuclear Speckles. Cold Spring Harb Perspect Biol. 2011 Feb;3(2).
236. Cardinale S, Cisterna B, Bonetti P, Aringhieri C, Biggiogera M, Barabino SM. Subnuclear localization and dynamics of the Pre-mRNA 3' end processing factor mammalian cleavage factor I 68-kDa subunit. Mol Biol Cell. 2007 Apr;18(4):1282-92.
237. Fox AH, Lamond AI. Paraspeckles. Cold Spring Harb Perspect Biol. 2010 Jul;2(7).
238. Chan JY, Li L, Fan YH, Mu ZM, Zhang WW, Chang KS. Cell-cycle regulation of DNA damage-induced expression of the suppressor gene PML. Biochem Biophys Res Commun. 1997 Nov 26;240(3):640-6.
239. Borden KLB, Campbell Dwyer EJ, Salvato MS. The promyelocytic leukemia protein PML has a pro-apoptotic activity mediated through its RING domain. FEBS Lett. 1997 Nov 24;418(1-2):30-4.
240. Ferbeyre G, de Stanchina E, Querido E, Baptiste N, Prives C, Lowe SW. PML is induced by oncogenic ras and promotes premature senescence. Genes Dev. 2000 Aug 15;14(16):2015-27.
241. Montanaro L, Trere D, Derenzini M. Nucleolus, ribosomes, and cancer. Am J Pathol. 2008 Aug;173(2):301-10.
242. Dai MS, Sun XX, Lu H. Aberrant expression of nucleostemin activates p53 and induces cell cycle arrest via inhibition of MDM2. Mol Cell Biol. 2008 Jul;28(13):4365-76.
243. Colombo E, Marine JC, Danovi D, Falini B, Pelicci PG. Nucleophosmin regulates the stability and transcriptional activity of p53. Nat Cell Biol. 2002 Jul;4(7):529-33.
244. Colombo E, Marine J-C, Danovi D, Falini B, Pelicci PG. Nucleophosmin regulates the stability and transcriptional activity of p53. Nat Cell Biol. [10.1038/ncb814]. 2002 07//print;4(7):529-33.
245. Ma H, Pederson T. Nucleostemin: a multiplex regulator of cell-cycle progression. Trends in Cell Biology. 2008 12//;18(12):575-9.
246. Dai MS, Zeng SX, Jin Y, Sun XX, David L, Lu H. Ribosomal protein L23 activates p53 by inhibiting MDM2 function in response to ribosomal perturbation but not to translation inhibition. Mol Cell Biol. 2004 Sep;24(17):7654-68.
247. Vazquez-Martin A, Cufi S, Lopez-Bonet E, Corominas-Faja B, Cuyas E, Vellon L, Iglesias JM, Leis O, Martin AG, Menendez JA. Reprogramming of non-genomic estrogen signaling by the stemness factor SOX2 enhances the tumor-initiating capacity of breast cancer cells. Cell Cycle. 2013 Nov 15;12(22):3471-7.
248. Stanley E, Lin CY, Jin S, Liu J, Sottas CM, Ge R, Zirkin BR, Chen H. Identification, proliferation, and differentiation of adult Leydig stem cells. Endocrinology. 2012 Oct;153(10):5002-10.
249. Bregman DB, Du L, van der Zee S, Warren SL. Transcription-dependent redistribution of the large subunit of RNA polymerase II to discrete nuclear domains. J Cell Biol. 1995 Apr;129(2):287-98.
250. Mortillaro MJ, Blencowe BJ, Wei X, Nakayasu H, Du L, Warren SL, Sharp PA, Berezney R. A hyperphosphorylated form of the large subunit of RNA polymerase II is associated with splicing complexes and the nuclear matrix. Proceedings of the National Academy of Sciences. 1996 August 6, 1996;93(16):8253-7.
251. van Royen ME, Cunha SM, Brink MC, Mattern KA, Nigg AL, Dubbink HJ, Verschure PJ, Trapman J, Houtsmuller AB. Compartmentalization of androgen receptor protein-protein interactions in living cells. J Cell Biol. 2007 Apr 9;177(1):63-72.
252. Koba M, Konopa J. [Actinomycin D and its mechanisms of action]. Postepy Hig Med Dosw (Online). 2005;59:290-8.

253. Schneider-Poetsch T, Ju J, Eyler DE, Dang Y, Bhat S, Merrick WC, Green R, Shen B, Liu JO. Inhibition of Eukaryotic Translation Elongation by Cycloheximide and Lactimidomycin. Nat Chem Biol. 2010 Mar;6(3):209-17.
254. Bunone G, Briand PA, Miksicek RJ, Picard D. Activation of the unliganded estrogen receptor by EGF involves the MAP kinase pathway and direct phosphorylation. EMBO Journal. 1996;15(9):2174-83.
255. Kato S, Endoh H, Masuhiro Y, Kitamoto T, Uchiyama S, Sasaki H, Masushige S, Gotoh Y, Nishida E, Kawashima H, Metzger D, Chambon P. Activation of the estrogen receptor through phosphorylation by mitogen-activated protein kinase. Science. 1995 Dec 1;270(5241):1491-4.
256. Sutherland RL, Hall RE, Taylor IW. Cell proliferation kinetics of MCF-7 human mammary carcinoma cells in culture and effects of tamoxifen on exponentially growing and plateau-phase cells. Cancer Res. 1983 Sep;43(9):3998-4006.
257. GM C. The Cell: A Molecular Approach. 2nd edition ed. Sunderland (MA): Sinauer Associates; 2000.
258. Prescott DM, Bender MA. Synthesis of RNA and protein during mitosis in mammalian tissue culture cells. Exp Cell Res. 1962 Mar;26:260-8.
259. Hartl P, Gottesfeld J, Forbes DJ. Mitotic repression of transcription in vitro. J Cell Biol. 1993 Feb;120(3):613-24.
260. Jackman J, O'Connor PM. Methods for synchronizing cells at specific stages of the cell cycle. Curr Protoc Cell Biol. 2001 May;Chapter 8:Unit 8 3.
261. Guppy M, Leedman P, Zu X, Russell V. Contribution by different fuels and metabolic pathways to the total ATP turnover of proliferating MCF-7 breast cancer cells. Biochem J. 2002 May 15;364(Pt 1):309-15.
262. De Stefano I, Zannoni GF, Prisco MG, Fagotti A, Tortorella L, Vizzielli G, Mencaglia L, Scambia G, Gallo D. Cytoplasmic expression of estrogen receptor beta (ERbeta) predicts poor clinical outcome in advanced serous ovarian cancer. Gynecol Oncol. 2011 Sep;122(3):573-9.
263. Zannoni GF, Prisco MG, Vellone VG, De Stefano I, Vizzielli G, Tortorella L, Fagotti A, Scambia G, Gallo D. Cytoplasmic expression of oestrogen receptor beta (ERbeta) as a prognostic factor in vulvar squamous cell carcinoma in elderly women. Histopathology. 2011 Nov;59(5):909-17.
264. Inoue A, Tsugawa K, Tokunaga K, Takahashi KP, Uni S, Kimura M, Nishio K, Yamamoto N, Honda K, Watanabe T, Yamane H, Tani T. S1-1 nuclear domains: characterization and dynamics as a function of transcriptional activity. Biol Cell. 2008 Sep;100(9):523-35.
265. Fong K-w, Li Y, Wang W, Ma W, Li K, Qi RZ, Liu D, Songyang Z, Chen J. Whole-genome screening identifies proteins localized to distinct nuclear bodies. The Journal of Cell Biology. 2013 03/27/received 08/19/accepted;203(1):149-64.
266. Ullah MF, Ahmad A, Zubair H, Khan HY, Wang Z, Sarkar FH, Hadi SM. Soy isoflavone genistein induces cell death in breast cancer cells through mobilization of endogenous copper ions and generation of reactive oxygen species. Mol Nutr Food Res. 2011 Apr;55(4):553-9.